Patent Application
Docket No. USF-T150CX
Serial No. 09/955,174

IN THE UNITED STATES PATENT AND TRADEMARK OFFICE

Examiner	:	Jane J. Zara
Art Unit	:	1635
Applicant	:	William G. Kerr
Serial No.	:	09/955,174
Filed	:	September 19, 2001
For	:	Control of NK Cell Function and Survival by Modulation of SHIP Activity

MS AMENDMENT
Commissioner for Patents
P.O. Box 1450
Alexandria, VA 22313-1450

DECLARATION OF WILLIAM G. KERR, Ph.D., UNDER 37 C.F.R. §1.132

Sir:

I, William G. Kerr, Ph.D., of the University of South Florida, hereby declare:

THAT, I am a named inventor on the above-referenced patent application (hereinafter the '174 application);

THAT, my *curriculum vitae* is already of record in the '174 application;

THAT, I have read and understood the specification and claims of the '174 application and the Office Actions dated February 18, 2004 and October 6, 2004;

AND, being thus duly qualified, do further declare:

1. The above-referenced Office Action dated October 6, 2004 indicates that claims 38-73 are rejected under 35 U.S.C. §112, first paragraph, as lacking sufficient written description by the patent application.

2. As indicated at page 8, lines 14-20, and page 31, lines 3-13, of the '174 application, the invention is based on the unexpected finding that reducing the activity of hematopoietic-specific SH2-containing inositol-5-phosphatase (SHIP-1) has physiological effects, such as alteration of natural

killer (NK) cell-mediated activities, which provide therapeutic benefits such as suppression of transplant rejection and treatment of graft-versus-host disease (GVHD).

3. The Reviewer indicates that the '174 application does not provide adequate written description for the breadth of the genus claimed (*i.e.*, mammalian SHIP-1 mRNA). The Reviewer points out that mammalian SHIP-1 mRNA encompasses SHIP-1 mRNA from mammals other than human and mouse (*e.g.*, monkey, rabbit, horse), and encompasses multiple existing isoforms within a given mammalian species.

4. As indicated in my previous Declaration dated July 16, 2004, and as evidenced by Exhibits B and C, which accompanied that Declaration, the mRNA sequences of human and mouse SHIP-1 were known at the time '174 application was filed. The degree of homology between human SHIP-1 and mouse SHIP-1 nucleotide sequences is high. It is reasonable to expect that there would be a high degree of homology between humans or mice and many other mammals. Submitted herewith as Exhibit A (four pages) is mammalian orthology data for SHIP-1 obtained from the National Center for Biotechnology Information's (NCBI) HomoloGene database (http://www.ncbi.nlm.nih.gov/HomoloGene/), which is a publicly available system for automated detection of homologs among the annotated genes of several completely sequenced eukaryotic genomes and is readily utilized by those of ordinary skill in the art. The SHIP-1 sequence of rat (*R. norvegicus*) has now been determined and a potential chimpanzee (*P. troglodytes*) SHIP-1 orthologue has also recently been identified. Exhibit A includes a table of pair wise alignment scores, showing levels of SHIP-1 homology among humans, mice, rats, and (potentially) chimpanzees. As shown in Exhibit A, each sequence has the SHIP-1 enzymatic domain (inositol 5'-phosphatase) and the degree of nucleotide homology between human SHIP-1 and mouse and rat SHIP1 is over 85%. Although the potential chimpanzee orthologue is shown on the database to lack a detectable amino-terminal src-homology domain (SH2), it is noteworthy that there is nonetheless 97% nucleotide homology between human SHIP-1 and the chimpanzee sequence. Furthermore, mice and humans are believed to have the same five SHIP-1 protein isoforms. There would be no difficulty in identifying target mRNA sequences shared by all known hematopoietic SHIP-1 isoforms in humans and mice, due to the extensive amount of sequence overlap between the

isoforms (see Figure 2A of Rohrschneider *et al.*, *Genes & Development*, 2000, 14:505-520, the full text of which is submitted herewith as Exhibit B). Moreover, the SHIP-1 enzymatic domain, which one of ordinary skill in the art would likely consider the starting point for selecting any inhibitory hybridizing nucleic acid molecule for SHIP-1, is very high in all five isoforms. Four of the five isoforms also contain the SH2 domain. Thus, based on the high degree of homology between known mammalian SHIP-1 orthologues, and the high degree of conservation between SHIP-1 isoforms (particularly, in the SHIP-1 enzymatic domain), the '174 application provides an adequate written description of mammalian SHIP-1 mRNA. Therefore, having the sequence of the target gene, one skilled in the art could readily envision target nucleic acid sequences within the recipient mammal's mRNA. Due to nucleotide complementarity, nucleic acid molecules likely to hybridize with SHIP-1 mRNA and interfere with its expression could then be determined.

5. The above-referenced Office Action dated October 6, 2004 indicates that claims 38-66 are rejected under 35 U.S.C. §112, first paragraph, as lacking enablement by the patent application. The Reviewer indicates that, in order for the full scope of the instant invention to be enabled, the results obtained using ablation experiments cannot be substituted for the unpredictable endeavor of providing treatment effects including altering NK cell function and GVHD in any mammal using any RNAi targeting any mammalian SHIP-1 mRNA. Furthermore, the Reviewer indicates that it would be highly unpredictable that complete ablation will be obtained using the inhibitory molecules recited in the claims, and a measure of the extent of target gene inhibition required to achieve this treatment effect (observed in an ablated mouse model) must be determined empirically and, therefore, requires undue experimentation. The '174 patent application enables reducing mammalian SHIP-1 function *in vitro* or *in vivo*, altering NK function in a mammal, preventing (or reducing) transplant rejection in a patient, and preventing or treating graft-versus-host disease (GVHD) in a patient, each by administering an effective amount of interfering RNA (RNAi) specific for mammalian SHIP-1 mRNA. As indicated above, the level of homology between known mammalian SHIP-1 isoforms is high. Having the sequence of the target gene, one skilled in the art could readily envision target nucleic acid sequences within the recipient mammal's mRNA. Due to nucleotide complementarity, nucleic acid molecules likely to hybridize with SHIP-1 mRNA and interfere with its expression could then be determined without resort to undue experimentation. The

following experiments support the enablement of the invention as claimed in the accompanying Amendment.

6. ShRNA vector specific for SHIP-1: C57BL6/J mice were injected i.p. on days 1, 2, and 3 with a SHIP-1 shRNA vector complexed with the cationic lipid DOTAP. The vector design and sequence is shown in Exhibit H of my Declaration dated July 16, 2004. The mice showed significant suppression of all detectable SHIP-1 isoforms in the spleen, as shown in Figure A of Exhibit G of my Declaration dated July 16, 2004.

7. SHIP-1-specific siRNA molecules: Four different SHIP-1-specific siRNAs (#1-4) were screened *in vitro* for knockdown of SHIP-1 in mouse cells. The sequences of siRNAs #1-4 and respective target sites within the open reading frame of mouse SHIP-1 are shown in Exhibit I of my Declaration dated July 16, 2004. siRNAs #1 and #4 were pooled and tested *in vivo* by injecting i.v. the siRNAs complexed with DOTAP into C57BL6/J mice. As with SHIP-1 shRNA-treated mice, there was partial suppression of SHIP-1 expression in peripheral mononuclear cells (PBMC), as determined by Western blotting 20 hours post-treatment (as stated in my Declaration dated July 16, 2004). The myeloid compartments of the mice were also analyzed by fluorescence activated cell sorting (FACS), which showed a significant increase in Mac+Gr1-monocytes and circulating Mac1+GR1+ cells (myeloid suppressor cells) was observed in the SHIP-1-specific siRNA treated mice, relative to controls, as shown in Figure B of Exhibit G of my Declaration dated July 16, 2004. These findings show that SHIP-1-specific interfering RNA can have profound physiological effects in a rapid fashion, even when complete knockdown is not achieved.

8. Partial Induction of SHIP-1 deficiency in adult mice increases Mac1+Gr1+ MSC and suppresses allogeneic T cell priming in lymphoid tissues: Figures A-C of Exhibit C, which is submitted herewith for the Reviewer's consideration, shows that induction of SHIP-1 deletion in the adult MXCreSHIPflox/- mice dramatically increases MSC numbers in the lymph node (LN) and spleens of mice, and leads to compromised priming of allogeneic T cells. This occurs within approximately one to three weeks of SHIP-1 deletion and does not require complete ablation of SHIP-1 expression, as mice with partial SHIP-1 ablation also show significantly reduced priming of allogeneic T cells.

The MXCre mouse represents a stringent model for assessment of altered SHIP-1 function, and is recognized by those in the field as a valid tool for determining the physiological effects of endogenous gene ablation *in vivo*. Figures D and E of Exhibit C, which is submitted herewith, show that SHIPflox/- mice with myeloid-specific expression of Cre (LysCre) have a significant increase in MSC that leads to a profound suppression of allogeneic T cell priming. Again, only a partial deletion of SHIP-1 in the myeloid lineage is required to achieve significant suppression of allogeneic T cell responses, which mediate GVHD and organ graft rejection. These findings demonstrate that even partial induction of SHIP-1 deficiency *in vivo* can increase the representation of cells capable of suppressing allogeneic T cell priming. A reduced allogeneic T cell response is considered by those in the field as a key determinant to successful engraftment. Thus, this physiologic response is clinically favorable and reasonably correlates with a therapeutic benefit in mediating GVHD and organ graft rejection.

The undersigned declares further that all statements made herein of his own knowledge are true and that all statements made on information and belief are believed to be true; and further that these statements were made with the knowledge that willful false statements and the like so made are punishable by fine or imprisonment, or both, under Section 1001 of Title 18 of the United States Code and that such willful false statements may jeopardize the validity of the application or of any patent issuing thereon.

Further declarant sayeth naught.

Signed: 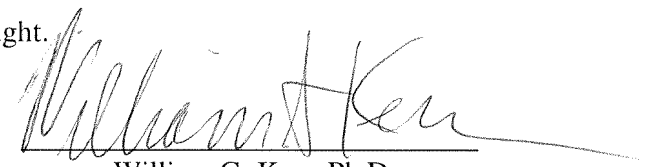
William G. Kerr, Ph.D.

Date: 1/18/05

Exhibit A

NCBI Homologene Discover Homologs

Help

Entrez PubMed Nucleotide Protein Genome Structure Map Viewer LocusLink UniGene OMIM

Search HomoloGene for Go Clear

Limits Preview/Index History Clipboard Details

Display HomoloGene Show: 20 Send to Text

1: HomoloGene:4046. Gene conserved in Mammalia Links

Genes
Genes identified as putative homologs of one another during the construction of HomoloGene

- H.sapiens INPP5D
  inositol polyphosphate-5-phosphatase, 145kDa.
- P.troglodytes LOC470683
  LOC470683.
- M.musculus Inpp5d
  inositol polyphosphate-5-phosphatase D.
- R.norvegicus Inpp5d
  inositol polyphosphate-5-phosphatase D.

Proteins
Proteins used in sequence comparisons and their conserved domain architectures.

- NP_005532.2
  1188 aa
- XP_526066.1
  972 aa
- NP_034696.1
  1191 aa
- NP_062184.1
  1190 aa

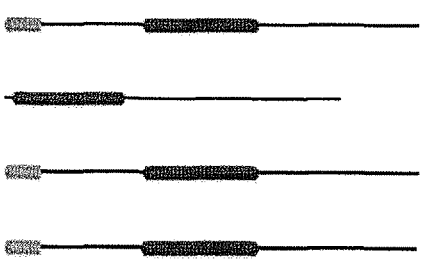

Alignment Scores
Various evolutionary parameters derived from pairwise alignments have been saved.

Show Table of Pairwise Scores

Alignments can be regenerated using BLAST for any selected pair of proteins.

Regenerate Alignments

Conserved Domains
Conserved Domains from CDD found in protein sequences by rpsblast searching.

- cd00173
  - SH2. Src homology 2 domains
- smart00128
  - IPPc. Inositol polyphosphate phosphatase, catalytic domain homologues

NP_005532.2(H.sapiens. INPP5D)
XP_526066.1(P.troglodytes. LOC470683)
BLAST

Related Homology Resources

Links to curated and computed homology information found in other databases.

MGI:107357
Orthology group for M.musculus Inpp5d includes H.sapiens INPP5D.

UniGene

Links to groups of transcribed sequences established by tblastn searching of UniGene.

B.taurus Bt.6453
Transcribed locus, moderately similar to NP_005532.2 inositol polyphosphate-5-phosphatase, 145kDa [Homo sapiens]

B.taurus Bt.26676
Transcribed locus, highly similar to NP_005532.2 inositol polyphosphate-5-phosphatase, 145kDa [Homo sapiens]

H.sapiens Hs.262886
Inositol polyphosphate-5-phosphatase, 145kDa

M.musculus Mm.15105
Inositol polyphosphate-5-phosphatase D

R.norvegicus Rn.10659
Inositol polyphosphate-5-phosphatase D

X.laevis Xl.34826
Hypothetical protein MGC68993

Display HomoloGene Show: 20 Send to Text

Questions or Comments?
E-mail the NCBI Help Desk

FIRSTGOV

HomoloGene Home
National Center for Biotechnology Information
U.S. National Library of Medicine
National Institutes of Health

U.S. DEPARTMENT OF HEALTH & HUMAN SERVICES

Jan 4 2005 07:12:41

Alignment Scores

Species	Gene	aa%ID	nt%ID	D	Ka/Ks	Knr/Knc	
H.sapiens	**INPP5D**						
vs. M.musculus	Inpp5d	88.2	85.2	0.165	0.090	0.543	Blast
vs. R.norvegicus	Inpp5d	88.4	85.4	0.162	0.096	0.567	Blast
vs. P.troglodytes	LOC470683	97.1	97.0	0.030	0.463	1.050	Blast
M.musculus	**Inpp5d**						
vs. H.sapiens	INPP5D	88.2	85.2	0.165	0.090	0.543	Blast
vs. R.norvegicus	Inpp5d	96.5	94.9	0.052	0.089	0.483	Blast
vs. P.troglodytes	LOC470683	85.5	82.3	0.201	0.109	0.603	Blast
R.norvegicus	**Inpp5d**						
vs. H.sapiens	INPP5D	88.4	85.4	0.162	0.096	0.567	Blast
vs. M.musculus	Inpp5d	96.5	94.9	0.052	0.089	0.483	Blast
vs. P.troglodytes	LOC470683	85.6	82.9	0.194	0.124	0.602	Blast
P.troglodytes	**LOC470683**						
vs. H.sapiens	INPP5D	97.1	97.0	0.030	0.463	1.050	Blast
vs. M.musculus	Inpp5d	85.5	82.3	0.201	0.109	0.603	Blast
vs. R.norvegicus	Inpp5d	85.6	82.9	0.194	0.124	0.602	Blast

Questions or Comments?
E-mail the NCBI Help Desk

Jan 4 2005 07:12:41

Exhibit B

REVIEW

Structure, function, and biology of SHIP proteins

Larry R. Rohrschneider,[1] John F. Fuller, Ingrid Wolf, Yan Liu, and David M. Lucas[2]

Fred Hutchinson Cancer Research Center, Division of Basic Sciences, Seattle, Washington 98109-1024 USA

One of the "simple" curiosities of life, at least for a biological scientist, is how the growth and development of a complete organism from a single cell is controlled. Part of the answer includes growth factor receptors and their respective ligands, which transduce signals across cell membranes and into the nucleus for transcriptional readout. The molecular nature of these intracellular signals determines the type of signals, the pathways involved, subsequent regulatory interactions, and eventual transcription factor activation/repression. Hematopoietic cell development has been a fruitful system for the analysis of these signals because mature blood cells develop from a small population of self-replicating stem cells in the bone marrow, providing a convenient model cell system to study these mechanisms. In recent years a new signaling protein component of many growth factor receptor signaling pathways has been identified, called SHIP (SH2-containing Inositol 5′-Phosphatase). This review presents current structural information on the SHIP protein and its various roles in cellular regulation.

SHIP was initially observed as a tyrosine-phosphorylated protein after stimulation of blood cells by any of a broad number of cytokines and growth factors (Damen et al. 1993; Kavanaugh and Williams 1994; Lioubin et al. 1994; Liu et al. 1994; Matsuguchi et al. 1994; Saxton et al. 1994; Drachman et al. 1995; Chacko et al. 1996; Crowley et al. 1996). cDNAs for the cognate protein were cloned by several laboratories. The cloning methods varied, and some utilized the biochemically identified interactions of SHIP with Grb2, Shc, or Fc receptors to isolate a ~145-kD protein, obtain peptide sequences, and screen a cDNA library with degenerate probes (Damen et al. 1996; Kavanaugh et al. 1996; Ono et al. 1996; Odai et al. 1997). A novel approach employing a modified yeast two-hybrid screen was used in two cases in which the yeast expressed an exogenous tyrosine kinase. This allowed identification of tyrosine-phosphorylated SHIP cDNA segments by specific interactions with the PTB domain of Shc (Lioubin et al. 1996) or the cytoplasmic sequence of an Fc receptor (Osborne et al. 1996). Other cloning methods obtained SHIP cDNA from EST probes (Q. Liu et al. 1997) or by general cloning of inositol 5′-phosphatases using degenerate PCR (Drayer et al. 1996). Subsequent studies have begun to examine the in vivo biological function of SHIP, and the following sections will cover sequential details on the structure and biological function with a critical analysis of the overall role of SHIP in cellular regulation.

[1]Corresponding author.
E-MAIL lrohrsch@fhcrc.org; FAX (206) 667-3308.
[2]Present address: Department of Internal Medicine, Ohio State University, Columbus, Ohio 43210 USA.

SHIP structure and protein interaction motifs

SHIP structure

The domain and motif structure of p145 SHIP is shown in Figure 1. SHIP contains 1190 amino acids, with a calculated molecular mass of 133 kD, and contains several identifiable motifs important for protein–protein interactions. The amino-terminal Src homology 2 (SH2) domain (Schaffhausen 1995) was an early identifying characteristic of SHIP and is vital in the interactions of SHIP with a large number of intracellular signaling proteins. As will be discussed below, the numerous SH2-mediated interactions of SHIP are currently being exploited to investigate its function. The central 400–500 amino acid portion of SHIP encodes an enzymatic activity for removal of phosphate from the 5′ position of inositol polyphosphate, and ~300 amino acids of undefined function separate the SH2 domain from the 5′-phosphatase domain. About 350 amino acids comprise a distinct carboxy-terminal domain, which encodes two NPXY motifs (in single-letter amino acid designation). Upon tyrosine phosphorylation of this motif, proteins containing a phosphotyrosine binding (PTB) domain (van der Geer and Pawson 1995) are known to interact with SHIP at these sites. For example, the PTB domain of Shc is known to bind to both these sites in phosphorylated SHIP (Lioubin et al. 1996; Lamkin et al. 1997). Phosphorylation of the NPXY motifs may also serve as potential interaction sites for SH2 domain-containing proteins, depending on the three amino acids adjacent to the carboxyl side of the tyrosine. Finally, several PxxP motifs are present within the carboxyl terminus and may serve as binding sites for proteins containing SH3 domains. The potential PxxP motifs are shown within the carboxy-terminal domain of SHIP in Figure 1, with the broader dark green bands as

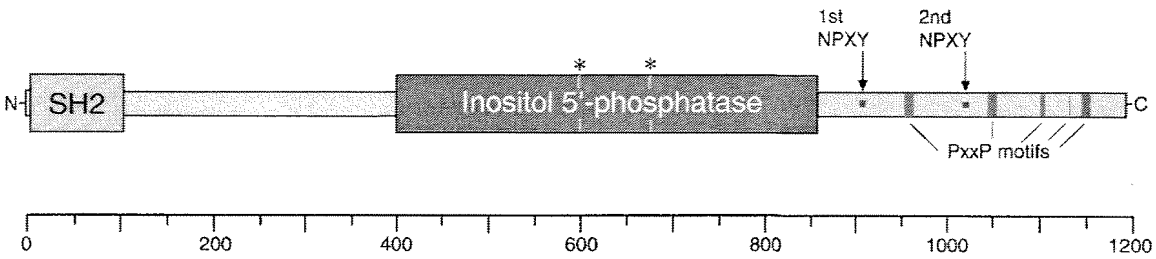

Figure 1. The domain structure of p145 SHIP. The SH2, inositol 5′-phosphatase, and carboxy-terminal domains are shown in light orange, blue, and green, respectively. The region between the SH2 and inositol 5′-phosphatase domains is of unknown function and is shaded gray. Two asterisks above the central enzymatic domain mark the locations of homology regions with all 5′-phosphatases; and two NPXY motifs, when tyrosine phosphorylated, have potential for binding PTB or possibly SH2 domains. These are designated with red in the carboxy-terminal region. The remainder of the carboxy-terminal domain has several potential polyproline motifs (PxxP) for binding SH3 domains. These polyproline motifs are shown in dark green. Three of the motifs show very good consensus for SH3 domain binding; two others have weaker homology and are shown with narrower dark green bands. The scale *below* the SHIP domain structure designates its length in amino acids.

the more likely SH3-domain binding sites. Together, these structural features describe a unique signaling protein, whose functional significance will be dependent upon the subsequent interactions and enzymatic activity. Each of these aspects of SHIP will be discussed in the following sections.

SHIP isoforms—an armada of SHIPs

The endogenous SHIP protein is usually detectable as multiple protein bands upon PAGE, with a 145-kD species as the largest band consistently detected. A lower abundance 160-kD SHIP protein has been observed at times (Ono et al. 1996; Geier et al. 1997), but detection may be cell-type or antibody specific, and further characterization has not been reported. Full-length SHIP, 1190 amino acid residues, is the product of a 3570-nucleotide ORF. However, SHIP protein products (either endogenous or exogenously expressed) frequently exhibit discrete size variability. In general, SHIP proteins of 145, 135, 125, and 110 kD have been described in different laboratories (Lioubin et al. 1996; Ono et al. 1996; Lucas and Rohrschneider 1999). The significance of these SHIP isoforms was enhanced by the observation that bone marrow or immature hematopoietic cell lines express increasingly larger SHIP proteins as differentiation proceeds to mature blood cells (Geier et al. 1997). Therefore, the provenance of these isoforms is an important question in determining the function of the SHIP proteins.

Possible mechanisms for isoform production include alternative transcriptional initiation, alternative translational initiation, mRNA splicing, protein degradation, and post-translational modification such as phosphorylation. Several of these possibilities have been examined. A study by Damen et al. (1998) used several domain-specific anti-SHIP antibodies to show that the SHIP protein is subject to specific proteolytic degradation from the carboxy-terminal end, possibly by a member of the calpain family. Several discrete protein bands were observed following expression of the cDNA for p145 SHIP. The smallest SHIP protein obtained, p110, was associated with the cellular cytoskeleton.

Kavanaugh et al. (1996) described a 110-kD form of SHIP in human cells, SIP-110, proposed to be a product of alternative splicing (Fig. 2). SIP-110 lacks the 214 amino-terminal amino acids, including the SH2 domain. The SIP-110 protein is not tyrosine phosphorylated after growth factor stimulation and was identified through its binding to the SH3 domain of Grb2 in a phosphotyrosine-independent manner, showing its ability to participate in interactions despite its lack of an SH2 domain. Although 110-kD forms of SHIP are seen in murine cells, it has not been demonstrated that these forms are the result of SIP-110 or a SIP-110-like mRNA splice. On the other hand, at least part of the postulated splice is consistent with the exon–intron SHIP genomic information and would link a unique nucleotide sequence encoding a start methionine plus eight amino acids to the beginning of exon 6 before the 5′-phosphatase domain (I. Wolf, D.M. Lucas, P.A. Algate, and L.R. Rohrschneider, in prep.). Alternatively, Kerr et al.(unpubl.) have identified a very similar *SHIP* cDNA encoding a related p110 product (GenBank accession no. AF184912); however, this latter SHIP protein would not require splicing but would arise from utilization of a transcriptional start different than that used for p145 SHIP. Presumably, a second promoter within the *SHIP* locus would regulate transcription for this p110 SHIP.

In our laboratory RT–PCR analyses using SHIP-specific oligonucleotides identified a SHIP cDNA with an internal 183-nucleotide deletion immediately following the first NPXY motif (Lucas and Rohrschneider 1999). When translated, this deletion results in the elimination of 61 amino acids after which SHIP translation proceeds in-frame. Because the deleted fragment contains intron splice donor and acceptor consensus sequences, it is likely to be the result of specific mRNA splicing. Several cDNAs encoding the Δ183 SHIP protein have been cloned from a murine myeloid cell library. The product of this Δ183 mRNA is calculated to be 8 kD smaller than full-length SHIP, correlating well with observations from immunoblot data showing a p135 SHIP isoform. Further studies using RT–PCR showed that this Δ183 cDNA is present in all of the full-length SHIP-expressing

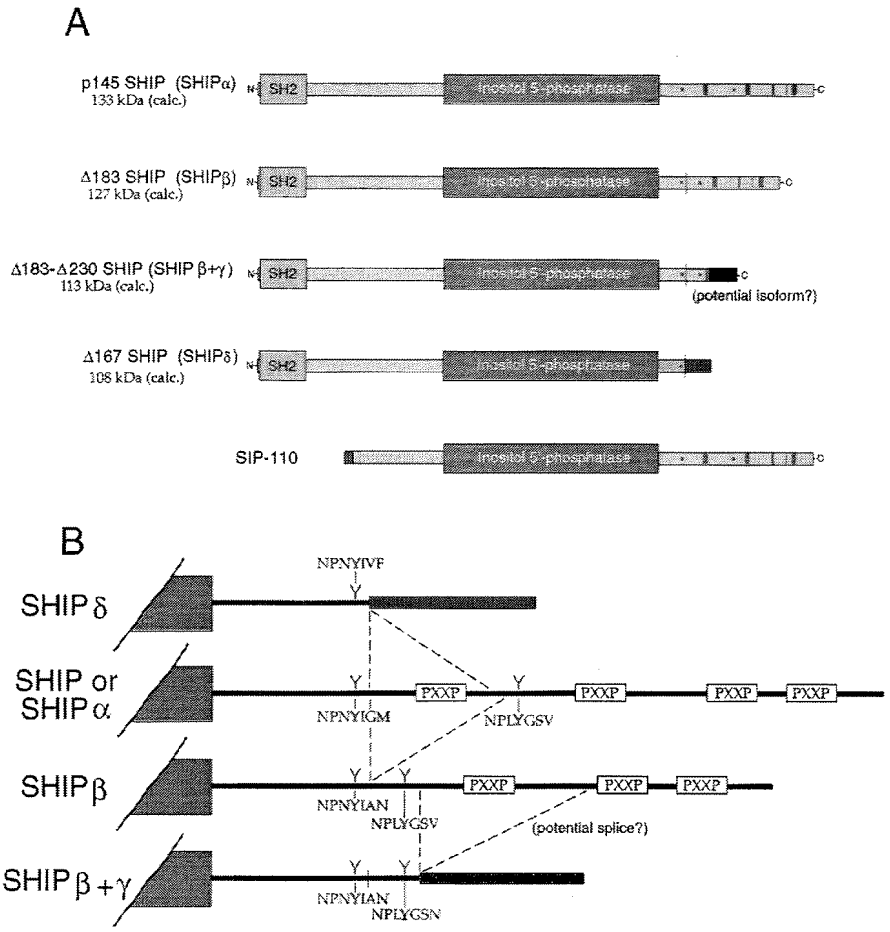

Figure 2. SHIP protein isoforms and derivation of the spliced protein products. (*A*) The structure of five SHIP isoforms is shown with p145 SHIP (SHIPα) at the *top*, followed in descending order by smaller size SHIP isoforms. The second structure down (SHIPβ) is an in-frame spliced product deleting 183 nucleotides, which affects the amino acids between the two NPXY motifs. The third SHIP isoform contains two spliced-out regions, Δ183 and Δ230; the latter removes 230 additional nucleotides from the region immediately downstream of the second NPXY motif in the SHIP. The out-of-frame Δ230 deletion would produce a protein with 67 new carboxy-terminal amino acids (dark green), and the protein product of this modification alone would be designated SHIPγ. The mRNA and protein for this latter splice are yet uncharacterized and the protein product should be considered as potential. The SHIPδ protein results from another out-of-frame splice in the region encoding the carboxyl terminus and produces 41 new amino acids at the carboxyl terminus (purple). An additional SHIP isoform, lacking the SH2 domain, has been called SIP-110. This product is proposed to result from splicing, but this possibility is controversial. (*B*) Derivation of the SHIP isoforms by splicing reactions. Details of the protein structures affected by splicing within the region encoding the carboxy-terminal domain of SHIP are shown. SHIP (or SHIPα) is the longest protein, and the other isoforms are derived from this product. The location of four polyproline motifs are shown, and the tyrosine (Y) of the two NPXY motifs are in red. The amino acid sequences surrounding each Y are shaded gray with the relevant Y in red. Both Δ167 and Δ183 splices begin at the same nucleotide, but terminate at different sites resulting in production of SHIPδ and SHIPβ, respectively. The Δ183 splice is in-frame; the Δ167 is out-of-frame producing the new carboxy-terminal tail sequence (purple). The Δ230 splice, shown at the bottom, also would produce an out-of-frame deletion with a new C-terminal sequence of 67 amino acids (dark green). Both Δ183 and Δ230 splicing would begin at a site near the first or second NPXY motifs, respectively, and change the three amino acid motif on the carboxyl side of each Y. Therefore, both Δ183 and Δ230 splices have the potential for altering any SH2 domains binding to these phosphorylated sites but the PTB domain sites remain the same.

cells tested so far, and thus does not appear to be subject to separate regulatory mechanisms. Using several SHIP-specific monoclonal antibodies, we were able to demonstrate that the 135-kD form of SHIP seen by SDS-PAGE is the product of Δ183 message and identical to p135 SHIP. An additional monoclonal antibody (P2A8) made using an immunogen spanning the spliced junction independently confirmed these results (Lucas and Rohrschneider 1999). The amino acid sequence removed by the Δ183 splice contains several PxxP sequences. In addition, the splice junction changes the third amino acid downstream of the phosphorylated Y in the first NPXY motif. This change could have significance for altering the specificity of binding via SH2 domains; however, at present, the potential for SH2 domain-containing proteins binding to this site is not well understood.

A SHIP-spliced form similar to the murine Δ183 is also present in human myeloid cells. This human SHIP was detected by RT–PCR analysis in human ML-1 cells treated with TPA and in human peripheral blood leukocytes. The deletion in the human cells is slightly larger and lacks 282 nucleotides, including those encoding the first NPXY motif. These 282 nucleotides encompass an entire exon instead of the intraexonic splice observed in the murine gene. Like the Δ183 deletion, the Δ282 deletion remains in the original reading frame following the splice but produces a SHIP cDNA isoform, which if translated, would lack 94 amino acids totaling 10 kD (Lucas and Rohrschneider 1999). A SHIP polyclonal antibody detects a 135-kD band in human hematopoietic cells, but we have not yet confirmed that this corresponds to the Δ282 human SHIP. The biological significance of the p135(Δ183) SHIP isoform is not yet understood, but because both human and murine forms appear to delete or modify the first NPXY motif along with the deletion of a potential SH3-binding motif, it is likely that at least part of its function relates to protein(s) binding to this region.

Two additional *SHIP* splice variants have been detected in the murine myeloid cells. A 167-nucleotide deletion of *SHIP* beginning at the same nucleotide as the Δ183 deletion, but ending 16 nucleotides before that of Δ183, has been characterized (I. Wolf, D.M. Lucas, P.A. Algate, and L.R. Rohrschneider, in prep.). This deletion is also flanked by consensus splice donors and acceptors and appears to be the result of mRNA splicing. However, following the splice, the sequence continues in a different reading frame and produces 41 unique amino acids at the carboxyl terminus before reaching a stop codon. The calculated size of this Δ167 cDNA is 108 kD, potentially explaining one of the multiple 110-kD bands seen in murine SHIP immunoblots. An additional splice event has been observed by RT–PCR analysis just downstream of the region encoding the second NPXY motif; however, it has not been characterized further and its existence in vivo is uncertain. This potential splice would delete 230 nucleotides in the last coding exon with a frameshift in translation. Splice donor and acceptor nucleotides flank the deletion, and the proposed splice junction would change the third amino acid on the carboxy-terminal side of the phosphorylated Y in the second NPXY motif. Thus, there might be some recapitulation of translational modifications at both the first and second NPXY motifs; however, the latter splice modification is speculative.

SHIP nomenclature

Several aspects of SHIP expression present a difficulty in nomenclature. Protein degradation of p145 SHIP protein from the carboxyl terminus creates multiple distinct SHIP proteins as described by Damen et al. (1998), and multiple *SHIP* splicing can generate SHIP proteins each unique from those created by proteolytic degradation. In addition, the proteolytic degradation of SHIP also may occur on each spliced form of SHIP identified. One example is the Δ183 *SHIP* cDNA encoding a 135-kD SHIP protein. A similar size SHIP band is detected as a degradation product from the 145-kD full-length SHIP, but these two ~135-kD proteins are distinguishable by using several monoclonal antibodies (Lucas and Rohrschneider 1999). These numerous SHIP proteins, plus the cloning of a new homolog, *SHIP2* (Pesesse et al. 1997), indicates that a better nomenclature is required.

The body of SHIP literature is large and rapidly growing, and because of the number of references to the 145-kD form as SHIP, no modification needs to be made to this designation. However, recently published work refers to this form as SHIP1 to differentiate it from the newly described SHIP2 (Pesesse et al. 1997). To permit better identification of the multiple smaller spliced isoforms of SHIP1, we propose that these be labeled with Greek letters by their successively smaller size, as has been done with other protein systems. Thus, the 145-kD product can be named SHIP, SHIP1, or SHIPα; the product of the Δ183 deletion can be termed SHIPβ; the 125-kD SHIP (if characterized better in vivo) can be referred to as SHIPγ; and the newly described Δ167 spliced form can be termed SHIPδ. These designations of each SHIP isoform along with its structure are listed in Figure 2.

Expression

SHIP was initially detected in the more mature cells of the blood, but it is now apparent that almost all cells of the bone marrow and blood express at least one form of this protein. The presence of *SHIP* mRNA has been detected at the earliest stages of hematopoietic cell development in mouse embryos (Q. Liu et al. 1998), and protein expression has been observed in all blood cell lineages, to various degrees, using flow cytometric analysis of bone marrow and blood (Geier et al. 1997). This latter study also demonstrated the differential expression of various SHIP isoforms during differentiation of the human ML-1 myeloid leukemia cell line from an immature myeloid state to mature macrophages or granulocytes. The immature cells expressed a p110 SHIP isoform primarily (e.g., SHIPδ), whereas the mature cells expressed mostly SHIPα and SHIPβ. This expression pattern also was observed in murine bone marrow cells and mature macrophages derived from these bone marrow cells (Lucas and Rohrschneider 1999). These results indicate complex splicing events for SHIP expression during hematopoietic cell development, with potentially different functions for each isoform and cell lineage.

Many reports have demonstrated *SHIP* mRNA expression in tissues such as spleen, testis, liver, lung, and brain by Northern blot analysis. This method of analysis is prone to contaminations with blood cells and should also be combined with histochemical detection. Q. Liu et al. (1998) performed both analyses and demonstrated SHIP expression primarily in cells of the blood and testes. Within the testes, SHIP-positive cells were restricted to the spermatids and localized to the cell membrane. The function of SHIP in spermatogenesis is not yet known.

SHIP enzymatic activity

Inositol 5′-phosphatase

The central enzymatic domain of SHIP was identified by its sequence similarity to previously identified inositol phosphatases and is tightly conserved (96% identical) between murine and human SHIP (Ware et al. 1996; Geier et al. 1997). Its enzymatic activity removes the phosphate group from the 5′ position of both phosphatidylinositol 3,4,5-trisphosphate [PI(3,4,5)P3] and 1,3,4,5-tetrakisphosphates (IP_4) (Damen et al. 1996; Lioubin et al. 1996). The 3′ position of the inositol phospholipid must be phosphorylated before SHIP can dephosphorylate the 5′ position (Damen et al. 1996) suggesting that SHIP acts sequentially with phosphatidylinositol 3′ kinase (PI3′K) in an inositol phospholipid pathway. This 5′-phosphatase activity is not regulated by tyrosine phosphorylation or interaction with adaptor proteins. Rather, it is believed that localization is the determining factor in its

mechanism of action. Upon cell stimulation with a growth factor, cytoplasmic SHIP is transported to sites near the lipid substrates at the plasma membrane.

Most assays for SHIP enzymatic activity have been in vitro. However, when inositol phospholipids have been quantified from cells either lacking SHIP or induced for tyrosine phosphorylation of SHIP, the results have consistently supported the in vivo role for SHIP in the conversion of PI(3,4,5)P3 to PI(3,4)P2 (Giuriato et al. 1997; Scharenberg et al. 1998; Gupta et al. 1999; Huber et al. 1999; Liu et al. 1999).

SHIP homologs

SHIP belongs to a family of inositolpolyphosphate phosphatases, comprised of two major classes: the general class of inositol phosphatases and the more closely related SH2-containing 5′-phosphatases. The former class of general inositol phosphatases can be subdivided further into those proteins removing phosphate from positions other than the 5′ position on the inositol ring, and a more related group composed of inositol 5′-phosphatases only (Majerus et al. 1999). All inositol 5′-phosphatases (including SHIP and SHIP2) contain two main amino acid sequence motifs defining this class of enzymes. Thus, the SHIP family tree shows the closest relationship to other SH2-containing inositol 5′-phosphatases, followed by the general class of inositol 5′-phosphatases (lacking an SH2 domain), and finally, all other inositol phosphatases removing phosphate from positions not including 5′ on the inositol ring. The SHIP homologs and their relationships will be discussed in order of descending relationship to SHIP itself.

The closest relative to SHIP is called SHIP2, and both proteins contain the same major structural features and exhibit an overlapping tissue expression pattern (Pesesse et al. 1997; Wisniewski et al. 1999). SHIP2 was originally cloned as a product potentially complementing the Fanconi anemia group A gene defect (Hejna et al. 1995), but the SH2 domain was not included in this clone. This gene product was called 51C. Interestingly, one strategy for the original cloning of SHIP employed the PTB domain of Shc to recognize tyrosine-phosphorylated target proteins from myeloid cells. In addition to SHIP itself, the 51C protein was identified as a Shc PTB domain target in the same screen (Lioubin et al. 1996). Subsequent work with myeloid cells identified the complete cDNA for 51C and renamed the product SHIP2 (Pesesse et al. 1997; Wisniewski et al. 1999).

The SHIP2 protein exhibits highest amino acid identity to SHIP: ~38% overall identity. The highest identity occurs within the 5′-phosphatase domains (64%), with slightly less identity in the amino-terminal SH2 domains (54%). The carboxy-terminal region of SHIP2 exhibits even less identity; however, all of the sequence motif hallmarks of SHIP are present including numerous polyproline regions (perhaps eight) for potential SH3-domain binding, and a single NPXY motif, which no doubt accounts for Shc binding through its PTB domain. SHIP2 protein is observed as a 155-kD protein on polyacrylamide gels, and it is not known whether the 160-kD protein seen in some SHIP preparations represents antigenic cross-reactivity with SHIP2. Despite their similarities, important differences between these two proteins have been identified. First, although SHIP's expression is restricted to hematopoietic and spermatogenic cells, SHIP2 expression is much more ubiquitous with primary expression not only in blood cells (Pesesse et al. 1997; Bruyns et al. 1999) but also in skeletal muscle, heart, placenta, and pancreas. Second, although enzymatic activity of both SHIP homologs requires that its phosphoinositide substrate have the 3′ position phosphorylated, presumably by PI3′K, 5′-phosphatase assays demonstrate that these two proteins exhibit different substrate specificity. Only SHIP removes the 5′ phosphate from both PI(3,4,5)P3 and the soluble Ins(1,3,4,5)P_4; whereas SHIP2 utilizes the PI(3,4,5)P3 substrate only (Wisniewski et al. 1999). These data suggest that SHIP and SHIP2 may not be completely redundant in function and that, even when expressed in the same cell, each may either regulate different pathways of inositide metabolism or interact differently with downstream effector proteins.

The presence of one close SHIP homolog suggests that others may yet exist. The existence of additional homologs is plausible considering the ubiquitous distribution of PI3′K, phosphoinositol lipids, and the necessity of their metabolism; however, more distantly related 5′-phosphatases could perform some of these functions. At present, evidence for the presence of only one additional potential SHIP homolog in insulin-stimulated CHO cells is available (Guilherme et al. 1996).

Moving down the SHIP homology and function scale, we come to the ubiquitously expressed inositol 5′-phosphatases synaptojanin 1 and 2, the X-linked OCRL (oculocerebrorenal-Lowe's) syndrome 5′-phosphatase, and the platelet type II enzyme with similar specificity. The grouping of these enzymes is determined both by lack of an SH2 domain and the presence of 5′-phosphatase enzymatic activity. In this class, however, the substrate does not need to be phosphorylated at the 3′ position of the inositol ring (and is therefore PI3′K independent). The synaptojanins are thought to be involved in synaptic vesicle trafficking and form complexes with dynamin and amphiphysin to promote vesicle recycling (Cremona et al. 1999; McPherson et al. 1996; Chung et al. 1997b; Nemoto et al. 1997). Both synaptojanins 1 and 2 have brain-specific and ubiquitously expressed isoforms (McPherson et al. 1996; Khvotchev and Südhof 1998); like SHIP, both are subject to tissue-specific alternative splicing, which alters the carboxy-terminal region of the protein (Seet et al. 1998; Nemoto and De Camilli 1999). In addition to the inositol phosphatase activity, the synaptojanins also possess a carboxy-terminal proline-rich region allowing interaction with SH3 domains. These multiple synaptojanin forms present an intriguing parallel to SHIP, but their biological function is clearly distinct.

The two additional members of this class, the OCRL/IP5P and type II IP5P, display 44%–52% similarity to

SHIP in the catalytic domain but are divergent outside this region and lack the protein–protein interaction motifs found on SHIP (Attree et al. 1992; Lioubin et al. 1996). The OCRL protein is an interesting example of a lipid metabolizing enzyme whose defect leads to an abnormal phenotype in humans: namely, OCRL syndrome characterized by renal failure, mental retardation, and blindness (Kawano et al. 1998). The OCRL protein is expressed broadly, but as the name implies, defects in the X-linked human OCRL gene (destroying the 5′-phosphatase activity) affect primarily lens, brain, and kidney cells. Cells from OCRL patients still express active type II inositol 5′-phosphatase but accumulate PI(4,5)P2. These results suggest the strong compartmentalization of 5′-phosphatases and the importance of inositol lipids in cell physiology.

Much farther down the SHIP homology scale are found a range of inositol phosphatases hydrolyzing the phosphate at positions of the inositol ring not including 5′. Many are not well characterized but include those phosphatases acting on the 1, 3, or 4 positions of the phosphorylated inositol ring. Inositol phosphatases in this class have very little sequence identity to SHIP: however, in this instance, the importance of sequence identity is superceded by other considerations. For example, members of this class of phosphatases probably operate in the same lipid-metabolizing pathway as SHIP. The inositol polyphosphate 4-phosphatases function in a group that metabolize PI(3,4)P2, the lipid product produced by SHIP and its substrate PI(3,4,5)P3 (Norris et al. 1995, 1997). Another member of this group is the tumor suppressor protein PTEN (for review, see Maehama and Dixon 1999). The phosphatase activity of PTEN removes the phosphate at the 3′ position from PI(3,4,5)P3, producing PI(4,5)P2. Like SHIP, PTEN's substrate requires phosphorylation by PI3′K, but unlike SHIP, the net effect is the apparent reversal of PI3′K enzymatic activity. Interestingly, even though the 4-phosphatase and PTEN remove phosphate from different sites on the inositol ring, both have the same amino acid sequence motif at the active site, $C(X)_5R$ (Zhang et al. 1994; Zhou et al. 1994; Fauman and Saper 1996). SHIP and SHIP2, exhibiting little overall sequence relationship to the 4-phosphatase or PTEN, both contain, in addition to the two signature motifs for the 5′-phosphatase family (Majerus et al. 1999), the related amino acid sequence motif $C(X)_5K$. The second signature motif is probably the phosphatase active site and the $C(X)_5K$ motif may be part of that active site. It is not known whether the additional $C(X)_5K$ motif has any role in the 5′-phosphatase enzymatic activity.

Analysis of genomic sequencing databases have revealed no identifiable nonmammalian homologs of SHIP. Members of the 5′-inositol phosphatase family have been found in *Caenorhabditis elegans* and *Drosophila melanogaster*; however, these sequences lack the protein–protein interaction motifs that make the SHIP protein unique. The lack of close SHIP homologs in these organisms suggests that SHIP may be a late evolutionary modification.

SHIP interactions with other proteins

As described above, the protein structure of SHIP contains numerous recognizable protein–protein interaction motifs. As in any signaling pathway, the function of SHIP must depend on its interaction with other upstream proteins, as well as downstream effector proteins and potential regulatory interactions. The observation that the different isoforms of SHIP either delete or otherwise modify these motifs further suggests that these regions play important individual roles in guiding the function of SHIP and that this function can be tailored by expressing these different isoforms. The following is an examination of the known and potential protein binding partners interacting with SHIP.

ITIM/ITAM motifs

The amino-terminal SHIP SH2 domain binds to phosphotyrosine residues and is a key feature mediating the interactions of numerous signal transduction proteins. A screen of a degenerate phosphopeptide library has shown a SHIP SH2 domain preference for a pY(Y/D)X(L/I/V) motif on target proteins (Osborne et al. 1996). This target motif matches sequences found in the so-called immmunoreceptor tyrosine-based activation motif (ITAM, $YXXLX_{6-8}YXXL$ in single-letter amino acid code) and the immunoreceptor tyrosine inhibition motif [ITIM, (V/I)XYXX(L/V)] (for review, see Unkeless and Jin 1997). During B-cell activation, the ITAM located on the cytoplasmic tail of the B-cell receptor (BCR) becomes phosphorylated on tyrosine and coordinates a proliferative signal in response to engagement and coclustering of BCRs by soluble-immunoglobulin bound to antigen (Kurosaki 1999). This is a critical first step in positive activation of naive B cells. Negative signaling in B cells is mediated by the FcγRIIB receptor. The binding of the SHIP SH2 domain to the ITIM motif of FcγRIIB is an important component of this negative signaling (Ono et al. 1996; Tridandapani et al. 1997; Coggeshall 1998) and will be discussed in greater detail below.

The ITIM motif is a component of the killer cell inhibitor receptors (KIR) found on natural killer (NK) and T cells (for review, see Saito 1998) and the KIR-like receptor gp49B1 on mast cells (Kuroiwa et al. 1998). However, whereas SHIP does not bind the ITIM of the KIR on NK cells (Gupta et al. 1997; Vély et al. 1997), it does bind the ITIM motif of gp49B1. Interestingly, gp49B1 contains two ITIM motifs, and SHIP displays a preference for binding to the ITIM proximal to the carboxyl side of the receptor. Additionally, the platelet cell endothelial adhesion molecule 1 (PECAM-1 or CD31) also contains two ITIM motifs, and SHIP has been shown to have preferential binding to just one of these. Therefore, it appears that the binding of the SHIP SH2 domain to ITIM sequences is not promiscuous and is possibly restricted by additional amino acid residues outside the ITIM motif unique to each protein.

The SH2 domain of SHIP also binds to ITAM motifs of the FcγRIIa and FcγRI-associated γ chain on monocytes

(Maresco et al. 1999), the FcεRIγ chain on mast cells, the CD3 complex, and the T-cell receptor ζ chain (Osborne et al. 1996). However, these interactions have only been suggested through in vitro binding studies. With the exception of SHIP binding to FcγRI (discussed in detail below) the biological relevance of these interactions with ITAM-containing receptors is unknown.

SHP-2

The protein tyrosine phosphatase SHP-2 has been reported to interact with the SH2 domain of SHIP (Sattler et al. 1997; L. Liu et al. 1997b). In one of these reports, it was demonstrated that IL-3 stimulation of B6SUtA1 cells results in the coimmunoprecipitation of SHIP and SHP-2 and that the SHIP SH2 domain alone was able to precipitate SHP-2 from cell lysates. As with other studies of this type, these data do not completely rule out the possibility that this association could be indirect and mediated by other molecules. Regardless of how the interaction takes place, both reports suggest that the association of SHIP with SHP-2 is exclusive of the well-described SHIP–Shc interaction. Furthermore, the oncogene *BCR–ABL* shifts the association in favor of the SHIP–SHP-2 complex, in which *BCR–ABL* also participates (Sattler et al. 1997). SHIP is rapidly tyrosine phosphorylated and dephosphorylated following growth factor stimulation, and the potential significance of the SHIP–SHP-2 interaction may reside in the possibility that SHP-2 is responsible for the observed dephosphorylation of SHIP or a protein associated with SHIP.

Gab family proteins

Gab family members, including Gab1 and Gab2 in mammalian cells and DOS in *Drosophila*, are scaffolding proteins that participate in many signaling pathways activated by various cytokines and growth factors (for review, see Huyer and Alexander 1999). These molecules contain an amino-terminal pleckstrin homology (PH) domain, a central proline-rich domain and multiple tyrosine phosphorylation sites spanning the length of the protein, which act as docking sites for the SH2 domain-containing proteins. Direct associations of Gab family members with Grb2, p85-subunit of PI3-kinase and the tyrosine phosphatase SHP-2 have been found in diverse signaling pathways (Holgado-Madruga et al. 1996; Carlberg and Rohrschneider 1997; Gu et al. 1998; Nishida et al. 1999). Recently, it was found that SHIP can also form complexes with Gab family members. An association of SHIP with Gab1 and Gab2 was detected in EPO-stimulated UT-7 cells and M-CSF-stimulated FD/fms cells, respectively (Lecoq-Lafon et al. 1999; Y. Liu, B.J. Jenkins, and L.R. Rohrschneider, in prep.). The interactions between SHIP and tyrosine phosphorylated Gab family members are presumably through the SH2 domain of SHIP. In support of this hypothesis, we found that a GST-fusion protein of the SHIP- SH2 domain is sufficient to pull down Gab2 after M-CSF stimulation in FD/fms cells (Y. Liu, B.J. Jenkins, and L.R. Rohrschneider, in prep.). However, it is still not clear whether the interactions are direct or through proteins such as Grb2, p85/PI3'K, or SHP-2. More experiments, including in vitro binding assay and mutant analyses, are required to address this question and, more importantly, to explore the functional significance of the interaction between these two interesting molecules.

Shc and Grb2

Shc and Grb2 are ubiquitously expressed adaptor proteins, first identified as important mediators of growth factor receptor signaling through the Ras/MAPK pathway (Rozakis-Adcock et al. 1992; for review, see Lewis et al. 1998). The SH3 domain of Grb2 presumably interacts with one of the polyproline motifs in the SHIP carboxyl terminus (Damen et al. 1996), and the PTB domain of Shc binds to the tyrosine-phosphorylated NPXY motifs in SHIP (Lamkin et al. 1997). In vitro pull-down experiments using GST fused to the SHIP SH2 domain and synthetic phosphopeptides provide evidence that tyrosine-phosphorylated Shc can also bind to the SHIP SH2 domain directly (L. Liu et al. 1997a; Pradhan and Coggeshall 1997; Tridandapani et al. 1999). In vivo data support this model of SHIP–Shc interaction because experiments show that SHIP mutated at the SH2 domain is incapable of coimmunoprecipitaing Shc from a murine hematopoietic cell line, whereas wild-type SHIP can (L. Liu et al. 1997a). However, the interpretation of this work is difficult, as the mutated SHIP also fails to become tyrosine phosphorylated in response to IL-3 stimulation like wild-type SHIP. Therefore, the decrease in Shc binding may arise due to decreased phosphorylation of the SHIP NPXY motifs mediating Shc PTB domain binding and may not represent a direct interaction with the SH2 domain.

Mechanistically, it would seem unnecessary for SHIP to bind to Shc through both the SH2 domain and the NPXY motifs. However, Tridandapani et al. (1999) have observed that isolates of FcγRIIB contain SHIP but not Shc, whereas isolates of Shc contain SHIP but not FcγRIIB. This suggests that Shc binding is somehow excluded from SHIP binding when the SHIP SH2 domain is engaged to FcγRIIB. From this work, Tridandapani et al. have proposed a model for FcγRIIB-mediated signaling in which the SH2 domain of SHIP first engages the FcγRIIB. SHIP is then phosphorylated at the NPXY motifs by an undefined kinase, and the PTB domain of Shc interacts with SHIP. Shc then becomes tyrosine phosphorylated itself (Ingham et al. 1999), promoting the interaction of the SHIP SH2 domain with Shc. This would sever the interaction of SHIP with FcγRIIB through the SHIP SH2 domain and thereby remove SHIP activity at the receptor. This is an intriguing hypothesis, and clearly, the interaction of the SH2 domain of SHIP and Shc demands further investigation.

Shc is also a ligand for Grb2, with the SH2 domains of Grb2 binding to phosphorylated tyrosine residues on Shc. This situation raises several questions. Do SHIP,

Shc, and Grb2 form a heterotrimeric complex, or does the binding of just two of these molecules preclude the binding of the third member? Data from Harmer and DeFranco (1999), employing a Grb2-deficient cell line, suggest that efficient binding of SHIP and Shc requires Grb2, in a situation analogous to the Sos/Shc/Grb2 complex formation. Shc and Grb2 together form a complex with Sos as part of the Ras/MAPK pathway. The binding of SHIP to Shc and Grb2 may interfere with the Sos/Shc/Grb2 complex formation and subsequently block activation of the Ras pathway. FcγRII-mediated negative signaling in B cells is associated with a decrease in Ras activation accompanied by a decrease in Shc/Grb2/Sos formation (Tridandapani et al. 1997). Whether SHIP may be involved in this function by acting as a competitor for Shc/Grb2 binding versus Sos is unclear. Activation of the MAPK cascade seems unaffected in chicken B cells that do not express SHIP (Okada et al. 1998). Additionally, although microinjection of SHIP into *Xenopus* oocytes blocks activation of the MAPK pathway induced by insulin, injection of a catalytically inactive SHIP does not, suggesting that this inhibition is dependent on the inositol phosphatase domain of SHIP and not any portions of SHIP mediating Shc and Grb2 interactions (Deuter-Reinhard et al. 1997).

Perhaps the simplest explanation for why SHIP binds Shc and Grb2 is because these adaptors serve to localize SHIP to various destinations inside the cell. Shc and Grb2 are known to interact with a variety of membrane-bound proteins; therefore, SHIP may employ interactions via these adapters to become localized to the cell membrane, where the substrates for its catalytic activity reside. Alternatively, the combination of Shc and Grb2 is linked to not only Sos and SHIP, but also to the Gab family of proteins and numerous growth factor receptors. This suggests that Shc and Grb2 together may be involved in a common, perhaps universal, mechanistic step, which is currently not appreciated.

PI3′K

PI3′K, the enzyme responsible for PI(3,4,5)P3 production, is a heterodimer of a 85-kD regulatory subunit and a 110-kD catalytic subunit. The p85 subunit of PI3′K contains two SH2 domains, both with similar binding specificity [pY-(M/V/I/E)-x-M] when tested against tyrosine-phosphorylated peptide motifs in vitro (Felder et al. 1993; Songyang et al. 1993). Interestingly, a p85 SH2-domain recognition motif is present in SHIP as the sequences immediately adjacent to the tyrosine of the first NPXY motif (i.e., NPXpYIGM). Experiments using a GST–p85 SH2 fusion protein show that this domain binds to full-length tyrosine-phosphorylated SHIP, but not to nonphosphorylated SHIP (Gupta et al. 1999; Lucas and Rohrschneider 1999). The SHIPβ isoform retains the NPXpY motif, but the upstream splice junction near the 3′ side of this motif disrupts the potential p85 SH2-domain binding motif by changing the amino acid sequence to NPXpYIAN. The sequence alteration in this motif results in the decreased ability of the p85 SH2 domain binding to SHIPβ. The association of p85/PI3′K with SHIP could represent an interesting complex of enzymes favoring the conversion of PI(4,5)P2 to PI(3,4,5)P3, and finally, PI(3,4)P2. Such conversion may be important in signaling for the membrane localization, or turnover of various PH domain-containing proteins. On the other hand, the human SHIP protein contains a slightly different motif at this site and its association with p85 has not been tested. Support for the biological significance of the SHIP–p85/PI3′K interaction would be greatly enhanced if p85 were also found to interact with the human SHIP.

PIAS1 interaction with SHIP

In our laboratory, the carboxyl tail of SHIP was used as bait in a yeast two-hybrid screen to look for murine hematopoietic-cell proteins interacting with the SHIP tail. No exogenous protein kinase activity was incorporated into the screen, and it was therefore anticipated that target proteins might contain SH3 domains or interact with the SHIP carboxyl tail via other nonphosphorylated amino acid sequences. The screen identified five interacting proteins; three of these each contained at least one SH3 domain. Not surprisingly, Grb2 was one of these proteins. Two additional SH3 domain-containing adaptor proteins were obtained, one of which was novel. Also identified in the same screen was an interaction between SHIP and a protein inhibitor of STAT1 called PIAS1 (protein inhibitor of activated STAT1) (B. Liu et al. 1998). Biochemical analyses have demonstrated that SHIP and PIAS1 interact constitutively in the unstimulated monocytic precursor cell line FD/Fms (J.F. Fuller and L.R. Rohrschneider, in prep.). Furthermore, PIAS1 interacts directly with the nonphosphorylated carboxyl terminus of SHIP, and conversely, SHIP interacts only with PIAS1 and not the PIAS3 homolog (Chung et al. 1997a). Given the large number of protein interaction sites within the SHIP carboxyl terminus, further effector or regulatory proteins of SHIP inteacting with this domain are likely to be identified.

DAB-1

The neuronal protein Dab-1 binds via its PTB domain to the NPXY motifs on SHIP in vitro (Howell et al. 1999). Dab-1 is expressed in both neuronal and hematopoietic cells and could interact with SHIP in the blood cells. Dab-1 binds both membrane inositol phospholipids and transmembrane receptors in neuronal cells, and thus may link receptor signaling with phosphatidylinositol polyphosphate metabolism. A physical interaction between SHIP and Dab-1 in vivo has not been reported; although an association would be interesting, it remains speculative.

General biology of SHIP proteins

SHIP is tyrosine phosphorylated and participates in signaling by a large number of hematopoietic growth fac-

tors and cytokines. Despite this contribution to very early events in apparent positive growth factor signaling, overexpression studies of p145 SHIP in myeloid cell lines indicated a negative role for SHIP in cell growth (Lioubin et al. 1996), and apoptosis was detected in some SHIP-overexpressing cell lines (L. Liu et al. 1997a). A negative role for SHIP signaling also has been described in B cells (Chacko et al. 1996; Ono et al. 1996; Kiener et al. 1997); however, the biochemical nature for the signaling in the hematopoietic cell types varies considerably. One must therefore wonder whether SHIP interactions are cell-type specific, or whether the differences indicate that the details are yet incomplete.

Gene-targeted knockout of *SHIP* in mice (Helgason et al. 1998; Liu et al. 1999) results in animals that are viable and fertile, but the life span of the homozygous-null animals is decreased due to myeloid cell infiltration of vital organs. Within the *SHIP*-null animals, a chronic progressive hyperplasia of the granulocytes and macrophages is observed, perhaps at the expense of B-cell production, whereas erythroid cell numbers show little or no change from the *SHIP* wild-type mice. The increased myeloid cell proliferation in the *SHIP*-null mice is associated with both increased PI(3,4,5)P3 production and the wortmannin-sensitive activation of serine/threonine kinase Akt/PKB. These cells are also less sensitive to apoptosis. Therefore, the most pronounced role for SHIP is in maintaining balanced growth regulation for specific myeloid cells, perhaps through governing the levels of growth-stimulated PI(3,4,5)P3 and the subsequent activation of Akt/PKB. In the lymphoid cell compartment, the B-cell numbers are also affected by SHIP deficiency, but whether this results from a direct or indirect effect of SHIP is not clear.

SHIP and PTEN

The role of SHIP in the enzymatic conversion of PI(3,4,5)P3 to PI(3,4)P2 stimulates the question of whether SHIP is a tumor suppressor like the PTEN protein, which utilizes the same lipid substrate but produces a different lipid product, PI(4,5)P2. Two lines of evidence indicate that SHIP is clearly not a tumor suppressor. First, the PTEN protein is encoded by a chromosomal location (10p23.3) associated in humans with an increased cancer incidence due to abnormalities and loss of heterozygosity (Li et al. 1997; Steck et al. 1997). The human SHIP protein is encoded by a locus (2q36–q37) in which the occasional overt defects (i.e., large deletions) exhibit only sporadic association with tumor formation (Geier et al. 1997). Second, whereas mice heterozygous for a functionally defective *PTEN* allele incur an increased cancer incidence (exacerbated by sublethal radiation) (Di Cristofano et al. 1998; Suzuki et al. 1998; Podsypanina et al. 1999), mice heterozygous for *SHIP* loss are virtually normal (Helgason et al. 1998; Liu et al. 1999). Even the homozygous *SHIP*-null mice do not have an increased susceptibility to cancer; however, the myeloproliferative disorder resulting in a decreased life span may preclude complete assessment of susceptibility changes to cancer in these animals. Nevertheless, despite the fact that SHIP is a negative regulator of cell growth, none of the main hallmarks of tumor suppressor activity indicate that SHIP's function falls within this category.

A more interesting question is why SHIP is not a tumor suppressor like PTEN, as they both have a common lipid substrate—PI(3,4,5)P3. Part of the answer may be obtained from comparison of knockout animals for each gene: $PTEN^{-/-}$ mice exhibit a much more severe phenotype than $SHIP^{-/-}$ mice do. The former knockout result in embryonic lethality, whereas the latter mice are physically almost indistinguishable from wild-type mice (but with a shorter life span as discussed above). There are two possibilities for this difference in biological activity. One, the pathology in $SHIP^{-/-}$ mice may not be as severe as expected because a SHIP homolog compensates for the loss. The SHIP2 protein is a logical candidate because it too is expressed in blood cells (Pesesse et al. 1997; Wisniewski et al. 1999). Second, the PTEN protein may have a more critical role than SHIP in cell growth and development. Perhaps PTEN performs some additional functions, not overlapping with those of SHIP, thus accounting for the activities of tumor suppression and embryonic lethality. It is not possible to distinguish between these possibilities at present.

Summary of SHIP interactions and possible functions

The overriding theme for SHIP function has consistently emphasized its negative regulatory role in cell growth and development. SHIP does not appear to be necessary for growth or differentiation per se; however, it has discernible effects on regulating these activities. The experimental specifics of the mechanism for this negative function differ depending upon the hematopoietic cell type and the portion of the SHIP protein under investigation. We will first describe the most prominent mechanisms uncovered for B-lineage cells, mast cells, and myeloid cells, and critically discuss the overall mechanisms.

B cells

Naive B cells have the innate capability of each expressing one of an extraordinarily large number ($\sim 10^{11}$) of antibody specificities on their cell surface encoded as the variable region of the BCR. With such a large antibody repertoire, some specificities will be directed against the individual harboring these B cells, whereas other specificities will be needed to fight infection by various invading microorganisms. B cells expressing BCRs with the former specificity must be eliminated, whereas B cells with the latter BCR specificity should be amplified to provide protection. This occurs through negative and positive selection of individual naive B cells, respectively.

The proposed positive and negative B-cell signaling

mechanisms are shown in Figure 3. Positive signaling is observed after BCR cross-linking with multivalent antigen (or Fab'_2 antibody with specificity for the BCR). Crucial steps in this signaling are PI3'K activation (Hippen et al. 1997; Kiener et al. 1997), with production of PI(3,4,5)P3 from the more abundant lipid, PI(4,5)P2. The PH domain of the nonreceptor tyrosine kinase, Btk, binds to PI(3,4,5)P3 with high affinity (Fukuda et al. 1996; Salim et al. 1996; Rameh et al. 1997) and the downstream phospholipid C γ2 (PLCγ2) becomes tyrosine phosphorylated and activated. The subsequent action of PLCγ2 on the lipid PI(4,5)P2 produces diacylglycerol and IP3, which activate PKC and induce release of Ca^{2+} from cytoplasmic stores, respectively. Each of these steps is essential for the positive signals because inhibitors or mutations in critical regions of these proteins eliminates the increased influx of intracellular Ca^{2+} and the positive signal for growth and further development (Kurosaki 1999).

The positive signal results in amplification of B cells expressing high-affinity antibodies beneficial to the host. However, if an individual B cell is producing a nonbeneficial antibody (e.g., directed against the host), that cell must be eliminated. In that case, the positive signal must be attenuated, and that mechanism is shown in the gray-shaded area of Figure 3. The negative signal is initiated by cross-linking the BCR with the primarily B cell-specific isotype of the FcγRII receptor (e.g., FcγRIIB1). Cross-linking is achieved in vivo when the concentrations of antigen and antibody approach equivalence. In vitro this is achieved by exposure of B cells to intact IgG with immune specificity for the BCR (the Fc portion of the IgG then naturally attaches to the FcγRII). The FcγRIIB1 receptor contains an immunoreceptor tyrosine-based inhibitory motif (ITIM) in its short 62-amino-acid cytoplasmic tail, and tyrosine phosphorylation of the tail region, by a kinase such as Lyn, marks a docking site for the amino-terminal SHIP SH2 domain. Thus, the constitutively active phosphatidylinositol 5'-phosphatase domain of SHIP is tethered to the cytoplasmic plasma membrane surface where its substrate [PI(3,4,5)P3] is being produced by the activated PI3'K. The SHIP enzymatic activity converts PI(3,4,5)P3 to PI(3,4)P2 and eliminates the higher affinity binding site for the PH domain of Btk (Salim et al. 1996; Bolland et al. 1998; Scharenberg et al. 1998). The disruption of the Btk PH domain interaction with the membrane appears sufficient to block positive signaling, because Btk-deficient cells lack the positive response (induced by BCR cross-linking and measured by increased Ca^{2+} influx and growth stimulation) (Rawlings and Witte 1994; Fluckiger et al. 1998). The positive signal can be reinstated in the Btk-deficient cells by introduction of a wild-type Btk (Fluckiger et al. 1998). Furthermore, spontaneous mutations in broad regions encoding the Btk protein that arise in both humans and mice result in X-linked agammaglobulinemia, a disease characterized by failure of positive B-cell signaling. Individual mutations in the Btk PH domain alone are sufficient to abrogate the positive growth signal (Conley and Rohrer 1995; Rawlings and Witte 1995). Therefore, the positive signal for B-cell growth and development induced by BCR cross-linking, is substantially attenuated upon coligation of the BCR with FcγRIIB1. The inositol 5'-phosphatase enzymatic activity of SHIP, tethered to the Fc receptor, depletes the intracellular membrane surface of the $PI(3,4,5)P_3$ needed for Btk activation. The Ca^{2+} influx from intracellular sources is prevented and these B cells do not proliferate or develop further.

This mechanism may be close to the truth, but the overall picture is incomplete. The SHIP 5'-phosphatase activity is required for attenuating the positive Ca^{2+} influx in B-cell signal (Ono et al. 1997), but other domains of SHIP also may be required. For example, the carboxyl terminus of SHIP has the potential for interacting with many different proteins, but its role in negative signaling has not been examined. Perhaps a block in the Ca^{2+} in-

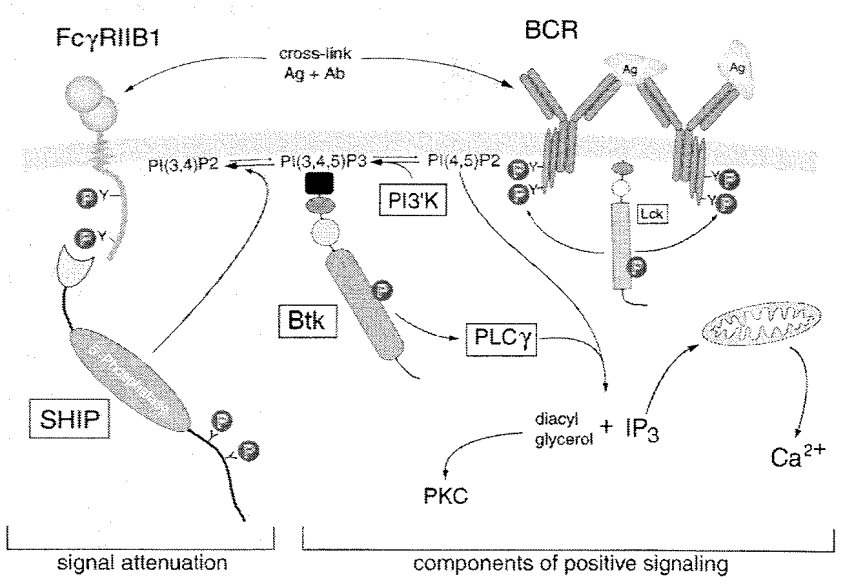

Figure 3. Role of SHIP in B-cell negative signaling. Positive signals for B-cell growth and development are triggered by cross-linking the BCR and are shown in the *right* side. Resultant activation of PI3'K produces the lipid PI(3,4,5)P3, a high-affinity ligand for the PH domain of the tyrosine kinase Btk. The activation of Btk leads to cytolpasmic influx of Ca^{2+} from intracellular sources, ultimately resulting in growth and further B-cell development. The positive signal is attenuated greatly by the events shown within the gray-shaded area. Cross-linking the BCR to the FcγRIIB receptor at the cell surface begins the process that preempts the activation signal. The SHIP protein binds to a tyrosine-phosphorylated motif in the cytoplasmic sequence of the FcγRIIB via its SH2 domain and converts PI(3,4,5)P3 to PI(3,4)P2 at the membrane activation sites. The loss of PI(3,4,5)P3 is believed to prevent Btk activation; and thus, both intracellular Ca^{2+} influx and growth are attenuated.

flux due to the SHIP 5′-phosphatase domain, plus additional negative activities are needed for a complete block in B-cell development. A good example of an additional negative signaling protein that may participate in this process is the Dok protein. Dok contributes to B cell-negative signaling but does not affect Ca^{2+} influx and therefore could contribute other negative functions (Yamanashi et al. 2000).

Myeloid cells (mast cells, neutrophils, macrophages, and their progenitors)

Mast cells provide an early line of defense against invading organisms or allergens. The release of a defensive mixture of molecules, stored in cytoplasmic granules, is triggered in these cells by immune complexes of monomeric IgE cross-linking the high-affinity cell-surface IgE receptor, FcγRI. This receptor is comprised of three subunit proteins, two of which contain ITAM motifs in their short (<50 amino acid) cytoplasmic tail. Like the FcγRIIB1 receptor in B cells, the tyrosine-phosphorylated cytoplasmic region of the FcεRI receptor on mast cells also binds the SH2 domain of SHIP upon aggregation (Osborne et al. 1996; Kimura et al. 1997). The mast cells undergo a large cytoplasmic Ca^{2+} influx, which presumably triggers, at least in part, the degranulation and release of defensive molecules. Mast cells, derived from *SHIP*$^{+/+}$ mouse bone marrow, exhibit the Ca^{2+} influx, whereas those derived from *SHIP*$^{-/-}$ animals ehibit a more pronounced Ca^{2+} influx, especially subsequent to the initial spike of Ca^{2+} influx, suggesting a role of SHIP as the "gatekeeper" in setting the threshold for the overall signal (Huber et al. 1998). The exact mechanism for SHIP attenuation of the Ca^{2+} influx in mast cells has not been worked out, but aspects of the mechanism described for B cells might be presupposed.

In addition to the SHIP-regulated Ca^{2+} influx demonstrated in mast and B cells, other potential mechanisms of negative regulation have been described. The diagram in Figure 4A illustrates some of the interactions of SHIP within a generic myeloid cell. Cells from *SHIP*-null mice have been used to demonstrate the requirement for this protein in down-modulating a growth factor receptor-mediated Akt/PKB activation and survival signal in myeloid cells (Liu et al. 1999). IL-3 or GM-CSF stimulation of mast cells or neutrophils from *SHIP*$^{+/+}$ mice activates PI3′K producing PI(3,4,5)P3. The PH domain of Akt/PKB interacts with the new phospholipids and becomes activated by phosphorylation at Ser-473 and Thr-308 in a PI(3,4,5)P3-dependent manner. Subsequent phosphorylation of the Akt/PKB substrates occurs [e.g., proapoptic signaling protein (BAD) and glycogen synthese kinase-3 (GSK-3)] and cell survival is extended. The PTEN protein (as discussed above) may regulate the basal levels of PI(3,4,5)P3 (Myers et al. 1997). SHIP is proposed to regulate the growth factor induced levels of PI(3,4,5)P3, because mast cells from *SHIP*$^{-/-}$ animals exhibit greater Akt/PKB activation (measured by serine/threonine phosphoryaltion and GSK-3 phosphorylation), and it remains activated for extended times following IL-3 stimulation (Liu et al. 1999). *SHIP*$^{-/-}$ cells also exhibit an increased resistance to inducers of apoptosis, consistent with the role of Akt/PKB in this process. Additionally,

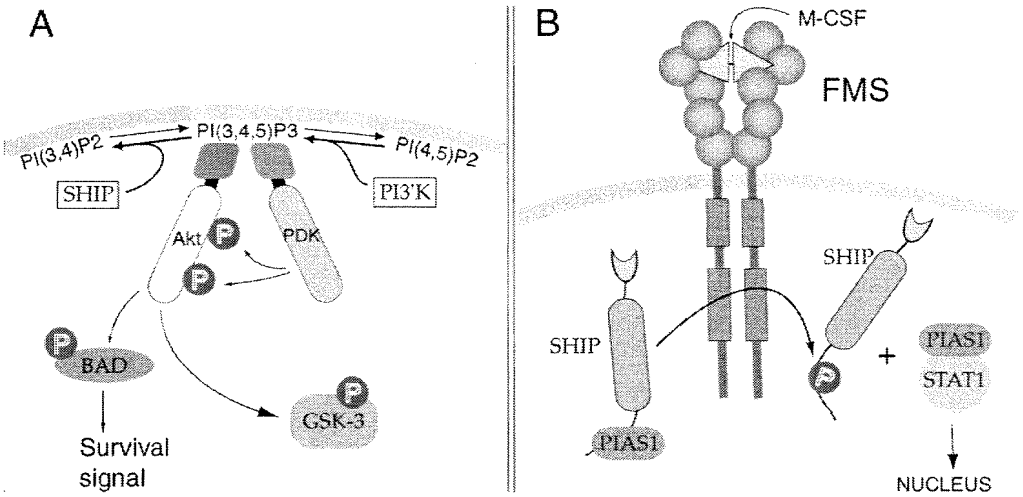

Figure 4. Negative regulation of cell growth and/or survival by SHIP may be achieved by different mechanisms. (*A*) Localized PI3′K activity, resulting from growth factor stimulation, produces the lipid PI(3,4,5)P3, which serves as a binding site for the PH domains of the Akt/PKB kinase, as well as the PDK1 kinase, which activates Akt/PKB. The continued survival signal depends on activated Akt/PKB and the presence of the PI(3,4,5)P3 lipid at the membrane. SHIP ablates the positive survival signal by metabolizing the PI(3,4,5)P3 to PI(3,4)P2, a form that presumably is unable to support activation Akt/PBK. (*B*) An alternative mechanism for SHIP signaling is illustrated with the M-CSF receptor FMS. Activation of FMS by its ligand, M-CSF, results in tyrosine phosphorylation of several cytoplasmic proteins. SHIP becomes tyrosine phosphorylated by a yet unknown kinase, at one or both of the carboxy-terminal NPXY motifs. PIAS1 interacts with the carboxyl terminus of the unphosphorylated SHIP and is released from SHIP upon tyrosine phosphorylation. PIAS1 is known to interact with STAT1 and may modify STAT1 transcription following M-CSF stimulation.

the PI3'K inhibitor wortmannin prevents PI(3,4,5)P3 accumulation and Akt/PKB activation, and sensitizes cells to apoptosis. These data indicate that PI3'K is essential for the resistance to apoptosis and Akt/PKB activation observed in *SHIP*$^{+/+}$ cells.

Phospholipids regulate Akt/PKB activation; however, this regulation is more complex than shown in Figure 4 because the PH domains of Akt/PKB and PDK1 can interact with either PI(3,4,5)P3 or PI(3,4)P2 in the activation process (Stephens et al. 1998). Therefore, the overall mechanism becomes more complex than shown. Considering additional variables associated with phospholipid metabolism, there is definitely more to be learned about this step.

The complex nature of PI(3,4,5)P3 in this overall process is also illustrated by the finding that in the B cell system, wortmannin also affected binding of the PH domain of Btk to this same lipid. SHIP also mediates the inhibition of Akt/PKB activation in B cells (Aman et al. 1998); therefore, activation of both Akt/PKB and Btk require binding to PI(3,4,5)P3 via their PH domains.

A distinct mechanism for SHIP's negative role in cell growth and development may utilize proteins binding to the carboxy-terminal sequences of SHIP. In FDC-P1 cells expressing an exogenous M-CSF receptor (FMS), M-CSF stimulation recapitulates most features of macrophage differentiation (Rohrschneider and Metcalf 1989). SHIP participates in the FMS signaling, and as described above, the PIAS1 protein was found to bind constitutively to the carboxyl terminus of SHIP in unstimulated cells. Interestingly, M-CSF stimulation resulted in SHIP tyrosine phosphorylation and decreased interaction between SHIP and PIAS1. The fate of PIAS1 in this system is not yet clear, but its specific interaction with activated STAT1 (B. Liu et al. 1998) suggests a role in transcriptional regulation. STAT1 is necessary for transcriptional activation of genes mediating innate immunity to viral disease (Durbin et al. 1996), and PIAS1 might modify that response. Thus, whereas the functions of SHIP described in Figures 3 and 4A rely primarily on the 5'-phosphatase enzymatic domain, the activity diagramed in Figure 4B depends on effector proteins attached to SHIP. The role of effector proteins in SHIP function has not been thoroughly explored but should provide additional clues for understanding the mechanisms of SHIP's negative functions.

Role of SHIP in human disease

Research on potential physiological roles of SHIP proteins in human maladies has, so far, yielded no direct connection with tumor suppression or tumor formation, as measured by over expression studies, mutational analysis, or examination of the SHIP chromosomal abnormalities associated with disease states. Results from the *SHIP* knockout studies in mice largely agree that SHIP deficiency in the blood cells results in myeloproliferation and hyper-responsiveness to growth factor stimulation. A similar spectrum of abnormalities is seen in *BCR–ABL*-induced transformation of mice, and Sattler et al. (1999) have exploited this relationship to show that *BCR–ABL*, a causative oncogene for chronic myelogenous leukemia (CML) in both humans and mice, inhibits expression of the SHIP protein. The kinase activity of BCR–ABL is necessary for the SHIP suppression because a chemical inhibitor of the ABL kinase activity restored SHIP expression. This same inhibitor (Novartis, CGP57148B) has now undergone clinical trials in humans, and the results indicate successful drug therapy against CML (B. Druker, pers. comm.). Although the role of SHIP in the CML drug therapy trial was not examined, these results raise the possibility of a more fundamental role for SHIP in regulating the preleukemic stages of disease formation. Examination of potential roles of SHIP in related disease states of blood cell formation may be worthwhile. Such disease states would include myeloproliferative disorders, polycythemia vera, agnogenic myeloid metaplasia, primary thrombocythemia, and chronic monocytic or neutrophilic leukemias.

Acknowledgments

This review represents the collective thinking of our laboratory; therefore, we apologize for omitting any alternative references or views. We greatly appreciate the comments, suggestions, and help from reviewers and numerous colleagues, as well as permission from Dr. Brian Druker to use clinical trial results before publication. Research in our laboratory was supported by the Fred Hutchinson Center and grants from the National Cancer Institute (CA20551 and CA4987). D.M.L. was supported in part by an NRSA fellowship (DK09774), and J.E.F. was supported by a training grant from the University of Washington (CA09437).

References

Aman, M.J., T.D. Lamkin, H. Okada, T. Kurosaki, and K.S. Ravichandran. 1998. The inositol phosphatase SHIP inhibits Akt/PKB activation in B cells. *J. Biol. Chem.* **273:** 33922–33928.

Attree, O., I.M. Olivos, I. Okabe, L.C. Bailey, D.L. Nelson, R.A. Lewis, R.R. McInnes, and R.L. Nussbaum. 1992. The Lowe's oculocerebrorenal syndrome gene encodes a protein highly homologous to inositol polyphosphate-5-phosphatase. *Nature* **358:** 239–242.

Bolland, S., R.N. Pearse, T. Kurosaki, and J.V. Ravetch. 1998. SHIP modulates immune receptor responses by regulating membrane association of Btk. *Immunity* **8:** 509–516.

Bruyns, C., X. Pesesse, C. Moreau, D. Blero, and C. Erneux. 1999. The two SH2-domain-containing inositol 5-phosphatases SHIP1 and SHIP2 are coexpressed in human T lymphocytes. *Biol. Chem.* **380:** 969–974.

Carlberg, K. and L.R. Rohrschneider. 1997. Characterization of a novel tyrosine phosphorylated 100 kDa protein that binds to SHP-2 and phosphatidylinositol 3'-kinase in hematopoietic cells. *J. Biol. Chem.* **272:** 15943–15950.

Chacko, G.W., S. Tridandapani, J.E. Damen, L. Liu, G. Krystal, and K.M. Coggeshall. 1996. Negative signaling in B lymphocytes induces tyrosine phosphorylation of the 145-kDa inositol polyphosphate 5-phosphatase, SHIP. *J. Immunol.* **157:** 2234–2238.

Chung, C.D., J. Liao, B. Liu, X. Rao, P. Jay, P. Berta, and K. Shuai.

1997a. Specific inhibition of Stat3 signal transduction by PIAS3. *Science* **278:** 1803–1805.

Chung, J.K., F. Sekiya, H.S. Kang, C. Lee, J.S. Han, S.R. Kim, Y.S. Bae, A.J. Morris, and S.G. Rhee. 1997b. Synaptojanin inhibition of phospholipase D activity by hydrolysis of phosphatidylinositol 4,5-bisphosphate. *J. Biol. Chem.* **272:** 15980–15985.

Coggeshall, K.M. 1998. Inhibitory signaling by B cell FcgRIIb. *Curr. Opin. Immunol.***10:** 306–312.

Conley, M.E. and J. Rohrer. 1995. The spectrum of mutations in Btk that cause X-linked agammaglobulinemia. *Clin. Immunol. Immunopathol.* **76:** S192–S197.

Cremona, O., G. Di Paolo, M.R. Wenk, A. Luthi, W.T. Kim, K. Takei, L. Daniell, Y. Nemoto, S.B. Shears, R.A. Flavell et al. 1999. Essential role of phosphoinositide metabolism in synaptic vesicle recycling. *Cell* **99:** 179–188.

Crowley, M.T., S.L. Harmer, and A.L. DeFranco. 1996. Activation-induced association of a 145-kDa tyrosine-phosphorylated protein with Shc and Syk in B lymphocytes and macrophages. *J. Biol. Chem.* **271:** 1145–1152.

Damen, J.E., L. Liu, R.L. Cutler, and G. Krystal. 1993. Erythropoietin stimulates the tyrosine phosphorylation of Shc and its association with Grb2 and a 145-Kd tyrosine phosphorylated protein. *Blood* **82:** 2296–2303.

Damen, J.E., L. Liu, P. Rosten, R.K. Humphries, A.B. Jefferson, P.W. Majerus, and G. Krystal. 1996. The 145-kDa protein induced to associate with Shc by multiple cytokines is an inositol tetraphosphate and phosphatidylinositol 3,4,5-trisphosphate 5-phosphatase. *Proc. Natl. Acad. Sci.* **93:** 1689–1693.

Damen, J.E., L. Liu, M.D. Ware, M. Ermolaeva, P.W. Majerus, and G. Krystal. 1998. Multiple forms of the SH2-containing inositol phosphatase, SHIP, are generated by C-terminal truncation. *Blood* **92:** 1199–1205.

Deuter-Reinhard, M., G. Apell, D. Pot, A. Klippel, L.T. Williams, and W.M. Kavanaugh. 1997. SIP/SHIP inhibits Xenopus oocyte maturation induced by insulin and phosphatidylinositol 3-kinase. *Mol. Cell. Biol.* **17:** 2559–2565.

Di Cristofano, A., B. Pesce, C. Cardon-Cardo, and P.P. Pandolfi. 1998. *Pten* is essential for embryonic development and tumour suppression. *Nat. Genet.* **19:** 348–355.

Drachman, J.G., J.D. Griffin, and K. Kaushansky. 1995. The c-Mpl ligand (thrombopoietin) stimulates tyrosine phosphorylation of Jak2, Shc, and c-Mpl. *J. Biol. Chem.* **270:** 4979–4982.

Drayer, A.L., X. Pesesse, F. De Smedt, R. Woscholski, P. Parker, and C. Erneux. 1996. Cloning and expression of a human placenta inositol 1,3,4,5-tetrakisphosphate and phosphatidylinositol 3,4,5-trisphosphate 5-phosphatase. *Biochem. Biophys. Res. Common.* **225:** 243–249.

Durbin, J.E., R. Hackenmiller, M.C. Simon, and D.E. Levy. 1996. Targeted disruption of the mouse *Stat1* gene results in compromised innate immunity to viral disease. *Cell* **84:** 443–450.

Fauman, E.B. and M.A. Saper. 1996. Structure and function of the protein tyrosine phosphatases. *Trends Biochem. Sci.* **21:** 413–417.

Felder, S., M. Zhou, P. Hu, J. Ureña, A. Ullrich, M. Chaudhuri, M. White, S.E. Shoelson, and J. Schlessinger. 1993. SH2 domains exhibit high-affinity binding to tyrosine-phosphorylated peptides yet also exhibit rapid dissociation and exchange. *Mol. Cell. Biol.* **13:** 1449–1455.

Fluckiger, A.-C., Z. Li, R.M. Kato, M.I. Wahl, H.D. Ochs, R. Longnecker, J.-P. Kinet, O.N. Witte, A.M. Scharenberg, and D.J. Rawlings. 1998. Btk/Tec kinases regulate sustained increases in intracellular Ca^{2+} following B-cell receptor activation. *EMBO J.* **17:** 1973–1985.

Fukuda, M., T. Kojima, H. Kabayama, and K. Mikoshiba. 1996. Mutation of the pleckstrin homology domain of Bruton's tyrosine kinase in immunodeficiency impaired inositol 1,3,4,5-tetrakisphosphate binding capacity. *J. Biol. Chem.* **271:** 30303–30306.

Geier, S.J., P.A. Algate, K. Carlberg, D. Flowers, C. Friedman, B. Trask, and L.R. Rohrschneider. 1997. The human SHIP gene is differentially expressed in cell lineages of the bone marrow and blood. *Blood* **89:** 1876–1885.

Giuriato, S., B. Payrastre, A.L. Drayer, M. Plantavid, R. Woscholski, P. Parker, C. Erneux, and H. Chap. 1997. Tyrosine phosphorylation and relocation of SHIP are integrin-mediated in thrombin-stimulated human blood platelets. *J. Biol. Chem.* **272:** 26857–26863.

Gu, H., J.C. Pratt, S.J. Burakoff, and B.G. Neel. 1998. Cloning of p97/Gab2, the major SHP2-binding protein in hematopoietic cells, reveals a novel pathway for cytokine-induced gene activation. *Mol. Cell* **2:** 729–740.

Guilherme, A., J.K. Klarlund, G. Krystal, and M.P. Czech. 1996. Regulation of phosphatidylinositol 3,4,5-trisphosphate 5'-phosphatase activity by insulin. *J. Biol. Chem.* **271:** 29533–29536.

Gupta, N., A.M. Scharenberg, D.N. Burshtyn, M.N. Lioubin, L.R. Rohrschneider, J.-P. Kinet, and E.O. Long. 1997. Negative signaling pathways of killer cell inhibitory receptors and FcγRIIb1 require distinct phosphatases. *J. Exp. Med.* **186:** 473–478.

Gupta, N., A.M. Scharenberg, D.A. Fruman, L.C. Cantley, J.-P. Kinet, and E.O. Long. 1999. The SH2 domain-containing inositol 5'-phosphatase (SHIP) recruits the p85 subunit of phosphoinositide 3-kinase during FcγRIIb1-mediated inhibition of B cell receptor signaling. *J. Biol. Chem.* **274:** 7489–7494.

Harmer, S.L. and A.L. DeFranco. 1999. The src homology domain 2-containing inositol phosphatase SHIP forms a ternary complex with Shc and Grb2 in antigen receptor-stimulated B lymphocytes. *J. Biol. Chem.* **274:** 12183–12191.

Hejna, J.A., H. Saito, L.S. Merkens, T.V. Tittle, P.M. Jakobs, M.A. Whitney, M. Grompe, A.S. Friedberg, and R.E. Moses. 1995. Cloning and characterization of a human cDNA (INPPL1) sharing homology with inositol polyphosphate phosphatases. *Genomics* **29:** 285–287.

Helgason, C.D., J.E. Damen, P. Rosten, R. Grewal, P. Sorenson, S.M. Chappel, A. Borowski, F. Jirik, G. Krystal, and R.K. Humphries. 1998. Targeted disruption of *SHIP* leads to hemopoietic perturbations, lung pathology, and a shortened life span. *Genes & Dev.* **12:** 1610–1620.

Hippen, K.L., A.M. Buhl, D. D'Ambrosio, K. Nakamura, C. Persin, and J.C. Cambier. 1997. FcγRIIb11 inhibtion of BCR mediated phosphoinositide hydrolysis and Ca^{2+} mobilization is integrated by CD19 dephosphorylation. *Immunity* **7:** 49–58.

Holgado-Madruga, M., D.R. Emlet, D.K. Moscatello, A.K. Godwin, and A.J. Wong. 1996. A Grb2-associated docking protein in EGF- and insulin-receptor signalling. *Nature* **379:** 560–564.

Howell, B.W., L.M. Lanier, R. Frank, F.B. Gertler, and J.A. Cooper. 1999. The disabled 1 phosphotyrosine-binding domain binds to the internalization signals of transmembrane glycoproteins and to phospholipids. *Mol. Cell. Biol.* **19:** 5179–5188.

Huber, M., C.D. Helgason, J.E. Damen, L. Liu, R.K. Humphries, and G. Krystal. 1998. The src homology 2-containing inositol phosphatase (SHIP) is the gatekeeper pf mast cell degranulation. *Proc. Natl. Acad. Sci.* **95:** 11330–11335.

Huber, M., C.D. Helgason, J.E. Damen, M.P. Scheid, V. Duronio,

V. Lam, R.K. Humphries, and G. Krystal. 1999. The role of the SRC homology 2-containing insitol 5'-phosphatase in Fc epsilon R1-induced signaling. *Curr. Top. Microbiol. Immunol.* **244:** 29–41.

Huyer, G. and D.R. Alexander.1999. Immune signalling: SHP-2 docks at multiple ports. *Curr. Biol.* **9:** R129–R132.

Ingham, R.J., H. Okada, M. Dang-Lawson, J. Dinglasan, and P. van der Geer. 1999. Tyrosine phosporylation of Shc in response to B cell antigen receptor engagement depends on the SHIP inositol phosphatase. *J. Immunol.* **163:** 5891–5895.

Kavanaugh, W.M. and L.T. Williams. 1994. An alternative to SH2 domains for binding tyrosine-phosphorylated proteins. *Science* **266:** 1862–1865.

Kavanaugh, W.M., D.A. Pot, S.M. Chin, M. Deuter-Reinhard, A.B. Jefferson, F.A. Norris, F.R. Masiarz, L.S. Cousens, P.W. Majerus, and L.T. Williams. 1996. Multiple forms of an inositol polyphosphate 5-phosphatase form signaling complexes with Shc and Grb2. *Curr. Biol.* **6:** 438–445.

Kawano, T., Y. Indo, H. Nakazato, M. Shimadzu, and I. Matsuda. 1998. Oculocerebrorenal syndrome of Lowe: Three mutations in the OCRL1 gene derived from three patients with different phenotypes. *Am. J. Med. Genet.* **77:** 348–355.

Khvotchev, M. and T.C. Südhof. 1998. Developmentally regulated alternative splicing in a novel synaptojanin. *J. Biol. Chem.* **273:** 2306–2311.

Kiener, P.A., M.N. Lioubin, L.R. Rohrschneider, J.A. Ledbetter, S.G. Nadler, and M.L. Diegel. 1997. Co-ligation of the antigen and Fc receptors gives rise to the selective modulation of intracellular signaling in B cells. *J. Biol. Chem.* **272:** 3838–3844.

Kimura, T., H. Sakamoto, E. Appella, and R. P. Siraganian. 1997. The negative signaling molecule SH2 domain-containing inositol-polyphosphate 5-phosphatase (SHIP) binds to the tyrosine-phosphorylated beta subunit of the high affinity IgE receptor. *J. Biol. Chem.* **272:** 13991–13996.

Kuroiwa, A., Y. Yamashita, M. Inui, T. Yuasa, M. Ono, A. Nagabukuro, Y. Matsuda, and T. Takai. 1998. Association of tyrosine phosphatases SHP-1 and SHP-2, inositol 5-phosphatase SHIP with gp49B1, and chromosomal assignment of the gene. *J. Biol. Chem.* **273:** 1070–1074.

Kurosaki, T. 1999. Genetic analysis of B cell antigen receptor signaling. *Annu. Rev. Immunol.* **17:** 555–592.

Lamkin, T.D., S.F. Walk, L. Liu, J.E. Damen, G. Krystal, and K.S. Ravichandran. 1997. Shc interaction with Src homology 2 domain containing isositol phosphatase (SHIP) *in vivo* requires the Shc-phosphotyrosine binding domain and two specific phosphotyrosines on SHIP. *J. Biol. Chem.* **272:** 10396–10401.

Lecoq-Lafon, C., F. Verdier, S. Fichelson, S. Chrétien, S. Gisselbrecht, C. Lacombe, and P. Mayeux. 1999. Erythropoietin induces the tyrosine phosphorylation of GAB1 and its association with SHC, SHP2, SHIP, and phosphatidylinositol 3-kinase. *Blood* **93:** 2578–2585.

Lewis, T.S., P.S. Shapiro, and N.G. Ahn. 1998. Signal transduction through MAPK cascades. *Adv. Cancer Res.* **74:** 49–139.

Li, J., C. Yen, D. Liaw, K. Podsypanina, S. Bose, S.I. Wang, J. Puc, C. Miliaresis, L. Rodgers, R. McCombie et al. 1997. *PTEN*, a putative protein tyrosine phosphatase gene mutated in human brain, breast, and prostate cancer. *Science* **275:** 1943–1947.

Lioubin, M.N., G.M. Myles, K. Carlberg, D. Bowtell, and L.R. Rohrschneider. 1994. SHC, GRB2, SOS1 and a 150-kilodalton tyrosine-phosphorylated protein form complexes with Fms in hematopoietic cells. *Mol. Cell. Biol.* **14:** 5682–5691.

Lioubin, M.N., P.A. Algate, S. Tsai, K. Carlberg, R. Aebersold, and L.R. Rohrschneider. 1996. $p150^{Shir}$, a signal transduction molecule with inositol polyphosphate-5-phosphatase activity. *Genes & Dev.* **10:** 1084–1095.

Liu, B., J. Liao, X. Rao, S.A. Kushner, C.D. Chung, D.D. Chang, and K. Shuai. 1998. Inhibition of Stat1-mediated gene activation by PIAS1. *Proc. Natl. Acad. Sci.* **95:** 10626–10631.

Liu, L., J.E. Damen, R.L. Cutler, and G. Krystal. 1994. Multiple cytokines stimulate the binding of a common 145-kilodalton protein to Shc at the Grb2 recognition site of Shc. *Mol. Cell. Biol.* **14:** 6926–6935.

Liu, L., J.E. Damen, M.R. Hughes, I. Babic, F.R. Jirik, and G. Krystal. 1997a. The Src homology 2 (SH2) domain of SH2-containing inositol phosphatase (SHIP) is essential for tyrosine phosphorylation of SHIP, its association with Shc, and its induction of apoptosis. *J. Biol. Chem.* **272:** 8983–8988.

Liu, L., J. E. Damen, M.D. Ware, and G. Krystal. 1997b. Interleuken-3 induces the association of the inositol 5-phosphatase SHIP with SHP2. *J. Biol. Chem.* **272:** 10998–11001.

Liu, Q., Amgen E.S.T. Program, and D.J. Dumont. 1997. Molecular cloning and chromosomal localization in human and mouse of the SH2-containing inositol phosphatase, *INPP5D* (SHIP). *Genomics* **39:** 109–112.

Liu, Q., F. Shalaby, J. Jones, D. Bouchard, and D.J. Dumont. 1998. The SH2-containing inositol polyphosphate 5-phosphatase, Ship, is expressed during hematopoiesis and spermatogenesis. *Blood* **91:** 2753–2759.

Liu, Q., T. Sasaki, I. Kozieradzki, A. Wakeham, A. Itie, D.J. Dumont, and J.M. Penninger. 1999. SHIP is a negative regulator of growth factor receptor-mediated PKB/Akt activation and myeloid cell survival. *Genes & Dev.* **13:** 786–791.

Lucas, D.M. and L.R. Rohrschneider. 1999. A novel spliced form of SH2-containing inositol phosphatase SHIP is expressed during myeloid development. *Blood* **93:** 1922–1933.

Maehama, T. and J.E. Dixon. 1999. PTEN: A tumour suppressor that functions as a phospholid phosphatase. *Trends Cell Biol.* **9:** 125–128.

Majerus, P.W., M.V. Kisseleva, and F.A. Norris. 1999. The role of phosphatases in inositol signaling reactions. *J. Biol. Chem.* **274:** 10669–10672.

Maresco, D.L., J.M. Osborne, D. Cooney, K.M. Coggeshall, and C.L. Anderson. 1999. The SH2-containing 5'-inositol phosphatase (SHIP) is tyrosine phosphorylated after Fc gamma receptor clustering in monocytes. *J. Immunol.* **162:** 6458–6465.

Matsuguchi, T., R. Salgia, M. Hallek, M. Eder, B. Druker, T.J. Ernst, and J.D. Griffin. 1994. Shc Phosphorylation in myeloid cells is regulated by granulocyte macrophage colony-stimulating factor, Interleukin-3, and steel factor is constitutively increased by $p210^{BCR/ABL}$. *J. Biol. Chem.* **269:** 5016–5021.

McPherson, P.S., E.P. Garcia, V.I. Slepnev, C. David, X. Zhang, D. Grabs, W.S. Sossin, R. Bauerfeind, Y. Nemeto, and P. De Camilli. 1996. A presynaptic inositol-5-phosphatase. *Nature* **379:** 353–357.

Myers, M.P., J.P. Stolarov, C. Eng, J. Li, S.I. Wang, M.H. Wigler, R. Parsons, and N.K. Tonks. 1997. PTEN, the tumor suppressor from human chromosome 10q23, is a dual-specificity phosphatase. *Proc. Natl. Acad. Sci.* **94:** 9052–9057.

Nemoto, Y. and P. De Camilli. 1999. Recruitment of an alternatively spliced form of synaptojanin 2 to mitochondria by the interaction with the PDZ domain of a mitochondrial outer membrane protein. *EMBO J.* **18:** 2991–3006.

Nemoto, Y., M. Arribas, C. Haffner, and P. De Camilli. 1997. Synaptojanin 2, a novel synaptojanin isoform with a distinct targeting domain and expression pattern. *J. Biol. Chem.* **272:** 30817–30821.

Nishida, K., Y. Yoshida, M. Itoh, T. Fukada, T. Ohtani, T. Shi-

rogane, T. Atsumi, M. Takahashi-Tezuka, K. Ishihara, M. Hibi, and T. Hirano. 1999. Gab-family adapter proteins act downstream of cytokine and growth factor receptors and T- and B-cell antigen receptors. *Blood* **93:** 1809–1816.

Norris, F., V. Auethavekiat and P.W. Majerus. 1995. The isolation and characterization of cDNA encoding human and rat brain inositol polyphosphate 4-phosphatase. *J. Biol. Chem.* **270:** 16128–16133.

Norris, F.A., R.C. Atkins, and P.W. Majerus. 1997. Inositol polyphosphate 4-phosphatase is inactivated by Calpain-mediated ptoteolysis in stimulated human platelets. *J. Biol. Chem.* **272:** 10987–10989.

Odai, H., K. Sasaki, A. Iwamatsu, T. Nakamoto, H. Ueno, T. Yamagata, K. Mitani, Y. Yazaki, and H. Hirai. 1997. Purification and molecular cloning of SH2- and SH3-containing inositol polyphosphate-5-phosphatase, which is involved in the signaling pathway of granulocyte-macrophage colony-stimulating factor, erythropoietin, and Bcr-Abl. *Blood* **89:** 2745–2756.

Okada, H., S. Bolland, A. Hashimoto, M. Kurosaki, Y. Kabuyama, M. Iino, J.V. Ravetch and T. Kurosaki. 1998. Cutting edge: Role of the inositol phosphatase SHIP in B cell receptor-induced Ca^{2+} oscillatory response. *J. Immunol.* **161:** 5129–5132.

Ono, M., S. Bolland, P. Tempst, and J. . Ravetch. 1996. Role of the inositol phosphatase SHIP in negative regulation of the immune system by the receptor FcγRIIB. *Nature* **383:** 263–266.

Ono, M., H. Okada, S. Bolland, S. Yanagi, T. Kurosaki, and J.V. Ravetch. 1997. Deletion of SHIP or SHP-1 reveals two distinct pathways for inhibitory signaling. *Cell* **90:** 293–301.

Osborne, M.A., G. Zenner, M. Lubinus, X. Zhang, Z. Songyang, L.C. Cantley, P. Majerus, P. Burn, and J.P. Kochan. 1996. The inositol 5'-phosphatase SHIP binds to immunoreceptor signaling motifs and responds to high affinity IgE receptor aggregation. *J. Biol. Chem.* **271:** 29271–29278.

Pesesse, X., S. Deleu, F. De Smedt, L. Drayer, and C. Erneux. 1997. Identification of a second SH2-domain-containing protein closely related to the phosphatidylinositol polyphosphate 5-phosphatase SHIP. *Biochem. Biophys. Res. Comm.* **239:** 697–700.

Podsypanina, K., L.H. Ellenson, A. Nemes, J. Gu, M. Tamura, K.M. Yamada, C. Cordon-Cardo, G. Catoretti, P.E. Fisher, and R. Parsons. 1999. Mutation of *Pten/Mmac1* in mice causes neoplasia in multiple organ systems. *Proc. Natl. Acad. Sci.* **96:** 1563–1568.

Pradhan, M. and K. M. Coggeshall. 1997. Activation-induced bi-dentate interaction of SHIP and Shc in B lymphocytes. *J. Cell. Biochem.* **67:** 32–42.

Rameh, L.E., A.K. Arvidsson, K.L. Carraway III, A.D. Couvillon, G. Rathbun, A. Crompton, B. VanRenterghem, M.P. Czech, K.S. Ravichandran, S.J. Burakoff et al. 1997. A comparative analysis of the phosphoinositide binding specificity of pleckstrin homology domains. *J. Biol. Chem.* **272:** 22059–22066.

Rawlings, D.J. and O.N. Witte. 1994. Bruton's tyrosine kinase is a key regulator in B cell development. *Immunol. Rev.* **138:** 105–119.

———. 1995. The Btk subfamily of cytoplasmic tyrosine kinases: Structure, regulation, and function. *Semin. Immunol.* **7:** 237–246.

Rohrschneider, L.R. and D. Metcalf. 1989. Induction of macrophage colony stimulating factor-dependent growth and differentiation after introduction of the murine c-fms gene into FDC-P1 cells. *Mol. Cell. Biol.* **9:** 5081–5092.

Rozakis-Adcock, M., J. McGlade, G. Mbamula, G. Pelicci, R. Daly, W. Li, A. Batzer, S. Thomas, J. Brugge, P. G. Pelicci et al. 1992. Association of the Shc and Grb2/Sem5 SH2-containing proteins is implicated in activation of the Ras pathway by tyrosine kinases. *Nature* **360:** 689–692.

Saito, T. 1998. Negative regulation of T cell activation. *Curr. Opin. Immunol.* **10:** 313–321.

Salim, K., M.J. Bottomley, E. Querfurth, M.J. Zvelebil, I. Gout, R. Scaife, R.L. Margolis, R. Gigg, C.I.E. Smith, P.C. Driscoll et al. 1996. Distinct specificity in the recognition of phosphoinositides by the pleckstrin homology domains of dynamin and Bruton's tyrosine kinase. *EMBO J.* **15:** 6241–6250.

Sattler, M., R. Salgia, G. Shrikhande, S. Verma, J.-L. Choi, L.R. Rohrschneider, and J.D. Griffin. 1997. The phosphatidylinositol polyphosphate 5-phosphatase SHIP and the protein tyrosine phosphatase SHP2 form a complex in hematopoietic cells which can be regulated by BCR/ABL and growth factors. *Oncogene* **15:** 2379–2384.

Sattler, M., S. Verma, C.H. Byrne, G. Shrikhande, T. Winkler, P.A. Algate, L.R. Rohrschneider, and J.D. Griffin. 1999. BCR/ABL directly inhibits expression of SHIP, an SH2-containing polyinositol-5-phosphatase involved in the regulation of hematopoiesis. *Mol. Cell. Biol.* **19:** 7473–7480.

Saxton, T.M., I. van Oostveen, D. Bowtell, R. Aebersold, and M.R. Gold. 1994. B cell antigen receptor cross-linking induces phosphorylation of the p21iras oncoprotein activators SHC and mSOS1 as well as assembly of complexes containing SHC, GRB-2, mSOS1, and a 145-kDa tyrosine-phosphorylated protein. *J. Immunol.* **153:** 623–636.

Schaffhausen, B. 1995. SH2 domain structure and function. *Biochim. Biophys. Acta* **1242:** 61–75.

Scharenberg, A.M., O. El-Hillal, D.A. Fruman, L.O. Beitz, Z. Li, S. Lin, I. Gout, L.C. Cantley, D.J. Rawlings, and J.-P. Kinet. 1998. Phosphatidylinositol-3,4,5-trisphosphate (PtdIns-3,4,5-P_3)/Tec kinase-dependent calcium signaling pathway: A target for SHIP-mediated inhibitory signals. *EMBO J.* **17:** 1961–1972.

Seet, L.F., S. Cho, A. Hessel, and D.J. Dumont. 1998. Molecular cloning of multiple isoforms of synaptojanin 2 and assignment of the gene to mouse chromosome 17A2-3.1. *Biochem. Biophys. Res. Comm.* **247:** 116–122.

Songyang, Z., S.E. Shoelson, M. Chaudhuri, G. Gish, T. Pawson, W.G. Haser, F. King, T. Roberts, S. Ratnofsky, R.J. Lechleider et al. 1993. SH2 domains recognize specific phosphopeptide sequences. *Cell* **72:** 767–778.

Steck, P.A., M.A. Pershouse, S.A. Jasser, W.K.A. Yung, H. Lin, A.H. Ligon, L.A. Langford, M.L. Baumgard, T. Hattier, T. Davis et al. 1997. Identification of a candidate tumor suppressor gene, MMAC1, at chromosome 10q23.3 that is mutated in multiple advanced cancers. *Nat. Genet.* **15:** 356–362.

Stephens, L., K. Anderson, D. Stokoe, H. Erdjument-Bromage, G.F. Painter, A.B. Holmes, P.R.J. Gaffney, C.B. Reese, F. McCormick, P. Tempst et al. 1998. Protein kinase B kinases that mediate phosphatidylInositol 3,4,5-trisphosphate-dependent activation of protein kinase B. *Science* **279:** 710–715.

Suzuki, A., J.L. de la Pompa, V. Stambolic, A.J. Elia, T. Sasaki, I.d.B. Barrantes, A. Ho, A. Wakeham, A. Itie, W. Khoo et al. 1998. High cancer susceptibility and embryonic lethality associated with mutation of the *PTEN* tumor suppressor gene in mice. *Curr. Biol.* **8:** 1169–1178.

Tridandapani, S., G.W. Chacko, J.R. Van Brocklyn, and K.M. Coggeshall. 1997. Negative signalling in B cells causes reduced Ras activity by reducing Shc-Grb2 interactions. *J. Immunol.* **158:** 1125–1132.

Tridandapani, S., M. Pradhan, J.R. LaDine, S. Garber, C.L. Anderson, and K.M. Coggeshall. 1999. Protein interactions

of Src homology 2 (SH2) domain-containing inositol phosphatase (SHIP): Association with Shc displaces SHIP from FcγRIIb in B cells. *J. Immunol.* **162:** 1408–1414.

Unkeless, J.C. and J. Jin. 1997. Inhibitory receptors, ITIM sequences and phospatases. *Curr. Opin. Immunol.* **9:** 338–343.

van der Geer, P. and T. Pawson. 1995. The PTB domain: A new protein module implicated in signal transduction. *Trends Biochem. Sci.* **20:** 277–280.

Vély, F., S. Olivero, L. Olcese, A. Moretta, J.E. Damen, L. Liu, G. Krystal, J.C. Cambier, M. Daëron, and E. Vivier. 1997. Differential association of phosphatases with hematopoietic coreceptors bearing immunoreceptor tyrosine-based inhibition motifs. *Eur. J. Immunol.* **27:** 1994–2000.

Ware, M.D., P. Rosten, J.E. Damen, L. Liu, K. Humphries, and G. Krystal. 1996. Cloning and characterization of human SHIP, the 145-kD inositol 5-phosphatase that associates with SHC after cytokine stimulation. *Blood* **88:** 2833–2840.

Wisniewski, D., A. Strife, S. Swendeman, H. Erdjument-Bromage, S. Geromanos, W.M. Kavanaugh, P. Tempst, and B. Clarkson. 1999. A novel SH2-containing phosphatidylinositol 3,4,5-trisphosphate 5-phosphatase (SHIP2) is constitutively tyrosine phosphorylated and associated with src homologous and collagen gene (SHC) in chronic myelogenous leukemia progenitor cells. *Blood* **93:** 2707–2720.

Yamanashi, Y., T. Tamura, T. Kanamori, H. Yamane, H. Nariuchi, T. Yamamoto, and D. Baltimore. 2000. Role of the rasGAP-associated docking protein $p62^{dok}$ in negative regulation of B cell receptor-mediated signaling. *Genes & Dev.* **14:** 11–16.

Zhang, Z.-Y., Y. Wang, E.B. Fauman, J.A. Stuckey, H.L. Schubert, M.A. Saper, and J.E. Dixon. 1994. The $Cys(X)_5Arg$ catalytic motif in phosphoester hydrolysis. *Biochemistry* **33:** 15266–15270.

Zhou, G., J.M. Denu, and J.E. Dixon. 1994. The catalytic role of $Cyst^{124}$ in the dual specificity phosphatase VHR. *J. Biol. Chem.* **269:** 28084–28090.

Exhibit C

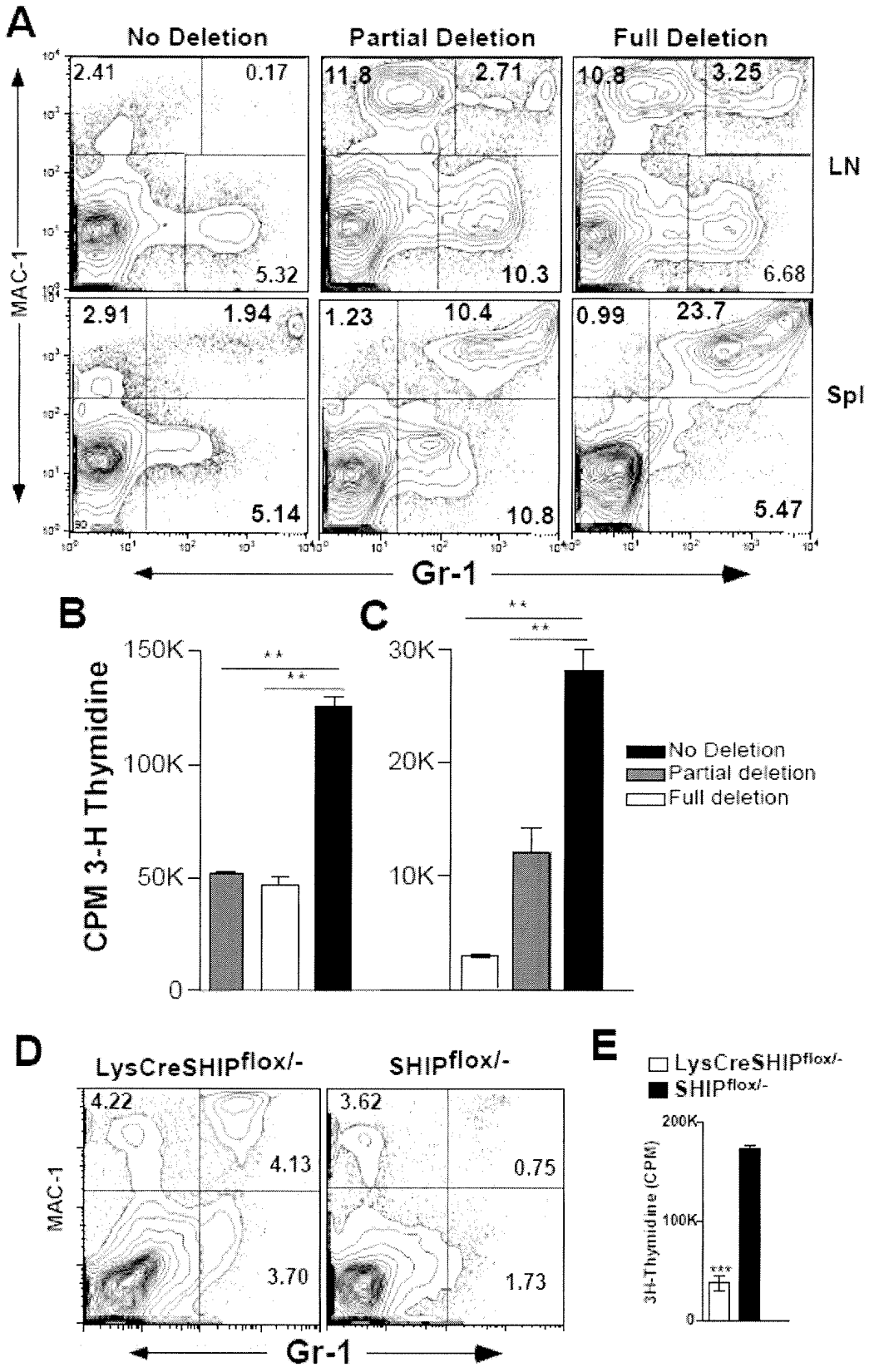
A
No Deletion
Partial Deletion
Full Deletion
2.41
0.17
5.32
11.8
2.71
10.3
10.8
3.25
6.68
LN
2.91
1.94
5.14
1.23
10.4
10.8
0.99
23.7
5.47
Spl
MAC-1
Gr-1
B
C
CPM 3-H Thymidine
150K
100K
50K
0
30K
20K
10K
**
**
No Deletion
Partial deletion
Full deletion
D
LysCreSHIPflox/-
SHIPflox/-
4.22
4.13
3.70
3.62
0.75
1.73
MAC-1
Gr-1
E
LysCreSHIPflox/-
SHIPflox/-
3H-Thymidine (CPM)
200K
100K
0
***

Induction of Mac1+Gr1+ MSC in adult mice and myeloid cells suppresses allogenic T cell priming. (A) FACS detection of MSC in LN and spleens (Spl) of MXCreSHIPflox/- and SHIPflox/-mice treated with poly(I/C) (625_g, 3X over 6 days). Two weeks later, the mice were sacrificed and their spleens and mesenteric LN analyzed by FACS for Mac1 and Gr1 staining. The "Partial Deletion" animal showed SHIP protein in the blood at 10-20% of WT controls. The "Full Deletion" animal had no detectable SHIP signal. The contour plots show staining on viable splenocytes and LN cells. (B, C) SHIP-ablated Spl and LN cells from MX-CreSHIPflox/- mice prime allogeneic BALB/C LN or Spl cells poorly relative to Cre- controls in the one-way MLR. (D) FACS detection of MSC in spleens (Spl) of LysCreSHIPflox/- and SHIPflox/- mice. (E) Spleen cells from LysCreSHIPflox/- prime allogeneic BALB/C Spl cells poorly relative to Cre- controls in the one-way MLR (***, $p<0.001$).

Patent Application
Docket No. USF-T150CX
Serial No. 09/955,174

IN THE UNITED STATES PATENT AND TRADEMARK OFFICE

Examiner	:	Jane J. Zara
Art Unit	:	1635
Applicant	:	William G. Kerr
Serial No.	:	09/955,174
Filed	:	September 19, 2001
For	:	Control of NK Cell Function and Survival by Modulation of SHIP Activity

MS AMENDMENT
Commissioner for Patents
P.O. Box 1450
Alexandria, VA 22313-1450

DECLARATION OF WILLIAM G. KERR, Ph.D., UNDER 37 C.F.R. §1.132

Sir:

I, William G. Kerr, Ph.D., of the University of South Florida, hereby declare:

THAT, my *curriculum vitae* is attached hereto as Exhibit A;

THAT, I am a named inventor on the above-referenced patent application;

THAT, I have read and understood the specification and claims of the subject application and the Office Action dated February 18, 2004;

AND, being thus duly qualified, do further declare:

1. The above-referenced Office Action indicates that claims 1-5, 7-13, 15, and 16 are rejected under 35 U.S.C. §112, first paragraph, as lacking sufficient written description by the patent application.

2. Our invention is based on the unexpected finding that reducing the activity of hematopoietic-specific SH2-containing inositol-5-phosphatase (SHIP) has physiological effects, such as suppression of natural killer (NK) cell-mediated activities, which provide therapeutic benefits in the suppression of transplant rejection and treatment of graft-versus-host disease (GVHD), for example.

3. The Reviewer indicates that the subject patent application does not provide the distinguishing attributes identifying members of "the genus comprising SHIP mRNA". As indicated above, and as recited in the claims of the accompanying Amendment, the subject invention involves the reduction of SHIP function. SHIP (which is also known in the art as SHIP-1, SHIP1, SHIPI, and SHIP-I) was also the subject of Helgason, *et al.* (1998), Huber *et al.* (1998), Liu *et al.* (1999), Liu *et al.* (1998), US. Patent No. 6,090,621 (Kavanaugh *et al.*), PCT publication WO 9710252A1 (Rohrschneider, L.R.), and PCT publication WO 9712039A2 (Krystal, G.), which are cited at pages 2 and 3 of the subject patent application. The methods recited in the claims of the accompanying Amendment involve administering an interfering RNA to a mammal that is specific for SHIP-1 mRNA within the mammal. The mRNA sequences of mouse SHIP-1 and human SHIP-1 have been publicly available since the late 1990s, as evidenced by Exhibits B and C (which are attached hereto), accession numbers NM_10566 and NM_005541, respectively, from the National Center for Biotechnology Information (NCBI) database. Although some nucleotide changes may have been subsequently made to update the GenBank sequences, Exhibits B and C show that the mouse and human SHIP-1 sequences were deposited in GenBank by papers published in 1996 and 1997. Therefore, having the sequence of the target gene, one skilled in the art could readily envision target nucleic acid sequences within the recipient mammal's mRNA. Due to nucleotide complementarity and the mechanism of RNA interference (RNAi), RNA molecules likely to interfere with expression of SHIP-1 could then be determined.

4. The Reviewer indicates that the subject patent application fails to provide particular guidance resolving issues associated with *in vivo* delivery of oligonucleotides and treatment effects. RNAi has been demonstrated to facilitate gene silencing in a variety of animal models including *C. elegans*, zebrafish, and in other biological systems such as *Drosophila* and mammalian cell culture, as reported or described in Zamore *et al.* (*Cell*, 2000, 101:25-33) and Svoboda *et al.* (*Development*, 2000, 127:4147-4156), attached hereto as Exhibit D and E, respectively. As indicated in Exhibits D and E, during the RNAi reaction, both strands of dsRNA are processed to RNA segments 21 to 23 nucleotides in length. The processing of the dsRNA to these fragments does not require the presence

of the targeted mRNA, and the targeted mRNA is cleaved only in the regions of identity to the dsRNA and at sites that are 21 to 23 nucleotides apart (the same interval observed for the dsRNA itself). It was confirmed that the 21 to 23 nucleotide RNA was sufficient to cause sequence specific interference *in vitro* (see page 30, column 2, lines 45-50, of Zamore *et al.*).

5. Exhibit F, which is attached hereto, shows suppression of SHIP-1 expression in embryonic stem (ES) cells *in vitro* by RNAi. ES cells that express the SHIP-1 gene were transfected with an irrelevant shRNA vector (Lane 3) or with two different shRNA vectors that produced siRNAS specific for SHIP-1 (Lanes 4 and 5). The cells were then lysed and equal quantities of whole cell extracts were immuno-blotted with either anti-SHIP-1 (Panel A) or anti-Actin (Panel B). Lane 2 shows untreated ES cells. Lane 1 shows untreated RAW264.7 mouse myeloid cells that express the SH2-containing SHIP-1 p135 and p145 isoforms. Panel A shows significant reduction of SHIP expression in primary ES cells after transfection of SHIP-1-specific shRNA vectors in the absence of selection. It would be expected that these vectors would also interfere with expression of the larger SH2-containing isoforms in differentiated hematopoietic cells.

6. Exhibit G, which is attached hereto, shows induction of SHIP-1 deficiency *in vivo* by RNAi increases the frequency of circulating myeloid cells including cells with a myeloid suppressor cell phenotype. In this experiment, it was confirmed that RNAi can effectively knockdown SHIP-1 expression *in vivo* using techniques described in the subject patent application. Two mice were injected with a SHIP-1 shRNA vector complexed with the cationic lipid 1,2-dioleoyloxy-3-trimethylammonium propane (DOTAP) while two additional mice received an irrelevant shRNA vector specific for the human LRBA gene. The design and sequence of the shRNA vector is shown in Exhibit H, which is attached hereto. The mice that received the SHIP-1-specific shRNA vector showed significant suppression of all major SHIP isoforms in the spleen, while β-actin levels were essentially unaltered, as shown in Figure A of Exhibit G. We also screened four different SHIP-1 specific siRNAs for knockdown of SHIP-1 in the RAW264.7 mouse myeloid cell line or ES cells. The two best siRNAs, #1 and #4, were pooled and tested *in vivo*. SiRNAs #1 and #4 were pooled,

complexed with DOTAP and injected intravenously into two separate mice. Two additional mice received the same mass of irrelevant GL2 siRNA control. As with SHIP-1 shRNA-treated mice, there was partial suppression of SHIP-1 expression in peripheral blood mononuclear cells (PBMC) by Western blotting 20 hours after the treatment (data not shown). We also examined the impact on the myeloid compartment in PBMC and found a significant increase in Mac+Gr1-monocytes and circulating Mac1+GR1+ cells (myeloid suppressor cells) in the SHIP-1 siRNA treated mice, relative to the GL2 control animals, as shown in Figure B of Exhibit G. The sequences of siRNAs #1-4 and their respective target sites within the open reading frame of mouse SHIP-1 are shown in Exhibit I, which is attached hereto. These findings show that knockdown of SHIP-1 expression *in vivo* by RNAi is a feasible approach that can exert physiological effect even with partial knockdown of SHIP-1 expression.

7. As indicated at page 11, lines 10-34, and page 12, lines 1-8, of the subject patent application, polycationic molecules such as liposomes can be used as gene delivery vehicles to deliver genetic constructs for reduction of SHIP expression. Cationic liposomes such as DOTAP are positively charged and interact with the negatively charged DNA molecules to form a stable positively charged DNA/liposome complex that binds to the negatively charged surface of the cell, where it is internalized. Column 17 of U.S. Patent No. 6,025,198, which is cited by the Reviewer in the Office Action, indicates that cationic liposomes may be used to deliver antisense oligonucleotides to inhibit expression of SHIP-2. DOTAP has been used for transfection of mammalian cells *in vitro* and *in vivo* for some time (see, for example, Porteous D.J. *et al.*, "Evidence for safety and efficacy of DOTAP cationic liposome mediated CFTR gene transfer to the nasal epithelium of patients with cystic fibrosis", *Gene Ther.*, 1997, Mar., 4(3):210-218; Song Y.K. *et al.*, "Characterization of cationic liposome-mediated gene transfer *in vivo* by intravenous administration", *Hum. Gene Ther.*, 1997, Sept., 8(13):1585-1594). However, in addition to such non-viral delivery vehicles, viral delivery vehicles such as adenovirus and adeno-associated virus could also be utilized to deliver interfering RNA to reduce SHIP-1 expression, as taught at pages 12 and 13 of the subject patent application.

8. Based on the experimental data demonstrating the ability to reduce expression of SHIP-1 *in vivo* in accordance with the teaching of the subject patent application, and the observed effects of SHIP-1 deficiency on NK cell function and GVHD in SHIP-/- transgenic mice (Examples 2-6 of the subject patent application), there is no reason to doubt that reduction of SHIP-1 function by RNA interference or other means of SHIP-1 inhibition will be of therapeutic benefit in suppressing transplant rejection and graft-versus-host disease in mammals, including humans.

The undersigned declares further that all statements made herein of his own knowledge are true and that all statements made on information and belief are believed to be true; and further that these statements were made with the knowledge that willful false statements and the like so made are punishable by fine or imprisonment, or both, under Section 1001 of Title 18 of the United States Code and that such willful false statements may jeopardize the validity of the application or of any patent issuing thereon.

Further declarant sayeth naught.

Signed: William A Kerr

William G. Kerr, Ph.D.

Date: 7/16/04

Exhibit A

Curriculum Vitae
William G. Kerr

Date: May 6, 2003

Home Address: 4421 W. Watrous Ave.
Tampa, FL 33629

Office Address: SRB2
Immunology Program
Moffitt Cancer Center
University of South Florida
12902 Magnolia Dr.
Tampa, FL 33612

Education:
1978-1982 B.S. Lehigh University (Chemistry/Molecular Biophysics)
1982-1987 Ph.D. University of Alabama at Birmingham (Molecular and Cellular Biology)

Postgraduate Training and Fellowship Appointments:
1987-1993 Post-doctoral Fellow
Department of Genetics
Stanford University

Industrial Employment:
1993-1995 Research Group Leader,
Cancer Gene Therapy, SyStemix, Inc.
Palo Alto, CA

1996 Visiting Scientist
DNAX Research Institute
Palo Alto, CA

Academic Appointments:
1996-2000 Assistant Professor
Dept. of Molecular and Cellular Engineering
University of Pennsylvania School of Medicine
Philadelphia, PA

2000-present Associate Professor (with tenure)
Dept. of Interdisciplinary Oncology
H. Lee Moffitt Comprehensive Cancer Center
University of South Florida
Tampa, FL

2000-present Associate Professor
Dept. of Biochemistry and Molecular Biology
H. Lee Moffitt Comprehensive Cancer Center
University of South Florida
Tampa, FL

2000–2001 Vice Director
Institute for Biomolecular Sciences
University of South Florida

Awards, Honors and Membership in Honorary Societies:

1981 Dean's List - Lehigh University
1981-1982 Bethlehem Fabricators Scholarship - Lehigh University
1986-1987 Pre-Doctoral Fellow - NIH (UAB)
1987 First Place - Sigma Xi Graduate Research Competition (UAB)
1987-1989 Post-Doctoral Fellow - NIH (Stanford Univ.)
1990-1993 Fellow - Irvington Institute for Medical Research (Stanford Univ.)
1997 McCabe Fund (University of Pennsylvania)
2002-2007 The Newman Scholar of the Leukemia and Lymphoma Society
2003 Outstanding Faculty Research Achievement Award (University of South Florida)
2004-present Full Member, Sigma Xi

Other Activities:

Member, Massachusetts Breast Cancer Research Review Panel (1997-2000)
Member, Univ. of California Breast Cancer Research Program (2000-2003)
Member, Special Emphasis Review Panel - Novel HIV Therapies: Integrated Preclinical/Clinical Program, NIAID/NIH (1999)
Member, Special Emphasis Review Panel – T/NK Cell Immunity, NIAID/NIH (2003-2004)
Member, Biomedical Resource Review Panel/NIH, P41 National Resource for Imaging Mass Spectrometry (1999-2000)
Ad Hoc Reviewer, VA Intramural Grants Program (1998-1999)
Ad Hoc Reviewer, Israel Science Foundation (1998)
Ad Hoc Reviewer, *Human Gene Therapy, Gene Therapy, Cytometry, Leukemia, J. Immunotherapy. J. Immunology, BLOOD, Gene, Proc. Natl. Acad. Sciences*
Member, American Association of Immunologists (1999 – present)
Active Member, American Society of Hematology (2001– present)
Member, International Society for Stem Cell Research (2003-present)
Consultant, Genentech (1998)
Consultant, Sunkyong Group (2000)
Consultant, Saneron Ccell (2003-2005)

Publications:

1. **Kerr, W.G.**, Cooper, M.D., Feng, L., Burrows, P.D., Hendershot, L.M. Mu heavy chains can associate with a pseudo-light chain complex (ΨL) in human pre-B cell lines. *International Immunology* 1: 355-361, 1989.

2. **Kerr, W.G.**, Nolan, G.P., Herzenberg, L.A. *In situ* detection of transcriptionally-active chromatin and genetic regulatory elements in individual viable mammalian cells. *Immunology* 68[Suppl. 2]: 74-79, 1989.

3. **Kerr, W. G.**, Nolan, G.P., Serafini, A.T., Herzenberg, L.A. : Transcriptionally-defective retroviruses containing *lacZ* for the *in situ* detection of endogenous genes and developmentally-regulated chromatin. *Cold Spring Harbor Symposium on Quantitative Biology* 54: 767-776, 1989.

4. Burrows, P.D., Kubagawa, H., Nishimoto, N., **Kerr, W.G.**, Borzillo, G.V., Hendershot, L.M., Cooper, M.D. Differences in human B cell differentiation. *Adv. Exp. Biol. Med.* 292: 215-226, 1991.

5. **Kerr, W.G.**, Herzenberg, L.A. Gene-search viruses and FACS-Gal permits the detection, isolation and characterization of mammalian cells with *in situ* fusions between cellular genes and *E. coli lacZ. Methods: A Companion to Methods in Enzymology* 2: 261-271, 1991.

6. **Kerr, W.G.**, Hendershot, L.M., Burrows, P.D. Regulation of IgM and IgD expression in human B-lineage cells. *J. Immunol.* 146: 3314-3321, 1991.

7. **Kerr, W.G.**, Nolan, G.P., Johnsen, J., Herzenberg, L.A. *In situ* detection of stage-specific genes and enhancers in B cell differentiation via gene-search retroviruses. *Adv. Exp. Biol. Med.* 292: 187-200, 1991.

8. **Kerr, W.G.**, Burrows, P.D. Stage-specific transcription of germline IgH Cγ and Cα regions during human B cell differentiation. *International Immunology* 3: 1059-1065, 1991.

9. **Kerr, W.G**. and Mulé, J.J. Gene therapy: Current status and future prospects. *J. Leuko. Biol.* 56: 210-214, 1994.

10. Gerard, C.J., Arboleda, M.J., Solar, G., Mulé, J.J., **Kerr, W.G.** A rapid and quantitative assay to estimate gene transfer into retrovirally-transduced hematopoietic stem/progenitor cells using a 96-well format PCR and fluorescent detection system universal for MMLV-based proviruses. *Human Gene Therapy* 7: 343-354, 1996.

11. **Kerr, W.G.** Progress towards a new wave of immune-based therapeutics. *Trends in Biotechnology*, 14: 359-360, 1996.

12. **Kerr, W.G.**, Heller, M.R., Herzenberg, L.A. Analysis of LPS-response genes in B-lineage cells demonstrates that they can have differentiation stage-restricted expression and contain SH2 domains. *Proc. Natl. Acad. Sci. (USA)* 93, 3947-3952, 1996.

13. Zambrowicz, B.P., Imamoto, A., Fiering, S., Herzenberg, L.A., **Kerr, W.G.**, Soriano, P. Disruption of overlapping transcripts in the ROSA βgeo26 gene trap strain leads to widespread expression of βgalactosidase in mouse embryos and hematopoietic cells. *Proc. Natl. Acad. Sci. (USA)* 94, 3789-3794, 1997.

14. Lorincz, M., Herzenberg, L.A., Diwu, Z., Barranger, J.A., and **Kerr, W.G.** Detection and isolation of gene-corrected cells in Gaucher disease via a FACS assay for lysosomal glucocerebrosidase activity. *BLOOD* 89, 3412-3420, 1997.

15. Kapasi, Z.F., Quin, D., **Kerr, W.G.**, Kosko-Vilbois, M.H., Schultz, L., Tew, J.G., and Szakal, A.K. Follicular dendritic cell (FDC) precursors in primary lymphoid tissues. *J. Immunol.* 160, 1078-1084, 1998.

16. Solar, G., **Kerr, W.G.**, Ziegler, F., Hess, D., Donahue, C., DeSavauge, F.J., and Eaton, D. *Special Focus:* Role of *c-mpl* in early hematopoiesis. *BLOOD* 92, 4-10, 1998.

17. **Kerr, W.G.** Genetic modification of the hematolymphoid compartment for therapeutic purposes. *Hematology/Oncology Clinics of North America: Gene Therapy* 12: 503-518, 1998.

18. Spain, L. and **W.G Kerr.** Lymphoid development. ENCYCLOPEDIA OF LIFE SCIENCES (Macmillan Reference Ltd), 1999.

19. Greenberg, A.W., ***Kerr, W.G.**, *Hammer, D.A. Relationship between selectin-mediated rolling of hematopoietic stem/progenitor cells and progression in hematopoietic development. *BLOOD* 95, 478-486, 2000. (**Senior authorship is shared on this manuscript*)

20. Wang JW, Howson J, Ghansah T, Ninos J, Kerr WG. Inhibition of apoptosis by the BEACH domain and WD repeats of gene lba that has key features of both protein kinase A anchor and chs1/beige genes. Scientific World Journal 1(1 Suppl. 3), 96, 2001.

21. Wang, J.W., Howson, J., Haller, E. and **Kerr, W.G.** Identification of a novel LPS-inducible gene that has key features of both protein kinase A anchor and CHS1/BEIGE proteins. *Journal of Immunology* 166, 4586-4595, 2001.

22. Ghansah, T., Ninos, J. and **Kerr, W.G**. A role for the SH2-containing Inositol Phosphatase (SHIP) in the biology of stem cells and natural killer cells. In *Activating and Inhibitory Immunoglobulin-Like Receptors (Eds, M.D. Cooper, T. Takai and J.V. Ravetch, Springer-Verlag),* pp. 129-140, 2001.

23. Zheng Tu, John M. Ninos, Zhengyu Ma, Jia-Wang Wang, Maria P. Lemos, Caroline Desponts, Tomar Ghansah, Julie M. Howson and **Kerr, W.G.** *Plenary Paper:* Embryonic and hematopoietic stem cells express a novel SHIP isoform that partners with the Grb2 adapter protein. *BLOOD* 98, 2028-2038, 2001.

24. **Kerr, W.G.**, Eaton, D.L. and Solar, G.P. Monoclonal antibodies specific for *c-mpl* for the study of human megakaryopoiesis and stem cell biology. In: *Leukocyte Typing VII,* Ed. D. Mason, Oxford University Press, UK, pp.561-563, 2002.

25. Wang, J.W., Howson, J.M., Ghansah, T., Desponts, C., Ninos, J.M., May, S.L., Nguyen, K.H.T., Sorimachi, N. and **Kerr, W.G.** Influence of SHIP on the NK repertoire and allogeneic bone marrow transplantation. *SCIENCE* 295, 2094-2097, 2002.

26. Cheng, F., Wang, H., Cuenca, A., Huang, M. Ghansah, T., Brayer, J., **Kerr, W.,** Takeda, K., Akira, S., Schoenberger, S., Yu, H., Jove, R. and E. Sotomayor. Critical role for Stat3 signaling in immune tolerance. *Immunity* 19, 425-436, 2003.

27. Wang, J.W., Gamsby, J., Bloom, G., Yeatman, T., Chodosh, L., Cress, W.D., Chen, J. and **Kerr, W.G.** Deregulated expression of LRBA facilitates cancer cell growth. *Oncogene* 23, 4089-4097, 2004.

28. Eason, D.D., Litman, R.T., Luer, C.A., **Kerr, W.G.** and Litman, G.W. Expression of Individual immunoglobulin genes occurs in an unusual system consisting of multiple

independent loci. *European Journal of Immunology*, in press (2004).

29. Perez, L., Desponts, C, Parquet, N and Kerr, W.G. A role for SHIP-1 in the control of megakaryocytopoiesis. *Submitted.*

30. Ninos, J.M., Eaton, D., and **Kerr, W.G.** The TPO receptor, *c-mpl,* demarcates human hematopoietic stem cells from multiple sources and is expressed by cells capable of multi-lineage repopulation following serial transfer. *Submitted.*

31. Ghansah, T., Nguyen, K.H.T., Highfill, S., Desponts, C., May, S., McIntosh, J.K., Brayer, J., Cheng, F., Sotomayor, E. and **Kerr, W.G.** Expansion of myeloid suppressor cells in $SHIP^{-/-}$ mice represses allogeneic T cell responses. *Submitted and under revision.*

32. Hess, D., Brown-Whitehorn, T, Howson, J., Ford, B., McIntosh, H. and **Kerr, W.G.** Repopulation of human lymph node grafts and long-term IgG production in immunodeficient mice co-transplanted with primary and secondary human lymphoid tissue. *Submitted and under revision.*

Current Extramural Grant Support:

1999-2004 PO1 NS27405: *In Vivo* Model of Human Microglia Development and Infection (Project Leader)

2002-2006 RO1 HL72523: Role of SHIP in the Control of NK Cell Function (Principal Investigator)

2002-2007 Scholar Award, Leukemia and Lymphoma Society of America (PI)

2004-2006 Antibody Therapeutics in Multiple Myeloma, Genentech (PI)

Lectures by Invitation:

September, 1994 "Retroviral Transduction of $CD34^{+}Thy^{+}Lin^{-}$ Hematopoietic Stem Cells From Adult Mobilized Peripheral Blood" - Gene Therapy Conference, Cold Spring Harbor, NY

December, 1994 "Retroviral Transduction of $CD34^{+}Thy^{+}Lin^{-}$ Hematopoietic Stem Cells From Adult Mobilized Peripheral Blood" - Annual Meeting of the American Society of Hematology, Nasheville, TN

December, 1994 "Retroviral Transduction of $CD34^{+}Thy^{+}Lin^{-}$ Hematopoietic Stem Cells From Adult Mobilized Peripheral Blood" - Third International Conference on Gene Therapy for Inherited Deficiencies and Disease, London, UK

July, 1995 "High-Efficiency Transduction of Highly-Purified $CD34^{+}Thy^{+}Lin^{-}$ Human Peripheral Blood Hematopoietic Stem Cells with Pseudotyped Retroviruses" - International Congress of Immunology, San Francisco, CA

September 29, 1995 "Gene Transfer Into Highly Purified Human Stem Cells Using Amphotropic and Pseudotyped MMLV-Based Vectors"

– First Conference on Hematopoietic Stem Cell Gene Therapy: Biology and Technology, Bethesda, MD

November, 1995 "High-Efficiency Transduction of Highly-Purified $CD34^{+}Thy^{+}Lin^{-}$ Human Peripheral Blood Hematopoietic Stem Cells with Pseudotyped Retroviruses" - Fourth International Conference on Gene Therapy of Cancer, San Diego, CA

December, 1995 "Directed Immunity" - Immunotherapeutic Strategies for Cancer: Novel Vaccine Strategies, San Diego, CA

March, 1996 "Gene Transfer Into Human Hematopoietic Stem/Progenitor Cells and Potential Therapeutic Applications" - Institute for Genetics, University of Cologne, Cologne, Germany

March, 1996 "Gene Transfer Into Human Hematopoietic Stem/Progenitor Cells and Potential Therapeutic Applications" - Max Planck Institute for Immunobiology, Freiburg, Germany

May, 1996 "Gene Transfer Into Human Hematopoietic Stem/Progenitor Cells and Potential Therapeutic Applications" - Genomic Sciences Series Conference on Gene Therapy, Hilton Head, SC

June, 1996 "Directing Immunity to Cancer Cells via HSC-Based Gene Therapy" - Antigen Processing and Presentation: Novel Therapeutics Development, Bethesda, MD

November, 1996 "Hematopoietic Stem Cell Based Gene Therapies for Cancer: Potential Therapeutic Approaches and Technologies" - Immunotherapeutic Strategies for Cancer, San Diego, CA (Chairman - Session on *Hematopoietic Stem Cell-Based Therapies*)

March 27, 1997 "Hematopoietic Stem Cell Gene Therapy: Will It Cure What Ails Us?", Genentech, South San Francisco, CA

April 23, 1997 "Progress Toward Stem Cell Gene Therapy", Laboratory of Tumor Biology and Immunology, National Cancer Institute, Bethesda, MD

May 9, 1997 "Progress Toward Stem Cell Gene Therapy and SCID-*hu* Models to Assist Us", Symposium on Nonhuman Primate Gene Therapy, New Orleans, LA

February 25, 1998 "*In Vivo* Models of the Human Lymph Node to Study Function and Pathogenesis in the Human Immune System", Immunotherapeutic Strategies for Cancer: Moving Towards the Clinic, San Diego, CA.

June 2, 1998 "Role of *c-mpl* in the Biology of Hematopoietic Stem Cells in Mouse and Man", Center for Molecular Pathogenesis, Umea University, Umea, Sweden.

January 21, 1999 "Modeling the Human Hematolymphoid System in Mice", Penn State Medical College, Hershey, PA.

March 18, 1999 "Role of *c-mpl* in the Hematopoietic Stem Cell Biology", Dept. of Pathology and Lab Medicine, University of Pennsylvania.

March 23, 1999 "Modeling the Human Hematolymphoid System in Immunodeficient Mice", Genzyme Corp., Cambridge, MA.

March 29, 1999 "Modeling the Human Hematolymphoid System in Immunodeficient Mice", Genentech, Inc., South San Francisco, CA.

May 18, 1999 "Studying the Function of the Human Hematopoietic Stem Cell and the Lymphoid System in Immunodeficient Mice", Philadelphia City-Wide AIDS Symposium, Jefferson Medical College, Philadelphia, PA

August 16, 1999 "Role of *c-mpl* in the Hematopoietic Stem Cell Biology", Immunotherapeutic Approaches to Cancer, San Diego, CA.

June 19-24, 2000 "Monoclonal antibodies specific for human *c-mpl* for clustering and study of hematopoiesis", Platelet Workshop - 7th Workshop and Conference on Human Leucocyte Differentiation Antigens, Harrogate, United Kingdom

September 19-20, 2000 "The SH2-Containing Inositol Phosphatase (SHIP) is a crucial regulator of NK cell repertoire and function.", The CREST International Symposium on Immunoglobulin-Like Receptors, Sendai, Japan

October 11-15, 2000 "The SH2-Containing Inositol Phosphatase (SHIP) is a crucial regulator of NK cell repertoire and function", Aegean Conference On Innate Immunity, Santorini, Greece.

October 27, 2000 "Key Genetic Determinants of Stem Cell Biology and Transplantation", Hematopoiesis and Immunology Seminar Series, Johns Hopkins University School of Medicine

April 13, 2001 "The SH2-Containing Inositol Phosphatase (SHIP) is a crucial regulator of NK cell repertoire and function", NCI/Frederick, Frederick, Maryland

April 27, 2001 "The SH2-Containing Inositol Phosphatase (SHIP) is a crucial regulator of NK cell repertoire and function", Dept. of Microbiology and Immunology, Univ. of California San Francisco

July 25, 2001 "SHIP is Critical for Repertoire Diversity and Function in the Adult NK Cell Compartment", Workshop: The role of NK and NKT cells in immune effector mechanisms, 11th International Congress of Immunology, Stockholm, Sweden.

September 4, 2001 "Critical role for SHIP in engraftment of histo-incompatible stem cells", Millenium International Conference: Stem Cell Differentiation, Genetic Reprogramming and Programmed Cell Death, Santorini, Greece.

March 20, 2002 "SHIP Influences the NK Repertoire and Allogeneic Bone Marrow Transplantation", Keystone Symposium: Molecular and Cellular Biology of Leukocyte Regulatory Receptors, Tahoe City, California

April 9, 2002 "Role for SHIP in Stem Cell Biology and Transplantation" Genentech, South San Francisco, California

October 13, 2002 "A Role for SHIP in Allogeneic Bone Marrow Transplantation", Molecular Targets for Cancer Therapy: 2nd Biennial Meeting, St. Petersburg, FL

November 12, 2002, "Role for SHIP in Stem Cell Biology and Transplantation", Molecular and Cellular Biology Seminar Series, UAB, Birmingham, Alabama

January 6, 2003 "A Role for SHIP in Allogeneic Bone Marrow Transplantation" Suntory Pharmaceuticals Research Laboratory, Cambridge, MA

January 14, 2003 "SHIP and LRBA: Two Novel Targets in Cancer Therapy?", Sidney Kimmel Cancer Center, Thomas Jefferson University, Philadelphia, PA

June 13, 2003 "Role for SHIP in Stem Cell Biology and Transplantation" Immunology Seminar Series, National Cancer Institute, Frederick, MD

September 7-9, 2003 Session Chair, Lymphopoiesis II: 70th Birthday Symposium for Max Cooper, M.D. UAB, Birmingham, AL

September 19, 2003 "Role for SHIP in Stem Cell Biology and Transplantation", Dept. of Biology Seminar Series, University of North Florida, Jacksonville, Florida (*invited*)

March 21-23, 2004 "A Role for SHIP in Stem Cell Biology and Transplantation", Session: Stem Cells and Cancer (Chair), *Emerging Cancer Treatment Modalities: From Research to Practice*, Copper Mountain, Colorado

April 29, 2004 "A Role for SHIP in Stem Cell Biology and Bone Marrow Transplantation", University Hospital Utrecht, The Netherlands

May 4, 2004 "A Role for SHIP in Stem Cell Biology and Bone Marrow Transplantation", Central Laboratory for the Blood (CLB/Sanquin), Amsterdam, The Netherlands

June 10, 2004 "A Role for SHIP in Stem Cell Biology and Transplantation",

University of California at San Francisco, San Francisco, CA (*Invited*)

June 22, 2004 "A Role for SHIP in Stem Cell Biology and Bone Marrow Transplantation", Amgen, Thousand Oaks, CA (*Invited*)

Teaching Responsibilities at the University of Pennsylvania (1996-1999):

Member, Cellular and Molecular Biology (CAMB) Graduate Group (1996-1999)
Member, Immunology Graduate Group (1997-1999)
Chair, Thesis Committee for Steven Suter, Ph.D., Candidate in Cell and Molecular Biology
Member, Thesis Committee for Adam Greenberg, Ph.D. Candidate in Bioengineering
Committee Member, Preliminary Exam of Xiarong Wang, Ph.D. candidate Cell and Molecular Biology Graduate Group
Committee Member, Preliminary Exam of Matthew McLeod, Ph.D. candidate Cell and Molecular Biology Graduate Group (1999)
Mentor, Second Preliminary Exam of Fang Zhao, Ph.D. candidate Immunology Graduate Group (1998)
Mentor, Second Preliminary Exam of Zhengyu Ma, Ph.D. candidate Immunology Graduate Group (1999)
Thesis Advisor, Zheng Tu, Ph.D. candidate, Cell and Molecular Biology Graduate Group (1998)
CAMB 610: Molecular Basis of Gene Therapy (1996)
Lecture 1: The hematopoietic stem cell
Lecture 2: Adenosine deaminase deficiency
CAMB 610: Molecular Basis of Gene Therapy (1997-1999)
Lecture 1: Hematopoiesis
Lecture 2: Discussion session
CAMB 633: Advanced Seminar in Cancer Gene Therapy (Co-Director) (1997)
Lecture 1: Immunotherapy I: Cytokine stimulated tumor immunity
Lecture 2: Immunotherapy II: Genetic modification to directly alter effector function
Lecture 3: Immunotherapy IV: Second generation tumor vaccine approaches
Lecture 4: Selective infection and induction of apoptosis in tumore cells to purge bone marrow
CAMB 633: Advanced Seminar in Gene Therapy (1997)
Lecture: Gaucher Disease
Immunology 660: Developmental Immunology (1996)
Lecture: The Hematopoietic Stem Cell
Immunology 506: Immune Mechanisms (1997-98)
Lecture: Acquired Immunity
Immunology 506: Immune Mechanisms (1998-1999)
Lecture: Role of the Antigen Receptor in B Cell Biology
Immunology 508: Immune Responses (1997-1999)
Lecture: Gene therapy approaches to correcting immunodeficiency states
CAMB 633: Advanced Seminar in Gene Therapy (1998)
Lecture: Modeling the human immune system in immunodeficient mice

CAMB 605: CAMB First Year Ph.D. Student Seminar (Fall 1998)

Teaching and Service at the University of South Florida (2000-present):
Lecturer, Biochemistry 6806: Biochemical Signal Transduction
Lecture: Inositol Phospholipid Signaling (Spring 2000)
Course Director, Stem Cell Biology (Spring 2001)
Course Director, GMS 6055: Immunology and Immunotherapy (2002,2004)
Member, Cancer Biology Education Committee (2000 - present)
Chair, Cancer Biology Graduate Admissions Committee (2001 - 2002)
Member, Biochemistry Graduate Admissions Committee

Lecturer, GMS 6055: Immunology and Applied Cancer Biology (2002-3)
Chair, Thesis Committee for Deborah Kuhn (Ph.D. Candidate in Cancer Biology)
Ph.D. Thesis Advisor, Caroline Desponts (Biochemistry/IBS), Joshua Gamsby (Biochemistry), Joseph Wahle (Cancer Biology)
Mentor, Acquanetta Henry, Undergraduate Honors Student/USF McNair Scholar
Chair, Thesis Committee for Deborah Kuhn (Ph.D. Candidate in Cancer Biology)
Organizer, Moffitt Cancer Center Immunology Colloquium (2002-2004)
Member, Organizing Committee for the Moffitt Cancer Center Molecular Targets Symposium, St. Petersburg, FL (2002)

Exhibit B

1: NM_010566. Mus musculus inos...[gi:6754355]

```
LOCUS       NM_010566                4865 bp    mRNA    linear   ROD 24-DEC-2003
DEFINITION  Mus musculus inositol polyphosphate-5-phosphatase D (Inpp5d), mRNA.
ACCESSION   NM_010566
VERSION     NM_010566.1  GI:6754355
KEYWORDS    .
SOURCE      Mus musculus (house mouse)
  ORGANISM  Mus musculus
            Eukaryota; Metazoa; Chordata; Craniata; Vertebrata; Euteleostomi;
            Mammalia; Eutheria; Rodentia; Sciurognathi; Muridae; Murinae; Mus.
REFERENCE   1  (bases 1 to 4865)
  AUTHORS   Giuriato,S., Pesesse,X., Bodin,S., Sasaki,T., Viala,C., Marion,E.,
            Penninger,J., Schurmans,S., Erneux,C. and Payrastre,B.
  TITLE     SH2-containing inositol 5-phosphatases 1 and 2 in blood platelets:
            their interactions and roles in the control of phosphatidylinositol
            3,4,5-trisphosphate levels
  JOURNAL   Biochem. J. 376 (Pt 1), 199-207 (2003)
   PUBMED   12885297
  REMARK    GeneRIF: SHIP1 plays a major role in controlling
            phosphatidylinositol 3,4,5-trisphosphate levels in platelets.
REFERENCE   2  (bases 1 to 4865)
  AUTHORS   Jiang,X., Stuible,M., Chalandon,Y., Li,A., Chan,W.Y., Eisterer,W.,
            Krystal,G., Eaves,A. and Eaves,C.
  TITLE     Evidence for a positive role of SHIP in the BCR-ABL-mediated
            transformation of primitive murine hematopoietic cells and in human
            chronic myeloid leukemia
  JOURNAL   Blood 102 (8), 2976-2984 (2003)
   PUBMED   12829595
  REMARK    GeneRIF: SHIP expression appears to be differently altered in the
            early and late stages of differentiation of BCR-ABL-transformed
            cells
REFERENCE   3  (bases 1 to 4865)
  AUTHORS   Baran,C.P., Tridandapani,S., Helgason,C.D., Humphries,R.K.,
            Krystal,G. and Marsh,C.B.
  TITLE     The inositol 5'-phosphatase SHIP-1 and the Src kinase Lyn
            negatively regulate macrophage colony-stimulating factor-induced
            Akt activity
  JOURNAL   J. Biol. Chem. 278 (40), 38628-38636 (2003)
   PUBMED   12882960
  REMARK    GeneRIF: SHIP-1 and Lyn have roles in the negative regulation of
            M-CSF-R-induced Akt activation
REFERENCE   4  (bases 1 to 4865)
  AUTHORS   Moody,J.L., Pereira,C.G., Magil,A., Fritzler,M.J. and Jirik,F.R.
  TITLE     Loss of a single allele of SHIP exacerbates the immunopathology of
            Pten heterozygous mice
  JOURNAL   Genes Immun. 4 (1), 60-66 (2003)
   PUBMED   12595903
  REMARK    GeneRIF: Reduced expression of SHIP, achieved by generating mice
            doubly heterozygous for Pten and SHIP, leads to a worsening of the
            Pten+/-phenotype.
```

REFERENCE 5 (bases 1 to 4865)
AUTHORS Nakamura,K., Malykhin,A. and Coggeshall,K.M.
TITLE The Src homology 2 domain-containing inositol 5-phosphatase negatively regulates Fcgamma receptor-mediated phagocytosis through immunoreceptor tyrosine-based activation motif-bearing phagocytic receptors
JOURNAL Blood 100 (9), 3374-3382 (2002)
PUBMED 12384440
REMARK GeneRIF: SHIP negatively regulates FcgammaR-mediated phagocytosis through all ITAM-containing IgG receptors using a molecular mechanism distinct from that in B cells.
REFERENCE 6 (bases 1 to 4865)
AUTHORS Takeshita,S., Namba,N., Zhao,J.J., Jiang,Y., Genant,H.K., Silva,M.J., Brodt,M.D., Helgason,C.D., Kalesnikoff,J., Rauh,M.J., Humphries,R.K., Krystal,G., Teitelbaum,S.L. and Ross,F.P.
TITLE SHIP-deficient mice are severely osteoporotic due to increased numbers of hyper-resorptive osteoclasts
JOURNAL Nat. Med. 8 (9), 943-949 (2002)
PUBMED 12161749
REMARK GeneRIF: SHIP negatively regulates osteoclast formation and function and the absence of this enzyme results in severe osteoporosis
REFERENCE 7 (bases 1 to 4865)
AUTHORS Huber,M., Kalesnikoff,J., Reth,M. and Krystal,G.
TITLE The role of SHIP in mast cell degranulation and IgE-induced mast cell survival
JOURNAL Immunol. Lett. 82 (1-2), 17-21 (2002)
PUBMED 12008029
REMARK GeneRIF: a review of SHIP's role in mast cell degranulation and IgE-induced mast cell survival
REFERENCE 8 (bases 1 to 4865)
AUTHORS Kalesnikoff,J., Baur,N., Leitges,M., Hughes,M.R., Damen,J.E., Huber,M. and Krystal,G.
TITLE SHIP negatively regulates IgE + antigen-induced IL-6 production in mast cells by inhibiting NF-kappa B activity
JOURNAL J. Immunol. 168 (9), 4737-4746 (2002)
PUBMED 11971024
REMARK GeneRIF: SHIP negatively regulates IgE + antigen-induced IL-6 production in mast cells
REFERENCE 9 (bases 1 to 4865)
AUTHORS Wang,J.W., Howson,J.M., Ghansah,T., Desponts,C., Ninos,J.M., May,S.L., Nguyen,K.H., Toyama-Sorimachi,N. and Kerr,W.G.
TITLE Influence of SHIP on the NK repertoire and allogeneic bone marrow transplantation
JOURNAL Science 295 (5562), 2094-2097 (2002)
PUBMED 11896280
REMARK GeneRIF: influences the repertoire of NK receptors;plays an important role in two processes that limit the success of allogeneic marrow transplantation: graft rejection and graft-versus-host disease
REFERENCE 10 (bases 1 to 4865)
AUTHORS Tu,Z., Ninos,J.M., Ma,Z., Wang,J.W., Lemos,M.P., Desponts,C., Ghansah,T., Howson,J.M. and Kerr,W.G.
TITLE Embryonic and hematopoietic stem cells express a novel SH2-containing inositol 5'-phosphatase isoform that partners with the Grb2 adapter protein
JOURNAL Blood 98 (7), 2028-2038 (2001)
PUBMED 11567986
REFERENCE 11 (bases 1 to 4865)
AUTHORS Wolf,I., Lucas,D.M., Algate,P.A. and Rohrschneider,L.R.

```
  TITLE     Cloning of the genomic locus of mouse SH2 containing inositol
            5-phosphatase (SHIP) and a novel 110-kDa splice isoform, SHIPdelta
  JOURNAL   Genomics 69 (1), 104-112 (2000)
   PUBMED   11013080
REFERENCE   12 (bases 1 to 4865)
  AUTHORS   Lucas,D.M. and Rohrschneider,L.R.
  TITLE     A novel spliced form of SH2-containing inositol phosphatase is
            expressed during myeloid development
  JOURNAL   Blood 93 (6), 1922-1933 (1999)
   PUBMED   10068665
REFERENCE   13 (bases 1 to 4865)
  AUTHORS   Liu,Q. and Dumont,D.J.
  TITLE     Molecular cloning and chromosomal localization in human and mouse
            of the SH2-containing inositol phosphatase, INPP5D (SHIP). Amgen
            EST Program
  JOURNAL   Genomics 39 (1), 109-112 (1997)
   PUBMED   9027494
REFERENCE   14 (bases 1 to 4865)
  AUTHORS   Lioubin,M.N., Algate,P.A., Tsai,S., Carlberg,K., Aebersold,A. and
            Rohrschneider,L.R.
  TITLE     p150Ship, a signal transduction molecule with inositol
            polyphosphate-5-phosphatase activity
  JOURNAL   Genes Dev. 10 (9), 1084-1095 (1996)
   PUBMED   8654924
REFERENCE   15 (bases 1 to 4865)
  AUTHORS   Damen,J.E., Liu,L., Rosten,P., Humphries,R.K., Jefferson,A.B.,
            Majerus,P.W. and Krystal,G.
  TITLE     The 145-kDa protein induced to associate with Shc by multiple
            cytokines is an inositol tetraphosphate and phosphatidylinositol
            3,4,5-triphosphate 5-phosphatase
  JOURNAL   Proc. Natl. Acad. Sci. U.S.A. 93 (4), 1689-1693 (1996)
   PUBMED   8643691
COMMENT     PROVISIONAL REFSEQ: This record has not yet been subject to final
            NCBI review. The reference sequence was derived from U52044.1.
FEATURES             Location/Qualifiers
     source          1..4865
                     /organism="Mus musculus"
                     /mol_type="mRNA"
                     /db_xref="taxon:10090"
                     /chromosome="1"
                     /map="1 57.0 cM"
     gene            1..4865
                     /gene="Inpp5d"
                     /note="synonyms: SHIP, 145kDa, s-SHIP"
                     /db_xref="GeneID:16331"
                     /db_xref="LocusID:16331"
                     /db_xref="MGI:107357"
     CDS             111..3686
                     /gene="Inpp5d"
                     /note="inositol polyphosphate-5-phosphatase, 145 kDa; Src
                     homology 2 domain-containing inositol-5-phosphatase;
                     go_function: signal transducer activity [goid 0004871]
                     [evidence IEA];
                     go_function: inositol/phosphatidylinositol phosphatase
                     activity [goid 0004437] [evidence ISS] [pmid 12466851];
                     go_function: ATP binding [goid 0005524] [evidence ISS]
                     [pmid 12466851];
                     go_function: protein binding [goid 0005515] [evidence IPI]
                     [pmid 11567986];
                     go_process: signal transduction [goid 0007165] [evidence
```

```
                     IEA];
                     go_process: intracellular signaling cascade [goid 0007242]
                     [evidence ISS] [pmid 12466851]"
                     /codon_start=1
                     /product="inositol polyphosphate-5-phosphatase D"
                     /protein_id="NP_034696.1"
                     /db_xref="GI:6754356"
                     /db_xref="GeneID:16331"
                     /db_xref="LocusID:16331"
                     /db_xref="MGI:107357"
                     /translation="MPAMVPGWNHGNITRSKAEELLSRAGKDGSFLVRASESIPRAYA
                     LCVLFRNCVYTYRILPNEDDKFTVQASEGVPMRFFTKLDQLIDFYKKENMGLVTHLQY
                     PVPLEEEDAIDEAEEDTVESVMSPPELPPRNIPMSAGPSEAKDLPLATENPRAPEVTR
                     LSLSETLFQRLQSMDTSGLPEEHLKAIQDYLSTQLLLDSDFLKTGSSNLPHLKKLMSL
                     LCKELHGEVIRTLPSLESLQRLFDQQLSPGLRPRPQVPGEASPITMVAKLSQLTSLLS
                     SIEDKVKSLLHEGSESTNRRSLIPPVTFEVKSESLGIPQKMHLKVDVESGKLIVKKSK
                     DGSEDKFYSHKKILQLIKSQKFLNKLVILVETEKEKILRKEYVFADSKKREGFCQLLQ
                     QMKNKHSEQPEPDMITIFIGTWNMGNAPPPKKITSWFLSKGQGKTRDDSADYIPHDIY
                     VIGTQEDPLGEKEWLELLRHSLQEVTSMTFKTVAIHTLWNIRIVVLAKPEHENRISHI
                     CTDNVKTGIANTLGNKGAAGVSFMFIGTSLGFVNSHLTSGSEKKLRRNQNYMNILRFL
                     ALGDKKLSPFNITHRFTHLFWLGDLNYRVELPTWEAEAIIQKIKQQQYSDLLAHDQLL
                     LERKDQKVFLHFEEEEITFAPTYRFERLTRDKYAYTKQKATGMKYNLPSWCDRVLWKS
                     YPLVHVVCQSYGSTSDIMTSDHSPVFATFEAGVTSQFVSKNGPGTVDSQGQIEFLACY
                     ATLKTKSQTKFYLEFHSSCLESFVKSQEGENEEGSEGELVVRFGETLPKLKPIISDPE
                     YLLDQHILISIKSSDSDESYGEGCIALRLETTEAQHPIYTPLTHHGEMTGHFRGEIKL
                     QTSQGKMREKLYDFVKTERDESSGMKCLKNLTSHDPMRQWEPSGRVPACGVSSLNEMI
                     NPNYIGMGPFGQPLHGKSTLSPDQQLTAWSYDQLPKDSSLGPGRGEGPPTPPSQPPLS
                     PKKFSSSTANRGPCPRVQEARPGDLGKVEALLQEDLLLTKPEMFENPLYGSVSSFPKL
                     VPRKEQESPKMLRKEPPPCPDPGISSPSIVLPKAQEVESVKGTSKQAPVPVLGPTPRI
                     RSFTCSSSAEGRMTSGDKSQGKPKASASSQAPVPVKRPVKPSRSEMSQQTTPIPAPRP
                     PLPVKSPAVLQLQHSKGRDYRDNTELPHHGKHRQEEGLLGRTAMQ"
misc_feature         126..395
                     /gene="Inpp5d"
                     /note="SH2; Region: Src homology 2 domains"
                     /db_xref="CDD:22728"
misc_feature         1323..2258
                     /gene="Inpp5d"
                     /note="IPPc; Region: Inositol polyphosphate phosphatase,
                     catalytic domain homologues"
                     /db_xref="CDD:113"
polyA_site           4865
                     /gene="Inpp5d"
                     /note="17 A nucleotides"

ORIGIN
        1 ggcaatttct gagaggcaac aggcggcagg tctcagccta gagagggccc tgaactactt
       61 tgctggagtg tccgtcctgg gagtggctgc tgacccagtc caggagaccc atgcctgcca
      121 tggtccctgg gtggaaccat ggcaacatca cccgctccaa ggcagaggag ctactttcca
      181 gagccggcaa ggacgggagc ttccttgtgc gtgccagcga gtccatcccc cgggcctacg
      241 cactctgcgt gctgttccgg aattgtgttt acacttacag gattctgccc aatgaggacg
      301 ataaattcac tgttcaggca tccgaaggtg tccccatgag gttcttcacg aagctggacc
      361 agctcatcga cttttacaag aaggaaaaca tggggctggt gacccacctg cagtaccccg
      421 tgcccctgga ggaggaggat gctattgatg aggctgagga ggacactgta gaaagtgtca
      481 tgtcaccacc tgagctgcct cccagaaaca ttcctatgtc tgccgggccc agcgaggcca
      541 aggaccttcc tcttgcaaca gagaaccccc gagcccctga ggtcacccgg ctgagtctct
      601 ccgagacact gtttcagcgt ctacagagca tggataccag tgggcttccc gaggagcacc
      661 tgaaagccat ccaggattat ctgagcactc agctcctcct ggattccgac tttttgaaga
      721 cgggctccag caacctccct cacctgaaga agctgatgtc actgctctgc aaggagctcc
      781 atggggaagt catcaggact ctgccatccc tggagtctct gcagaggttg tttgaccaac
      841 agctctcccc aggccttcgc ccacgacctc aggtgcccgg agaggccagt cccatcacca
      901 tggttgccaa actcagccaa ttgacaagtc tgctgtcttc cattgaagat aaggtcaagt
```

```
 961 ccttgctgca cgagggctca gaatctacca acaggcgttc ccttatccct ccggtcacct
1021 ttgaggtgaa gtcagagtcc ctgggcattc ctcagaaaat gcatctcaaa gtggacgttg
1081 agtctgggaa actgatcgtt aagaagtcca aggatggttc tgaggacaag ttctacagcc
1141 acaaaaaaat cctgcagctc attaagtccc agaagtttct aaacaagttg gtgattttgg
1201 tggagacgga gaaggagaaa atcctgagga aggaatatgt ttttgctgac tctaagaaaa
1261 gagaaggctt ctgtcaactc ctgcagcaga tgaagaacaa gcattcggag cagccagagc
1321 ctgacatgat caccatcttc attggcactt ggaacatggg taatgcaccc cctcccaaga
1381 agatcacgtc ctggtttctc tccaaggggc agggaaagac acgggacgac tctgctgact
1441 acatccccca tgacatctat gtgattggca cccaggagga tccccttgga gagaaggagt
1501 ggctggagct actcaggcac tccctgcaag aagtcaccag catgacattt aaaacagttg
1561 ccatccacac cctctggaac attcgcatag tggtgcttgc caagccagag catgagaatc
1621 ggatcagcca tatctgcact gacaacgtga agacaggcat cgccaacacc ctgggaaaca
1681 agggagcagc gggagtgtcc ttcatgttca ttggaacctc cttggggttc gtcaacagcc
1741 acttgacttc tggaagtgaa aaaaagctca ggagaaatca aaactatatg aacatcctgc
1801 ggttcctggc cctgggagac aagaagctaa gcccatttaa catcacccac cgcttcaccc
1861 acctcttctg gcttggggat ctcaactacc gcgtggagct gcccacttgg gaggcagagg
1921 ccatcatcca gaagatcaag caacagcagt attcagacct tctggcccac gaccaactgc
1981 tcctggagag gaaggaccag aaggtcttcc tgcactttga ggaggaagag atcaccttcg
2041 cccccaccta tcgatttgaa agactgaccc gggacaagta tgcatacacg aagcagaaag
2101 caacagggat gaagtacaac ttgccgtcct ggtgcgaccg agtcctctgg aagtcttacc
2161 cgctggtgca tgtggtctgt cagtcctatg gcagtaccag tgacatcatg acgagtgacc
2221 acagccctgt ctttgccacg tttgaagcag gagtcacatc tcaattcgtc tccaagaatg
2281 gtcctggcac tgtagatagc caagggcaga tcgagtttct tgcatgctac gccacactga
2341 agaccaagtc ccagactaag ttctacttgg agttccactc aagctgctta gagagttttg
2401 tcaagagtca ggaaggagag aatgaagagg gaagtgaagg agagctggtg gtacggtttg
2461 gagagactct tcccaagcta aagcccatta tctctgaccc cgagtactta ctggaccagc
2521 atatcctgat cagcattaaa tcctctgaca gtgacgagtc ctatggtgaa ggctgcattg
2581 cccttcgctt ggagaccaca gaggctcagc atcctatcta cacgcctctc acccaccatg
2641 gggagatgac tggccacttc aggggagaga ttaagctgca gacctcccag ggcaagatga
2701 gggagaagct ctatgacttt gtgaagacag agcgggatga atccagtgga atgaaatgct
2761 tgaagaacct caccagccat gaccctatga ggcaatggga gccttctggc agggtccctg
2821 catgtggtgt ctccagcctc aatgagatga tcaatccaaa ctacattggt atggggcctt
2881 ttggacagcc cctgcatggg aaatcaaccc tgtccccaga tcagcaactc acagcttgga
2941 gttatgacca gctacccaaa gactcctccc tggggcctgg gaggggggag ggtcctccaa
3001 cccctccctc ccaaccacct ctgtcgccaa agaagttttc atcttccaca gccaaccgag
3061 gtccctgccc cagggtgcaa gaggcaagac ctggggatct gggaaaggtg gaagctctgc
3121 tccaggagga cctgctgctg acgaagcccg agatgtttga gaacccactg tatggatccg
3181 tgagttcctt ccctaagctg gtgcccagga aagagcagga gtctcccaag atgctgcgga
3241 aggagccccc gccctgtcca gacccaggaa tctcatcacc cagcatcgtg ctccccaaag
3301 cccaagaggt ggagagtgtc aaggggacaa gcaaacaggc ccctgtgcct gtccttggcc
3361 ccacaccccg gatccgctcc tttacctgtt cttcttctgc tgagggcaga atgaccagtg
3421 gggacaagag ccaagggaag cccaaggcct cagccagttc ccaagcccca gtgccagtca
3481 agaggcctgt caagccttcc aggtcagaaa tgagccagca gacaacaccc atcccagctc
3541 cacggccacc cctgccagtc aagagtcctg ctgtcctgca gctgcaacat tccaaaggca
3601 gagactaccg tgacaacaca gaactccccc accatggcaa gcaccgccaa gaggaggggc
3661 tgcttggcag gactgccatg cagtgagctg ctggtgatcg gagcctggag gaacagcaca
3721 aagcagacct gcgcctctct caggatgcct ctctcaggat gcctcttgga ggacctcctg
3781 ctagctcttc ttgcctagct tcaagtccca ggctgtgtat ttttttttcag gaaacggcct
3841 cacttctctg tggtccaaga agtgtgctgc tggctgccac actgtgcggc agatgctaaa
3901 gctggatgac aaacgcacgc catacagaca gcagacagcg gcactgggtc tcagaacttg
3961 gattcctggg ccttcttcca gtcgccgttt taaagaaagg aactaacgga gctgctcatc
4021 cgagggtgaa gatataaata ataatattat taataataat aacagtcagg tgccatgtgc
4081 tgtgttaagt gctttatgaa catttgtcgg gctggcctcc agtgctgagg tgccagtcag
4141 cctgaaccct atgcccaggc ccactaatcc caaatggtgg gtcctgagat gtttttaaaa
4201 agcattaaag aaaaccatcg gtctcttaga gctaaccggc cgggctctac tgcagggacc
4261 cgaacagtct gcatggctaa gtggcacaag gagcctggcc ctgtccagct tcagagatcc
4321 aagctgcttt ttgctggggt tctgtcacag gcctgatcct cttggttttt atggggtttc
4381 aagtctgcca gagtcagaaa tcagctctaa ctcgccagtg aagagatctg gccttaactt
4441 aagccagcca cgtcaggccc ctgctgagcc tatggaccaa taaatactcc ccgtgccact
4501 ggaggtgggc agctatcacc ataccctgag ttgggccaag cccaccccac ccctaccctg
```

```
     4561 caacatttct gatgtwctga ggaagagtct ccaccatagt ccccaagggc tgagttctcc
     4621 agcctgctat cagggaaggt gagcattggt cccaggctct caaaatagtg cagcctcttc
     4681 ttcccaagct ctggggtgca ccctgtgtcc ttggttacca ggagactagg gttgtgatat
     4741 cttttcttgt cttgcttttt gatatatcag gattaatgta ggaaaccaga cctagattat
     4801 tcaggagagt aggtatatcc cctgtgtttc ccagtctgag tgaccaataa aattgtgcct
     4861 ttcta
//
```


Jul 8 2004 07:07:40

Exhibit C

1: NM_005541. Homo sapiens inos...[gi:40254822]

LOCUS NM_005541 5273 bp mRNA linear PRI 08-JUL-2004
DEFINITION Homo sapiens inositol polyphosphate-5-phosphatase, 145kDa (INPP5D), mRNA.
ACCESSION NM_005541
VERSION NM_005541.2 GI:40254822
KEYWORDS .
SOURCE Homo sapiens (human)
ORGANISM Homo sapiens
Eukaryota; Metazoa; Chordata; Craniata; Vertebrata; Euteleostomi; Mammalia; Eutheria; Primates; Catarrhini; Hominidae; Homo.
REFERENCE 1 (bases 1 to 5273)
AUTHORS Krahn,A.K., Ma,K., Hou,S., Duronio,V. and Marshall,A.J.
TITLE Two distinct waves of membrane-proximal B cell antigen receptor signaling differentially regulated by Src homology 2-containing inositol polyphosphate 5-phosphatase
JOURNAL J. Immunol. 172 (1), 331-339 (2004)
PUBMED 14688341
REMARK GeneRIF: SHIP positively, rather than negatively, regulates in vitro membrane recruitment of pleckstrin homology domain-containing signaling proteins Bam32 and TAPP2, which therefore specify a distinct wave of phosphatidylinositol 3-kinase signaling in B cells.
REFERENCE 2 (bases 1 to 5273)
AUTHORS Jiang,X., Stuible,M., Chalandon,Y., Li,A., Chan,W.Y., Eisterer,W., Krystal,G., Eaves,A. and Eaves,C.
TITLE Evidence for a positive role of SHIP in the BCR-ABL-mediated transformation of primitive murine hematopoietic cells and in human chronic myeloid leukemia
JOURNAL Blood 102 (8), 2976-2984 (2003)
PUBMED 12829595
REMARK GeneRIF: SHIP expression appears to be differently altered in the early and late stages of differentiation of BCR-ABL-transformed cells
REFERENCE 3 (bases 1 to 5273)
AUTHORS Baran,C.P., Tridandapani,S., Helgason,C.D., Humphries,R.K., Krystal,G. and Marsh,C.B.
TITLE The inositol 5'-phosphatase SHIP-1 and the Src kinase Lyn negatively regulate macrophage colony-stimulating factor-induced Akt activity
JOURNAL J. Biol. Chem. 278 (40), 38628-38636 (2003)
PUBMED 12882960
REMARK GeneRIF: SHIP-1 and Lyn have roles in the negative regulation of M-CSF-R-induced Akt activation
REFERENCE 4 (bases 1 to 5273)
AUTHORS Galandrini,R., Tassi,I., Mattia,G., Lenti,L., Piccoli,M., Frati,L. and Santoni,A.
TITLE SH2-containing inositol phosphatase (SHIP-1) transiently translocates to raft domains and modulates CD16-mediated cytotoxicity in human NK cells

JOURNAL Blood 100 (13), 4581-4589 (2002)
PUBMED 12393695
REMARK GeneRIF: data demonstrate that CD16 engagement on NK cells induces membrane targeting and activation of SHIP-1, which acts as negative regulator of antibody-dependent cellular cytotoxicity function
REFERENCE 5 (bases 1 to 5273)
AUTHORS Freeburn,R.W., Wright,K.L., Burgess,S.J., Astoul,E., Cantrell,D.A. and Ward,S.G.
TITLE Evidence that SHIP-1 contributes to phosphatidylinositol 3,4,5-trisphosphate metabolism in T lymphocytes and can regulate novel phosphoinositide 3-kinase effectors
JOURNAL J. Immunol. 169 (10), 5441-5450 (2002)
PUBMED 12421919
REMARK GeneRIF: SHIP-1 contributes to degradation of phosphatidylinositol trisphosphate (PI(3,4,5)P3) in T cells and thus influences signaling away from PI(3,4,5)P3-dependent effectors toward effectors that are exclusively driven by phosphatidylinositol 3,4-bisphosphate.
REFERENCE 6 (bases 1 to 5273)
AUTHORS MacDonald,S.M. and Vonakis,B.M.
TITLE Association of the Src homology 2 domain-containing inositol 5' phosphatase (SHIP) to releasability in human basophils
JOURNAL Mol. Immunol. 38 (16-18), 1323-1327 (2002)
PUBMED 12217402
REMARK GeneRIF: Association of SHIP with releasability in human basophils.
REFERENCE 7 (bases 1 to 5273)
AUTHORS Gardai,S., Whitlock,B.B., Helgason,C., Ambruso,D., Fadok,V., Bratton,D. and Henson,P.M.
TITLE Activation of SHIP by NADPH oxidase-stimulated Lyn leads to enhanced apoptosis in neutrophils
JOURNAL J. Biol. Chem. 277 (7), 5236-5246 (2002)
PUBMED 11724799
REMARK GeneRIF: SHIP localization to membrane receptors and subsequent activation along with the observed inability of SHIP -/- neutrophils to exhibit enhanced apoptosis with the stimulus combination.
REFERENCE 8 (bases 1 to 5273)
AUTHORS Vonakis,B.M., Gibbons,S. Jr., Sora,R., Langdon,J.M. and MacDonald,S.M.
TITLE Src homology 2 domain-containing inositol 5' phosphatase is negatively associated with histamine release to human recombinant histamine-releasing factor in human basophils
JOURNAL J. Allergy Clin. Immunol. 108 (5), 822-831 (2001)
PUBMED 11692111
REMARK GeneRIF: implicated as regulator of histamine release in basophils
REFERENCE 9 (bases 1 to 5273)
AUTHORS Geier,S.J., Algate,P.A., Carlberg,K., Flowers,D., Friedman,C., Trask,B. and Rohrschneider,L.R.
TITLE The human SHIP gene is differentially expressed in cell lineages of the bone marrow and blood
JOURNAL Blood 89 (6), 1876-1885 (1997)
PUBMED 9058707
REFERENCE 10 (bases 1 to 5273)
AUTHORS Ware,M.D., Rosten,P., Damen,J.E., Liu,L., Humphries,R.K. and Krystal,G.
TITLE Cloning and characterization of human SHIP, the 145-kD inositol 5-phosphatase that associates with SHC after cytokine stimulation
JOURNAL Blood 88 (8), 2833-2840 (1996)
PUBMED 8874179
REFERENCE 11 (bases 1 to 5273)

AUTHORS Drayer,A.L., Pesesse,X., De Smedt,F., Woscholski,R., Parker,P. and Erneux,C.
TITLE Cloning and expression of a human placenta inositol 1,3,4,5-tetrakisphosphate and phosphatidylinositol 3,4,5-trisphosphate 5-phosphatase
JOURNAL Biochem. Biophys. Res. Commun. 225 (1), 243-249 (1996)
PUBMED 8769125
REFERENCE 12 (bases 1 to 5273)
AUTHORS Kavanaugh,W.M., Pot,D.A., Chin,S.M., Deuter-Reinhard,M., Jefferson,A.B., Norris,F.A., Masiarz,F.R., Cousens,L.S., Majerus,P.W. and Williams,L.T.
TITLE Multiple forms of an inositol polyphosphate 5-phosphatase form signaling complexes with Shc and Grb2
JOURNAL Curr. Biol. 6 (4), 438-445 (1996)
PUBMED 8723348
REFERENCE 13 (bases 1 to 5273)
AUTHORS Damen,J.E., Liu,L., Rosten,P., Humphries,R.K., Jefferson,A.B., Majerus,P.W. and Krystal,G.
TITLE The 145-kDa protein induced to associate with Shc by multiple cytokines is an inositol tetraphosphate and phosphatidylinositol 3,4,5-triphosphate 5-phosphatase
JOURNAL Proc. Natl. Acad. Sci. U.S.A. 93 (4), 1689-1693 (1996)
PUBMED 8643691
COMMENT PROVISIONAL REFSEQ: This record has not yet been subject to final NCBI review. The reference sequence was derived from U57650.1.
On Dec 20, 2003 this sequence version replaced gi:5031798.

FEATURES Location/Qualifiers

source 1..5273
/organism="Homo sapiens"
/mol_type="mRNA"
/db_xref="taxon:9606"
/chromosome="2"
/map="2q36-q37"

gene 1..5273
/gene="INPP5D"
/note="synonym: SHIP"
/db_xref="GeneID:3635"
/db_xref="LocusID:3635"
/db_xref="MIM:601582"

CDS 513..4079
/gene="INPP5D"
/note="hp51CN; inositol polyphosphate-5-phosphatase, 145kD;
go_function: inositol-polyphosphate 5-phosphatase activity [goid 0004445] [evidence TAS] [pmid 8769125];
go_function: inositol/phosphatidylinositol phosphatase activity [goid 0004437] [evidence IEA];
go_process: phosphate metabolism [goid 0006796] [evidence TAS] [pmid 8769125];
go_process: intracellular signaling cascade [goid 0007242] [evidence IEA]"
/codon_start=1
/product="inositol polyphosphate-5-phosphatase, 145kDa"
/protein_id="NP_005532.2"
/db_xref="GI:40254823"
/db_xref="GeneID:3635"
/db_xref="LocusID:3635"
/db_xref="MIM:601582"
/translation="MVPCWNHGNITRSKAEELLSRTGKDGSFLVRASESISRAYALCV
LYRNCVYTYRILPNEDDKFTVQASEGVSMRFFTKLDQLIEFYKKENMGLVTHLQYPVP

LEEEDTGDDPEEDTESVVSPPELPPRNIPLTASSCEAKEVPFSNENPRATETSRPSLS
ETLFQRLQSMDTSGLPEEHLKAIQDYLSTQLAQDSEFVKTGSSSLPHLKKLTTLLCKE
LYGEVIRTLPSLESLQRLFDQQLSPGLRPRPQVPGEANPINMVSKLSQLTSLLSSIED
KVKALLHEGPESPHRPSLIPPVTFEVKAESLGIPQKMQLKVDVESGKLIIKKSKDGSE
DKFYSHKKILQLIKSQKFLNKLVILVETEKEKILRKEYVFADSKKREGFCQLLQQMKN
KHSEQPEPDMITIFIGTWNMGNAPPPKKITSWFLSKGQGKTRDDSADYIPHDIYVIGT
QEDPLSEKEWLEILKHSLQEITSVTFKTVAIHTLWNIRIVVLAKPEHENRISHICTDN
VKTGIANTLGNKGAVGVSFMFNGTSLGFVNSHLTSGSEKKLRRNQNYMNILRFLALGD
KKLSPFNITHRFTHLFWFGDLNYRVDLPTWEAETIIQKIKQQQYADLLSHDQLLTERR
EQKVFLHFEEEEITFAPTYRFERLTRDKYAYTKQKATGMKYNLPSWCDRVLWKSYPLV
HVVCQSYGSTSDIMTSDHSPVFATFEAGVTSQFVSKNGPGTVDSQGQIEFLRCYATLK
TKSQTKFYLEFHSSCLESFVKSQEGENEEGSEGELVVKFGETLPKLKPIISDPEYLLD
QHILISIKSSDSDESYGEGCIALRLEATETQLPIYTPLTHHGELTGHFQGEIKLQTSQ
GKTREKLYDFVKTERDESSGPKTLKSLTSHDPMKQWEVTSRAPPCSGSSITEIINPNY
MGVGPFGPPMPLHVKQTLSPDQQPTAWSYDQPPKDSPLGPCRGESPPTPPGQPPISPK
KFLPSTANRGLPPRTQESRPSDLGKNAGDTLPQEDLPLTKPEMFENPLYGSLSSFPKP
APRKDQESPKMPRKEPPPCPEPGILSPSIVLTKAQEADRGEGPGKQVPAPRLRSFTCS
SSAEGRAAGGDKSQGKPKTPVSSQAPVPAKRPIKPSRSEINQQTPPTPTPRPPLPVKS
PAVLHLQHSKGRDYRDNTELPHHGKHRPEEGPPGPLGRTAMQ"

misc_feature 525..815
/gene="INPP5D"
/note="SH2; Region: Src homology 2 domains"
/db_xref="CDD:16538"

misc_feature 1713..2648
/gene="INPP5D"
/note="IPPc; Region: Inositol polyphosphate phosphatase, catalytic domain homologues"
/db_xref="CDD:25290"

ORIGIN

```
      1 ctagggcatg gcatcccacg tgggtgtcag cacggccgca gaagaaccac ttctctggcc
     61 cacccatgcc tgctaggcca tgcttcttca gaagtggcca caactctcct gacgtctcca
    121 gagccggtca ttccacccag ggggacttca gctgccactg gacacttcaa ttgtacgctg
    181 cgaccagttg ccaggaagga gagggctggc aagaaagccg cggcagccgt ggcagggtgt
    241 atgggacggt ggacggccag ggccccccgc tctctctctt tctctctctc tctcttgctt
    301 ggtttctgta atgaggaagt tctccgcagc tcagtttcct ttccctcact gagcgcctga
    361 aacaggaagt cagtcagtta agctggtggc agcagccgag gccaccaaga ggcaacgggc
    421 ggcaggttgc agtggagggg cctccgctcc cctcggtggt gtgtgggtcc tgggggtgcc
    481 tgccggccca gccgaggagg cccacgccca ccatggtccc ctgctggaac catggcaaca
    541 tcacccgctc caaggcggag gagctgcttt ccaggacagg caaggacggg agcttcctcg
    601 tgcgtgccag cgagtccatc tcccgggcat acgcgctctg cgtgctgtat cggaattgcg
    661 tttacactta cagaattctg cccaatgaag atgataaatt cactgttcag gcatccgaag
    721 gcgtctccat gaggttcttc accaagctgg accagctcat cgagttttac aagaaggaaa
    781 acatggggct ggtgacccat ctgcaatacc ctgtgccgct ggaggaagag gacacaggcg
    841 acgaccctga ggaggacaca gaaagtgtcg tgtctccacc cgagctgccc ccaagaaaca
    901 tcccgctgac tgccagctcc tgtgaggcca aggaggttcc tttttcaaac gagaatcccc
    961 gagcgaccga gaccagccgg ccgagcctct ccgagacatt gttccagcga ctgcaaagca
   1021 tggacaccag tgggcttcca gaagagcatc ttaaggccat ccaagattat ttaagcactc
   1081 agctcgccca ggactctgaa tttgtgaaga cagggtccag cagtcttcct cacctgaaga
   1141 aactgaccac actgctctgc aaggagctct atggagaagt catccggacc ctcccatccc
   1201 tggagtctct gcagaggtta tttgaccagc agctctcccc gggcctccgt ccacgtcctc
   1261 aggttcctgg tgaggccaat cccatcaaca tggtgtccaa gctcagccaa ctgacaagcc
   1321 tgttgtcatc cattgaagac aaggtcaagg ccttgctgca cgagggtcct gagtctccgc
   1381 accggccctc ccttatccct ccagtcacct ttgaggtgaa ggcagagtct ctggggattc
   1441 ctcagaaaat gcagctcaaa gtcgacgttg agtctgggaa actgatcatt aagaagtcca
   1501 aggatggttc tgaggacaag ttctacagcc acaagaaaat cctgcagctc attaagtcac
   1561 agaaatttct gaataagttg gtgatcttgg tggaaacaga gaaggagaag atcctgcgga
   1621 aggaatatgt ttttgctgac tccaaaaaga gagaaggctt ctgccagctc ctgcagcaga
   1681 tgaagaacaa gcactcagag cagccggagc ccgacatgat caccatcttc atcggcacct
   1741 ggaacatggg taacgccccc cctcccaaga agatcacgtc ctggtttctc tccaaggggc
   1801 agggaaagac gcgggacgac tctgcggact acatccccca tgacatttac gtgatcggca
```

```
1861 cccaagagga ccccctgagt gagaaggagt ggctggagat cctcaaacac tccctgcaag
1921 aaatcaccag tgtgactttt aaaacagtcg ccatccacac gctctggaac atccgcatcg
1981 tggtgctggc caagcctgag cacgagaacc ggatcagcca catctgtact gacaacgtga
2041 agacaggcat tgcaaacaca ctggggaaca agggagccgt gggggtgtcg ttcatgttca
2101 atggaacctc cttagggttc gtcaacagcc acttgacttc aggaagtgaa aagaaactca
2161 ggcgaaacca aaactatatg aacattctcc ggttcctggc cctgggcgac aagaagctga
2221 gtccctttaa catcactcac cgcttcacgc acctcttctg gtttggggat cttaactacc
2281 gtgtggatct gcctacctgg gaggcagaaa ccatcatcca aaaaatcaag cagcagcagt
2341 acgcagacct cctgtcccac gaccagctgc tcacagagag gagggagcag aaggtcttcc
2401 tacacttcga ggaggaagaa atcacgtttg ccccaaccta ccgttttgag agactgactc
2461 gggacaaata cgcctacacc aagcagaaag cgacagggat gaagtacaac ttgccttcct
2521 ggtgtgaccg agtcctctgg aagtcttatc ccctggtgca cgtggtgtgt cagtcttatg
2581 gcagtaccag cgacatcatg acgagtgacc acagccctgt ctttgccaca tttgaggcag
2641 gagtcacttc ccagtttgtc tccaagaacg gtcccgggac tgttgacagc caaggacaga
2701 ttgagtttct caggtgctat gccacattga agaccaagtc ccagaccaaa ttctacctgg
2761 agttccactc gagctgcttg gagagttttg tcaagagtca ggaaggagaa aatgaagaag
2821 gaagtgaggg ggagctggtg gtgaagtttg gtgagactct tccaaagctg aagcccatta
2881 tctctgaccc tgagtacctg ctagaccagc acatcctcat cagcatcaag tcctctgaca
2941 gcgacgaatc ctatggcgag ggctgcattg cccttcggtt agaggccaca gaaacgcagc
3001 tgcccatcta cacgcctctc acccaccatg gggagttgac aggccacttc caggggggaga
3061 tcaagctgca gacctctcag ggcaagacga gggagaagct ctatgacttt gtgaagacgg
3121 agcgtgatga atccagtggg ccaaagaccc tgaagagcct caccagccac gaccccatga
3181 agcagtggga agtcactagc agggcccctc cgtgcagtgg ctccagcatc actgaaatca
3241 tcaaccccaa ctacatggga gtggggccct ttgggccacc aatgcccctg cacgtgaagc
3301 agaccttgtc ccctgaccag cagcccacag cctggagcta cgaccagccg cccaaggact
3361 ccccgctggg gccctgcagg ggagaaagtc ctccgacacc tcccggccag ccgcccatat
3421 cacccaagaa gtttttaccc tcaacagcaa accggggtct ccctcccagg acacaggagt
3481 caaggcccag tgacctgggg aagaacgcag gggacacgct gcctcaggag gacctgccgc
3541 tgacgaagcc cgagatgttt gagaaccccc tgtatgggtc cctgagttcc ttccctaagc
3601 ctgctcccag gaaggaccag gaatccccca aaatgccgcg gaaggaaccc ccgccctgcc
3661 cggaacccgg catcttgtcg cccagcatcg tgctcaccaa agcccaggag gctgatcgcg
3721 gcgaggggcc cggcaagcag gtgcccgcgc cccggctgcg ctccttcacg tgctcatcct
3781 ctgccgaggg cagggcggcc ggcggggaca agagccaagg gaagcccaag accccggtca
3841 gctcccaggc cccggtgccg gccaagaggc ccatcaagcc ttccagatcg gaaatcaacc
3901 agcagacccc gcccaccccg acgccgcggc cgccgctgcc agtcaagagc ccggcggtgc
3961 tgcacctcca gcactccaag ggccgcgact accgcgacaa caccgagctc ccgcatcacg
4021 gcaagcaccg gccggaggag gggccaccag ggcctctagg caggactgcc atgcagtgaa
4081 gccctcagtg agctgccact gagtcgggag cccagaggaa cggcgtgaag ccactggacc
4141 ctctcccggg acctcctgct ggctcctcct gcccagcttc ctatgcaagg ctttgtgttt
4201 tcaggaaagg gcctagcttc tgtgtggccc acagagttca ctgcctgtga ggcttagcac
4261 caagtgctga ggctggaaga aaaacgcaca ccagacgggc aacaaacagt ctgggtcccc
4321 agctcgctct tggtacttgg gaccccagtg cctcgttgag ggcgccattc tgaagaaagg
4381 aactgcagcg ccgatttgag ggtggagata tagataataa taatattaat aataataatg
4441 gccacatgga tcgaacactc atgatgtgcc aagtgctgtg ctaagtgctt tacgaacatt
4501 cgtcatatca ggatgacctc gagagctgag gctctagcca cctaaaacac gtgcccaaac
4561 ccaccagttt aaaacggtgt gtgttcggag gggtgaaagc attaagaagc ccagtgccct
4621 cctggagtga gacaagggct cggccttaag gagctgaaga gtctgggtag cttgtttagg
4681 gtacaagaag cctgttctgt ccagcttcag tgacacaagc tgctttagct aaagtcccgc
4741 gggttccggc atggctaggc tgagagcagg gatctacctg gcttctcagt tctttggttg
4801 gaaggagcag gaaatcagct cctattctcc agtggagaga tctggcctca gcttgggcta
4861 gagatgccaa ggcctgtgcc aggttccctg tgccctcctc gaggtgggca gccatcacca
4921 gccacagtta agccaagccc cccaacatgt attccatcgt gctggtagaa gagtctttgc
4981 tgttgctccc gaaagccgtg ctctccagcc tggctgccag ggagggtggg cctcttggtt
5041 ccaggctctt gaaatagtgc agccttttct tcctatctct gtggctttca gctctgcttc
5101 cttggttatt aggagaatag atgggtgatg tctttcctta tgttgctttt tcaacatagc
5161 agaattaatg tagggagcta aatccagtgg tgtgtgtgaa tgcagaaggg aatgcacccc
5221 acattcccat gatggaagtc tgcgtaacca ataaattgtg cctttcttaa aaa
```

//

Jul 8 2004 07:07:40

Exhibit D

Cell, Vol. 101, 25–33, March 31, 2000, Copyright ©2000 by Cell Press

RNAi: Double-Stranded RNA Directs the ATP-Dependent Cleavage of mRNA at 21 to 23 Nucleotide Intervals

Phillip D. Zamore,*# Thomas Tuschl,†# Phillip A. Sharp,‡§ and David P. Bartel§‖
*Department of Biochemistry and Molecular Biology
University of Massachusetts Medical School
Worcester, Massachusetts 01655
†Department of Cellular Biochemistry
Max-Planck-Institute for Biophysical Chemistry
Am Faßberg 11
D-37077 Göttingen
Germany
‡Center for Cancer Research and
§Department of Biology
Massachusetts Institute of Technology
Cambridge, Massachusetts 02139
‖The Whitehead Institute for Biomedical Research
9 Cambridge Center
Cambridge, Massachusetts 02142

Summary

Double-stranded RNA (dsRNA) directs the sequence-specific degradation of mRNA through a process known as RNA interference (RNAi). Using a recently developed *Drosophila* in vitro system, we examined the molecular mechanism underlying RNAi. We find that RNAi is ATP dependent yet uncoupled from mRNA translation. During the RNAi reaction, both strands of the dsRNA are processed to RNA segments 21–23 nucleotides in length. Processing of the dsRNA to the small RNA fragments does not require the targeted mRNA. The mRNA is cleaved only within the region of identity with the dsRNA. Cleavage occurs at sites 21–23 nucleotides apart, the same interval observed for the dsRNA itself, suggesting that the 21–23 nucleotide fragments from the dsRNA are guiding mRNA cleavage.

Introduction

The term RNA interference, or "RNAi," was initially coined by Fire and coworkers (Fire et al., 1998) to describe the observation that double-stranded RNA (dsRNA) can block gene expression when it is introduced into worms (for reviews see Fire, 1999; Hunter, 2000; Hunter, 1999; Montgomery and Fire, 1998; Sharp, 1999; Wagner and Sun, 1998). Their discovery built upon the previous, puzzling observation that sense and antisense RNA (asRNA) were equally effective in suppressing specific gene expression (Guo and Kemphues, 1995), a paradox resolved by the finding that small amounts of dsRNA contaminate sense and antisense preparations (Fire et al., 1998). RNAi has since been discovered in a wide variety of animals, including flies (Kennerdell and Carthew, 1998; Misquitta and Paterson, 1999), trypanosomes (Ngo et al., 1998), planaria (Sánchez-Alvarado and Newmark, 1999), hydra (Lohmann et al., 1999), zebrafish (Wargelius et al., 1999), and mice (Wianny and Zernicka-Goetz, 2000), and appears to be related to gene silencing phenomena in plants ("cosuppression"; Vaucheret et al., 1998; Waterhouse et al., 1998, 1999; Baulcombe, 1999) and the fungus *Neurospora* ("quelling"; Cogoni et al., 1996; Cogoni and Macino, 1999a, 1999b).

RNAi occurs posttranscriptionally and involves mRNA degradation (Montgomery et al., 1998; Ngo et al., 1998). In addition to providing a powerful tool for creating gene-specific phenocopies of loss-of-function mutations, RNAi may also play an important biological role in protecting the genome against instability caused by the accumulation of transposons and repetitive sequences (Ketting et al., 1999; Tabara et al., 1999). In *C. elegans*, dsRNA blocks specific gene expression even when expressed by bacteria fed to the worms (Timmons and Fire, 1998). RNAi in animals may also represent an ancient antiviral response, just as posttranscriptional gene silencing appears to protect plants from viral infection (Baulcombe, 1999; Grant, 1999; Ratcliff et al., 1999). The breadth of RNAi-like processes suggests that RNAi may encompass gene silencing phenomena, including cellular strategies for gene regulation, well beyond the initial observation that dsRNA can produce RNAi.

Genetic screens in both *C. elegans* and *Neurospora* have identified genes required for RNAi (Cogoni and Macino, 1997; Tabara et al., 1999). Mutations in a subset of these genes, including *rde-2*, *rde-3*, *mut-2*, and *mut-7*, permit the mobilization of transposons in the worm germline (Ketting et al., 1999; Tabara et al., 1999; Grishok et al., 2000). A second class of mutants, including the *rde-1* and *rde-4* loci, are defective for RNAi but show no other phenotypic abnormalities (Tabara et al., 1999). The *rde-1* and *rde-4* genes are required for the initiation of heritable RNAi, a phenomenon in which RNAi established by injection of dsRNA in a worm leads to heritable gene silencing in the F2 generation and beyond (Grishok et al., 2000). In contrast, *rde-2* and *mut-7* are not required for the initiation of heritable interference but are required downstream in the tissue where the interference occurs. Mello and colleagues have proposed that *rde-1* and *rde-4* respond to dsRNA by producing a secondary extragenic agent that is used by the downstream genes *rde-2* and *mut-7* to target specific mRNAs for posttranscriptional gene silencing (Grishok et al., 2000). In this view, *rde-1* and *rde-4* act as initiators of RNAi, whereas *rde-2* and *mut-7* are effectors. These authors propose that other stimuli that lead to gene silencing, such as the accumulation of transposons or repetitive DNA in the genome or the introduction of a transgene, are interpreted by a separate set of initiator genes that produce the same secondary extragenic agent.

In *Neurospora*, the *qde-3* gene, which is required for quelling (a form of posttranscriptional silencing in which an endogenous gene is silenced by the introduction of a transgenic copy of the gene), may be an example of an initiator gene that responds to the presence of a transgene (Cogoni and Macino, 1999b). *qde-3* is a member of the RecQ DNA helicase family, which includes

To whom correspondence should be addressed (e-mail: phillip.zamore@umassmed.edu [P. D. Z.], ttuschl@mpibpc.gwdg.de [T. T.]).

the human genes for Bloom's syndrome and Werner's syndrome.

One candidate for the secondary extragenic agent itself is the 25 nucleotide–long RNAs associated with posttranscriptional gene silencing in plants (Hamilton and Baulcombe, 1999). These RNAs, which correspond to both the sense and antisense strands of the silenced gene, are only detected in plants undergoing silencing. The level of expression of these short RNAs also correlates with the extent of gene silencing. It remains to be shown if the 25 nt RNAs are the actual agents or merely the products of gene silencing.

Two other genes implicated in posttranscriptional gene silencing, *qde-1* in *Neurospora* (Cogoni and Macino, 1999a) and *ego-1* in *C. elegans* (Smardon et al., 2000), are homologous to a tomato protein that displays RNA-directed RNA-polymerase activity in vitro (Schiebel et al., 1993a, 1993b, 1998). RNA-directed RNA polymerases have been implicated in the initial formation of the silencing agent or in the amplification of dsRNA. Amplification of injected dsRNA by an endogenous RNA-directed RNA polymerase would help explain how a very small number of dsRNA molecules can inactivate a much larger population of mRNAs and how the dsRNA can apparently persist in the animal for many days and even into subsequent generations. *ego-1* mutants are defective for RNAi for maternally, but not zygotically, expressed mRNAs. Interestingly, *ego-1* is also required for germline development in *C. elegans* (Qiao et al., 1995).

Biochemical analysis of RNAi has become possible with the development of an in vitro *Drosophila* embryo lysate that recapitulates dsRNA-dependent silencing of gene expression (Tuschl et al., 1999). In the in vitro system, dsRNA—but not sense or asRNA—targets a corresponding mRNA for degradation yet does not affect the stability of an unrelated control mRNA. Furthermore, preincubation of the dsRNA in the lysate potentiates its activity for target mRNA degradation, suggesting that the dsRNA must be converted to an active form by binding proteins in the extract or by covalent modification (Tuschl et al., 1999).

Here, we use the in vitro system to analyze the requirements of RNAi and to determine the fate of the dsRNA and the mRNA. RNAi in vitro requires ATP but does not require either mRNA translation or recognition of the 7-methyl-guanosine cap of the targeted mRNA. The dsRNA but not single-stranded RNA is processed in vitro to a population of 21–23 nt species. Deamination of adenosines within the dsRNA does not appear to be required for formation of the 21–23 nt RNAs. Furthermore, we find that the mRNA is cleaved only in the region corresponding to the sequence of the dsRNA and that the mRNA is cleaved at 21–23 nt intervals, strongly suggesting that the 21–23 nt fragments from the dsRNA are targeting the cleavage of the mRNA.

Results and Discussion

RNAi Requires ATP

Drosophila embryo lysates faithfully recapitulate RNAi (Tuschl et al., 1999). Previously, dsRNA-mediated gene silencing was monitored by measuring the synthesis of

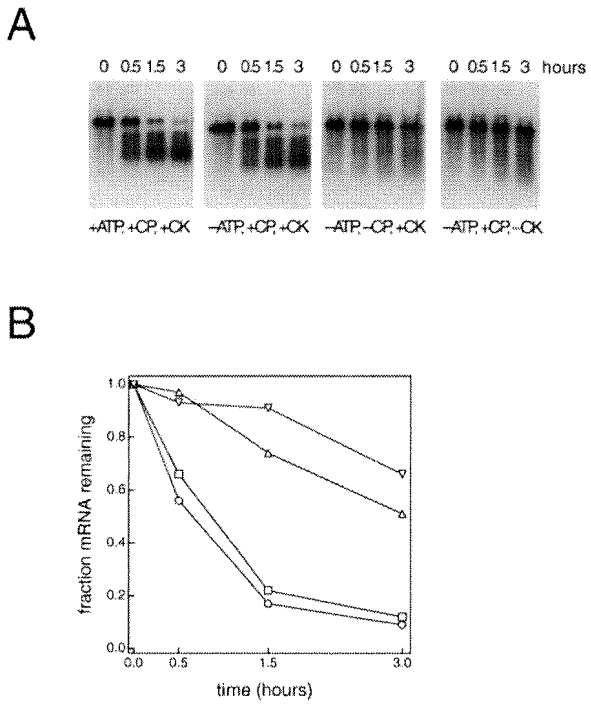

Figure 1. RNAi Requires ATP

(A) Denaturing agarose-gel analysis of 5′-^{32}P-radiolabeled *Rr*-luc mRNA incubated for the times indicated in an in vitro RNAi reaction with or without ATP, creatine phosphate (CP), or creatine kinase (CK), as indicated below each panel.

(B) Quantitation of the data in (A). Circles, +ATP, +CP, +CK; squares, -ATP, +CP, +CK; triangles, -ATP, -CP, +CK; inverted triangles, -ATP, +CP, -CK.

luciferase protein from the targeted mRNA. Thus, these RNAi reactions contained an ATP-regenerating system, needed for the efficient translation of the mRNA. To test if ATP was, in fact, required for RNAi, the lysates were depleted for ATP by treatment with hexokinase and glucose, which converts ATP to ADP, and RNAi was monitored directly by following the fate of ^{32}P-radiolabeled *Renilla reniformis* luciferase (*Rr*-luc) mRNA (Figure 1). Treatment with hexokinase and glucose reduced the endogenous ATP level in the lysate from 250 μM to below 10 μM (data not shown). ATP regeneration required both exogenous creatine phosphate and creatine kinase, which acts to transfer a high-energy phosphate from creatine phosphate to ADP. When ATP-depleted extracts were supplemented with either creatine phosphate or creatine kinase separately, no RNAi was observed. Therefore, RNAi requires ATP in vitro. When ATP, creatine phosphate, and creatine kinase were all added together to reactions containing the ATP-depleted lysate, dsRNA-dependent degradation of the *Rr*-luc mRNA was restored (Figure 1). The addition of exogenous ATP was not required for efficient RNAi in the depleted lysate, provided that both creatine phosphate and creatine kinase were present, demonstrating that the endogenous concentration (250 μM) of adenosine nucleotide is sufficient to support RNAi. RNAi with a *Photinus pyralis* luciferase (*Pp*-luc) mRNA was also ATP dependent (data not shown).

The stability of the *Rr*-luc mRNA in the absence of

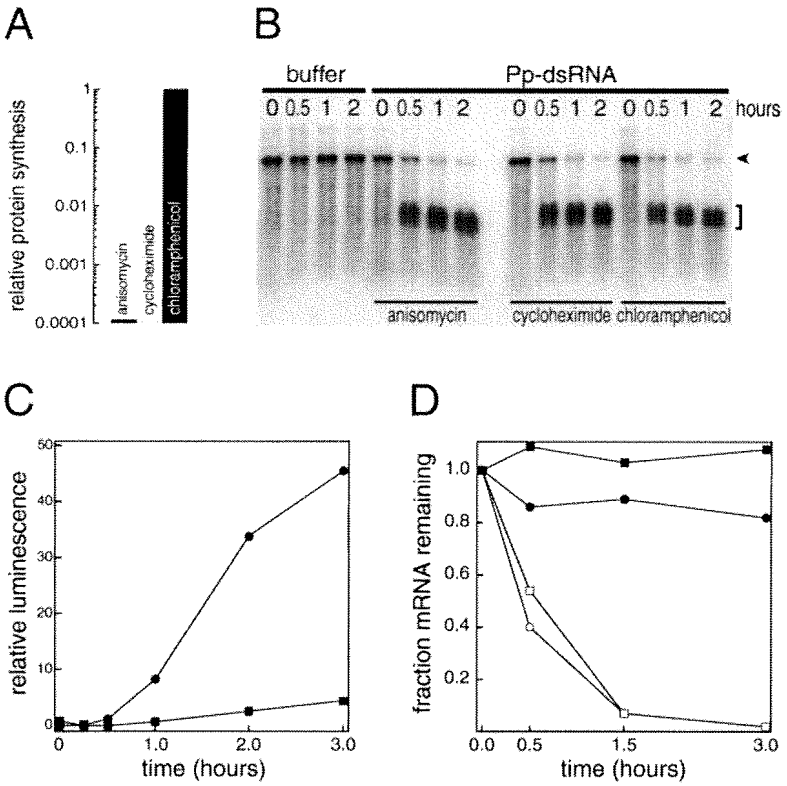

Figure 2. RNAi Does Not Require mRNA Translation

(A) Protein synthesis, as reflected by luciferase activity produced after incubation of *Rr*-luc mRNA in the in vitro RNAi reaction for 1 hr, in the presence of the protein synthesis inhibitors anisomycin, cycloheximide, or chloramphenicol, relative to a reaction without any inhibitor.

(B) Denaturing agarose-gel analysis of 5′-^{32}P-radiolabeled *Pp*-luc mRNA after incubation for the indicated times in a standard RNAi reaction with and without protein synthesis inhibitors. The arrowhead indicates the position of full-length mRNA in the gel, and the bracket marks the position of stable, 5′ cleavage products.

(C) Translation of 7-methyl-guanosine- and adenosine-capped *Pp*-luc mRNAs (circles and squares, respectively) in the RNAi reaction in the absence of dsRNA, as measured by luciferase activity produced in a 1 hr incubation.

(D) Incubation in an RNAi reaction of uniformly ^{32}P-radiolabeled 7-methyl-guanosine-capped *Pp*-luc mRNA (circles) and adenosine-capped *Pp*-luc mRNA (squares), in the presence (open symbols) and absence (filled symbols) of 505 bp *Pp*-luc dsRNA.

Rr-dsRNA was reduced in ATP-depleted lysates relative to that observed when the energy regenerating system was included, but decay of the mRNA under these conditions did not display the rapid decay kinetics characteristic of RNAi in vitro, nor did it generate the stable mRNA cleavage products characteristic of dsRNA-directed RNAi (data not shown). These experiments do not establish if the ATP requirement for RNAi is direct, implicating ATP in one or more steps in the RNAi mechanism, or indirect, reflecting a role for ATP in maintaining high concentrations of another nucleoside triphosphate in the lysate.

Translation Is Not Required for RNAi In Vitro

The requirement for ATP suggested that RNAi might be coupled to mRNA translation, a highly energy-dependent process. To test this possibility, various inhibitors of protein synthesis were added to the reaction. We tested the eukaryotic translation inhibitors anisomycin, an inhibitor of initial peptide bond formation, cycloheximide, an inhibitor of peptide chain elongation, and puromycin, a tRNA mimic that causes premature termination of translation (Cundliffe, 1981). Each of these inhibitors reduced protein synthesis in the *Drosophila* lysate by more than 1,900-fold (Figure 2A; data not shown). In contrast, chloramphenicol, an inhibitor of *Drosophila* mitochondrial protein synthesis (Page and Orr-Weaver, 1997), had no effect on translation in the lysates (Figure 2A). Despite the presence of anisomycin, cycloheximide, or chloramphenicol, RNAi proceeded at normal efficiency (Figure 2B). Puromycin also did not perturb efficient RNAi (data not shown). Thus, protein synthesis is not required for RNAi in vitro.

Translational initiation is an ATP-dependent process that involves recognition of the 7-methyl guanosine cap of the mRNA (Merrick and Hershey, 1996; Kozak, 1999). The *Drosophila* lysate used to support RNAi in vitro also recapitulates the cap dependence of translation: *Pp*-luc mRNA with a 7-methyl-guanosine cap was translated greater than 10-fold more efficiently than was the same mRNA with an A(5′)ppp(5′)G cap (Figure 2C). Both RNAs were equally stable in the *Drosophila* lysate, showing that this difference in efficiency cannot be merely explained by more rapid decay of the mRNA with an adenosine cap (also see Gebauer et al., 1999). Although the translational machinery can discriminate between *Pp*-luc mRNAs with 7-methyl-guanosine and adenosine caps, the two mRNAs were equally susceptible to RNAi in the presence of *Pp*-dsRNA (Figure 2D). These results suggest that steps in cap recognition are not involved in RNAi.

dsRNA Is Processed to 21–23 Nucleotide Species

RNAs 25 nt in length are generated from both the sense and antisense strands of genes undergoing posttranscriptional gene silencing in plants (Hamilton and Baulcombe, 1999). We find that dsRNA is also processed to small RNA fragments (Figures 3A and 3B). When incubated in lysate, approximately 15% of the input radioactivity of both the 501 bp *Rr*-dsRNA and the 505 bp *Pp*-dsRNA appeared in 21 to 23 nt RNA fragments. Because the dsRNAs are more than 500 bp in length, the 15% yield of fragments implies that multiple 21–23 nt RNAs are produced from each full-length dsRNA molecule. No other stable products were detected. The small RNA species were produced from dsRNAs in which both

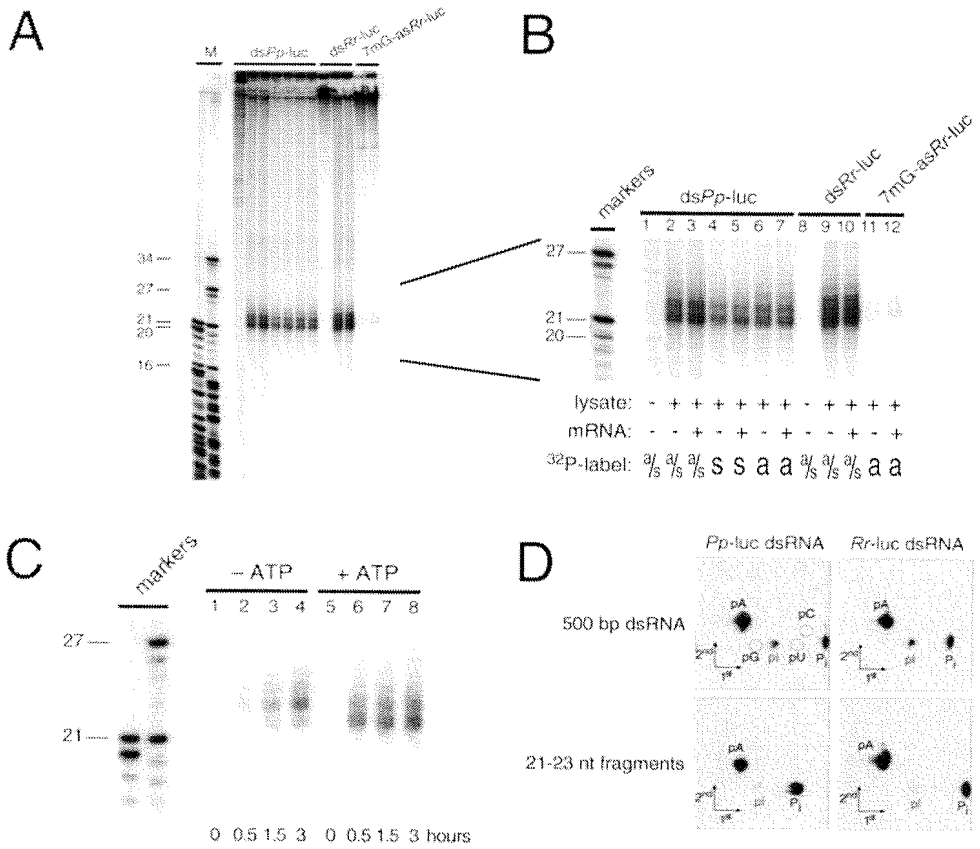

Figure 3. 21–23 nt RNA Fragments Are Produced upon Incubation of dsRNA in *Drosophila* Embryo Lysate

(A) Denaturing acrylamide-gel analysis of the products formed in a 2 hr incubation of uniformly ^{32}P-radiolabeled dsRNAs or capped asRNA in lysate under standard RNAi conditions, in the presence or absence of target mRNAs.

(B) An enlargement of the portion of the gel in (A) corresponding to 17 to 27 nt. For *Pp*-dsRNA, the sense (lanes 4 and 5) or the antisense (lanes 6 and 7) or both strands (lanes 1, 2, and 3) were labeled. For *Rr*-luc dsRNA, both strands were radioactive (lanes 8, 9, and 10).

(C) An enlargement of the 17 to 27 nt region of a gel showing the products formed upon incubation of uniformly ^{32}P-radiolabeled dsRNAs in lysate without and with ATP.

(D) Adenosine deamination in full-length dsRNA and the 21–23 nt RNA species assessed by two-dimensional thin-layer chromatography. Circles correspond to positions of unlabeled 5′-nucleotide monophosphate standards visualized under UV light. Inorganic phosphate (P_i) was produced by the degradation of mononucleotides by phosphatases that contaminate commercially available nuclease P1 (Auxilien et al., 1996).

strands were uniformly ^{32}P-radiolabeled (Figure 3B, lanes 2, 3, 9, and 10). Formation of the 21–23 nt RNAs from the dsRNA did not require the presence of the corresponding mRNA (Figure 3B, compare lane 2 with lane 3 and lane 9 with lane 10), demonstrating that the small RNA species is generated by processing of the dsRNA, rather than as a product of dsRNA-targeted mRNA degradation. We note that 22 nucleotides corresponds to two turns of an A-form RNA–RNA helix.

When dsRNAs radiolabeled within either the sense or the antisense strand were incubated with lysate in a standard RNAi reaction, 21–23 nt RNAs were generated with comparable efficiency (Figure 3B, compare lanes 4 and 6). These data support the idea that the 21–23 nt RNAs are generated by symmetric processing of the dsRNA. A variety of data support the idea that the 21–23 nt RNA is efficiently generated only from dsRNA and is not the consequence of an interaction between single-stranded RNA and the dsRNA. First, a ^{32}P-radiolabeled 505 nt *Pp*-luc sense RNA or asRNA was not efficiently converted to the 21–23 nt product when it was incubated with 5 nM nonradioactive 505 bp *Pp*-dsRNA (data not shown). Second, in the absence of mRNA, a 501 nt 7-methyl-guanosine-capped *Rr*-asRNA produced only a barely detectable amount of 21–23 nt RNA (Figure 3B, lane 11; capped single-stranded RNAs are as stable in the lysate as dsRNA [Tuschl et al., 1999]), probably due to a small amount of dsRNA contaminating the antisense preparation. However, when *Rr*-luc mRNA was included in the reaction with the ^{32}P-radiolabeled, capped *Rr*-asRNA, a small amount of 21–23 nt product was generated, corresponding to 4% of the amount of 21–23 nt RNA produced from an equimolar amount of *Rr*-dsRNA. This result is unlikely to reflect the presence of contaminating dsRNA in the *Rr*-asRNA preparation, since significantly more product was generated from the asRNA in the presence of the *Rr*-luc mRNA than in the absence (compare lanes 12 and 11). Instead, the data suggest that asRNA can interact with the complementary mRNA sequences to form dsRNA in the reaction and that the

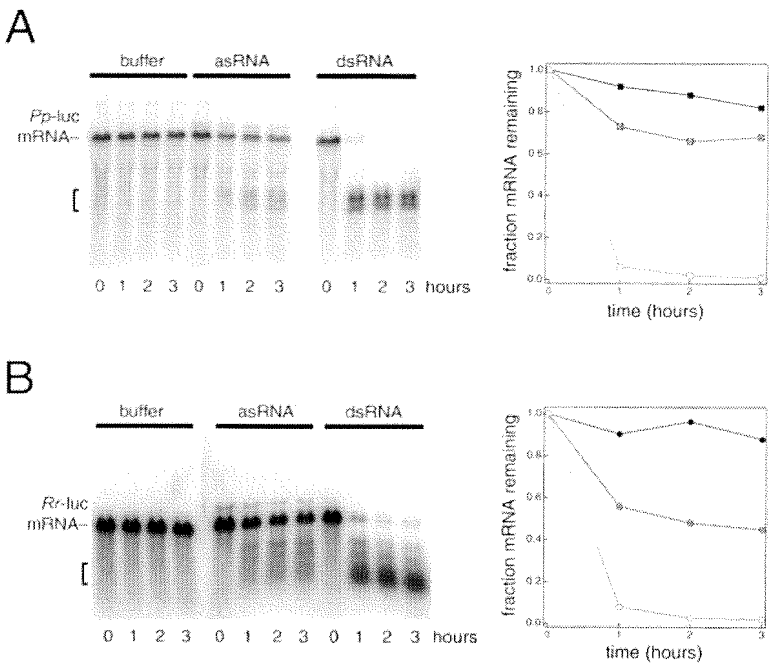

Figure 4. asRNA Causes a Small Amount of RNAi In Vitro

(A) Denaturing agarose-gel analysis of *Pp*-luc mRNA incubated in a standard RNAi reaction with buffer, 505 nt *Pp*-asRNA, or 505 bp *Pp*-dsRNA for the times indicated.

(B) The same analysis for the *Rr*-luc mRNA. Quantitation of the gel data in both (A) and (B) is given to the right of each panel. Buffer, black symbols; asRNA, blue symbols; dsRNA, red symbols.

resulting dsRNA is subsequently processed to the small RNA species. *Rr*-asRNA can support a low level of bona fide RNAi in vitro (see below), consistent with this explanation.

We next asked if production of the 21–23 nt RNAs from dsRNA required ATP (Figure 3C). When the 505 bp *Pp*-dsRNA was incubated in a lysate depleted for ATP by treatment with hexokinase and glucose, 21–23 nt RNA was produced (lanes 1–4, "−ATP"), albeit six times slower than when ATP was regenerated in the depleted lysate by the inclusion of creatine kinase and creatine phosphate (lanes 5–8, "+ ATP"). Therefore, ATP may not be required for production of the 21–23 nt RNA species but may instead simply enhance its formation. Alternatively, ATP may be required for processing of the dsRNA, but at a concentration less than that remaining after hexokinase treatment. We do not yet understand the molecular basis for the slower mobility of the small RNA fragments generated in the ATP-depleted lysate.

Wagner and Sun (1998) and Sharp (1999) have speculated that the requirement for dsRNA in gene silencing by RNAi reflects the involvement of a dsRNA-specific adenosine deaminase in the process. dsRNA adenosine deaminases unwind dsRNA by converting adenosine to inosine, which does not base pair with uracil. dsRNA adenosine deaminases function in the posttranscriptional editing of mRNA (reviewed by Bass, 1997). To test for the involvement of dsRNA adenosine deaminase in RNAi, we examined the degree of conversion of adenosine to inosine in the 501 bp *Rr*-luc and 505 bp *Pp*-luc dsRNAs after incubation with *Drosophila* embryo lysate in a standard in vitro RNAi reaction (Figure 3D). We also determined the degree of adenosine deamination in the 21–23 nt species. The full-length dsRNA radiolabeled with [^{32}P]-adenosine was incubated in the lysate, and both the full-length dsRNA and the 21–23 nt RNA products were purified from a denaturing acrylamide gel, cleaved to mononucleotides with nuclease P1, and analyzed by two-dimensional thin-layer chromatography.

A significant fraction of the adenosines in the full-length dsRNA were converted to inosine after 2 hr (3.1% and 5.6% conversion for *Pp*-luc and *Rr*-luc dsRNAs, respectively). In contrast, only 0.4% (*Pp*-dsRNA) or 0.7% (*Rr*-dsRNA) of the adenosines in the 21–23 nt species were deaminated. These data imply that fewer than 1 in 27 molecules of the 21–23 nt RNA species contain an inosine. Therefore, it is unlikely that dsRNA-dependent adenosine deamination within the 21–23 nt species is required for its production.

asRNA Generates a Small Amount of RNAi In Vitro

When mRNA was ^{32}P-radiolabeled within the 5′-7-methyl-guanosine cap, stable 5′ decay products accumulated during the RNAi reaction (see, for example, Figures 1A and 2B). Such stable 5′ decay products were observed for both the *Pp*-luc and *Rr*-luc mRNAs when they were incubated with their cognate dsRNAs (indicated by the brackets in Figures 4A and 4B). Previously, we reported that efficient RNAi does not occur when asRNA is used in place of dsRNA (Tuschl et al., 1999). Nevertheless, mRNA was measurably less stable when incubated with asRNA than with buffer (Figures 4A and 4B). This was particularly evident for the *Rr*-luc mRNA: approximately 90% of the RNA remained intact after a 3 hr incubation in lysate, but only 50% when asRNA was added. Less than 5% remained when dsRNA was added. Interestingly, the decrease in mRNA stability caused by asRNA was accompanied by the formation of a small amount of the stable 5′ decay products characteristic of the RNAi reaction with dsRNA. This finding parallels the observation that a small amount of 21–23 nt product formed from the asRNA when it was incubated with the mRNA (see above) and lends strength to the idea that asRNA can enter the RNAi pathway, albeit inefficiently.

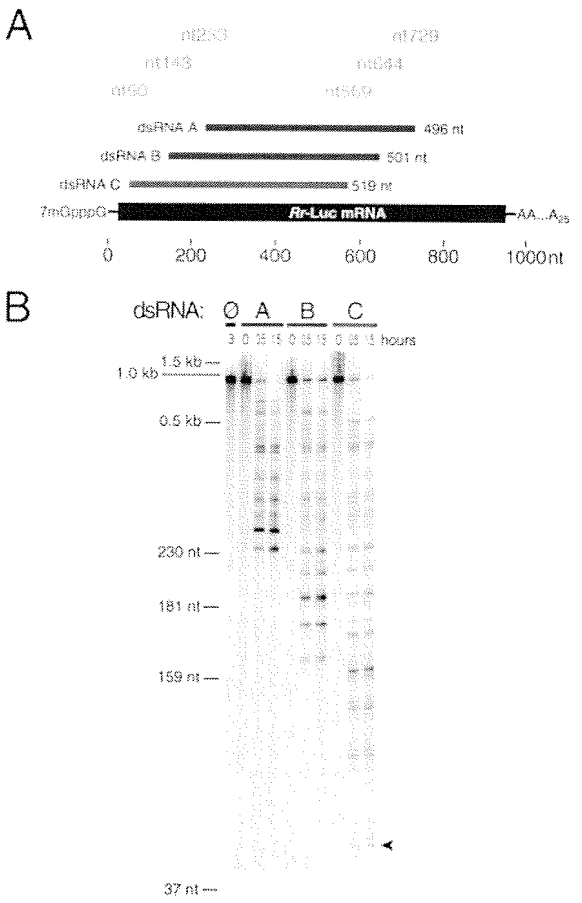

Figure 5. The dsRNA Determines the Boundaries of the Cleavage Products

(A) Schematic of the positions of the three dsRNAs, A, B, and C, relative to the *Rr*-luc mRNA.

(B) Denaturing acrylamide-gel analysis of the stable, 5′ cleavage products produced after incubation of the *Rr*-luc mRNA for the indicated times with each of the three dsRNAs, A, B, and C, or with buffer (zero with strikethrough). The positions of RNA markers radiolabeled within their 5′ cap is shown at left. The arrowhead denotes a faint cleavage site that is indicated with an open blue circle in Figure 6B.

mRNA Cleavage Sites Are Determined by the Sequence of the dsRNA

The sites of mRNA cleavage were examined using three different dsRNAs, "A," "B," and "C," displaced along the *Rr*-luc sequence by approximately 100 nt. The positions of these relative to the *Rr*-luc mRNA sequence are shown (Figure 5A). Each of the three dsRNAs was incubated in a standard RNAi reaction with *Rr*-luc mRNA ^{32}P-radiolabeled within the 5′ cap (Figure 5B). In the absence of dsRNA, no stable 5′ cleavage products were detected for the mRNA, even after 3 hr of incubation in lysate. In contrast, after a 20 min incubation, each of the three dsRNAs produced a ladder of bands corresponding to a set of mRNA cleavage products characteristic for that particular dsRNA. For each dsRNA, the stable, 5′ mRNA cleavage products were restricted to the region of the *Rr*-luc mRNA that corresponded to the dsRNA (Figures 5B and 6). For dsRNA A, the lengths of the 5′ cleavage products ranged from 236 to just under ~750 nt; dsRNA A spans nucleotides 233 to 729 of the *Rr*-luc mRNA. Incubation of the mRNA with dsRNA B produced mRNA 5′ cleavage products ranging in length from 150 to ~600 nt; dsRNA B spans nucleotides 143 to 644 of the mRNA. Finally, dsRNA C produced mRNA cleavage products from 66 to ~500 nt in length. This dsRNA spans nucleotides 50 to 569 of the *Rr*-luc mRNA. Therefore, the dsRNA not only provides specificity for the RNAi reaction, selecting which mRNA from the total cellular mRNA pool will be degraded, but also determines the boundaries of cleavage along the mRNA sequence.

The mRNA Is Cleaved at 21–23 Nucleotide Intervals

To gain further insight into the mechanism of RNAi, we mapped the positions of several mRNA cleavage sites for each of the three dsRNAs (Figure 6). Remarkably, most of the cleavages occurred at 21–23 nt intervals (Figure 6A). This spacing is especially striking in light of our observation that the dsRNA is processed to a 21–23 nt RNA species and the finding of Hamilton and Baulcombe that a 25 nt RNA correlates with posttranscriptional gene silencing in plants (Hamilton and Baulcombe, 1999). Of the 16 cleavage sites we mapped (two for dsRNA A, five for dsRNA B, and nine for dsRNA C), all but two reflect the 21–23 nt interval. One of the two exceptional cleavages was a weak cleavage site produced by dsRNA C (indicated by an arrowhead in Figure 5B and an open blue circle in Figure 6B). This cleavage occurred 32 nt 5′ to the next cleavage site. The other exception is particularly intriguing. After four cleavages spaced 21–23 nt apart, dsRNA C caused cleavage of the mRNA just 9 nt 3′ to the previous cleavage site (Figures 6A and 6B, red arrowhead). This cleavage occurred in a run of seven uracil residues and appears to "reset" the ruler for cleavage; the next cleavage site was 21–23 nt 3′ to the exceptional site. The three subsequent cleavage sites that we mapped were also spaced 21–23 nt apart. Curiously, of the sixteen cleavage sites mapped for the three different dsRNAs, fourteen occur at uracil residues. We do not yet understand the significance of this finding, but it suggests that mRNA cleavage is determined by a process that measures 21–23 nt intervals and that has a sequence preference for cleavage at uracil. In preliminary experiments, the 21–23 nt RNA species produced by incubation of ~500 bp dsRNA in the lysate caused sequence-specific interference in vitro when isolated from an acrylamide gel and added to a new RNAi reaction in place of the full-length dsRNA (our unpublished data).

A Model for dsRNA-Directed mRNA Cleavage

Our biochemical data, together with recent genetic experiments in *C. elegans* and *Neurospora* (Cogoni and Macino, 1999a; Ketting et al., 1999; Tabara et al., 1999; Grishok et al., 2000), suggest a model for how dsRNA targets mRNA for destruction (Figure 7). In this model, the dsRNA is first cleaved to 21 to 23 nt long fragments in a process likely to involve genes such as the *C. elegans* loci *rde-1* and *rde-4*. The resulting fragments, probably as short asRNAs bound by RNAi-specific proteins, would then pair with the mRNA and recruit a nuclease that cleaves the mRNA. Alternatively, strand exchange could occur in a protein–RNA complex that transiently

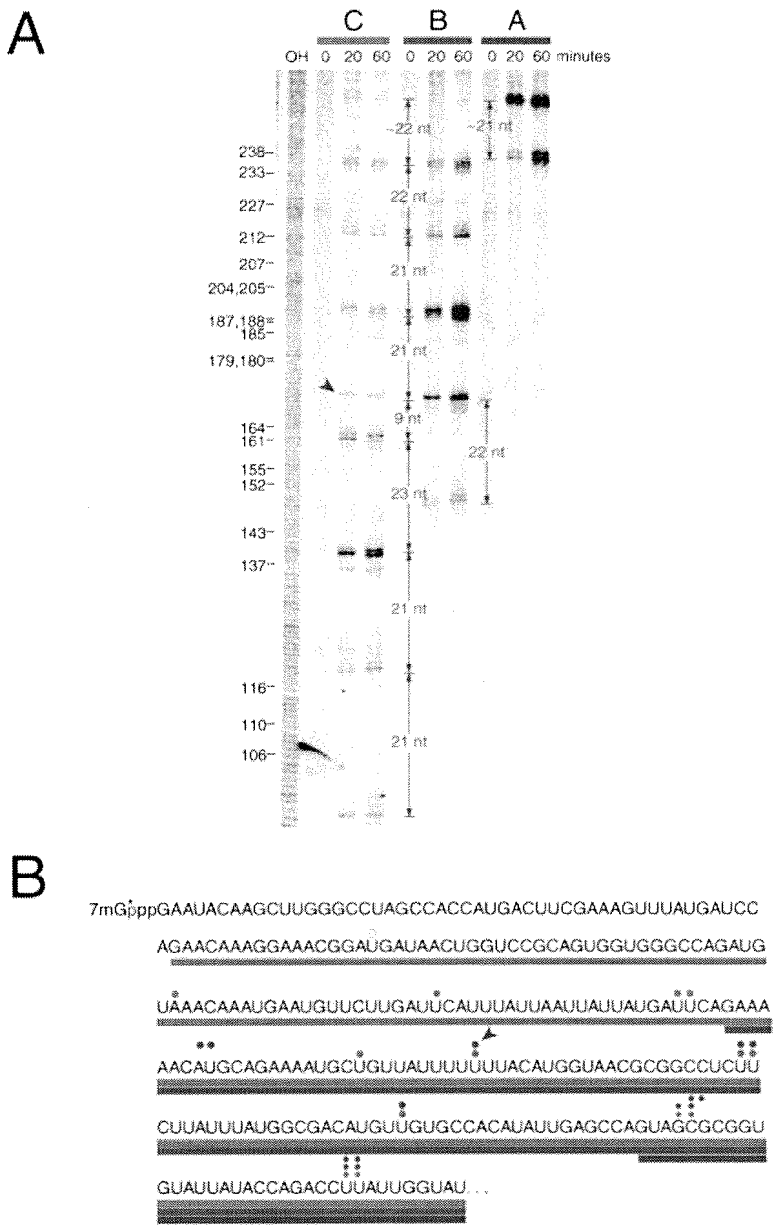

Figure 6. The mRNA Is cleaved in 21–23 nt Intervals

(A) High-resolution denaturing acrylamide-gel analysis of a subset of the 5′ cleavage products described in Figure 5B. The positions of some of the partial T1 digestion products of *Rr*-luc mRNA are indicated at left. "OH" marks the lane in which a partial base-hydrolysis ladder was loaded.

(B) The cleavage sites in (A) mapped onto the first 267 nt of the *Rr*-luc mRNA. The blue bar below the sequence indicates the position of dsRNA C, and blue circles indicate the position of cleavage sites caused by this dsRNA. The green bar denotes the position of dsRNA B, and green circles, the cleavage sites. The magenta bar indicates the position of dsRNA A, and magenta circles, the cleavages. An exceptional cleavage within a run of seven uracils is marked with a red arrowhead in both (A) and (B).

holds a 21–23 nt dsRNA fragment close to the mRNA. Separation of the two strands of the dsRNA following fragmentation might be assisted by an ATP-dependent RNA helicase, explaining the ATP enhancement of 21–23 nt RNA production we observed.

We envision that each small RNA fragment produces one, or at most two, cleavages in the mRNA, perhaps at the 5′ or 3′ ends of the 21–23 nt fragment. The small RNAs may be amplified by an RNA-directed RNA polymerase such as that encoded by the *ego-1* gene in *C. elegans* (Smardon et al., 2000) or the *qde-1* gene in *Neurospora* (Cogoni and Macino, 1999a), producing long-lasting posttranscriptional gene silencing in the absence of the dsRNA that initiated the RNAi effect. Heritable RNAi in *C. elegans* requires the *rde-1* and *rde-4* genes to initiate but not to persist in subsequent generations. The *rde-2*, *rde-3*, and *mut-7* genes in *C. elegans* are required in the tissue where RNAi occurs but are not required for initiation of heritable RNAi (Grishok et al., 2000). These "effector" genes (Grishok et al., 2000) are likely to encode proteins functioning in the actual selection of mRNA targets and in their subsequent cleavage. ATP may be required at any of a number of steps during RNAi, including complex formation on the dsRNA, strand dissociation during or after dsRNA cleavage, pairing of the 21–23 nt RNAs with the target mRNA, mRNA cleavage, and recycling of the targeting complex. Testing these ideas with the in vitro RNAi system will be an important challenge for the future.

Experimental Procedures

In Vitro RNAi

In vitro RNAi reactions and lysate preparation were as described previously (Tuschl et al., 1999) except that the reaction contained 0.03 μg/ml creatine kinase, 25 mM creatine phosphate (Fluka), and 1 mM ATP. Creatine phosphate was freshly dissolved at 500 mM in

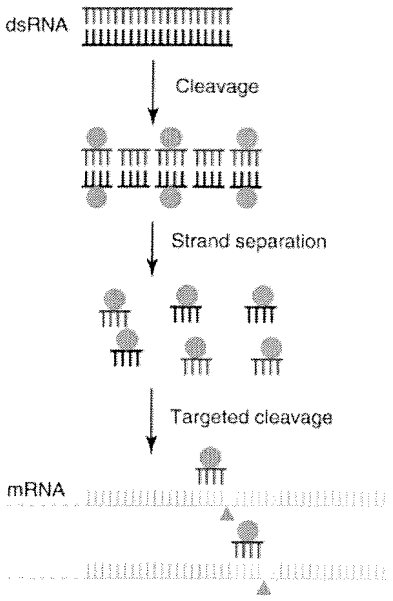

Figure 7. Proposed Model for RNAi

RNAi is envisioned to begin with cleavage of the dsRNA to 21–23 nt products by a dsRNA-specific nuclease, perhaps in a multiprotein complex. These short dsRNAs might then be dissociated by an ATP-dependent helicase, possibly a component of the initial complex, to 21–23 nt asRNAs that could then target the mRNA for cleavage. The short asRNAs are imagined to remain associated with the RNAi-specific proteins (ochre circles) that were originally bound by the full-length dsRNA, thus explaining the inefficiency of asRNA to trigger RNAi in vivo and in vitro. Finally, a nuclease (triangles) would cleave the mRNA.

water for each experiment. GTP was omitted from the reactions, except in Figures 2 and 3.

RNA Synthesis

Pp-luc and *Rr*-luc mRNAs and *Pp*- and *Rr*-dsRNAs (including dsRNA B in Figure 6) were synthesized by in vitro transcription as described previously (Tuschl et al., 1999). To generate transcription templates for dsRNA C, the 5′ sense RNA primer was gcgtaatacgactcactata GAACAAAGGAAACGGATGAT and the 3′ sense RNA primer was GAAGAAGTTATTCTCCAAAA; the 5′ asRNA primer was gcgtaatac gactcactataGAAGAAGTTATTCTCCAAAA and the 3′ asRNA primer was GAACAAAGGAAACGGATGAT. For dsRNA A, the 5′ sense RNA primer was gcgtaatacgactcactataGTAGCGCGGTGTATTATACC and the 3′ sense RNA primer was GTACAACGTCAGGTTTACCA; the 5′ asRNA primer was gcgtaatacgactcactataGTACAACGTCAGGTTT ACCA and the 3′ asRNA primer was GTAGCGCGGTGTATTATACC (lowercase, T7 promoter sequence).

mRNAs were 5′ end labeled using guanylyl transferase (Gibco/BRL), S-adenosyl methionine (Sigma), and α-^{32}P-GTP (3000 Ci/mmol; New England Nuclear) according to the manufacturer's directions. Radiolabeled RNAs were purified by poly(A) selection using the Poly(A) Tract III kit (Promega). Nonradioactive 7-methyl-guanosine- and adenosine-capped RNAs were synthesized in in vitro transcription reactions with a 5-fold excess of 7-methyl-G(5′)ppp(5′)G or A(5′)ppp(5′)G relative to GTP. Cap analogs were purchased from New England Biolabs.

ATP Depletion and Protein Synthesis Inhibition

ATP was depleted by incubating the lysate for 10 min at 25°C with 2 mM glucose and 0.1 U/μl hexokinase (Sigma). Protein synthesis inhibitors were purchased from Sigma and dissolved in absolute ethanol as 250-fold concentrated stocks. The final concentrations of inhibitors in the reaction were anisomycin, 53 μg/ml; cycloheximide, 100 μg/ml; and chloramphenicol, 100 mg/ml. Relative protein synthesis was determined by measuring the activity of *Rr* luciferase protein produced by translation of the *Rr*-luc mRNA in the RNAi reaction after 1 hr as described previously (Tuschl et al., 1999).

Analysis of dsRNA Processing

Internally α-^{32}P-ATP-labeled dsRNAs (505 bp *Pp*-luc or 501 *Rr*-luc) or 7-methyl-guanosine-capped *Rr*-luc antisense RNA (501 nt) were incubated at 5 nM final concentration in the presence or absence of unlabeled mRNAs in *Drosophila* lysate for 2 hr in standard conditions. Reactions were stopped by the addition of 2× proteinase K buffer and deproteinized as described previously (Tuschl et al., 1999). Products were analyzed by electrophoresis in 15% or 18% polyacrylamide sequencing gels. Length standards were generated by complete RNase T1 digestion of α-^{32}P-ATP-labeled 501 nt *Rr*-luc sense RNA and asRNA.

For analysis of mRNA cleavage, 5′-^{32}P-radiolabeled mRNA (described above) was incubated with dsRNA as described previously (Tuschl et al., 1999) and analyzed by electrophoresis in 5% (Figure 5B) and 6% (Figure 6C) polyacrylamide sequencing gels. Length standards included commercially available RNA size standards (FMC Bioproducts) radiolabeled with guanylyl transferase as described above and partial base hydrolysis and RNase T1 ladders generated from the 5′-radiolabeled mRNA.

Deamination Assay

Internally α-^{32}P-ATP-labeled dsRNAs (5 nM) were incubated in *Drosophila* lysate for 2 hr at standard conditions. After deproteinization, samples were run on 12% sequencing gels to separate full-length dsRNAs from the 21–23 nt products. RNAs were eluted from the gel slices in 0.3 M NaCl overnight, ethanol precipitated, collected by centrifugation, and redissolved in 20 μl water. The RNA was hydrolyzed into nucleoside 5′ phosphates with nuclease P1 (10 μl reaction containing 8 μl RNA in water, 30 mM KOAc [pH 5.3], 10 mM $ZnSO_4$, and 10 μg or 3 units nuclease P1, for 3 hr at 50°C). Samples (1 μl) were cospotted with nonradioactive 5′ mononucleotides (0.05 O. D. units [A_{260}] of pA, pC, pG, pI, and pU) on cellulose HPTLC plates (EM Merck) and separated in the first dimension in isobutyric acid/25% ammonia/water (66/1/33, v/v/v) and in the second dimension in 0.1 M sodium phosphate, pH 6.8/ammonium sulfate/1-propanol (100/60/2, v/w/v; Silberklang et al., 1979). Migration of the nonradioactive internal standards was determined by UV shadowing.

Acknowledgments

We acknowledge Heike Taubner, Sayda M. Elbashir, and Winfried Lendeckel for assistance, and Herbert Jäckle and his research group and members of the Bartel laboratory for their support and advice. The authors thank Terri Orr-Weaver for providing fly resources and Marlene Castle for maintaining population cages. This work was supported by a German BMBF Biofuture grant number 0311856 (T. T.), by the National Institutes of Health through a United States Public Health Service MERIT award, the National Science Foundation, and partially by the National Cancer Institute through a Cancer Center Support core grant (P. A. S.), and by the Searle Scholars Program/The Chicago Community Trust (D. P. B.).

Received March 2, 2000; revised March 10, 2000.

References

Auxilien, S., Crain, P.F., Trewyn, R.W., and Grosjean, H. (1996). Mechanism, specificity and general properties of the yeast enzyme catalysing the formation of inosine 34 in the anticodon of transfer RNA. J. Mol. Biol. *262*, 437–458.

Bass, B.L. (1997). RNA editing and hypermutation by adenosine deamination [published erratum appears in Trends Biochem Sci. 1997 Jul;22(7):278]. Trends Biochem. Sci. *22*, 157–162.

Baulcombe, D.C. (1999). Fast forward genetics based on virus-induced gene silencing. Curr. Opin. Plant Biol. *2*, 109–113.

Cogoni, C., and Macino, G. (1997). Isolation of quelling-defective (qde) mutants impaired in posttranscriptional transgene-induced

gene silencing in Neurospora crassa. Proc. Natl. Acad. Sci. USA *94*, 10233–10238.

Cogoni, C., and Macino, G. (1999a). Gene silencing in *Neurospora crassa* requires a protein homologous to RNA-dependent RNA polymerase. Nature *399*, 166–169.

Cogoni, C., and Macino, G. (1999b). Posttranscriptional gene silencing in Neurospora by a RecQ DNA helicase. Science *286*, 2342–2344.

Cogoni, C., Irelan, J.T., Schumacher, M., Schmidhauser, T.J., Selker, E.U., and Macino, G. (1996). Transgene silencing of the al-1 gene in vegetative cells of Neurospora is mediated by a cytoplasmic effector and does not depend on DNA-DNA interactions or DNA methylation. EMBO J. *15*, 3153–3163.

Cundliffe, E. (1981). Antibiotic inhibitors of ribosome function. In The Molecular Basis of Antibiotic Action, E. Gale et al., eds. (New York: Wiley), pp. 402–547.

Fire, A. (1999). RNA-triggered gene silencing. Trends Genet. *15*, 358–363.

Fire, A., Xu, S., Montgomery, M.K., Kostas, S.A., Driver, S.E., and Mello, C.C. (1998). Potent and specific genetic interference by double-stranded RNA in *Caenorhabditis elegans*. Nature *391*, 806–811.

Gebauer, F., Corona, D.F., Preiss, T., Becker, P.B., and Hentze, M.W. (1999). Translational control of dosage compensation in Drosophila by Sex-lethal: cooperative silencing via the 5′ and 3′ UTRs of msl-2 mRNA is independent of the poly(A) tail. EMBO J. *18*, 6146–6154.

Grant, S.R. (1999). Dissecting the mechanisms of posttranscriptional gene silencing: divide and conquer. Cell *96*, 303–306.

Grishok, A., Tabara, H., and Mello, C. (2000). Genetic requirements for inheritance of RNAi in *C. elegans*. Science, in press.

Guo, S., and Kemphues, K.J. (1995). par-1, a gene required for establishing polarity in *C. elegans* embryos, encodes a putative Ser/Thr kinase that is asymmetrically distributed. Cell *81*, 611–620.

Hamilton, A.J., and Baulcombe, D.C. (1999). A species of small antisense RNA in posttranscriptional gene silencing in plants. Science *286*, 950–952.

Hunter, C.P. (1999). A touch of elegance with RNAi. Curr. Biol. *9*, R440–R442.

Hunter, C. (2000). Gene silencing: shrinking the black box of RNAi. Curr. Biol. *10*, R137–R140.

Kennerdell, J.R., and Carthew, R.W. (1998). Use of dsRNA-mediated genetic interference to demonstrate that *frizzled* and *frizzled 2* act in the wingless pathway. Cell *95*, 1017–1026.

Ketting, R.F., Haverkamp, T.H., van Luenen, H.G., and Plasterk, R.H. (1999). Mut-7 of *C. elegans*, required for transposon silencing and RNA interference, is a homolog of Werner syndrome helicase and RNaseD. Cell *99*, 133–141.

Kozak, M. (1999). Initiation of translation in prokaryotes and eukaryotes. Gene *234*, 187–208.

Lohmann, J.U., Endl, I., and Bosch, T.C. (1999). Silencing of developmental genes in Hydra. Dev. Biol. *214*, 211–214.

Merrick, W., and Hershey, J. (1996). The pathway and mechanism of eukaryotic protein synthesis. In Translational Control, J. Hershey et al., eds. (Cold Spring Harbor, NY: Cold Spring Harbor Laboratory Press), pp. 31–69.

Misquitta, L., and Paterson, B.M. (1999). Targeted disruption of gene function in Drosophila by RNA interference (RNA-i): a role for nautilus in embryonic somatic muscle formation. Proc. Natl. Acad. Sci. USA *96*, 1451–1456.

Montgomery, M.K., and Fire, A. (1998). Double-stranded RNA as a mediator in sequence-specific genetic silencing and co-suppression. Trends Genet. *14*, 255–258.

Montgomery, M.K., Xu, S., and Fire, A. (1998). RNA as a target of double-stranded RNA-mediated genetic interference in *Caenorhabditis elegans*. Proc. Natl. Acad. Sci. USA *95*, 15502–15507.

Ngo, H., Tschudi, C., Gull, K., and Ullu, E. (1998). Double-stranded RNA induces mRNA degradation in *Trypanosoma brucei*. Proc. Natl. Acad. Sci. USA *95*, 14687–14692.

Page, A.W., and Orr-Weaver, T.L. (1997). Activation of the meiotic divisions in Drosophila oocytes. Dev. Biol. *183*, 195–207.

Qiao, L., Lissemore, J.L., Shu, P., Smardon, A., Gelber, M.B., and Maine, E.M. (1995). Enhancers of glp-1, a gene required for cell-signaling in Caenorhabditis elegans, define a set of genes required for germline development. Genetics *141*, 551–569.

Ratcliff, F.G., MacFarlane, S.A., and Baulcombe, D.C. (1999). Gene silencing without DNA. RNA-mediated cross-protection between viruses. Plant Cell *11*, 1207–1216.

Sánchez-Alvarado, A., and Newmark, P.A. (1999). Double-stranded RNA specifically disrupts gene expression during planarian regeneration. Proc. Natl. Acad. Sci. USA *96*, 5049–5054.

Schiebel, W., Haas, B., Marinkovic, S., Klanner, A., and Sanger, H.L. (1993a). RNA-directed RNA polymerase from tomato leaves. I. Purification and physical properties. J. Biol. Chem. *268*, 11851–11857.

Schiebel, W., Haas, B., Marinkovic, S., Klanner, A., and Sanger, H.L. (1993b). RNA-directed RNA polymerase from tomato leaves. II. Catalytic in vitro properties. J. Biol. Chem. *268*, 11858–11867.

Schiebel, W., Pelissier, T., Riedel, L., Thalmeir, S., Schiebel, R., Kempe, D., Lottspeich, F., Sanger, H.L., and Wassenegger, M. (1998). Isolation of an RNA-directed RNA polymerase-specific cDNA clone from tomato. Plant Cell *10*, 2087–2101.

Sharp, P.A. (1999). RNAi and double-strand RNA. Genes Dev. *13*, 139–141.

Silberklang, M., Gillum, A.M., and RajBhandary, U.L. (1979). Use of in vitro ^{32}P labeling in the sequence analysis of nonradioactive tRNAs. Methods Enzymol. *59*, 58–109.

Smardon, A., Spoerke, J., Stacey, S., Klein, M., Mackin, N., and Maine, E. (2000). EGO-1 is related to RNA-directed RNA polymerase and functions in germ-line development and RNA interference in *C. elegans*. Curr. Biol. *10*, 169–178.

Tabara, H., Sarkissian, M., Kelly, W.G., Fleenor, J., Grishok, A., Timmons, L., Fire, A., and Mello, C.C. (1999). The rde-1 gene, RNA interference, and transposon silencing in *C. elegans*. Cell *99*, 123–132.

Timmons, L., and Fire, A. (1998). Specific interference by ingested dsRNA. Nature *395*, 854.

Tuschl, T., Zamore, P.D., Lehmann, R., Bartel, D.P., and Sharp, P.A. (1999). Targeted mRNA degradation by double-stranded RNA in vitro. Genes Dev. *13*, 3191–3197.

Vaucheret, H., Beclin, C., Elmayan, T., Feuerbach, F., Godon, C., Morel, J.B., Mourrain, P., Palauqui, J.C., and Vernhettes, S. (1998). Transgene-induced gene silencing in plants. Plant J. *16*, 651–659.

Wagner, R., and Sun, L. (1998). Functional genomics: double-stranded RNA poses puzzle. Nature *391*, 744–745.

Wargelius, A., Ellingsen, S., and Fjose, A. (1999). Double-stranded RNA induces specific developmental defects in zebrafish embryos. Biochem. Biophys. Res. Commun. *263*, 156–161.

Waterhouse, P.M., Graham, M.W., and Wang, M.B. (1998). Virus resistance and gene silencing in plants can be induced by simultaneous expression of sense and antisense RNA. Proc. Natl. Acad. Sci. USA *95*, 13959–13964.

Waterhouse, P.M., Smith, N.A., and Wang, M.-B. (1999). Virus resistance and gene silencing: killing the messenger. Trends Plant Sci. *4*, 452–457.

Wianny, F., and Zernicka-Goetz, M. (2000). Specific interference with gene function by double-stranded RNA in early mouse development. Nat. Cell Biol. *2*, 70–75.

Note Added in Proof

Recently, Hammond et al. have shown that ~25 nt RNAs are generated in cultured *Drosophila* S2 cells transfected with *cyclin E* dsRNA (Hammond, S.M., Bernstein, E., Beach, D., and Hannon, G.J. [2000]. Nature *404*, 293–296.

Exhibit E

Development 127, 4147-4156 (2000)
Printed in Great Britain © The Company of Biologists Limited 2000
DEV3227

Selective reduction of dormant maternal mRNAs in mouse oocytes by RNA interference

Petr Svoboda*, Paula Stein*, Harutoshi Hayashi and Richard M. Schultz‡

Department of Biology, University of Pennsylvania, Philadelphia, PA 19104-6018, USA
*These authors contributed equally to this work
‡Author for correspondence (e-mail: rschultz@mail.sas.upenn.edu)

Accepted 17 July; published on WWW 7 September 2000

SUMMARY

Specific mRNA degradation mediated by double-stranded RNA (dsRNA), which is termed RNA interference (RNAi), is a useful tool with which to study gene function in several systems. We report here that in mouse oocytes, RNAi provides a suitable and robust approach to study the function of dormant maternal mRNAs. *Mos* (originally known as c-*mos*) and tissue plasminogen activator (tPA, *Plat*) mRNAs are dormant maternal mRNAs that are recruited during oocyte maturation; translation of *Mos* mRNA results in the activation of MAP kinase. dsRNA directed towards *Mos* or *Plat* mRNAs in mouse oocytes effectively results in the specific reduction of the targeted mRNA in both a time- and concentration-dependent manner. Moreover, dsRNA is more potent than either sense or antisense RNAs. Targeting the *Mos* mRNA results in inhibiting the appearance of MAP kinase activity and can result in parthenogenetic activation. *Mos* dsRNA, therefore, faithfully phenocopies the *Mos* null mutant. Targeting the *Plat* mRNA with *Plat* dsRNA results in inhibiting production of tPA activity. Finally, effective reduction of the *Mos* and *Plat* mRNA is observed with stoichiometric amounts of *Mos* and *Plat* dsRNA, respectively.

Key words: Maternal mRNA, RNA interference, mouse oocyte, *Mos*, *Plat*

INTRODUCTION

'Omne vivum ex ovo' (All living things come from eggs), which is attributed to William Harvey, is probably the first articulation of the current view that the program for early development is established during oogenesis. During oogenesis in the mouse, oocytes grow and acquire the ability to resume and complete meiosis (acquisition of meiotic competence) (Sorensen and Wassarman, 1976; Wickramasinghe et al., 1991), as well as the ability to be fertilized and develop to term (acquisition of developmental competence) (Eppig and O'Brien, 1996). Meiotic maturation and egg activation are accompanied by the recruitment of many maternal mRNAs (Schultz et al., 1979; Schultz and Wassarman, 1977; Van Blerkom, 1981), and presumably some of these direct the synthesis of proteins that are required for the formation of a fertilizable egg that is capable of developing to term. One such mRNA is the *Mos* mRNA. The mobilization of the *Mos* mRNA results in the ultimate activation of mitogen-activated protein (MAP) kinase, whose activity is required to maintain arrest at metaphase II (Gebauer and Richter, 1997; Sagata, 1997); oocytes lacking the *Mos* gene mature to metaphase II but then undergo spontaneous activation, i.e., they emit the second polar body and form a pronucleus (Colledge et al., 1994; Hasimoto et al., 1994). The tissue plasminogen activator (tPA, *Plat*) mRNA is another maternal mRNA that is recruited during oocyte maturation (Huarte et al., 1987; Vassalli et al., 1989). Although tPA is synthesized during maturation and secreted following fertilization, and then becomes associated with a cell-surface receptor on the embryo (Carroll et al., 1993), *Plat* knockout mice are viable and fertile, but do display mild perturbations in phenotype, e.g., retardation in neuronal migration (Seeds et al., 1999).

To date, an antisense RNA approach has been the most widely used method to assess the function of maternal mRNAs that are recruited during oocyte maturation. Nevertheless, this approach has problems. For example, an antisense RNA approach has been used to assess the role of *Mos* mRNA recruitment during maturation. The phenotypes observed range from permitting germinal vesicle breakdown but inhibiting emission of the first polar body (Paules et al., 1989; Zhao et al., 1991), to emission of the first polar body but entering interphase instead of proceeding to and arresting at metaphase II (O'Keefe et al., 1989). In contrast, the phenotype of a *Mos* null mutant generated by homologous recombination is that the oocytes proceed to metaphase II, but meiotic arrest is not maintained and the eggs spontaneously undergo parthenogenetic activation (Colledge et al., 1994; Hasimoto et al., 1994). This discrepancy between the phenotypes observed by the antisense approach with that of a 'true' knockout potentially confounds the use of antisense RNA to study the function of a dormant maternal mRNA. Antisense RNA can

also target and destroy the *Plat* mRNA. The efficacy of destruction of the untranslated *Plat* mRNA, however, appears restricted to antisense RNA directed towards the 3′ UTR (Strickland et al., 1988). Antisense RNAs directed at other portions of the *Plat* mRNA are far less effective and can form hybrids only following maturation and the concomitant recruitment of the *Plat* mRNA. Thus, the efficacy of this approach is compromised by the appropriate selection of the region of the mRNA to be targeted, and this can only be determined experimentally and not a priori.

Recently, RNA interference (RNAi), which employs double-stranded RNA (dsRNA), has been shown to ablate potently the targeted mRNA in a variety of species (Sanchez-Alvardado and Newmark, 1999; Fire et al., 1998; Kennerdell and Carthew, 1998; Li et al., 2000; Lohmann et al., 1999; Misquitta and Paterson, 1999; Ngo et al., 1998; Wargelius et al., 1999). The destruction of the targeted mRNA by dsRNA occurs prior to translation (Fire, 1999; Montgomery et al., 1998; Sharp, 1999; Zamore et al., 2000), and targets exon sequences; dsRNA directed against intron sequences is ineffective (Fire et al., 1998). Genetic approaches in *Caenorhabditis elegans* have identified genes with homology to eIF-2C, RNase D, and RNA-directed RNA polymerase (Ketting et al., 1999; Tabara et al., 1999; Smardon et al., 2000) that are involved in the RNAi-mediated pathway of mRNA degradation. Very recent studies suggest that a nuclease involved in the destruction of the targeted mRNA contains an essential RNA component containing approx. 25-nucleotide RNAs that are homologous to the dsRNA (Hammond et al., 2000). The processing of the dsRNA to these fragments does not require the presence of the targeted mRNA, and the targeted mRNA is cleaved only in the regions of identity to the dsRNA and at sites that are 21-23 nucleotides apart (Zamore et al., 2000).

We report here that dsRNA directed towards *Mos* and *Plat* mRNAs in mouse oocytes effectively results in the specific reduction of the targeted mRNA in both a time- and concentration-dependent manner. Moreover, dsRNA is more potent than either sense or antisense RNA. Targeting the *Mos* mRNA results in inhibiting the appearance of MAP kinase activity, as well as promoting parthenogenetic activation of the treated cells, and targeting *Plat* mRNA results in inhibiting production of tPA activity. Effective reduction of the *Mos* and *Plat* mRNA is observed with stoichiometric amounts of *Mos* and *Plat* dsRNA, respectively. While these studies were in progress, a paper appeared that has reported that oocytes injected with *Mos* dsRNA undergo egg activation, as evidenced by pronucleus formation (Wianny and Zernicka-Goetz, 2000).

MATERIALS AND METHODS

dsRNA preparation

For *Mos* amplification, a pair of primers was designed based on the cDNA sequence (Accession number J00372). The sequence of upstream *Mos* primer was 5′-CCATCAAGCAAGTAAACAAG-3′ and the downstream *Mos* primer was 5′-AGGGTGATTCCAAAAGA-GTA-3′. These primers generated a PCR product that was 535 bp in length and corresponded to the 3′ end of the coding region and the beginning of the 3′UTR. Likewise, for *Plat* amplification a pair of primers was designed based on the cDNA sequence (Accession number J03520). The sequence of the upstream *Plat* primer was 5′-CATGGGCAAGCGTTACACAG-3′ and the downstream *Plat* primer was 5′-CAGAGAAGAATGGAGACGAT-3′. These primers generated a PCR product that was 650 bp in length and corresponded to the middle part of the coding region.

To generate template for transcription in vitro, 5 μg of liver total RNA were reverse transcribed with Superscript II reverse transcriptase (Gibco BRL) according to the manufacturer's instructions using oligo-dT as the primer. PCR amplification conditions for both *Mos* and *Plat* were as follows: initial denaturation at 94°C for 4 minutes was followed by 36 cycles of 94°C for 30 seconds, 60°C for 30 seconds, 72°C for 1 minute and the final cycle had an extended incubation at 72°C for 7 minutes followed by decrease to 4°C. All PCR reactions were performed in either a PE2400 or PE9600 PCR thermocycler.

Gel-purified primary PCR products were diluted 1:500 and re-amplified to produce specific templates to generate sense and antisense transcripts by transcription in vitro. To do this, primers were made that contained an SP6 promoter attached to the 5′ end of both the forward and reverse primers. Following PCR under the above conditions, the secondary PCR products were purified using a Nucleospin Extraction Kit (Clontech). The template (500-1000 ng) was then transcribed with SP6 RNA polymerase (Promega) in order to obtain the corresponding sense and antisense RNAs.

The in vitro transcription products were resolved following electrophoresis in 1.5% NuSieve LM agarose (FMC, Rockland, ME, USA) and the bands corresponding to the sense and antisense single-stranded RNA were purified according to the manufacturer's protocol. Equimolar amounts of sense and antisense RNA were then annealed in 1 mM Tris-HCl (pH 7.5), containing 1 mM EDTA, or in DEPC-treated water supplemented with 5% RNasin (Promega); similar results were obtained using either procedure. Typically, 2-4 μg of RNA in 30 μl were mixed and heated in 500 ml of boiling water for 1 minute. The sample, still in the water bath, was allowed to cool to room temperature over the course of several hours. The dsRNA was phenol extracted, ethanol precipitated, washed in 75% ethanol and then dissolved in water. Samples were stored in water at −80°C prior to use.

RNA isolation and RT-PCR

RNA was isolated from oocytes and prepared for RT-PCR as previously described (Temeles et al., 1994). In each case, 0.125 pg of rabbit β-globin mRNA/oocyte was added prior to RNA isolation. The globin mRNA serves as an internal standard for the efficiency of the RT-PCR reactions (Temeles et al., 1994). For each set of gene-specific primers the linear region of semi-log plots of the amount of PCR product as a function of cycle number was determined and a cycle number for each primer pair was selected that was in this linear range; the amount of PCR product under these conditions is proportional to the number of cells used (Manejwala et al., 1991). This method permits the comparison of relative changes in the abundance of a particular transcript (Ho et al., 1995; Latham et al., 1994; Temeles et al., 1994).

Following reverse transcription two oocyte equivalents were used as a template for each PCR reaction. PCR products were labeled with [α-^{32}P]dCTP (Amersham, 0.25 μCi per 50 μl reaction). PCR amplification conditions for both *Mos* and *Plat* were as follows: initial denaturation at 94°C for 2 minutes was followed by 28 (*Plat*) or 31 (*Mos*) cycles of 94°C for 30 seconds, 60°C for 30 seconds and 72°C for 1 minute, followed by 4°C until the samples were removed. PCR amplification conditions for globin: initial denaturation at 94°C for 2 minutes was followed by 24 cycles of 94°C for 10 seconds and 62°C for 15 seconds followed by final 4°C. After PCR, the products were subjected to electrophoresis in an 8% polyacrylamide gel. The gel was dried under vacuum for 1 hour at 80°C, exposed in phosphorimager cassette for 4 to 24 hours and the signal was quantified using the Storm 860 PhosphorImager and ImageQuant software (Molecular Dynamics, Sunnyvale, CA, USA).

Oocyte collection, microinjection and culture

Fully grown, germinal vesicle (GV)-intact oocytes were obtained from pregnant mare's serum gonadotropin (PMSG)-primed six-week-old female CF-1 mice (Harlan) and freed of attached cumulus cells, as previously described (Schultz et al., 1983). The collection medium was bicarbonate-free minimal essential medium (Earle's salt) supplemented with polyvinylpyrrolidone (3 mg/ml) and 25 mM Hepes, pH 7.3. Germinal vesicle breakdown was inhibited by including 0.2 mM 3-isobutyl-1-methyl-xanthine (IBMX). The oocytes were transferred into CZB medium (Chatot et al., 1989) containing 0.2 mM IBMX (CZB+IBMX) and cultured in an atmosphere of 5% CO_2 in air at 37°C. Oocytes were microinjected in bicarbonate-free CZB containing 10 mM Hepes and 0.2 mM IBMX with 5 pl of the corresponding solution; the injections were performed as previously described (Kurasawa et al., 1989). The concentration of the undiluted stock solution was 0.2 μg/μl and injection of 5 pl of either *Mos* or *Plat* dsRNA corresponds to 1.7×10^6 and 1.4×10^6 molecules, respectively. When single-stranded RNA was injected, it was diluted to a concentration such that injection of 5 pl corresponded to the same number of molecules as when dsRNA was injected. In experiments in which either enzyme activity or phenotype was assayed, microinjected oocytes were cultured in CZB+IBMX for 10 or 20 hours. They were then washed through ten drops of IBMX-free CZB and cultured in CZB until oocyte collection and lysis. In experiments in which mRNA levels were measured, the oocytes were kept in medium containing IBMX for 10, 20, or 40 hours until they were collected and processed for RNA isolation.

tPA assay

tPA activity was assayed by zymography of single oocytes. Immobilon-P (Millipore) was soaked in methanol for 1 minute and then rinsed four times with 50 mM Tris-HCl (pH 8.0) containing 50 mM NaCl. The wet membrane was placed on Whatman paper soaked with this buffer and both were transferred to a 96-well dot blot apparatus (Milliblot Systems, Millipore) with the Immobilon-P facing upwards. A 96-well template was then placed on the stage and single oocytes were transferred in 1-2 μl of CZB medium to the middle of where the wells would form. The apparatus was completely assembled and the wet membrane with the oocytes was then exposed to vacuum suction for 2 minutes. The apparatus was then disassembled and the membrane was immediately applied on the detection gel; the detection gel, which contained 40 μg/ml of plasminogen (Fluka), was prepared as previously described (Vassalli et al., 1984). Zymograms were developed for 12-64 hours at 37°C, scanned with a black background and the lysed area was estimated using the ImageQuant software (Molecular Dynamics).

Histone H1 and MBP kinase assay

The activities of both histone H1 and myelin basic protein (MBP) kinases were determined in single eggs as follows: single eggs were transferred in 1.5 μl of culture medium into a tube containing 3.5 μl of double kinase lysis buffer (10 μg/ml aprotinin, 10 μg/ml leupeptin, 10 mM *p*-nitrophenyl phosphate, 20 mM β-glycerophosphate, 0.1 mM sodium orthovanadate, and 5 mM EGTA). The tubes were immediately frozen on dry ice and stored at −80°C until the assay was performed. The kinase reaction was initiated by the addition of 5 μl of double kinase buffer (24 mM *p*-nitrophenyl phosphate, 90 mM β-glycerophosphate, 24 mM $MgCl_2$, 24 mM EGTA, 0.2 mM EDTA, 4.6 mM sodium orthovanadate, 4 mM NaF, 1.6 mM dithiothreitol, 60 μg/ml aprotinin, 60 μg/ml leupeptin, 2 mg/ml polyvinyl alcohol, 2.2 μM protein kinase A inhibitor peptide (Sigma), 40 mM 3-(n-morpholino) propanesulfonic acid (MOPS), pH 7.2, 0.6 mM ATP, 2 mg/ml histone (type III-S, Sigma), 0.5 mg/ml MBP) with 500 μCi/ml [γ-^{32}P]ATP (3000 Ci/mmol; Amersham). To determine the background level of phosphorylation for H1 and MBP, 5 μl of double kinase lysis buffer was added instead of the egg lysate. The reaction was conducted for 30 minutes at 30°C and terminated by the addition of 10 μl double-strength concentrated SDS-PAGE sample buffer (Laemmli, 1970) and boiling for 3 minutes. Following SDS-PAGE, the 15% gel was fixed in 10% acetic acid/30% methanol, dried and exposed to a phosphorimager screen for 16 to 24 hours. Scanning and quantification of the signal were performed using a Storm 860 PhosphorImager and ImageQuant software (Molecular Dynamics, Inc., Sunnyvale, CA). For each experiment, the mean value of H1 or MBP kinase activities for oocytes microinjected with sense *Mos* RNA was arbitrarily set as 100% and the values obtained in the other groups of eggs were expressed relative to this amount.

RESULTS

Preparation of dsRNA

dsRNA for either *Mos* or *Plat* was prepared by hybridizing equimolar amounts of gel-purified, single-stranded sense and antisense transcripts that were generated by transcription in vitro of appropriate templates containing an SP6 promoter. In each case, the RNA was directed towards a coding portion of the transcript. Following hybridization, the single-stranded RNAs were essentially totally converted to dsRNA, as evidenced by the absence of any visible staining in the region of the gel that corresponded to single-stranded species (Fig. 1). The quantitative nature of hybridization permitted use of the dsRNA without any need for gel purification of the dsRNA species.

Effect of *Mos* and *Plat* dsRNA on *Mos* and *Plat* mRNA levels in mouse oocytes

Mos and *Plat* are two maternal mRNAs that are recruited during oocyte maturation (see Introduction). We selected to target the *Mos* mRNA since a *Mos* null oocyte has a defined phenotype, i.e., the oocyte matures to metaphase II, but rather than arresting at metaphase II, it undergoes spontaneous egg activation. In addition, it is possible to measure MAP kinase activity in a single oocyte; MAP kinase activity reflects the mobilization of *Mos* mRNA (see below). We also selected to target *Plat* mRNA, which like *Mos*, is a moderately abundant mRNA; it has been estimated that an oocyte contains approx. 10,000 transcripts each of *Mos* and *Plat* (Huarte et al., 1987;

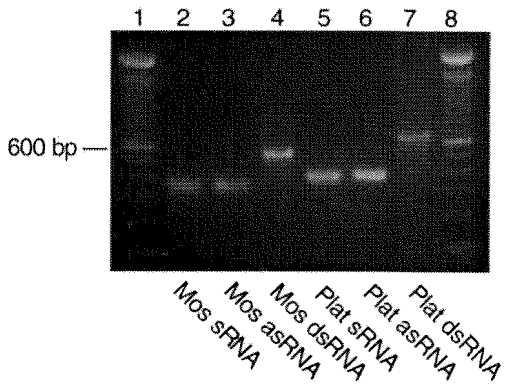

Fig. 1. Generation of *Mos* or *Plat* dsRNA. Sense or antisense *Mos* or *Plat* RNAs were produced by transcription in vitro and then gel purified. Equimolar concentrations of sense and antisense RNA were then hybridized and a portion of the reaction analyzed by electrophoresis. Shown is an ethidium bromide-stained gel demonstrating the quantitative formation of dsRNA. Lanes 1 and 8, 100 bp ladder.

Keshet et al., 1988). In addition, it is also possible to measure tPA activity in single oocytes.

Oocytes were injected with approx. 10^6 molecules of either *Plat* or *Mos* dsRNA that was directed towards the coding region of each transcript; this corresponds to approx. 10 nM final concentration (see Discussion). The oocytes were then cultured in medium containing IBMX to inhibit resumption of meiosis; a decrease in cAMP is associated with resumption of meiosis and including the membrane-permeable phosphodiesterase inhibitor IBMX in the medium prevents the decrease in cAMP and thus the resumption of meiosis (Schultz et al., 1983). Following culture, RNA was isolated and the relative amount of *Plat* and *Mos* transcripts were determined by a semi-quantitative RT-PCR assay that permits quantification of relative changes in transcript abundance. Prior to RNA isolation, a known amount of rabbit globin mRNA was added; this served as a control for RNA recovery, and for the efficiency of the RT-PCR (Temeles et al., 1994).

Oocytes injected with *Mos* dsRNA displayed a marked reduction in the amount of *Mos* transcript (approx. 80%), relative to water-injected or uninjected controls (Fig. 2, compare lane 2 with lanes 4 and 5). Likewise, oocytes injected with *Plat* dsRNA displayed an approx. 90% reduction in the amount of *Plat* transcript relative to the control (Fig. 2, lane 3). Specificity of this effect was demonstrated by the finding that *Mos* dsRNA did not reduce the abundance of *Plat* mRNA, and reciprocally, that *Plat* dsRNA did not reduce the abundance of *Mos* mRNA (Fig. 2). Results of these experiments indicated that the machinery for RNAi-mediated degradation of the targeted endogenous mRNA is present and functions in mouse oocytes.

Effect of *Mos* and *Plat* sense and antisense RNA on *Mos* and *Plat* mRNA levels in mouse oocytes

In other systems, antisense RNA can be ineffective. For example, injection of *C. elegans* with antisense RNA directed towards the *unc*-22 gene does not result in the mutant twitching phenotype, whereas dsRNA does (Fire et al., 1998). Nevertheless, antisense RNA can be effective in degrading oocyte mRNAs (Strickland et al., 1988). Accordingly, we determined the effect of sense and antisense *Mos* and *Plat* RNA on targeting the cognate oocyte transcript.

Oocytes were injected with approx. 10^6 copies of either sense, antisense or dsRNA, and incubated for 20 hours in medium containing IBMX, before the RNA was isolated and transcript abundance determined. As anticipated, dsRNA directed towards either *Mos* or *Plat* mRNA resulted in the reduction of the targeted mRNA, whereas the untargeted transcript remained essentially intact (Fig. 3A). As also anticipated, injection of sense RNA resulted in little, if any, decrease in the abundance of either the targeted or nontargeted mRNA. Injection of either *Mos* or *Plat* antisense RNA, however, did result in a decrease in the targeted, but not in the nontargeted, mRNA (Fig. 3A). Little, if any decrease in the targeted mRNA was observed when the amount of injected *Mos* or *Plat* antisense RNA was decreased by 10-fold (Fig. 3B). In contrast, this amount of dsRNA was effective in decreasing the amount of the targeted mRNA (Fig. 3B), e.g., the *Mos* dsRNA resulted in an approx. 85% decrease in *Mos* mRNA, and *Plat* dsRNA resulted in an approx. 30% decrease in *Plat* mRNA. Results of these experiments suggest that dsRNA is more effective in targeting mRNAs than antisense RNA.

Concentration- and time-dependence of dsRNA directed towards *Mos* and *Plat* mRNAs

In the experiments described above, the oocytes were injected

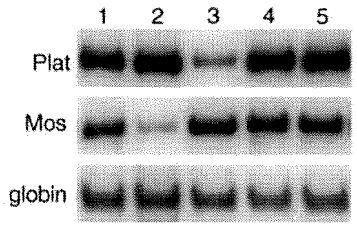

Fig. 2. Effect of *Mos* and *Plat* dsRNA on the relative abundance of *Mos* and *Plat* transcripts. Oocytes were injected with approx. 10^6 molecules of either *Mos* or *Plat* dsRNA and then cultured in the presence of IBMX for 20 hours. RNA was isolated and the relative amount of *Mos* and *Plat* transcripts were determined by RT-PCR, as described in Materials and Methods. The intensity of the globin band permits comparison of the different lanes, as it normalizes for RNA recovery, and for the efficiency of the RT-PCR part of the assay. Lane 1, relative amount of transcripts present in uninjected oocytes at t=0 hours; lane 2, relative amount of transcripts at t=20 hours in oocytes injected with *Mos* dsRNA; lane 3, relative amount of transcripts at t=20 hours in oocytes injected with *Plat* dsRNA; lane 4, relative amount of transcripts at t=20 hours in water-injected oocytes; lane 5, relative amount of transcripts at t=20 hours in uninjected oocytes.

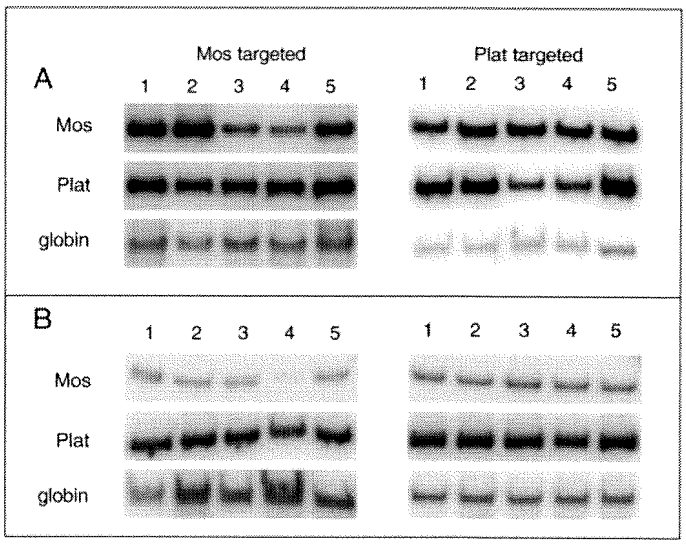

Fig. 3. Effect of *Mos* and *Plat* sense, antisense, and dsRNA on the relative abundance of *Mos* and *Plat* transcripts. (A) Oocytes were injected with approx. 10^6 molecules of either *Mos* or *Plat* sense, antisense or dsRNA and then cultured in the presence of IBMX for 20 hours. RNA was then isolated and the relative amount of *Mos* and *Plat* transcripts were determined by RT-PCR as described in the Materials and Methods. (B) Oocytes were injected with 10^5 molecules of either *Mos* or *Plat* sense, antisense or dsRNA and then processed as described in A. Lane 1, relative amount of transcripts present in water-injected oocytes; lane 2, relative amount of transcripts in sense RNA-injected oocytes; lane 3, relative amount of transcripts in antisense RNA-injected oocytes; lane 4, relative amount of transcripts in dsRNA-injected oocytes; lane 5, relative amount of transcripts in uninjected oocytes.

with approx. 10^6 molecules of dsRNA and cultured for 20 hours prior to determining the relative amount of targeted transcript. In order to determine further characteristics of the RNAi effect, the concentration- and time-dependence of this effect were determined. Oocytes were injected with 10^6, 10^4, or 10^2 molecules of either *Mos* or *Plat* dsRNA, and then incubated for 10, 20, or 40 hours prior to determining the relative abundance of the endogenous *Mos* and *Plat* transcripts (Fig. 4). For both *Mos* and *Plat* dsRNA-injected oocytes, the targeted message was destroyed in both a time- and concentration-dependent manner. In all cases, the nontargeted mRNA was not destroyed (data not shown).

Injection of 10^6 or 10^4 molecules of *Mos* dsRNA resulted in a substantial reduction in the amount of *Mos* mRNA, such that by 20 hours more than 75% of the mRNA was degraded; 10^2 molecules of injected *Mos* dsRNA had little, if any effect over the 40-hour timecourse. Although 10^6 molecules of injected *Plat* dsRNA also dramatically reduced the amount of *Plat* mRNA, the kinetics of *Plat* mRNA degradation were slower, when compared with those obtained for *Mos* dsRNA. In addition, 10^4 molecules of *Plat* dsRNA was not nearly effective as 10^4 molecules of *Mos* dsRNA. Similar to *Mos* dsRNA, the 100 molecules of injected *Plat* dsRNA was ineffective in reducing the amount of *Plat* mRNA.

Effect of Mos dsRNA on MAP kinase and p34^{cdc2}/cyclin B kinase activities

The experiments described above documented that both *Mos* and *Plat* dsRNA could result in the degradation of the targeted mRNA in a concentration- and time-dependent manner. We next demonstrated that the reduction of the targeted mRNA resulted in loss of formation of the encoded protein. The translation of *Mos* mRNA that initiates at the onset of oocyte maturation results in synthesis of MOS, which in turn activates MAP kinase kinase by phosphorylation (Gebauer and Richter, 1997; Sagata, 1997). MAP kinase kinase, which is a dual-specificity kinase, then phosphorylates MAP kinase on Thr183 and Tyr185 in the mammal, which in turn results in MAP kinase activation (Nishida and Gotoh, 1993). MAP kinase, which is a component of cytostatic factor (CSF) and is required to maintain metaphase II arrest, is frequently assayed by measuring the phoshorylation of MBP. Concomitant with germinal vesicle breakdown is the activation of p34^{cdc2}/cyclin B kinase (MPF) (Gebauer and Richter, 1997; Sagata, 1997), which is routinely assayed by phosphorylation of histone H1. In the mouse, MPF activation precedes MAP kinase activation by about 1-2 hours, and both activities reach maximal levels in the metaphase II-arrested egg (Verlhac et al., 1993). Following fertilization, MPF activity declines prior to MAP kinase activity (Moos et al., 1995; Verlhac et al., 1993).

Oocytes were injected with either *Mos* dsRNA, antisense RNA or sense RNA and cultured for 20 hours in IBMX-containing medium, then transferred to IBMX-free medium. The oocytes then matured to metaphase II, at which time both MAP and p34^{cdc2}/cyclin B kinase activities were assayed simultaneously in single eggs. As expected, sense RNA did not inhibit either kinase activity when compared with uninjected or water-injected eggs (data not shown). In contrast, both *Mos* antisense and dsRNA inhibited MAP kinase activity, although a greater degree of inhibition was observed with dsRNA (Fig. 5). This result was consistent with *Mos* dsRNA eliciting a greater decrease in *Mos* mRNA than *Mos* antisense RNA (Fig. 3). Although *Mos* antisense RNA did inhibit MAP kinase activity, the level of p34^{cdc2}/cyclin B kinase, i.e., histone H1 kinase, was reduced by only about 25% relative to control sense-injected or uninjected oocytes, while a 70% decrease was observed in the dsRNA-injected oocytes. This reduced amount of histone H1 kinase activity in the dsRNA-injected oocytes

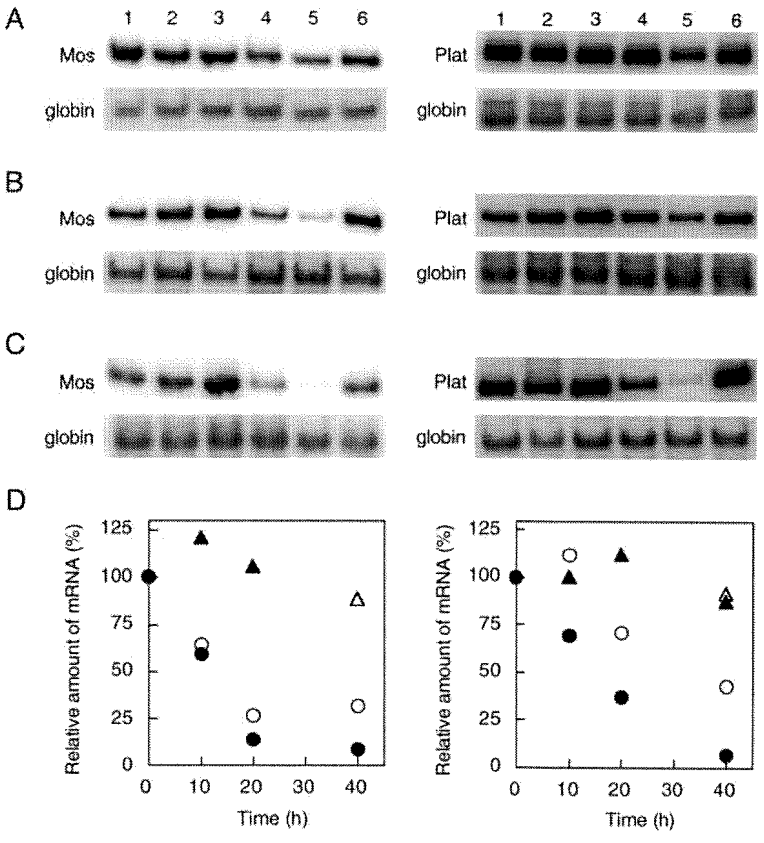

Fig. 4. Concentration- and time-dependence of *Mos* and *Plat* dsRNA-mediated reduction of the targeted mRNA. Oocytes were injected with 10^2 (lane 3), 10^4 (lane 4) or 10^6 (lane 5) molecules of either *Mos* or *Plat* dsRNA, and the relative abundance of either the *Mos* or *Plat* transcript was assayed after either 10 hours (A), 20 hours (B) or 40 hours (C) of culture in medium containing IBMX. Lane 1, relative amount of transcripts present in uninjected oocytes at t=0; lane 2, relative amount of transcripts in water-injected oocytes; lane 6, relative amount of transcripts in uninjected oocytes. (D) Quantification of the relative amount of *Mos* or *Plat* transcripts. The data are normalized to the amount present in the uninjected oocytes at the appropriate time following culture in IBMX-containing medium and all data are normalized to the globin signal, i.e., the ratio of the pixel volume of the transcript to that of the globin is set as 100%. (●), 10^6 molecules injected; (○), 10^4 molecules injected; (▲), 10^2 molecules injected; (△), the amount of *Plat* transcript present in oocytes injected with 10^6 molecules of *Mos* dsRNA or the amount of *Mos* transcript in oocytes injected with 10^6 molecules of *Plat* dsRNA. In order to keep the y-axis of similar scale, the value for oocytes injected with 10^2 molecules of *Mos* dsRNA and analyzed at 40 hours is not shown.

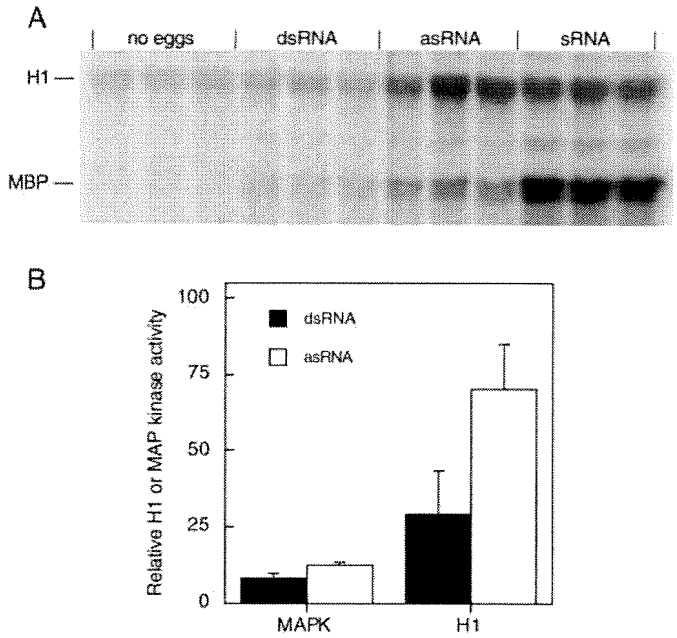

Fig. 5. Effect of *Mos* sense, antisense, and dsRNA on MAP kinase and MPF activities. Oocytes were injected with 10^6 molecules of either *Mos* sense (s), antisense (as) or dsRNA (ds), and then incubated for 20 hours in IBMX-containing medium. The oocytes were then transferred to IBMX-free medium and allowed to mature to metaphase II (about 18 hours), at which time single oocytes were assayed for both MAP kinase activity and MPF activity using MBP and histone H1, respectively as substrates. (A) Region of autoradiogram showing where phosphorylated histone H1 and MBP migrate. (B) Relative amount of kinase activity. The data have been normalized to that present in oocytes injected with sense RNA and this value does not differ from uninjected oocytes (data not shown). The data are expressed as the mean±s.e.m. and represent a total of 15, 15 and 13 dsRNA-, asRNA- and sRNA-injected oocytes, respectively.

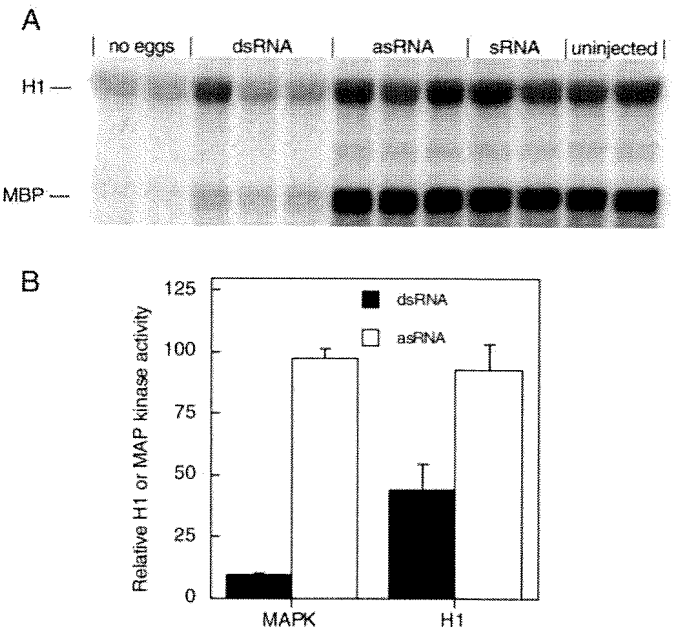

Fig. 6. Effect of *Mos* sense, antisense and dsRNA on MAP kinase and MPF activities. Oocytes were injected with 10^5 molecules of either *Mos* sense (s), antisense (as) or dsRNA (ds) and the experiment was then conducted as described in the legend to Fig. 5. (A) Region of autoradiogram showing where phosphorylated histone H1 and MBP migrate. (B) Relative amount of kinase activity. The data have been normalized to that present in oocytes injected with sense RNA and this value does not differ from uninjected oocytes. The data are expressed as the mean±s.e.m. and represent a total of 10, 10 and 6 dsRNA-, asRNA- and sRNA-injected oocytes.

was a consequence that in numerous cases these eggs underwent spontaneous egg activation, which results in a decrease in histone H1 kinase activity. In contrast, the antisense-injected oocytes never underwent egg activation.

Although *Mos* antisense RNA, which did result in a decrease in *Mos* mRNA, could inhibit MAP kinase activation, the results presented in Fig. 3 indicate that dsRNA is a more potent inhibitor than antisense RNA. Accordingly, oocytes were injected with 1/10 the amount of *Mos* sense, antisense, or dsRNA, cultured for 20 hours in IBMX-containing medium and then matured to metaphase II by transferring them to IBMX-free medium. The eggs were then assayed for both MAP and $p34^{cdc2}$/cyclin B kinase activities simultaneously in individual eggs. Whereas both *Mos* sense and antisense RNA did not inhibit the appearance of MAP kinase activity ($p34^{cdc2}$/cyclin B kinase activity was also high in these eggs), *Mos* dsRNA still elicited a dramatic inhibition in MAP kinase activity, and a corresponding decease in $p34^{cdc2}$/cyclin B kinase activity (Fig. 6). These results strengthen the conclusion that *Mos* dsRNA is more potent than *Mos* antisense RNA in promoting the reduction of the endogenous *Mos* mRNA.

Effect of Plat dsRNA on tPA activity

tPA is synthesized during oocyte maturation and its activity can be assayed in single oocytes by zymography (Huarte et al., 1985, 1987; Strickland et al., 1988). We observed only a single band (M_r 72,000) when metaphase II-arrested eggs were used; no activity was observed in GV-stage oocytes (data not shown). The presence of a single activity responsible for generating the lytic zone permitted analysis of tPA activity by simply spotting an oocyte/egg on a membrane, which was then overlaid with an agarose gel containing non-fat dry milk and plasminogen. The area of the lytic zone was linear as a function of time after a lag, which probably reflected the time to activate the zymogen cascade and degrade enough substrate to be visible to the eye (Fig. 7).

We assayed the effect of *Plat* sense, antisense and dsRNA on tPA activity in matured oocytes. Oocytes were injected with approx. 10^6 molecules of each RNA and cultured in IBMX-containing medium for 20 hours prior to initiating maturation by transfer to IBMX-free medium. Culture for 18 hours resulted in the production of metaphase II-arrested eggs that were then assayed for tPA activity. Injection of either antisense RNA or dsRNA resulted in a dramatic reduction in the amount of tPA activity, when compared with sense-injected oocytes (Fig. 8, black bars). The ability of *Plat* antisense RNA to inhibit the production of tPA activity following maturation is consistent with its ability to target the destruction of *Plat* mRNA (see Fig. 3A and Strickland et al., 1988), as well as its ability to inhibit translation of the *Plat* mRNA (Strickland et al., 1988). Nevertheless, injection of *Plat* sense RNA also modestly inhibited the production of tPA activity, although to

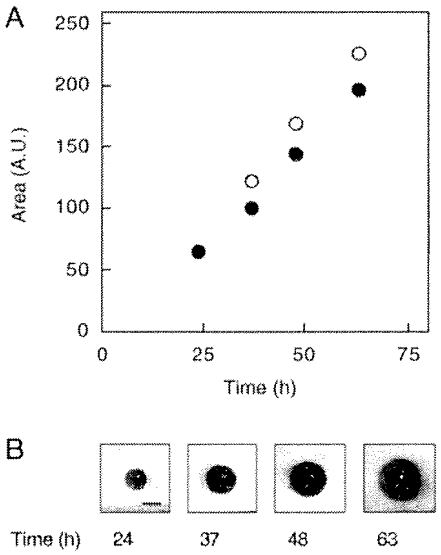

Fig. 7. Zymographic assay of tPA activity in single eggs. (A) Time-dependent increase in the area of the lytic zone of two eggs. (B) Photomicrographs of the lytic zone as a function of time of a single egg. Scale bar: 3 mm.

a lesser extent than either *Plat* antisense or dsRNA (Fig. 8, black bars). We observed that *Mos* sense RNA, which doesn't target the *Plat* mRNA, also resulted in a 50% decrease in tPA activity but had no inhibitory effect on the activation of MAP kinase (data not shown). The molecular basis underlying this inhibitory effect of sense RNA on the generation of tPA activity remains unresolved.

The results presented in Fig. 3 indicated that *Plat* dsRNA was more potent than *Plat* antisense RNA in targeting the reduction of endogenous *Plat* mRNA. As expected, a ten-fold dilution of *Plat* antisense RNA resulted in levels of tPA activity

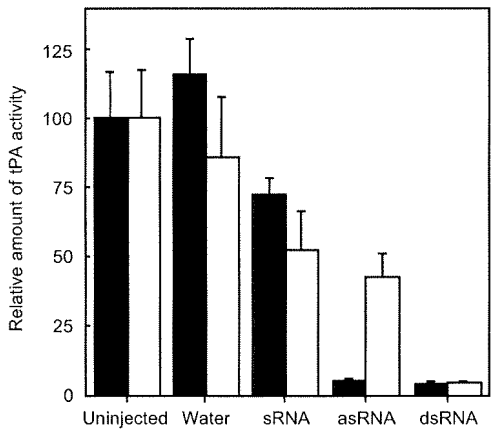

Fig. 8. Effect of *Plat* sense (s), antisense (as) and dsRNA (ds) on the appearance of tPA activity following oocyte maturation. Black bars, injection of approx. 10^6 molecules of RNA; white bars, injection of approx. 10^5 molecules of RNA. The value obtained in the uninjected oocytes was taken as 100% and the other samples are expressed relative to this amount. The data are expressed as the mean±s.e.m. and typically 5-12 eggs were assayed. The experiment was performed three times and similar results were obtained in each case; a representative experiment is shown.

similar to that of sense-injected oocytes, whereas injection of *Plat* dsRNA still promoted a dramatic inhibition (Fig. 8, white bars). Similar to the results obtained with *Mos* dsRNA, these results confirmed that *Plat* dsRNA was more potent than *Plat* antisense RNA in promoting the reduction of the endogenous *Plat* mRNA.

DISCUSSION

We have demonstrated that RNAi is an effective and efficient method to inhibit the translation of maternal mRNAs that are recruited during oocyte maturation. The reduction of the targeted mRNA, namely *Mos* and *Plat*, is specific, i.e., a nontargeted mRNA is not destroyed, and is both time- and concentration-dependent; mRNA levels can be decreased by up to 90%. In addition, dsRNA is more effective than antisense RNA. The reduction of *Mos* mRNA led to a failure in MAP kinase activation that normally accompanies oocyte maturation. A consequence of this failure is that metaphase II arrest was not maintained and that the eggs underwent parthenogenetic activation with the concomitant decrease in H1 kinase activity. Likewise, reduction of the endogenous *Plat* mRNA inhibited the production of tPA following oocyte maturation. A recent report also found that injection of *Mos* dsRNA results in parthenogenetic activation of mouse eggs (Wianny and Zernicka-Goetz, 2000); it was not shown in that study, however, that the *Mos* RNA is selectively degraded and that MAP kinase failed to activate. In the mouse, RNAi, which entails microinjection of the dsRNA, should prove far superior to antisense approaches that have been used in the past, but with variable success. It should be noted that culture of oocytes in medium containing either *Plat* or *Mos* dsRNA (2 μg/μl) does not reduce the amount of the targeted mRNA (P. S., P. S. and R. M. S., unpublished). Thus, in contrast to lower species such as *C. elegans* (Fire et al., 1998) and planaria (Sanchez-Alvarado and Newmark, 1999), in which injection of the dsRNA into the animal results in the reduction of the targeted mRNA, mouse oocytes apparently lack this uptake mechanism or, if it is present, it is very inefficient.

About 1.5×10^6 molecules of either *Plat* or *Mos* dsRNA were injected when undiluted dsRNA was used. This corresponds to an intracellular concentration of 10 nM, as the volume of an oocyte is approx. 250 pl. This concentration is similar to that required to ablate *frizzled* function in *Drosophila* embryos (Kennerdell and Carthew, 1998). In those experiments approx. 0.2 fmole of dsRNA was injected into syncytial blastoderm embryos whose volume is approx. 7.3 nl and this corresponds to approx. 25 nM. Concentrations of 10 nM dsRNA are effective in an in vitro system that supports the destruction of the targeted mRNA (Tuschl et al., 1999). Significant reduction of both *Mos* and *Plat* mRNAs are also observed when only 10,000 molecules of *Mos* or *Plat* dsRNA are injected. As the oocyte contains about 10,000 each of these transcripts (Huarte et al., 1987; Keshet et al., 1988), the reduction of the endogenous mRNA appears to be very efficient. A catalytic mechanism is possible, as in other systems the number of dsRNA molecules per cell is likely to be less than the number of endogenous transcripts. For example, in *C. elegans*, injection of 60,000 *unc*-22 dsRNA into adult animals results in the twitching phenotype in approx. 100 progeny (Fire et al.,

1998). *unc*-22 expression commences when the embryos contain about 500 cells, by which time the injected dsRNA would be diluted to only a few molecules per cell. Alternatively, the recent finding that an RNA-directed RNA polymerase is implicated in RNAi (Smardon et al., 2000) could provide an amplification mechanism that accounts for the efficacy of stoichiometric or substoichiometric amounts of dsRNA to promote the efficient reduction of the targeted mRNA.

When approx. 10^6 or 10^4 molecules of either *Mos* or *Plat* dsRNA are injected, the kinetics of *Plat* mRNA degradation are slower than that for *Mos* mRNA. As it has been estimated that oocytes contain approx. 10 000 transcripts of each of these mRNAs, the difference in kinetics of mRNA degradation may reflect that the *Mos* mRNA is more accessible to be targeted for destruction. It should be borne in mind, however, that estimate of the number of transcripts is relatively crude, and hence the difference in kinetics of mRNA degradation may reflect differences in transcript abundance, i.e., there is less *Mos* mRNA than *Plat* mRNA.

Both *Mos* and *Plat* antisense RNA are also effective in reducing the amount of endogenous *Mos* and *Plat* mRNA, respectively. Nevertheless, on a molar basis, the antisense RNA is not as effective as dsRNA. For example, *Mos* dsRNA more effectively inhibits the activation of MAP kinase when compared with *Mos* antisense RNA; parthenogenetic activation and the concomitant reduction in histone H1 kinase activity are only observed in *Mos* dsRNA-injected eggs, and not in *Mos* antisense RNA-injected eggs. This suggests in turn that MAP kinase activity must be reduced below a threshold level at which MAP kinase activity is almost absent, in order to make the eggs exit metaphase II arrest and enter interphase. Moreover, when the amount of injected *Mos* dsRNA and antisense RNA are reduced 10-fold, *Mos* dsRNA is still highly effective in inhibiting the increase in MAP kinase activity whereas *Mos* antisense RNA is essentially ineffective. Thus, *Mos* dsRNA is more efficient than *Mos* antisense RNA. A similar situation is also found with *Plat* antisense and dsRNA. Injection of 10^6 molecules of *Plat* antisense or dsRNA results in both destroying the *Plat* mRNA and inhibiting the increase in tPA activity that accompanies oocyte maturation. In contrast, injection of 10^5 molecules of *Plat* antisense RNA results in little reduction of the endogenous mRNA and little inhibition in the increase in tPA activity, while *Plat* dsRNA still results in the reduction of the endogenous mRNA and inhibition of the appearance of tPA activity.

The increased potency of dsRNA when compared with antisense RNA could, in principle, reflect differences in their stability, i.e., dsRNA is more stable than antisense RNA. This possibility is minimized by the observation that in a *Drosophila* cell lysate that supports RNAi-mediated mRNA destruction both capped antisense and capped dsRNA are stable but only the capped dsRNA is active (Tuschl et al., 1999). Moreover, results of recent experiments suggest that processing the dsRNA to discrete 20-25 nucleotide fragments is part of the mechanism that leads to destruction of the targeted mRNA (Hammond et al., 2000; Zamore et al., 2000). In fact, asRNA can give rise in an in vitro system to small amounts of stable 20-25 nucleotide fragments (Zamore et al., 2000). This could account for the activity, albeit reduced, of antisense RNA, relative to dsRNA.

dsRNAs in mammalian cells typically activate protein kinase PKR that phosphorylates and inactivates eIF2a (Fire, 1999). The ensuing inhibition of protein synthesis ultimately results in apoptosis. This sequence-independent response may reflect a form of primitive immune response, since the presence of dsRNA is a common feature of many viral lifecycles. Mouse oocytes, however, clearly lack this response, as oocyte maturation beyond germinal vesicle breakdown requires protein synthesis (Wassarman et al., 1976), which probably reflects a requirement for cyclin B synthesis, and the oocytes injected with dsRNAs resume meiosis and mature to metaphase II. Preimplantation mouse embryos also lack the response, as embryos injected with dsRNAs develop to the blastocyst stage (Wianny and Zernicka-Goetz, 2000). When the embryo acquires this response is unknown. It is not known if oocytes and preimplantation embryos contain PKR activity, which could account for the lack of the response. The lack of this response, however, cannot be attributed to a deficiency in the cell death machinery, because both oocytes (Perez et al., 1999) and preimplantation embryos (Brison and Schultz, 1997; Handyside and Hunter, 1986; Pierce et al., 1989; Weil et al., 1996) can undergo apoptosis.

The lack of this response to dsRNA may confer a selective advantage by minimizing reproductive wastage. Both oocytes and preimplantation embryos are exposed to viruses. Viral exposure throughout the lifespan of the female could deplete the pool of oocytes and compromise her reproductive capacity, because oocytes do not proliferate. The preimplantation embryo is also susceptible to viral infection from viruses present in the female reproductive tract. Infection of an early cleavage stage preimplantation embryo that results in blastomere death could result in a blastocyst containing an insufficient number of inner cell mass cells, and hence be incapable of development to term.

RNAi clearly offers several advantages to the current methods that employ generation of null mutants by homologous recombination, which requires (1) generating a suitable targeting construct, (2) selecting homologous recombination events in ES cells, (3) injecting blastocysts with these ES cells, and (4) establishing pure breeding lines from the chimeric offspring. The RNAi response will also likely be far more efficient and consistent than the antisense RNA approach that has been used with very inconsistent results in the mouse oocyte and embryo. Moreover, hypomorph phenotypes may become manifest, as RNAi does not appear to result in the total ablation of the targeted mRNA. Such hypomorph phenotypes may be as informative (or more informative) than the corresponding null mutation by providing novel insights into the presence of thresholds and/or the function of a gene. For example, as described above, a critical amount of MOS activity appears required for the development of a level of MAP kinase activity that is sufficient to maintain metaphase II arrest, a result consistent with a recently proposed switch mechanism for MAP kinase activation, as well as other cellular switches (Ferrell, 1999). In addition, modest changes in the levels of *Oct4* (*Pou5f1* – Mouse Genome Informatics) expression may also function as a developmental switch by regulating the fate of embryonic stem cells, e.g., high levels lead to differentiation into primitive endoderm and mesoderm, intermediate levels lead to pluripotent stem cells and reduced levels result in trophectoderm (Niwa et al., 2000).

As more dormant maternal mRNAs are identified, RNAi will be a valuable tool with which to study their function in oocyte maturation, fertilization and egg activation, and development. Moreover, the method can also be used to study the function of genes that are expressed in the early embryo, since dsRNA can inhibit the function of zygotically expressed genes (Wianny and Zernicka-Goetz, 2000; P. S., P. S. and R. M. S., unpublished). Whether dsRNA can also lead to DNA methylation of the targeted gene and result in long-term repression of transcription, as apparently occurs in plants (Wassenegger et al., 1994), is unknown.

This research was supported by a grant from the NIH (HD 22681 to R.M.S.). The authors would like to thank Johanna Mestach for help with preparing the dsRNA.

REFERENCES

Brison, D.R. and Schultz, R.M. (1997). Apoptosis during mouse blastocyst formation: evidence for a role for survival factors including transforming growth factor α. *Biol. Reprod.* **56**, 1088-1096.

Carroll, P.M., Richards, W.G., Darrow, A.L., Wells, J.M. and Strickland, S. (1993). Preimplantation mouse embryos express a cell surface receptor for tissue-plasminogen activator. *Development* **119**, 191-198.

Chatot, C.L., Ziomek, C.A., Bavister, B.D., Lewis, J.L. and Torres, I. (1989). An improved culture medium supports development of random-bred 1-cell mouse embryos *in vitro*. *J. Reprod. Fertil.* **86**, 679-688.

Colledge, W.H., Carlton, M.B.L., Udy, G.B. and Evans. M.J. (1994). Disruption of c-mos causes parthenogenetic development of unfertilized mouse eggs. *Nature* **370**, 65-68.

Eppig, J.J. and O'Brien, M.J. (1996). Development in vitro of mouse oocytes from primordial follicles. *Biol. Reprod.* **54**, 197-207.

Ferrell, J.E. Jr (1999). Building a cellular switch: more lessons from a good egg. *BioEssays* **21**, 866-870.

Fire, A. (1999). RNA-triggered gene silencing. *Trends Genet.* **15**, 358-363.

Fire, A., Xu, S., Montgomery, M.K., Kostas, S.A., Driver, S.E. and Mello, C.C. (1998). Potent and specific genetic interference by double-stranded RNA in Caenorhabditis elegans. *Nature* **391**, 806-811.

Gebauer, F. and Richter, J.D. (1997). Synthesis and function of Mos: the control switch of vertebrate oocyte meiosis. *BioEssays* **19**, 23-28.

Hammond, S.M., Berstein, E., Beach, D. and Hannon, G.J. (2000). An RNA-directed nuclease mediates post-transcriptional gene silencing in *Drosophila* cells. *Nature* **404**, 293-296.

Handyside, A.H. and Hunter, S. (1986). Cell division and death in the mouse blastocyst before implantation. *Roux's Arch. Dev. Biol.* **195**, 519-526.

Hasimoto, N., Watanabe, N., Y. Furuta, Y., H. Tamemoto, H., N. Sagata, N., M. Yokoyama, M., Okazaki, K., Nagayoshi, M., Takeda, N., Ikawa, Y. and Aizawa, S. (1994). Parthenogenetic activation of oocytes in c-*mos*-deficient mice. *Nature* **370**, 68-71.

Ho, Y., Wigglesworth, K., Eppig, J.J. and Schultz, R.M. (1995). Preimplantation development of mouse embryos in KSOM: Augmentation by amino acids and analysis of gene expression. *Mol. Reprod. Dev.* **41**, 232-238.

Huarte, J., Belin, D., Vassalli, A., Strickland, S. and Vassalli, J.-D. (1987). Meiotic maturation of mouse oocytes triggers the translation and polyadenylation of dormant tissue-type plasminogen activator mRNA. *Genes Dev.* **1**, 1201-1211.

Huarte, J., Belin, D. and Vassalli, J.-D. (1985). Plasminogen activator in mouse and rat oocytes: Induction during meiotic maturation. *Cell* **43**, 551-558.

Kennerdell, J.R. and Carthew, R.W. (1998). Use of dsRNA-mediated genetic interference to demonstrate that *frizzled* and *frizzled 2* act in the wingless pathway. *Cell* **95**, 1017-1026.

Keshet, E., Roenberg, M.P., Mercer, J.A., Propst, F., Vande Woude, G.F., Jenkins, N.A. and Copeland, N.G. (1988). Developmental regulation of ovarian-specific Mos expression. *Oncogene* **2**, 235-240.

Ketting, R.F., Haverkamp, T.H., van Luenen, H.G. and Plasterk, R.H. (1999). Mut-7 of *C. elegans*, required for transposon silencing and RNA interference, is a homolog of Werner syndrome helicase and RNaseD. *Cell* **99**, 133-141.

Kurasawa, S., Schultz, R.M. and Kopf, G.S. (1989). Egg-induced modifications of the *zona pellucida* of mouse eggs: effects of microinjected inositol 1,4,5-trisphosphate. *Dev. Biol.* **133**, 295-304.

Laemmli, U.K. (1970). Cleavage of structural proteins during the assembly of the head of bacteriophage T4. *Nature* **227**, 680-685.

Latham, K.E., Doherty, A.S., Scott, C.D. and Schultz, R.M. (1994). Igf2r and Igf2 gene expression in androgenetic, gynogenetic, and parthenogenetic preimplantation mouse embryos: absence of regulation by genomic imprinting. *Genes Dev.* **8**, 290-299.

Li, Y.-X., Farrell, M.J., Liu, R., Mohanty, N. and Kirby, M.L. (2000). Double-stranded RNA injection produces null phenotypes in zebrafish. *Dev. Biol.* **217**, 394-405.

Lohmann, J.U., Endl, I. and Bosch, T.C.G. (1999). Silencing of developmental genes in Hydra. *Dev. Biol.* **214**, 211-214.

Manejwala, F.M., Logan, C.Y. and Schultz, R.M. (1991). Regulation of hsp70 mRNA levels during oocyte maturation and zygotic gene activation in the mouse. *Dev. Biol.* **144**, 301-308.

Misquitta, L. and Paterson, B.M. (1999). Targeted disruption of gene function in *Drosophila* by RNA interference (RNA-i): A role for nautilus in embryonic somatic muscle formation. *Proc. Natl. Acad. Sci. USA* **96**, 1451-1456.

Montgomery, M.K., Xu, S. and Fire, A. (1998). RNA as a target of double-stranded RNA-mediated genetic interference in Caenorhabditis elegans. *Proc. Natl. Acad. Sci. USA* **95**, 15502-15507.

Moos, J., Visconti, P.E., Moore, G.D., Schultz, R.M. and Kopf, G.S. (1995). Potential role of mitogen-activated protein kinase in pronuclear envelope assembly and disassembly following fertilization of mouse eggs. *Biol. Reprod.* **53**, 692-699.

Ngo, H., Tschudi, C., Gull, K. and Ullu, E. (1998). Double-stranded RNA induces mRNA degradation in Trypanosoma brucei. *Proc. Natl. Acad. Sci. USA* **95**, 14687-92.

Nishida, E. and Gotoh, Y. (1993). The MAP kinase cascade is essential for diverse signal transduction pathways. *Trends Biochem. Sci.* **18**, 128-131.

Niwa, H., Miyazaki, J. and Smith, A.G. (2000). Quantitative expression of Oct-3/4 defines differentiation, dedifferentiation or self-renewal of ES cells. *Nature Genet.* **24**, 372-376.

O'Keefe, S.J., Wolfes, H., Kiessling, A.A. and Cooper, G.M. (1989). Microinjection of antisense *c-mos* oligonucleotides prevents meiosis II in the maturing mouse egg. *Proc. Natl. Acad. Sci. USA* **86**, 7038-7042.

Paules, R.S., Buccione, R., Moschel, R.C., Vande Woude, G.F. and Eppig, J.J. (1989). Mouse *Mos* protooncogene product is present and functions during oogenesis. *Proc. Natl. Acad. Sci. USA* **86**, 5395-5399.

Perez, G.I., Tao, X.-J. and Tilly, J.L. (1999). Fragmentation and death (a.k.a. apoptosis) of ovulated oocytes. *Mol. Hum. Reprod.* **5**, 414-420.

Pierce, G.B., Lewellyn, A.L. and Parchment, R.E. (1989). Mechanism of programmed cell death in the blastocyst. *Proc. Natl. Acad. Sci. USA* **86**, 3654-3658.

Sagata, N. (1997). What does Mos do in oocytes and somatic cells? *BioEssays* **19**, 13-21.

Sanchez-Alvarado, A. and Newmark, P.A. (1999). Double-stranded RNA specifically disrupts gene expression during planarian regeneration. *Proc. Natl. Acad. Sci. USA* **96**, 5049-5054.

Schultz, R.M., Letourneau, G.E. and Wassarman, P.M. (1979). Program of early development in the mammal: Changes in patterns and absolute rates of tubulin and total protein synthesis during oogenesis and early embryogenesis in the mouse. *Dev. Biol.* **68**, 341-359.

Schultz, R.M., Montgomery, R.R. and Belanoff, J.R. (1983). Regulation of mouse oocyte maturation: implication of a decrease in oocyte cAMP and protein dephosphorylation in commitment to resume meiosis. *Dev. Biol.* **97**, 264-273.

Schultz, R.M. and Wassarman, P.M. (1977). Specific changes in the pattern of protein synthesis during meiotic maturation of mammalian oocytes in vitro. *Proc. Natl. Acad. Sci. USA* **74**, 538-541.

Seeds, N.W., Basham, M.E. and Haffke, S.P. (1999). Neuronal migration is retarded in mice lacking the tissue plasminogen activator gene. *Proc. Natl. Acad. Sci. USA* **96**, 14118-14123.

Sharp, P.A. (1999). RNAi and double-strand RNA. *Genes Dev.* **13**, 139-141.

Smardon, A., Spoerke, J., Stacey, S., Klein, M., Mackin, N. and Maine, E. (2000). EGO-1 is related to RNA-directed RNA polymerase and functions in germ-line development and RNA interference in *C. elegans*. *Curr. Biol.* **10**, 169-178.

Sorensen, R.A. and Wassarman, P.M. (1976). Relationship between growth and meiotic maturation of the mouse oocyte. *Dev. Biol.* **50**, 531-536.

Strickland, S., Huarte, J., Belin, D., Vassalli, A., Rickles, R.J. and Vassalli, J.-D. (1988). Antisense RNA directed against the 3′ noncoding region prevents dormant mRNA activation in mouse oocytes. *Science* **241**, 680-684.

Tabara, H., Sarkissian, M., Kelly, W.G., Fleenor, J., Grishok, A., Timmons, L., Fire, A. and Mello, C.C. (1999). The rde-1 gene, RNA interference, and transposon silencing in C. elegans. *Cell* **99**, 123-132.

Temeles, G.L., Ram, P.T., Rothstein, J.L. and Schultz, R.M. (1994). Expression patterns of novel genes during mouse preimplantation embryogenesis. *Mol. Reprod. Dev.* **37**, 121-129.

Tuschl, T., Zamore, P.D., Lehmann, R., Bartel, D.P. and Sharp, P.A. (1999). Targeted mRNA degradation by double-stranded RNA *in vitro*. *Genes Dev.* **13**, 3191-3197.

Van Blerkom, J. (1981). Structural relationship and posttranslational modification of stage-specific proteins synthesized during early preimplantation development in the mouse. *Proc. Natl. Acad. Sci. USA* **78**, 7629-7633.

Vassalli, J.-D., Dayer, J.-M., Wohlwend, A. and Belin, D. (1984). Concomitant secretion of prourokinase and of a plasminogen activator-specific inhibitor by cultured human monocytes-macrophages. *J. Exp. Med.* **159**, 1653-1668.

Vassalli, J.-D., Huarte, J., Belin, D., Gubler, P., Vassalli, A., O'Connell, M.L., Parton, L.A., Rickles, R.J. and Strickland, S. (1989). Regulated polyadenylation controls mRNA translation during meiotic maturation of mouse oocytes. *Genes Dev.* **3**, 2163-2171.

Verlhac, M.-H., De Pennart, H., Maro, B., Cobb, M.H. and Clarke, H.J. (1993). MAP kinase becomes stably activated at metaphase and is associated with microtubule-organizing centers during meiotic maturation of mouse oocytes. *Dev. Biol.* **158**, 330-340.

Wargelius, A., Ellingsen, S. and Fjose, A. (1999). Double-stranded RNA induces specific developmental defects in zebrafish embryos. *Biochem. Biophys. Res. Commun.* **263**, 156-161.

Wassarman, P.M., Josefowicz, W.J. and Letourneau, G.E. (1976). Meiotic maturation of mouse oocytes in vitro: inhibition of maturation at specific stages of nuclear progression. *J. Cell Sci.* **22**, 531-545.

Wassenegger, M., Heimes, S., Riedel, L. and Sanger, H.L. (1994). RNA-directed de novo methylation of genomic sequences in plants. *Cell* **76**, 567-76.

Weil, W., Jacobson, M.D., Coles, H.S.R., Davies, T.J., Gardner, R.L., Raff, K.D. and Raff, M.C. (1996). Constitutive expression of the machinery for programmed cell death. *J. Cell Biol.* **133**, 1053-1059.

Wianny, F. and Zernicka-Goetz, M. (2000). Specific interference with gene function by double-stranded RNA in early mouse development. *Nat. Cell Biol.* **2**, 70-75.

Wickramasinghe, D., Ebert, K.M. and Albertini, D.F. (1991). Meiotic competence acquisition is associated with the appearance of M-phase characteristics in growing mouse oocytes. *Dev. Biol.* **143**, 162-172.

Zamore, P.D., Tuschl, T., Sharp, P.A. and Bartel, D.P. (2000). RNAi: Double-stranded RNA directs the ATP-dependent cleavage of mRNA at 21 to 23 nucleotide intervals. *Cell* **101**, 25-33.

Zhao, X., Singh, B. and Batten, B.E. (1991). The role of c-mos proto-oncoprotein in mammalian meiotic maturation. *Oncogene* **6**, 43-49.

Exhibit F

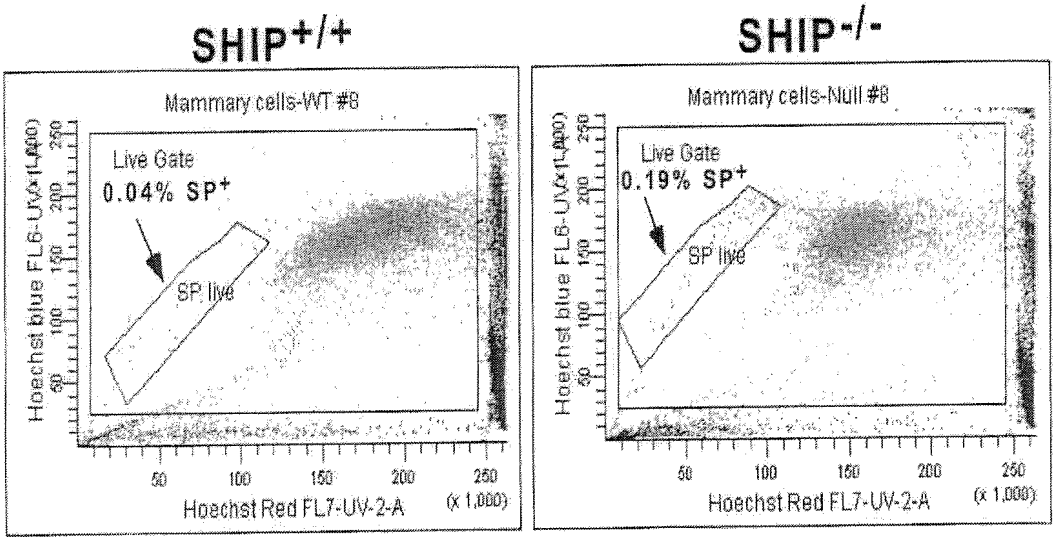
SHIP+/+
SHIP-/-
Mammary cells-WT #8
Mammary cells-Null #8
Live Gate
0.04% SP+
0.19% SP+
SP live
Hoechst blue FL6-UV-2-A
Hoechst Red FL7-UV-2-A
(x 1,000)
50
100
150
200
250

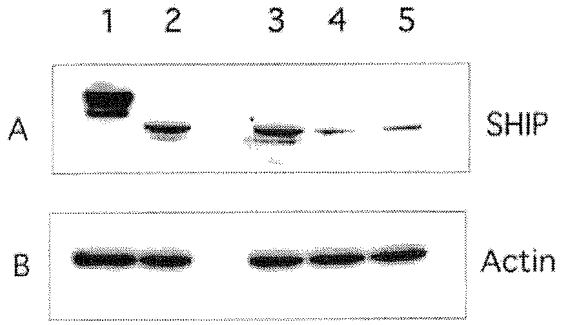
1
2
3
4
5
A
SHIP
B
Actin

Exhibit G

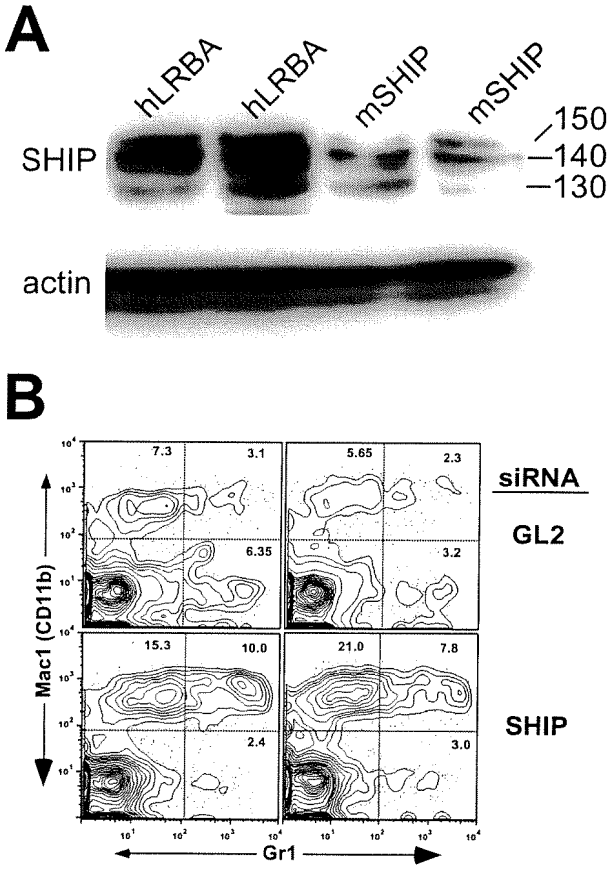
A
hLRBA
hLRBA
mSHIP
mSHIP
SHIP
150
140
130
actin
B
7.3
3.1
6.35
5.65
2.3
3.2
siRNA
GL2
15.3
10.0
2.4
21.0
7.8
3.0
SHIP
Mac1 (CD11b)
Gr1

Exhibit H

muSHIP1shRNA VECTOR

- pBluescript MCS: Bam H1 and Eco R1
- mouse RNA Pol III U6 promoter
- S-SHIP TARGET: 683-704 (AF184912)
  = SHIP TARGET: 1423-1444 (MMU52044)
- Hairpin Loop=Hind III
- Pol III Transcription Termination Signal

TACAGGGCGCGTCCCATTCGCCATTCAGCTGCGCAACTGTTGGGAAGGGCGAT-
CGGTGCGGGCCTCTTCGCTATTACGCCAGCTGGCGAAAGGGGGATGTGCTGCA-
AGGCGATTAAGTTGGGTAACGCCAGGGTTTTCCCAGTCACGACGTTGTAAAAC-
GACGGCCAGTGAGCGCGCGTAATACGACTCACTATAGGGCGAATTGGGTACCCGC
TCTAGAACTAGTGGATCCGACGCCGCCATCTCTAGGCCCGCGCCGGCCCCCTC-
GCACAGACTTGTGGGAGAAGCTCGGCTACTCCCCTGCCCCGGTTAATTTGCAT-
ATAATATTTCCTAGTAACTATAGAGGCTTAATGTGCGATAAAAGACAGATAATCTGT-
TCTTTTTAATACTAGCTACATTTTACATGATAGGCTTGGATTTCTATAAGAGATACAA
ATACTAAATTATTATTTTAAAAAACAGCACAAAAGGAAACTCACCCTAACTGTAAAG-
TAATTGTGTGTTTTGAGACTATAAATATCCCTTGGAGAAAAGCCTTGTTTGGGAC-
GACTCTGCTGACTACATAAGCTTATGTAGTCAGCAGAGTCGTCCCTTTTTGAATTC-
CTGCAGCCCGGGGGATCCACTAGTTCTAGAGCGGCCGCCACCGCGGTGGAGCTC
CAGCTTT

Transcribed siRNA

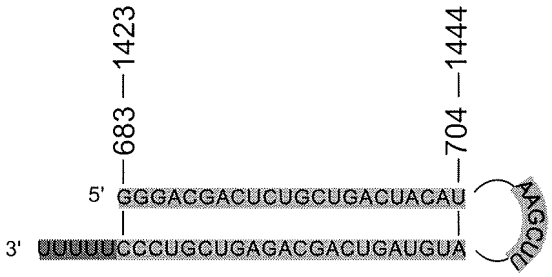

Exhibit I

1: 5′-GAAGAUCACGUCCUGGUUUdTdT-3′
3′-dTdTCUUCUAGUGCAGGACCAAA-5′

2: 5′-UGGUCCUGGCACUGUAGAUdTdT-3′
3′-dTdTACCAGGACCGUGACAUCUA-5′

3: 5′-UGAGAUGAUCAAUCCAAACdTdT-3′
3′-dTdTACUCUACUAGUUAGGUUUG-5′

4: 5′-GACGACUCUGCUGACUACAdTdT-3′
3′-dTdTCUGCUGAGACGACUGAUGU-5′

Accession #: NM_010566

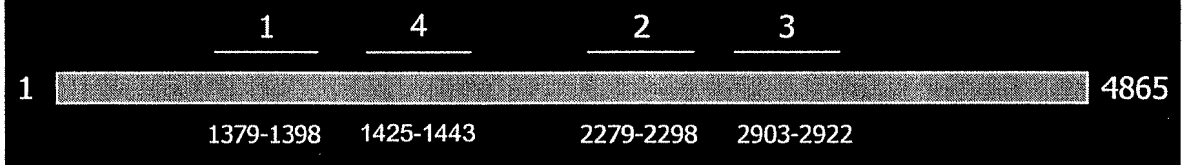

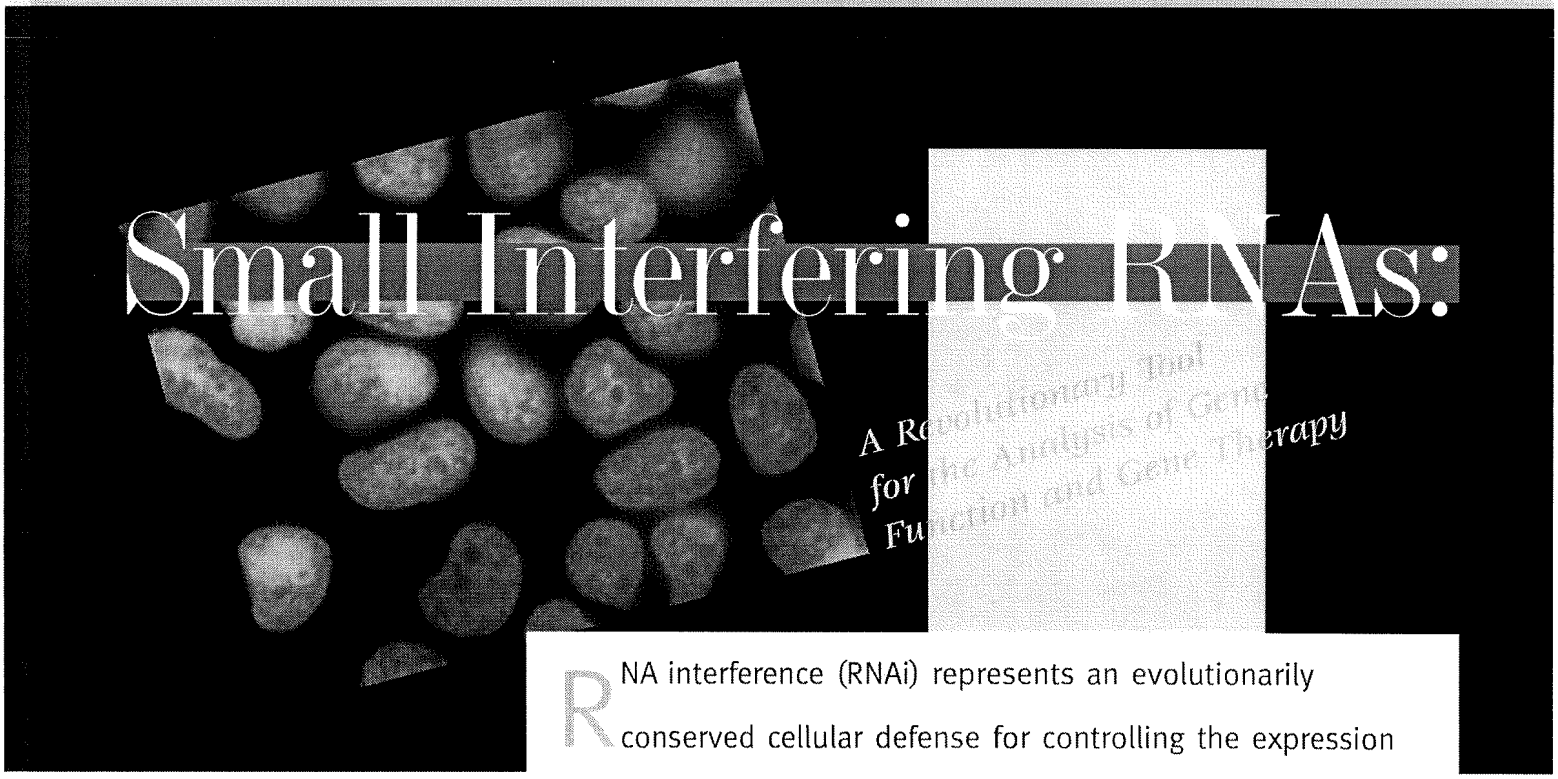

Small Interfering RNAs:

A Re... for ... Fu...

RNA interference (RNAi) represents an evolutionarily conserved cellular defense for controlling the expression of foreign genes in most eukaryotes including humans. RNAi is triggered by double-stranded RNA (dsRNA) and causes sequence-specific mRNA degradation of single-stranded target RNAs homologous in response to dsRNA. The mediators of mRNA degradation are small interfering RNA duplexes (siRNAs), which are produced from long dsRNA by enzymatic cleavage in the cell. siRNAs are approximately twenty-one nucleotides in length, and have a base-paired structure characterized by two-nucleotide 3'-overhangs. Chemically synthesized siRNAs have become powerful reagents for genome-wide analysis of mammalian gene function in cultured somatic cells. Beyond their value for validation of gene function, siRNAs also hold great potential as gene-specific therapeutic agents.

The ability of double-stranded RNA (dsRNA) to silence the expression of genes has been the focus of many studies in C. elegans and D. melanogaster. More recent research has looked for evidence of RNAi-mediated gene suppression in other model organisms. Now there is excitement that RNAi-based methodologies will allow for the rapid assessment and validation of proteins as potential drug targets. Additionally, we might now be standing on the edge of fundamentally new approaches to gene therapy as conducted through RNAi-mediated suppression of mutated genes.

Thomas Tuschl[1] and Arndt Borkhardt[2]
[1]Department of Cellular Biochemistry, Max-Planck-Institute for Biophysical Chemistry, D-37077 Goettingen, Germany
[2]Children's University Hospital, Pediatric Hematology and Oncology, 35392 Giessen, Germany

INTRODUCTION

When viruses infect eukaryotic cells, or when transposons and transgenes are randomly integrated into host genomes, dsRNA is frequently produced from the foreign genes. Most eukaryotes, including humans, possess an innate cellular immune surveillance system that specifically responds to the presence of dsRNA and activates processes that act post-transcriptionally to silence the expression of the interloping genes (*1–4*). This mechanism is now commonly referred to as RNA interference or RNAi (*5*). During RNAi, long transcripts of dsRNA are rapidly processed into small interfering RNAs (siRNAs), which represent RNA duplexes of specific length and structure that finally guide sequence-specific degradation of mRNAs homologous in sequence to the siRNAs (*6, 7*). The sequencing of the human genome has created an urgent need to ascertain efficiently the function of novel genes and to validate targets for drug discovery. Indeed, the rapid translation of the genomic DNA sequence information into therapeutic strategies for many common maladies—particularly infectious, cardiovascular, neoplastic, and neurological diseases—would be highly desirable. siRNAs may be the best tools for target validation in biomedical research today, because of their exquisite specificity, efficiency and endurance of gene-specific silencing. siRNAs are probably also suitable for the design of novel gene-specific therapeutics by directly targeting the mRNAs of disease-related genes.

The transfection of siRNAs into animal cells results in the potent, long-lasting post-transcriptional silencing of specific genes (*8, 9*). siRNA-mediated gene silencing is particularly useful in somatic mammalian cells, because these cells mount an additional, sequence-nonspecific innate immune response (i.e., responding with interferon-mediated defenses) when exposed to dsRNA greater than thirty base pairs, therefore prohibiting the application of longer dsRNAs (*10*). siRNAs are extraordinarily effective at lowering the amounts of targeted RNA—and by extension proteins—frequently to undetectable levels. The silencing effect is long lasting, typically several days, and extraordinarily specific, because one nucleotide mismatch between the target RNA and the central region of the siRNA is frequently sufficient to prevent silencing (*6, 7, 11, 12*). siRNAs can be rapidly synthesized and are now broadly available for the analyses of gene function in cultured mammalian cells. Similar to antisense oligonucleotide technology (*13*), the use of siRNAs also holds great promise for the application of gene-specific therapies in treating acute diseases such as viral infection, cancer, and, perhaps, acute inflammation.

The Mechanism of dsRNA Interference

A schematic illustration shows the mechanism of RNAi (Figure 1). The key enzyme required for processing of long dsRNAs to siRNA duplexes is the RNase III enzyme Dicer, which was characterized in extracts prepared from insect cells, *C. elegans* embryos, and

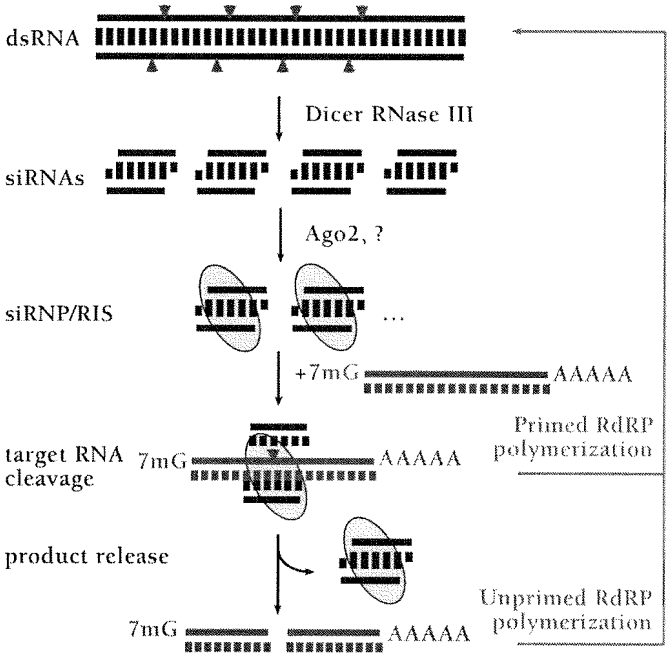

Figure 1. A model for RNA interference. dsRNA is processed to 21- to 23-nt siRNA duplexes by Dicer RNase III and possible other dsRNA-binding factors. The siRNA duplexes are incorporated into a siRNA-containing ribonucleoprotein complex (siRNP) (*21*) becoming the RNA-induced silencing complex (RISC) endonuclease, which targets homologous mRNAs for degradation. AGO2 and yet to be characterized proteins are thought to be required for RISC formation. The RISC mediates sequence-specific target RNA degradation. In plants and nematodes, targeted RNAs might also function as templates for double-strand RNA synthesis giving rise to transitive RNAi (*24, 80–83*), either through siRNA-primed dsRNA synthesis or through unprimed synthesis from aberrant RNA (which could represent the cleaved target RNA). In mammals or in fruitfly, however, RdRP genes have yet been identified, and the major mechanism of siRNA action is believed to be endonucleolytic target RNA cleavage guided by siRNA-protein complexes (RISC).

mouse cells (*14–16*). Dicer contains an N-terminal RNA helicase domain, a Piwi, Argonaute, Zwille/Pinhead (PAZ) domain (*17*), two RNase III domains, and a C-terminal dsRNA-binding motif. The PAZ domain is also present in Argonaute proteins, whose genes represent a poorly characterized family present in dsRNA-responsive organisms. Argonaute1 (AGO1) and Argonaute2 (AGO2), two of the five Argonaute proteins of *D. melanogaster*, appear to be important for forming the mRNA-degrading sequence-specific endonuclease complex, also referred to as the RNA-induced silencing complex (RISC) (*18, 19*). Dicer and AGO2 appear to interact in *D. melanogaster* Schneider 2 (S2) cells, probably through their PAZ domains; however, RISC and Dicer activity are separable, and RISC is unable to process dsRNA to siRNAs, suggesting that Dicer is not a component of RISC (*18, 20*). Possibly, the interaction between Dicer and AGO2 facilitates the incorporation of siRNA into RISC (*20*). The endonucleolytic subunit of RISC remains to be identified.

siRNA duplexes produced by the action of Dicer contain 5'-

Table 1. RNAi-Mediated Silencing in Cell Lines

Cell line	Tissue origin	Reference
A-431	human epidermoid carcinoma	(23)
A549	human lung carcinoma	(72)
BV173	human B-precursor leukemia	(77)
C-33A	human papilloma virus negative cervical carcinoma	(46)
CA46	human Burkitt's lymphoma	(77)
Caco2	human colon epithelial cells	(61)
CHO	Chinese hamster ovary	(23)
COS-7	African green monkey kidney	(9)
F5	rat fibroblast	(32)
H1299	human nonsmall cell lung carcinoma	(46)
HaCaT	human keratinocyte cell	(12)
HEK 293	human embryonic kidney	(9)
HeLa	human papilloma virus positive cervical carcinoma	(9)
Hep3B	human hepatocellular carcinoma	(64)
HUVEC	human umbilical vein endothelial cells	(54)
IMR-90	human diploid fibroblast	(41)
K562	human chronic myelogenous leukemia, blast crisis	(77)
Karpas 299	human T-cell lymphoma	(77)
MCF-7	human breast cancer	(84)
MDA-MB-468	human breast cancer	(84)
MV-411	human acute monocytic leukemia	(77)
NIH/3T3	mouse fibroblast	(9)
P19	mouse embryonic carcinoma	(42)
SD1	human acute lymphoblastic leukemia	(77)
SKBR3	human breast cancer	(23)
U2OS	human osteogenic sarcoma cell	(59)

phosphates and free 3'-hydroxyl groups. The central base-paired region is flanked by two-to-three nucleotides of single-stranded 3'-overhangs (6). The 5'-phosphate termini of siRNAs is essential for guiding mRNA degradation (21). Nevertheless, for their practical application in gene targeting experiments, siRNAs may be used without 5'-phosphate termini because a kinase activity in the cell rapidly phosphorylates the 5' ends of synthetic siRNA duplexes (9, 21, 22). Under certain circumstances (e.g., injection experiments in *D. melanogaster*), 5'-phosphorylated siRNA duplexes may have slightly enhanced properties as compared to 5'-hydroxyl siRNAs (22). In gene targeting experiments using human HeLa cells, no differences in siRNA-mediated "knockdown" of gene expression were observed, as a function of 5'-phosphorylation (23). Furthermore, a cell line that is unable to utilize synthetic 5'-hydroxyl siRNAs for RNAi has not been encountered (for cell lines supporting RNAi see Table 1).

In *C. elegans*, introduction of approximately 300 bp dsRNA corresponding to a segment of the targeted gene may also give rise to the phenomenon of transitive RNAi (24). Transitive RNAi is characterized by the spreading of silencing outside of the region targeted by the initiator dsRNA. Presumably, targeted mRNA serves as template for RNA-dependent RNA polymerase (RdRP) and forms new dsRNA that is processed by Dicer. Thus, secondary siRNAs are generated that may cleave the mRNA outside of the region targeted by the ancestral dsRNA. Although this appears to have important implications for RNAi-based analysis of gene function because silencing may spread between genes that share highly homologous sequences, phenotypic analysis of a large set of silenced genes in *C. elegans* suggests that transitive RNAi between naturally occurring homologous gene sequences is probably of no major concern (25, 26). It was also proposed that siRNAs might prime novel dsRNA synthesis; however, it should be pointed out that siRNAs, in comparison to longer dsRNAs, are extremely poor initiators of gene silencing in *C. elegans* (27, 28). Biochemical evidence for RdRP activity in *D. melanogaster* was recently reported (29), although genes encoding classical RdRP activity appear to be lacking from the *D. melanogaster* genome. Despite the beauty of the suggested model in *D. melanogaster*, which hypothesizes that siRNAs function as primers for target-RNA-dependent dsRNA synthesis, thus leading to amplification of the silencing signal (29), biochemical evidence for the spreading of gene silencing outside of regions targeted by dsRNAs has not been observed in other model systems (6, 12, 23, 30, 31). Rather, the predominant pathway of gene silencing appears to be siRNA-mediated target mRNA degradation by RISC formation, which may also act catalytically. Similar to the situation in *D. melanogaster*, genes encoding RdRPs have not been identified in mammals. Therefore it is important to remember that the mechanisms of silencing differ between different species.

Application of siRNAs in Somatic Mammalian Cells

siRNAs have brought reverse genetics to mammalian cultured cells, and have made large-scale functional genomic analysis a realistic possibility (32). Standard cell lines provide starting points for mammalian functional screens because siRNAs can be effectively delivered by electroporation or cationic liposome-mediated transfection (11, 23). For small scale-applications, the microinjection of siRNAs may represent an alternative method. Technical problems that result from low transfection efficiencies may be partially overcome by using cell sorting protocols, such as after the transfection of siRNAs together with sorting markers such as GFP-expression plasmids. Alternatively, siRNAs that target cell surface marker proteins may be co-transfected, and the reduced expression of the co-targeted cell surface marker could then be used to identify specific cell populations by cell sorting.

An obvious prerequisite for the application of siRNAs for validation and therapeutic applications is the need for functional

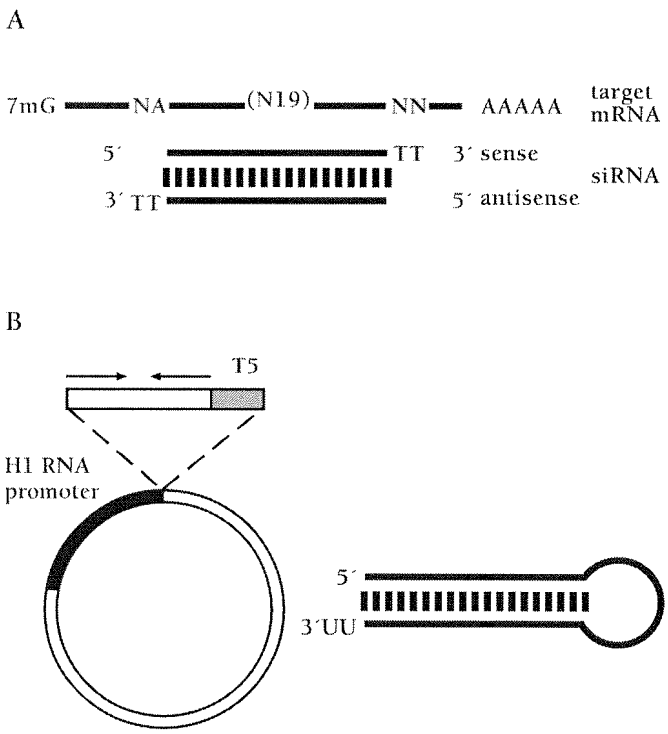

Figure 2. Methods for the delivery of siRNAs to somatic mammalian cells. (A) Synthetic 21-nt siRNA duplex prepared by chemical synthesis (23) aligned to a target mRNA. Target regions are selected such that siRNA sequences may contain uridine residues in the 2-nt overhangs. Uridine residues in the 2-nt 3'-overhang can be replaced by 2'-deoxythymidine without loss of activity, which significantly reduces costs of RNA synthesis and may also enhance nuclease resistance of siRNA duplexes when applied to mammalian cell (7). (B) Plasmid-based expression of short hairpin loops which give rise to siRNAs in vivo (11). The polymerase III promoter of H1 RNA (human RNase P RNA) drives the transcription of a nineteen-base-pair/nine-nucleotide-loop RNA hairpin. The transcription is terminated by the encounter of a polythymidine tract (T5) after the incorporation of two to three uridine residues encoded by the T5 element. Northern blot analysis showed that the hairpin RNAs were processed to siRNAs.

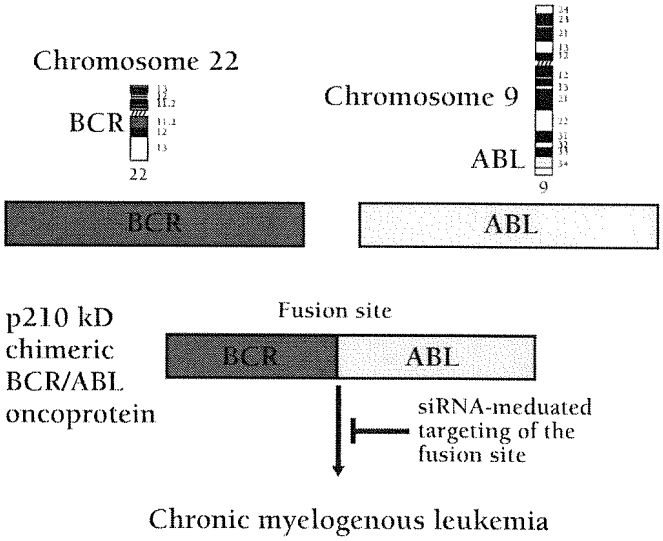

Figure 3. Scheme of the translocation t(9;22) in leukemia. The BCR-ABL fusion mRNA provides a leukemia-specific target that can be cleaved by siRNAs.

RNAi machinery within the targeted cells or tissue to bind to siRNAs and mediate mRNA degradation. In order to assay for the activity of this ribonucleoprotein complex in cells, a reporter assay was developed (9, 23). Plasmids coding for firefly and sea-pansy luciferase are transfected together with control or target-specific (i.e., luciferase) siRNAs into cells, and the relative luminescence of target versus control luciferase activity is measured.

siRNAs have been used to identify cytoskeletal proteins that are essential for cell growth (32). Even the targeting of non-essential genes resulted in cellular phenotypes that were identical to phenotypes previously observed in cells derived from transgenic knockout mice (32), illustrating the value of siRNA methodology for the analysis of mammalian gene function.

In certain situations, several-hundred-base-pair long dsRNA represents an alternative to siRNAs. Long dsRNA effectively silences genes expressed in insect cells (18, 33–35) and in embryonic mammalian cells that have not yet established the interferon system (15, 36–39). However, undifferentiated cells, such as embryonic stem (ES) cells or P19 teratocarcinoma cells, are difficult to work with because these progenitor cells are often poorly transfectable, making cell sorting prior to phenotypic analysis necessary (15).

Until recently, the application of siRNAs in somatic cells was restricted to the delivery of chemically or enzymatically synthesized siRNAs (9, 40–42) (Figure 2A), but methods for intracellular expression of small RNA molecules have now been developed. Endogenous delivery is possible by inserting DNA templates for siRNAs into RNA polymerase III (pol III) transcription units, which are based on the sequences of the natural transcription units of the small nuclear RNA U6 or the human RNase P RNA H1. Two approaches are available for expressing siRNAs: 1) The sense and antisense strands constituting the siRNA duplex are transcribed from individual promoters (42–44), or 2) siRNAs are expressed as fold-back stem-loop structures that give rise to siRNAs after intracellular processing by Dicer (11, 41, 42, 45, 46) (Figure 2B). The transfection of cells with plasmids that encode siRNAs, therefore, represents an alternative to direct siRNA transfection. Stable expression of siRNAs may facilitate certain applications such as the functional characterization of non-essential gene products in synthetic lethality screens or the construction of combinatorial libraries useful for loss-of-function screening in microarray assays (47). The insertion of siRNA expression cassettes into (retro)viral vectors will also enable the targeting of primary cells refractory to transfection or electroporation of plasmid DNA.

The function of several genes in cultured somatic mammalian cells have been analysed using siRNAs. The human vacuolar sorting protein Tsg101 was thus identified as essential for HIV-1 but not MLV budding (48). The reintroduction of a Tsg101-

expressing plasmid that encoded Tsg101 mRNA with silent mutations at the siRNA-targeting site restored the HIV-1 budding defect. siRNA-mediated depletion of endogenous targets and the re-introduction of siRNA-resistant rescue constructs (*30*) will become important for the analysis of protein function much like the complementation analyses used in traditional yeast genetic research. In other instances, siRNAs were applied for studying the role of proteins involved in DNA damage response and cell cycle control (*11*, *49–53*), general cell metabolism (*54–56*), signaling (*57–59*), cytoskeleton and its rearrangement during mitosis (*32*, *44*, *60*), membrane trafficking (*61*, *62*), transcription (*63*), and DNA methylation (*64*). These various examples reported by independent investigators illustrate the robustness of the siRNA gene silencing technology.

However, variations do exist in the efficiency of siRNAs to target the same genes (*12*, *23*, *32*). Our experience in targeting many different genes suggests that, on average, between seventy to ninety percent of randomly chosen siRNAs are able to reduce target gene expression by more than eighty percent. Some genes, encoding extremely abundant and extremely stable proteins (e.g., vimentin), may be more difficult to silence, and the probability for finding efficacious siRNAs may be lower (*23*, *32*). Nonetheless, difficulty in depleting the most abundant proteins does not appear to compromise the value of this new transient gene silencing technology.

siRNAs as Novel Therapeutic Platform Technology

siRNAs are highly sequence-specific reagents and discriminate between single mismatched target RNA sequences (*7*, *11*), and may represent a new avenue for gene therapy. The expression of mRNAs coding for mutated proteins, which give rise to dominant genetic disorders and neoplastic growth, might be decreased or blocked completely by specific siRNAs.

With respect to targeting viral gene products expressed in virus-infected cells, it is possible that infectious mammalian viruses could express inhibitors of RNAi similar to those identified in plant and insect viruses (*65–71*). Because viral inhibitors of the mammalian RNAi machinery have not yet been described, it seems feasible that the application of siRNAs could extend our understanding of viral protein function and viral life cycle. Bitko and Barik successfully used siRNAs to silence genes expressed from respiratory syncytial virus (RSV) (*72*), a negative strand RNA virus that causes sometimes severe respiratory disease, especially in neonates and infants. They also demonstrated that siRNAs do not induce interferon-mediated responses, by showing the absence of phosphorylation of the translation factor eIF-2α. Although mRNAs transcribed from the viral genome were effectively silenced and viral replication was inhibited, it was not possible to cleave the viral genomic or antigenomic RNA because of its chromatin-like condensed structure. Lee et al. recently reported effective siRNA-mediated degradation of HIV-1 *rev* transcripts in a cell assay by co-transfection of proviral DNA and siRNA expression vectors, thus raising the possibility that siRNAs may become useful to treat HIV infection (*43*).

In leukemias and lymphomas—the most frequent cancers in childhood—oncogene activation frequently occurs through reciprocal chromosomal translocations. These translocations lead to juxtaposition of gene segments normally found on different chromosomes, and the creation of a composite gene. The prototype of such a translocation is the generation of the Philadelphia chromosome by the translocation of the long arms of chromosomes 9 and 22 [t(9;22)] in patients with chronic myelogenous leukemia and acute lymphoblastic leukemia (*73*). The translocation fuses the BCR gene from chromosome 22 and ABL gene from chromosome 9, creating an oncogenic BCR-ABL hybrid gene (Figure 3) (*74*). The BCR-ABL fusion protein has dramatically increased the tyrosine kinase activity, as compared to that of the normal ABL protein, leading to aberrant phosphorylation of several downstream molecules. The kinase activities of both BCR-ABL and ABL can be inhibited by a specific tyrosine kinase inhibitor, STI 571 (Imatinib®), which is now used in the effective treatment of BCR-ABL-positive leukemia (*75*, *76*). RNAi was also used to target the BCR-ABL mRNA, and this approach was compared to that of STI 571–mediated cell killing in

Table 2. Selection of Possible Targets for Tumor Therapy by siRNAs

Genes or Fusion Genes	Aberration	Tumors
RAS	Point mutations	Pancreatic carcinoma, chronic leukemia, colon carcinoma, lung cancers
c-*MYC*, N-*MYC*	Overexpression, translocation, Point mutation, amplification	Burkitt's lymphoma, neuroblastoma
ERBB	overexpression	Breast cancer
ERBB2	Overexpression	Breast cancer
MLL fusion genes	Translocation	Acute leukemias
BCR-ABL	Translocation	Acute and chronic leukemia
TEL-AML1	Translocation	Childhood acute leukemia
EWS-FLI1	Translocation	Ewing sarcoma
TLS-FUS	Translocation	Myxoid liposarcoma
PAX3-FKHR	Translocation	Alvelolar rhabodomyosarcoma
BCL-2	Overexpression, translocation	Lung cancers, Non-Hodgkin lymphoma, prostate cancer
AML1-ETO	Translocation	Acute leukemia

a cell culture model. The siRNA treatment readily reduced the expression of BCR-ABL mRNA, followed by a reduction of BCR-ABL oncoprotein, leading to apotosis in leukemic cells (77). siRNA-based BCR-ABL silencing may become important considering that some patients develop drug resistance against STI 571 (e.g., by genomic amplification of BCR-ABL, increased expression of BCR-ABL mRNA or point mutation in the ABL gene). Alternative therapies, perhaps applied in combination with inhibitors such as STI 571, may help to overcome problems of such drug resistance.

The combined effort of many laboratories worldwide has led to the molecular clarification of numerous chromosomal translocations through the successful cloning of the genes adjacent to the chromosomal breakpoint regions. Silencing of these tumor-specific, chimeric mRNAs by siRNAs might become an effective fusion gene-specific tumor therapy. The extraordinary sequence specificity of the RNAi mechanism may also allow for the targeting of individual polymorphic alleles expressed in loss-of-heterozygosity tumor cells, as well as targeting point-mutated transcripts of transforming oncogenes such as Ras. Finally, the decrease of overexpressed apoptosis inhibitors such as Bcl-2 and c-Myc might also be beneficial for cancer therapy. A list of possible targets for siRNA-mediated therapy in human malignancies is shown in Table 2.

With respect to future medical applications, siRNAs were recently directed against a mutated mRNA associated with the spinobulbular muscular atrophy (SBMA) in tissue culture (78). SBMA, together with Huntington Disease, belongs to a growing group of neurodegenerative disorders caused by the expansion of trinucleotide repeats (79). Targeting the CAG-expanded mRNA transcript with dsRNA may be an attractive alternative to commonly used therapeutic strategies that, beyond symptomatic treatment, mainly focus on the inhibition of the toxic effects of the polyglutamine protein. Caplen et al. (78) successfully decreased the expression of mutated transcripts of the androgen receptor in human kidney 293T cells that were transfected with a plasmid encoding the expanded-CAG androgen receptor mutant. Most importantly, the authors achieved a rescue of the polyglutamine-induced cytotoxicity in cells treated with dsRNA molecules. Even though the study observed RNAi in transfected cells in vitro rather than in a more physiologically relevant context, the approach provides proof-of-principle, and underlines the remarkably broad potency and sequence-specificity of RNAi-mediated gene therapy. Whether the RNAi pathway is functionally active in various neuronal cells irrespective of their state of differentiation remains to be shown.

The delivery of siRNAs to the proper sites of therapy remains problematic. This is especially true for their delivery to primary cells, because such cells often do not tolerate treatment with liposome transfection reagents. Chemical modification of siRNAs, such as changing the lipophilicity of the molecule may be considered—for example, phosphorothioate modifications present in antisense oligodeoxynucleotides, or the attachment of lipophilic residues at the 3'-termini of the siRNA duplex. Delivery of siRNAs into organisms might be achieved with methods previously developed for the application of antisense oligonucleotides or nuclease-resistant ribozymes. Such methods consist of the injection of naked or liposome-encapsulated molecules. Studies that inform us about the possibility of exploiting RNAi in various cell types, tissues, and organs are urgently needed. Without doubt, these experiments will be performed in the near future in academic as well as industrial settings.

CONCLUSIONS

The pace with which siRNAs revolutionize the analysis of mammalian gene function is astounding, considering that siRNA-mediated gene silencing was only introduced last year (9, 78). siRNAs are poised to facilitate the genome-wide systematic analysis of gene function in cultured cells, and may soon become a valuable tool for target validation beyond in vitro tissue culture. siRNAs may yet provide a solution for gene-specific drug development, especially before highly specific small-molecule inhibitors become available.

Acknowledgments

We acknowledge Sayda Elbashir, Jens Harborth, Klaus Weber and Ulrike Krämer for critical comments on the manuscript. Our own studies were made possible by grants from the Deutsche Forschungsgemeinschaft.

References

1. Hammond, S.M., Caudy, A.A., and Hannon, G.J. Post-transcriptional gene silencing by double-stranded RNA. *Nat. Rev. Genet.* **2**, 110–119 (2001).
2. Hutvágner, G. and Zamore, P.D. RNAi: Nature abhors a double-strand. *Curr. Opin. Genet. Dev.* **12**, 225–232 (2002).
3. Sharp, P.A. RNA interference 2001. *Genes Dev.* **15**, 485–490 (2001).
4. Waterhouse, P.M., Wang, M.B., and Lough, T. Gene silencing as an adaptive defence against viruses. *Nature* **411**, 834–842 (2001).
5. Fire, A., Xu, S., Montgomery, M.K., Kostas, S.A., Driver, S.E., and Mello, C.C. Potent and specific genetic interference by double-stranded RNA in *Caenorhabditis elegans*. *Nature* **391**, 806–811 (1998).
6. Elbashir, S.M., Lendeckel, W., and Tuschl, T. RNA interference is mediated by 21 and 22 nt RNAs. *Genes Dev.* **15**, 188–200 (2001).
7. Elbashir, S.M., Martinez, J., Patkaniowska, A., Lendeckel, W., and Tuschl, T. Functional anatomy of

siRNAs for mediating efficient RNAi in *Drosophila melanogaster* embryo lysate. *EMBO J.* **20**, 6877–6888 (2001).

8. Caplen, N.J., Parrish, S., Imani, F., Fire, A., and Morgan, R.A. Specific inhibition of gene expression by small double-stranded RNAs in invertebrate and vertebrate systems. *Proc. Natl. Acad. Sci. U.S.A.* **98**, 9742–9747 (2001).

9. Elbashir, S.M., Harborth, J., Lendeckel, W., Yalcin, A., Weber, K., and Tuschl, T. Duplexes of 21-nucleotide RNAs mediate RNA interference in mammalian cell culture. *Nature* **411**, 494–498 (2001).

10. Stark, G.R., Kerr, I.M., Williams, B.R., Silverman, R.H., and Schreiber, R.D. How cells respond to interferons. *Annu. Rev. Biochem.* **67**, 227–264 (1998).

11. Brummelkamp, T.R., Bernards, R., and Agami, R. A system for stable expression of short interfering RNAs in mammalian cells. *Science* **296**, 550–553 (2002).

12. Holen, T., Amarzguioui, M., Wiiger, M.T., Babaie, E., and Prydz, H. Positional effects of short interfering RNAs targeting the human coagulation trigger Tissue Factor. *Nucleic Acids Res.* **30**, 1757–1766 (2002).

13. Flaherty, K.T., Stevenson, J.P., and O'Dwyer, P.J. Antisense therapeutics: Lessons from early clinical trials. *Curr. Opin. Oncol.* **13**, 499–505 (2001).

14. Bernstein, E., Caudy, A.A., Hammond, S.M., and Hannon, G.J. Role for a bidentate ribonuclease in the initiation step of RNA interference. *Nature* **409**, 363–366 (2001).

15. Billy, E., Brondani, V., Zhang, H., Muller, U., and Filipowicz, W. Specific interference with gene expression induced by long, double-stranded RNA in mouse embryonal teratocarcinoma cell lines. *Proc. Natl. Acad. Sci. U.S.A.* **98**, 14428–14433 (2001).

16. Ketting, R.F., Fischer, S.E., Bernstein, E., Sijen, T., Hannon, G.J., and Plasterk, R.H. Dicer functions in RNA interference and in synthesis of small RNA involved in developmental timing in *C. elegans*. *Genes Dev.* **15**, 2654–2659 (2001).

17. Cerutti, L., Mian, N., and Bateman, A. Domains in gene silencing and cell differentiation proteins: The novel PAZ domain and redefinition of the piwi domain. *Trends Biochem. Sci.* **25**, 481–482 (2000).

18. Hammond, S.M., Bernstein, E., Beach, D., and Hannon, G.J. An RNA-directed nuclease mediates post-transcriptional gene silencing in Drosophila cells. *Nature* **404**, 293–296 (2000).

19. Williams, R.W. and Rubin, G.M. ARGONAUTE1 is required for efficient RNA interference in Drosophila embryos. *Proc. Natl. Acad. Sci. U.S.A.* **99**, 6889–6894 (2002).

20. Hammond, S.M., Boettcher, S., Caudy, A.A., Kobayashi, R., and Hannon, G.J. Argonaute2, a link between genetic and biochemical analyses of RNAi. *Science* **293**, 1146–1150 (2001).

21. Nykänen, A., Haley, B., and Zamore, P.D. ATP requirements and small interfering RNA structure in the RNA interference pathway. *Cell* **107**, 309–321 (2001).

22. Boutla, A., Delidakis, C., Livadaras, I., Tsagris, M., and Tabler, M. Short 5'-phosphorylated double-stranded RNAs induce RNA interference in Drosophila. *Curr. Biol.* **11**, 1776–1780 (2001).

23. Elbashir, S.M., Harborth, J., Weber, K., and Tuschl, T. Analysis of gene function in somatic mammalian cells using small interfering RNAs. *Methods* **26**, 199-213 (2002).

24. Sijen, T., Fleenor, J., Simmer, F., Thijssen, K.L., Parrish, S., and Timmons, L., Plasterk, R.H., Fire, A. On the role of RNA amplification in dsRNA-triggered gene silencing. *Cell* **107**, 465–476 (2001).

25. Fraser, A.G., Kamath, R.S., Zipperlen, P., Martinez-Campos, M., Sohrmann, M., and Ahringer, J. Functional genomic analysis of *C. elegans* chromosome I by systematic RNA interference. *Nature* **408**, 325–330 (2000).

26. Gönczy, P., Echeverri, C., Oegema, K. et al. Functional genomic analysis of cell division in *C. elegans* using RNAi of genes on chromosome III. *Nature* **408**, 331–336 (2000).

27. Parrish, S., Fleenor, J., Xu, S., Mello, C., and Fire, A. Functional anatomy of a dsRNA trigger: Differential requirement for the two trigger strands in RNA Interference. *Mol. Cell* **6**, 1077–1087 (2000).

28. Tijsterman, M., Ketting, R.F., Okihara, K.L., and Plasterk, R.H. RNA helicase MUT-14–dependent silencing triggered in *C. elegans* by short antisense RNAs. *Science* **295**, 694–697 (2002).

29. Lipardi, C., Wei, Q., and Paterson, B.M. RNAi as Random Degradative PCR. siRNA primers convert mRNA into dsRNAs that are degraded to generate new siRNAs. *Cell* **107**, 297–307 (2001).

30. Kisielow, M., Kleiner, S., Nagasawa, M., Faisal, A., and Nagamine, Y. Isoform-specific knockdown and expression of adaptor protein ShcA using small interfering RNA. *Biochem. J.* **363**, 1–5 (2002).

31. Zamore, P.D., Tuschl, T., Sharp, P.A., and Bartel, D.P. RNAi: Double-stranded RNA directs the ATP-dependent cleavage of mRNA at 21 to 23 nucleotide intervals. *Cell* **101**, 25–33 (2000).

32. Harborth, J., Elbashir, S.M., Bechert, K., Tuschl, T., and Weber, K. Identification of essential genes in cultured mammalian cells using small

interfering RNAs. *J. Cell Sci.* **114**, 4557–4565 (2001).

33. Caplen, N.J., Fleenor, J., Fire, A., and Morgan, R.A. dsRNA–mediated gene silencing in cultured Drosophila cells: A ussue culture model for the analysis of RNA interference. *Gene* **252**, 95–105 (2000).

34. Clemens, J.C., Worby, C.A., Simonson-Leff, N., Muda, M., Maehama, T., Hemmings, B.A., and Dixon, J.E. Use of double-stranded RNA interference in Drosophila cell lines to dissect signal transduction pathways. *Proc. Natl. Acad. Sci. U.S.A.* **97**, 6499–6503 (2000).

35. Ui-Tei, K., Zenno, S., Miyata, Y., and Saigo, K. Sensitive assay of RNA interference in Drosophila and Chinese hamster cultured cells using firefly luciferase gene as target. *FEBS Lett.* **479**, 79–82 (2000).

36. Svoboda, P., Stein, P., Hayashi, H., and Schultz, R.M. Selective reduction of dormant maternal mRNAs in mouse oocytes by RNA interference. *Development* **127**, 4147–4156 (2000).

37. Wianny, F. and Zernicka-Goetz, M. Specific interference with gene function by double-stranded RNA in early mouse development. *Nat. Cell Biol.* **2**, 70–75 (2000).

38. Paddison, P.J., Caudy, A.A., and Hannon, G.J. Stable suppression of gene expression by RNAi in mammalian cells. *Proc. Natl. Acad. Sci. U.S.A.* **99**, 1443–1448 (2002).

39. Yang, S., Tutton, S., Pierce, E., and Yoon, K. Specific double-stranded RNA interference in undifferentiated mouse embryonic stem cells. *Mol. Cell. Biol.* **21**, 7807–7816 (2001).

40. Donzé, O. and Picard, D. RNA interference in mammalian cells using siRNAs synthesized with T7 RNA polymerase. *Nucleic Acids Res.* **30**, e46 (2002).

41. Paddison, P.J., Caudy, A.A., Bernstein, E., Hannon, G.J., and Conklin, D.S. Short hairpin RNAs (shRNAs) induce sequence-specific silencing in mammalian cells. *Genes Dev.* **16**, 948–958 (2002).

42. Yu, J.Y., DeRuiter, S.L., and Turner, D.L. RNA interference by expression of short-interfering RNAs and hairpin RNAs in mammalian cells. *Proc. Natl. Acad. Sci. U.S.A.* **99**, 6047–6052 (2002).

43. Lee, N.S., Dohjima, T., Bauer, G., Li, H., Li, M.J., Ehsani, A., Salvaterra, P., and Rossi, J. Expression of small interfering RNAs targeted against HIV-1 rev transcripts in human cells. *Nat. Biotech.* **20**, 500–505 (2002).

44. Miyagishi, M. and Taira, K. U6 promoter driven siRNAs with four uridine 3' overhangs efficiently suppress targeted gene expression in mammalian cells. *Nat. Biotech.* **20**, 497–500 (2002).

45. Paul, C.P., Good, P.D., Winer, I., and Engelke, D.R. Effective expression of small interfering RNA in human cells. *Nat. Biotech.* **20**, 505–508 (2002).

46. Sui, G., Soohoo, C., Affar el, B., Gay, F., Shi, Y., and Forrester, W.C. A DNA vector-based RNAi technology to suppress gene expression in mammalian cells. *Proc. Natl. Acad. Sci. U.S.A.* **99**, 5515–5520 (2002).

47. Ziauddin, J. and Sabatini, D.M. Microarrays of cells expressing defined cDNAs. *Nature* **411**, 107–110 (2001).

48. Garrus, J.E., von Schwedler, U.K., Pornillos, O.W. et al. Tsg101 and the vacuolar protein sorting pathway are essential for HIV-1 budding. *Cell* **107**, 55–65 (2001).

49. Cortez, D., Guntuku, S., Qin, J., and Elledge, S.J. ATR and ATRIP: Partners in checkpoint signaling. *Science* **294**, 1713–1716 (2001).

50. Mailand, N., Lukas, C., Kaiser, B.K., Jackson, P.K., Bartek, J., and Lukas, J. Deregulated human Cdc14A phosphatase disrupts centrosome separation and chromosome segregation. *Nat. Cell Biol.* **4**, 318–322 (2002).

51. Porter, L.A., Dellinger, R.W., Tynan, J.A., Barnes, E.A., Kong, M., Lenormand, J.L., and Donoghue, D.J. Human Speedy: A novel cell cycle regulator that enhances proliferation through activation of Cdk2. *J. Cell Biol.* **157**, 357–366 (2002).

52. Stucke, V.M., Sillje, H.H., Arnaud, L., and Nigg, E.A. Human Mps1 kinase is required for the spindle assembly checkpoint but not for centrosome duplication. *EMBO J.* **21**, 1723–1732 (2002).

53. Zou, L., Cortez, D., and Elledge, S.J. Regulation of ATR substrate selection by Rad17–dependent loading of Rad9 complexes onto chromatin. *Genes Dev.* **16**, 198–208 (2002).

54. Ancellin, N., Colmont, C., Su, J., Li, Q., Mittereder, N., Chae, S.S., Steffansson, S., Liau, G., and Hla, T. Extracellular export of sphingosine kinase-1 enzyme: Sphingosine 1-phosphate generation and the induction of angiogenic vascular maturation. *J. Biol. Chem.* **277**, 6667–6675 (2001).

55. Bai, X., Zhou, D., Brown, J.R., Crawford, B.E., Hennet, T., and Esko, J.D. Biosynthesis of the linkage region of glycosaminoglycan: Cloning and activity of galactosyltransferase II, the sixth member of the β1,3-galyctosyltransferase family (β3GalT6). *J. Biol. Chem.* **276**, 48189–48195 (2001).

56. Hutvágner, G., McLachlan, J., Bálint, É., Tuschl, T., and Zamore, P.D. A cellular function for the RNA interference enzyme Dicer in small temporal RNA maturation. *Science* **93**, 834–838 (2001).

57. Habas, R., Kato, Y., and He, X. Wnt/Frizzled activation of Rho regulates vertebrate gastrulation and

requires a novel Formin homology protein Daam1. *Cell* **107**, 843–854 (2001).

58. Li, L., Mao, J., Sun, L., Liu, W., and Wu, D. Second cysteine-rich domain of Dickkopf-2 activates canonical Wnt signaling pathway via LRP-6 independently of dishevelled. *J. Biol. Chem.* **277**, 5977–5981 (2001).

59. Martins, L.M., Iaccarino, I., Tenev, T. et al. The serine protease Omi/HtrA2 regulates apoptosis by binding XIAP through a Reaper-like motif. *J. Biol. Chem.* **277**, 439–444 (2002).

60. Du, Q., Stukenberg, P.T., and Macara, I.G. A mammalian partner of inscuteable binds NuMA and regulates mitotic spindle organization. *Nat. Cell Biol.* **3**, 1069–1075 (2001).

61. Moskalenko, S., Henry, D.O., Rosse, C., Mirey, G., Camonis, J.H., and White, M.A. The exocyst is a Ral effector complex. *Nat. Cell Biol.* **4**, 66–72 (2002).

62. Short, B., Preisinger, C., Korner, R., Kopajtich, R., Byron, O., and Barr, F.A. A GRASP55–rab2 effector complex linking Golgi structure to membrane traffic. *J. Cell Biol.* **155**, 877–883 (2001).

63. Ostendorff, H.P., Peirano, R.I., Peters, M.A., Schluter, A., Bossenz, M., Scheffner, M., and Bach, I. Ubiquitination-dependent cofactor exchange on LIM homeodomain transcription factors. *Nature* **416**, 99–103 (2002).

64. Bakker, J., Lin, X., and Nelson, W.G. Methyl-CpG binding domain protein 2 represses transcription from hypermethylated p-class glutathione S-transferase gene promoters in hepatocellular carcinoma cells. *J. Biol. Chem.*, in press. Published April 17, 2002 as 10.1074/jbc.M203009200 (2002).

65. Guo, H.S. and Ding, S.W. A viral protein inhibits the long range signaling activity of the gene silencing signal. *EMBO J.* **21**, 398–407 (2002).

66. Kasschau, K.D. and Carrington, J.C. A counterdefensive strategy of plant viruses: Suppression of posttranscriptional gene silencing. *Cell* **95**, 461–470 (1998).

67. Li, H.W., Lucy, A.P., Guo, H.S., Li, W.X., Ji, L.H., Wong, S.M., and Ding, S.W. Strong host resistance targeted against a viral suppressor of the plant gene silencing defence mechanism. *EMBO J.* **18**, 2683–2691 (1999).

68. Li, W.X. and Ding, S.W. Viral suppressors of RNA silencing. *Curr. Opin. Biotechnol.* **12**, 150–154 (2001).

69. Llave, C., Kasschau, K.D., and Carrington, J.C. Virus-encoded suppressor of posttranscriptional gene silencing targets a maintenance step in the silencing pathway. *Proc. Natl. Acad. Sci. U.S.A.* **97**, 13401–13406 (2000).

70. Lucy, A.P., Guo, H.S., Li, W.X., and Ding, S.W. Suppression of post-transcriptional gene silencing by a plant viral protein localized in the nucleus. *EMBO J.* **19**, 1672–1680 (2000).

71. Li , H., Li, W.X., and Ding, S.W. Induction and suppression of RNA silencing by an animal virus. *Science* **296**, 1319–1321 (2002).

72. Bitko, V. and Barik, S. Phenotypic silencing of cytoplasmic genes using sequence-specific double-stranded short interfering RNA and its application in the reverse genetics of wild type negative-strand RNA viruses. *BMC Microbiol.* **1**, 34 (2001).

73. Rowley, J.D. A new consistent chromosomal abnormality in chronic myelogenous leukaemia identified by quinacrine fluorescence and Giemsa staining. *Nature* **243**, 290–293 (1973).

74. de Klein, A., van Kessel, A.G., Grosveld, G. et al. A cellular oncogene is translocated to the Philadelphia chromosome in chronic myelocytic leukaemia. *Nature* **300**, 765–767 (1982).

75. Druker, B.J., Sawyers, C.L., Kantarjian, H., Resta, D.J., Reese, S.F., Ford, J.M., Capdeville, R., and Talpaz, M. Activity of a specific inhibitor of the BCR-ABL tyrosine kinase in the blast crisis of chronic myeloid leukemia and acute lymphoblastic leukemia with the Philadelphia chromosome. *N. Engl. J. Med.* **344**, 1038–1042 (2001).

76. Druker, B.J., Talpaz, M., Resta, D.J. et al. Efficacy and safety of a specific inhibitor of the BCR-ABL tyrosine kinase in chronic myeloid leukemia. *N. Engl. J. Med.* **344**, 1031–1037 (2001).

77. Wilda, M., Fuchs, U., Wössmann W., and Borkhardt, A., Killing of leukemic cells with a BCR/ABL fusion gene by RNA interference (RNAi). *Oncogene* in press.

78. Caplen, N.J., Taylor, J.P., Statham, V.S., Tanaka, F., Fire, A., and Morgan, R.A. Rescue of polyglutamine-mediated cytotoxicity by double-stranded RNA-mediated RNA interference. *Hum. Mol. Genet.* **11**, 175–184 (2002).

79. La Spada, A.R., Wilson, E.M., Lubahn, D.B., Harding, A.E., and Fischbeck, K.H. Androgen receptor gene mutations in X-linked spinal and bulbar muscular atrophy. *Nature* **352**, 77–79 (1991).

80. Cogoni, C. and Macino, G. Gene silencing in *Neurospora crassa* requires a protein homologous to RNA-dependent RNA polymerase. *Nature* **399**, 166–169 (1999).

81. Dalmay, T., Hamilton, A., Rudd, S., Angell, S., and Baulcombe, D.C. An RNA-dependent RNA polymerase gene in Arabidopsis is required for posttranscriptional gene silencing mediated by a transgene but not by a virus. *Cell* **101**, 543–553 (2000).

82. Mourrain, P., Beclin, C., Elmayan, T. et al. Arabidopsis SGS2 and SGS3 genes

are required for posttranscriptional gene silencing and natural virus resistance. *Cell* **101**, 533–542 (2000).

83. Smardon, A., Spoerke, J., Stacey, S., Klein, M., Mackin, N., and Maine, E. EGO-1 is related to RNA-directed RNA polymerase and functions in germ-line development and RNA interference in *C. elegans*. *Curr. Biol.* **10**, 169–178 (2000).

84. Hirai, I. and Wang, H.G. A role of the C-terminal region of hRad9 in nuclear transport of the hRad9-hRad1-hHus1 checkpoint complex. *J. Biol. Chem.*, in press. Published May 6, 2002 as 10.1074/jbc.M203079200 (2002).

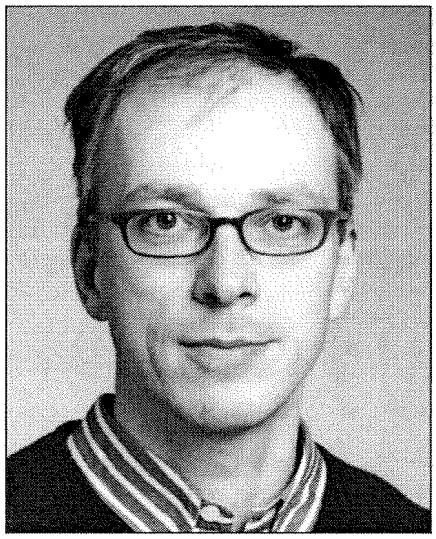

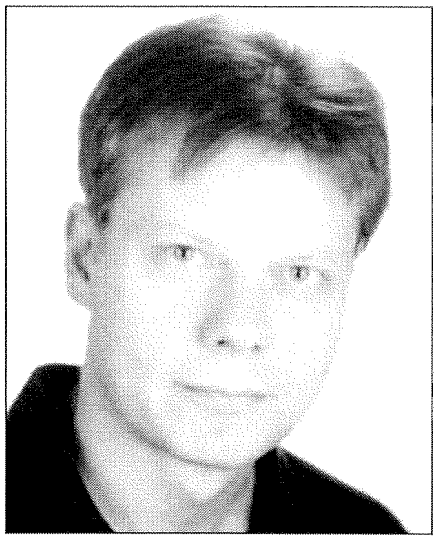

Thomas Tuschl, PhD, is an EMBO Young Investigator and leads the Combinatorial Biochemistry Research Group at the Department of Cellular Biochemistry, Max-Planck-Institute for Biophysical Chemistry, Goettingen, Germany. **Arndt Borkhardt, MD**, is a Principal Investigator in the Department of Pediatric Hematology and Oncology, at Children's University Hospital, Giessen, Germany. Address correspondence to either T.T. or A.B. E-mail ttuschl@mpibpc.gwdg.de; e-mail arndt.borkhardt@paediat.med.uni-giessen.de

TECHNOLOGY REPORT

Transient RNA Interference in Hematopoietic Progenitors With Functional Consequences

Daniela M. Oliveira and Margaret A. Goodell*

Center for Cell and Gene Therapy, Baylor College of Medicine, Houston, Texas

Received 25 April 2003; Accepted 5 June 2003

Summary: Short interfering (si) RNAs have now been shown to inhibit gene expression in several species, including mammals (Elbashir *et al.*: Nature 411:494–498, 2001; Fire *et al.*: Nature 391:806–811, 1998). RNA inhibition in primary cells such as stem cells would facilitate rapid gene discovery in a postgenome era. While retroviruses can deliver siRNA expression cassettes for stable expression (Barton and Medzhitov: Proc Natl Acad Sci USA 99:14943–14945, 2002; Paddison *et al.*: Proc Natl Acad Sci USA 99:1443–1448, 2002; Rubinson *et al.*: Nat Genet 33:401–406, 2003), an efficient method for direct transfer of siRNA to stem cells is still lacking. Here, we established electroporation to deliver siRNA to hematopoietic progenitors. On average, at least 80% of cells take up the RNA, and these display nearly 100% knockout of marker gene expression at both the RNA and protein level. Moreover, knockdown of the hematopoietic regulator, CD45, results in 3-fold more hematopoietic colonies in a progenitor assay. These results demonstrate that transient transfection of siRNA to primary cells can have substantial functional consequences. This technology may be applicable to a variety of primary cell types. genesis 36:203–208, 2003.

Key words: siRNA; electroporation; hematopoietic; stem cells; RNA

INTRODUCTION

Stem cells are self-renewing cells in the adult that retain the capacity for differentiation and replenish many tissues throughout life. In general, the molecular mechanisms governing stem cell commitment remain to be determined, despite the abundance of information generated recently by large-scale genomics efforts (Ivanova *et al.*, 2002; Ramalho-Santos *et al.*, 2002). Furthermore, characterization of many candidate stem cell "signature" genes is hampered by lack of methods for genetic manipulation of stem cells (Fire *et al.*, 1998).

To address this problem, we chose to pursue the possibility that RNA interference (RNAi) technology could be used in primary stem cells, using hematopoietic stem cells as a model system. RNAi is a posttranscriptional, sequence-specific gene silencing process initiated with double-stranded RNA (dsRNA) that is homologous in sequence to a portion of the gene to be silenced (Guo and Kemphues, 1995).

While retroviruses have been used to stably express short hairpin RNA (shRNA) in hematopoietic cells (Hemann *et al.*, 2003; Rubinson *et al.*, 2003), both retroviruses and lentiviruses infect most stem cell types poorly due to their quiescent status. Moreover, in many cases, even transient RNAi may be expected to have a significant impact on differentiation of a stem or progenitor cell. Thus, we established a methodology for highly efficient yet transient RNAi in primary mouse hematopoietic progenitors using short interfering RNA (siRNA), which has been shown to generate transient gene-specific silencing in mammalian cells lines (Elbashir *et al.*, 2001b).

RESULTS AND DISCUSSION

Since nondividing primary hematopoietic stem cells (HSCs) are difficult to transfect using nonviral approaches, we tested several transfection protocols and found that exposure of murine bone marrow cells to a pulse-electric field was the most efficient technique. We used the Gene Pulser™ electroporation apparatus to transfer dsRNA and determined the best parameters to introduce dsRNA into populations enriched for HSC and progenitors using Sca-1. All murine bone marrow HSC express the Sca-1 antigen (Spangrude *et al.*, 1988) and only ~5% of bone marrow cells express Sca-1, affording a ~20-fold enrichment for HSC and progenitors. By using siRNA labeled with FITC molecules, we found the optimal conditions (described in Materials and Methods) with transfection efficiencies averaging 80% (Fig. 1). We also observed that the transfection yield in mouse bone

* Correspondence to: M.A. Goodell, Center for Cell and Gene Therapy, Baylor College of Medicine, One Baylor Plaza, BCM 505, Houston, TX 77030.
E-mail: Goodell@bcm.tmc.edu

DOI: 10.1002/gene.10212

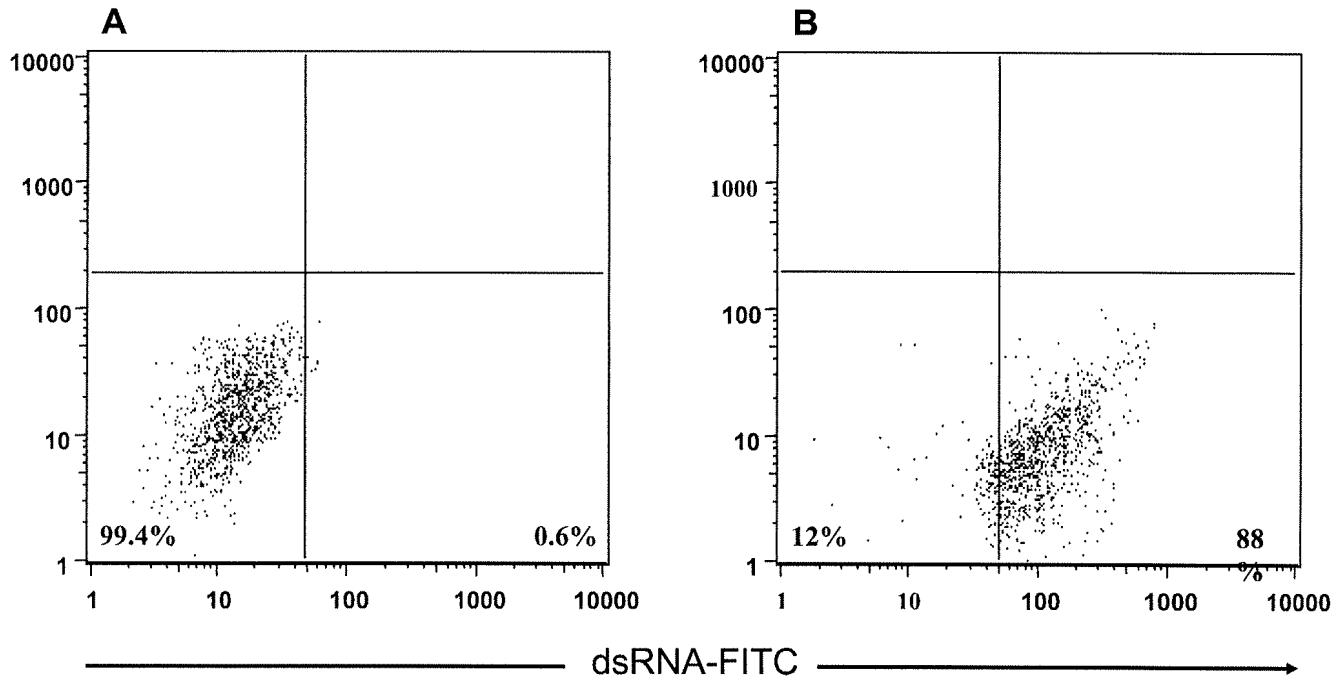

FIG. 1. **A:** Sca-1-positive mouse bone marrow cells that were electroporated in the absence of dsRNA (negative control). **B:** Cells that were electroporated with fluorescent siRNA, resulting in transfection of ~90% of the cells, measured 1 day after electroporation.

marrow increases proportionally with enrichment for Sca-1 (data not shown).

In order to determine whether RNAi would function in pulsed primary murine hematopoietic cells, we transfected Sca-1-positive bone marrow cells with chemically synthesized dsRNA against lacZ and GFP. For these studies we used Sca-1-enriched cells from C57/Bl/6-ROSA transgenic mice that express lacZ constitutively (Zambrowicz *et al.*, 1997) and Sca-1-GFP knockin mice (Hanson *et al.*, 2003). After siRNA electroporation, the proportion of cells expressing GFP or lacZ, measured by flow cytometry, was reduced to ~20% or 40% of control levels, respectively (Fig. 2A,B). Electroporation of cells in the absence of dsRNA or in the presence of a control siRNA had no significant effect on the number of positive cells.

Comparative analysis of lacZ mRNA levels by real-time quantitative PCR, using as a reference the level of the housekeeping β-actin mRNA, validated our observations and show a 90% reduction of lacZ mRNA compared to the control level (Fig. 2C). Since at least 10% of cells were probably untransfected (Fig. 1), this indicates that in cells receiving the siRNA the lacZ transcript is almost completely eliminated. The ~40% of electroporated cells that still exhibit lacZ protein as measured by FDG (Fig. 2B) could be explained by a number of factors, including a long protein half-life and the sensitivity of lacZ detection using FDG, due to the enzymatic nature of the semiquantitative assay. The dramatic knockdown in transfected cells indicates the efficiency of RNAi in primary mammalian is better than originally believed (Elbashir *et al.*, 2001a; Fire *et al.*, 1998).

To determine the viability of the pulsed cells, we analyzed their differentiation potential in methylcellulose medium containing hematopoietic growth factors. Pulsed cells were able to originate colonies when placed in methylcellulose medium (Fig. 3C). This observation is in agreement with previous studies performed with human cells that have shown that hematopoietic cell properties are preserved during electroporation, suggesting the use of pulsed electric field as a method for selection of human hematopoietic cells and depletion of contaminants (Eppich *et al.*, 2000).

Cells electroporated with siRNA-lacZ and cultured for 10 days in methylcellulose showed the same percentage of lacZ-positive cells as those transfected with siRNA control, indicating that the silencing was transient, prompting us to evaluate other siRNA expression strategies. We used a commercially available plasmid vector (pSILENCER, Ambion, Austin, TX) that expresses RNAi, inducing short hairpin RNA (shRNA) under the control of U6 promoter in mammalian cells (Sui *et al.*, 2002). In different culture cell lines, this shRNAi vector has generated stable loss-of-function phenotypes, mediating persistent suppression of gene expression and allowed the analysis of loss-of-function phenotypes that develop over long periods of time (Brummelkamp *et al.*, 2002; Sui *et al.*, 2002). We electroporated pSilencer containing shRNA-lacZ and analyzed the presence of lacZ in methylcellulose colonies originating from transfected cells. We found a reduction of about 30% in the number of lacZ-positive cells analyzed 10 days after the electroporation (Fig.

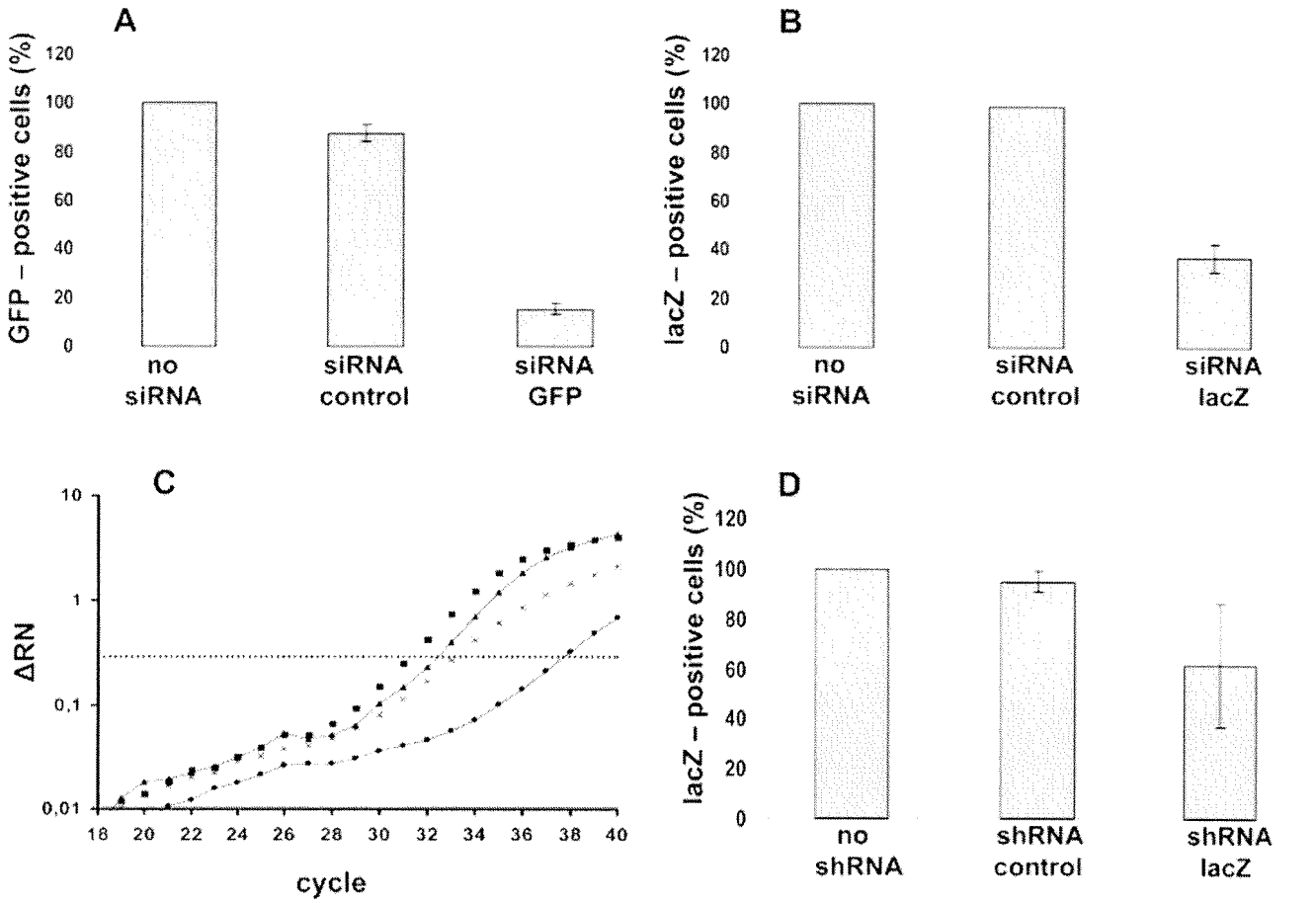

FIG. 2. RNAi in murine bone marrow cells. Effects of siRNA on the percentage of GFP-positive cells (**A**) and lacZ-positive cells (**B**) are shown. Bone marrow cells enriched for Sca-1 from transgenic mice which express lacZ constitutively and GFP in Sca-1 cells were used. Cells were transfected with siRNA against GFP, lacZ, control siRNA, or transfected in the absence of siRNA as indicated, and analyzed 3 days after electroporation and growth in liquid medium. The error bars indicate SDs with n = 3. The amplification plot of real-time quantitative PCR used to compare the intracellular levels of mRNA of lacZ and the housekeeping gene β-actin 2 days after electroporation is shown in (**C**). The x-axis shows the number of PCR cycles and y-axis fluorescence. A fluorescence threshold was set above the baseline (horizontal dashed line). The parameter threshold cycle (CT) is defined as the cycle number at which the fluorescence crosses the threshold. Amplification plots using lacZ primers from cell populations electroporated with siRNA against lacZ (circle) (CT = 37.6), siRNA control (triangle) (CT = 32.0), and β-actin primers in cells transformed with siRNA-control (squares) (CT = 30.5) and siRNA-lacZ (X) (CT = 33.1) are shown. Quantification of the amount of lacZ RNA relative to the amount of β-actin RNA in samples was accomplished by analyzing the CTs and normalizing the level of lacZ expression against the level of β-actin. The measuring of the CT values was performed using software of the 7700 system. **D:** Cells were transfected with a vector that expresses shRNA against lacZ (pSilencer). Values were normalized as a function of the number of positive cells observed in the absence siRNA or vector. The data are the average ± SD of at least five independent determinations.

2D), while cells kept in liquid long-term bone marrow medium for 3 days after the electroporation exhibited a reduction of about 40% in the number of lacZ-positive cells. This indicated that while the initial transfection of plasmid is less efficient than siRNA (likely due to size), the RNA inhibition in transfected cells was nevertheless more sustained. The reduction in inhibition over time was probably due to dilution and loss of the vector by the cells as they divided and differentiated.

Finally, we tested whether we could knockdown a natural endogenous gene with an observable effect in a functional assay such as colony formation in methylcellulose. The candidate for this study was CD45, a cell surface tyrosine phosphatase found in multiple isoforms on all nucleated hematopoietic cells (Trowbridge and Thomas, 1994). We interfered with the expression of CD45 by introducing siRNA in Sca-positive cells as described above. Three days after electroporation, we detected a significant reduction in the cell surface expression of CD45 (Fig. 3A) by flow cytometry of cells from the liquid culture. We also quantified the changes at the mRNA level using real-time quantitative PCR, which revealed a 16-fold reduction of CD45 mRNA in transfected cells (Fig. 3B). Remarkably, we observed that siRNA-transfected cells generated an average of 3-fold more methylcellulose colonies than controls, in-

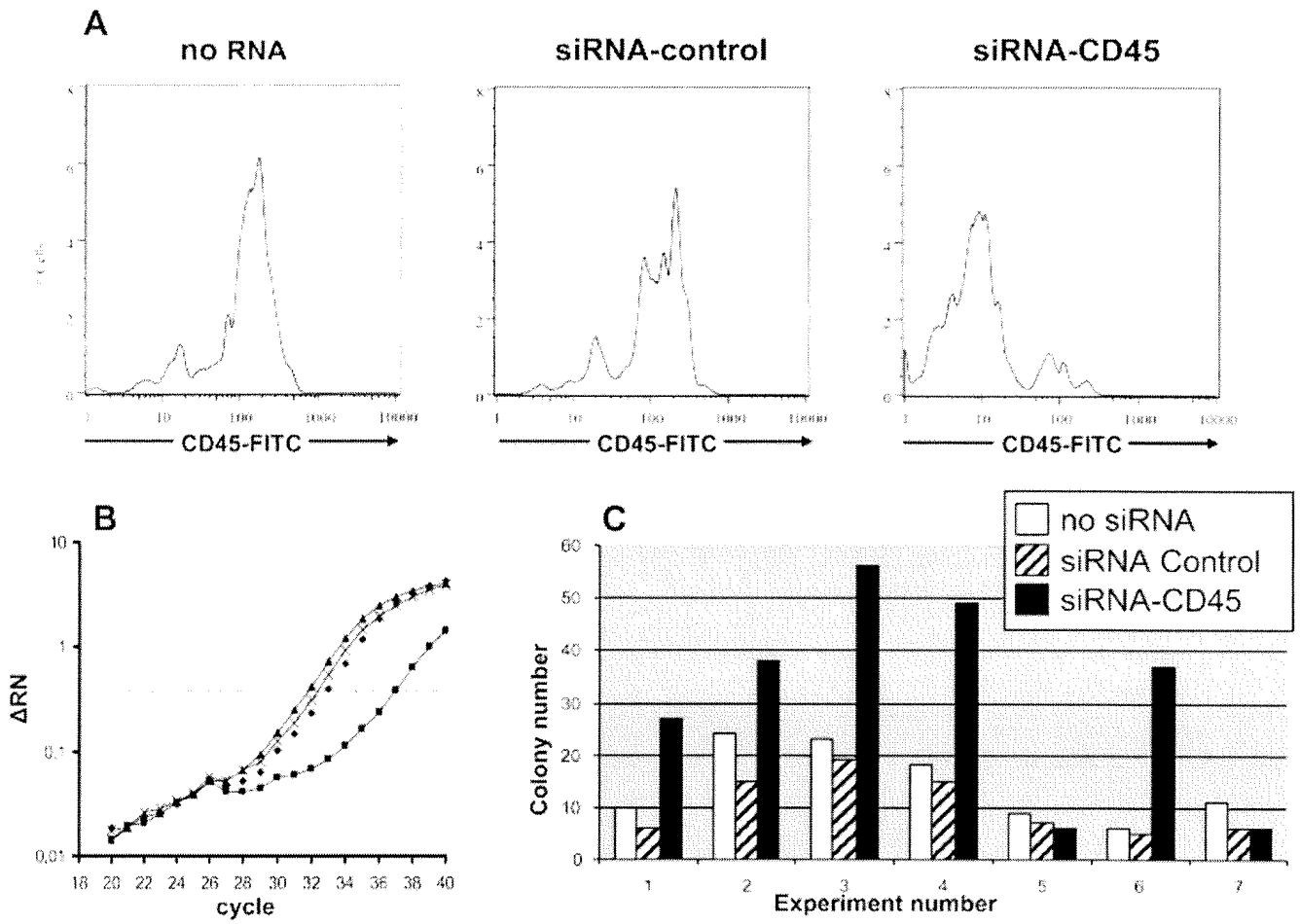

FIG. 3. Functional gene silencing in HSCs. Histograms showing the typical reduction of CD45 gene expression observed 3 days after siRNA transfection in bone marrow cells enriched for Sca-1 (**A**). Cells were electroporated with siRNA-CD45 (far right panel), siRNA-control (middle), and in the absence of dsRNA (left), as indicated. Analysis by flow cytometry after staining with CD45 antibody showed that ~80% of cells downregulated the surface expression of CD45. The knockdown of CD45 expression was validated by real-time PCR. The amplification plots of real-time quantitative PCR used to compare the intracellular levels of mRNA of CD45 and β-actin 2 days after electroporation are shown in (**B**). The plots used to estimate the alteration in the level of CD45 mRNA in cell populations electroporated with siRNA against CD45 (squares) (CT = 36.8), siRNA control (X) (CT = 32.2), and β-actin mRNA in cells transformed with siRNA-control (triangle) (CT = 31.6) and CD45 (diamonds) (CT = 33.0) are shown. Transfected cells were counted and then 10^5 cells were transferred to methylcellulose. Colonies were counted 7–10 days later as shown in (**C**).

dicating that knockdown of CD45 caused proliferation of the target cells. The degree of expansion observed was wide in range (0.9–7.4-fold, Fig. 3C), probably due to small differences in initial RNAi efficiency (due to variations in electroporation or siRNA quality) which become magnified during the initial 3-day culture period by differential proliferation rates of transfected cells. These data are in agreement with the current view that CD45 is involved in the suppression of proliferation of hematopoietic cells (Penninger *et al.*, 2001).

Here we have shown that the use of electroporation together with siRNA offers a straightforward method for rapidly testing the effect of knockdown of genes affecting proliferation and differentiation of hematopoietic progenitors. Coupled with simple strategies for siRNA production (Myers *et al.*, 2003; Sohail *et al.*, 2003), this method could be used for first-pass screening of genes potentially involved in stem cell function as identified by large scale studies (Ivanova *et al.*, 2002; Phillips *et al.*, 2000; Ramalho-Santos *et al.*, 2002; Terskikh *et al.*, 2001). Moreover, since there is a paucity of methods for transduction of embryonic as well as adult stem cell types, the methods described herein may be widely applicable.

MATERIALS AND METHODS

siRNA

Synthetic siRNA oligos (Dharmacon, Lafayette, CO; Ambion), were as follows (sense strand is given): lacZ, cucggcguuucaucugugg; GFP, aagcugacccugaaguucauc;

CD45, gucuuugucacagggcaaa. Synthetic fluorescent siRNA, which has FITC molecules attached to both 3′-ends was obtained from Orbigene (San Diego, CA).

Cells and Transfection of Primary Hematopoietic Cells

Bone marrow cells from C57Bl/6-ROSA26 transgenic mice (Zambrowicz *et al.*, 1997) (obtained from Jackson Laboratories, Bar Harbor, ME) and mice that express GFP in Sca-1 positive cells (Hanson *et al.*, 2003) were isolated as previously described (Bradfute and Goodell, 2003). Magnetic enrichment was performed by incubating the cells with Sca-1-biotin antibody (E13-161.7, Pharmingen, San Diego, CA) followed by streptavidin-conjugated microbeads (Miltenyi Biotec, Auburn, CA), then passing the cells through a magnetic column (Miltenyi Biotec). After magnetic enrichment, cell preparations were verified to be on average 90% Sca-1-positive.

For electroporation, Sca-1 positive bone marrow cells were resuspended at 1×10^6 cell/ml in DMEM serum-free medium (GIBCO BRL, Gaithersburg, MD). Samples of 500 μl each were placed in electrode gap cuvettes 4 mm gap (Life Technologies, Carlsbad, CA), gently mixed with dsRNA or pSilencer (Ambion), to a final concentration of 2 μmolar. The cell-nucleic acid was gently mixed and kept on ice 5 min prior to electroporation and then pulsed once at 320 mV, 1,600 μF with a Life Technologies Cell Porator, with the internal compartment for temperature control filled with water at room temperature. After electroporation the cells were washed in long-term bone marrow medium. The cells were then resuspended in long-term bone marrow medium and incubated in a humidified incubator at 37°C, 5% CO_2. A very detailed protocol can be found at http://www.bcm.tmc.edu/genetherapy/goodell/.

Flow cytometry analyses were performed by using FACScan (Becton Dickinson, Sunnyvale, CA). All antibodies used in this work were from Pharmingen. The presence of lacZ in the cells was determined by using FDG (Molecular Probes, Eugene, OR).

Real-Time RT-PCR

The quantification of the target mRNA relative to β-actin was performed using SYBR Green detection of products (Applied Biosystems, Warrington, UK) as described previously (Becker *et al.*, 1996), using an ABI 7700 sequence detector (Perkin-Elmer, Wellesley, MA). The following primers were used: lacZ (forward: tttctccggcggtaaa, reverse: cggtttcatctctggtgcaac); β-actin (forward: caaaagccaccccactcctaaga, reverse: gccctggctgcctcaacacctc); CD45 (forward: acacccagtgatggtgcca; reverse: ggcccagagtggatggtgta). RNA from murine Sca-1 positive cells was purified by using RNA-Aqueous (Ambion). Purified mRNA was digested, DNAase-treated, and reverse transcription PCR for first strand DNA synthesis was performed according to the instructions provided with Superscript II (Invitrogen, Carlsbad, CA).

Methylcellulose Culture

Hematopoietic colony assays were performed by plating 5,000 cells in Methocult m3434 (StemCell Techonolgy, Vancouver, BC) 1 day after electroporation. The cells were incubated in a humidified incubator at 37°C, 5% CO_2. The number of hematopoietic colonies was scored 7–12 days after the cultures were initiated.

LITERATURE CITED

Becker A, Reith A, Napiwotzki J, Kadenbach B. 1996. A quantitative method of determining initial amounts of DNA by polymerase chain reaction cycle titration using digital imaging and a novel DNA stain. Anal Biochem 237:204–207.

Bradfute SB, Goodell MA. 2003. Adenoviral transduction of mouse hematopoietic stem cells. Mol Ther 7:334–340.

Brummelkamp TR, Bernards R, Agami R. 2002. A system for stable expression of short interfering RNAs in mammalian cells. Science 296:550–553.

Elbashir SM, Harborth J, Lendeckel W, Yalcin A, Weber K, Tuschl T. 2001a. Duplexes of 21-nucleotide RNAs mediate RNA interference in cultured mammalian cells. Nature 411:494–498.

Elbashir SM, Lendeckel W, Tuschl T. 2001b. RNA interference is mediated by 21- and 22-nucleotide RNAs. Genes Dev 15:188–200.

Eppich HM, Foxall R, Gaynor K, Dombkowski D, Miura N, Cheng T, Silva-Arrieta S, Evans RH, Mangano JA, Preffer FI, Scadden DT. 2000. Pulsed electric fields for selection of hematopoietic cells and depletion of tumor cell contaminants. Nat Biotechnol 18:882–887.

Fire A, Xu S, Montgomery MK, Kostas SA, Driver SE, Mello CC. 1998. Potent and specific genetic interference by double-stranded RNA in Caenorhabditis elegans. Nature 391:806–811.

Guo S, Kemphues KJ. 1995. par-1, a gene required for establishing polarity in C. elegans embryos, encodes a putative Ser/Thr kinase that is asymmetrically distributed. Cell 81:611–620.

Hanson P, Mathews V, Marrus SH, Graubert TA. 2003. Enhanced green fluorescent protein targeted to the Sca-1 (Ly-6A) locus in transgenic mice results in efficient marking of hematopoietic stem cells in vivo. Exp Hematol 31:159–167.

Hemann MT, Fridman JS, Zilfou JT, Hernando E, Paddison PJ, Cordon-Cardo C, Hannon GJ, Lowe SW. 2003. An epi-allelic series of p53 hypomorphs created by stable RNAi produces distinct tumor phenotypes in vivo. Nat Genet 33:396–400.

Ivanova NB, Dimos JT, Schaniel C, Hackney JA, Moore KA, Lemischka IR. 2002. A stem cell molecular signature. Science 298:601–604.

Myers JW, Jones JT, Meyer T, Ferrell JE. 2003. Recombinant Dicer efficiently converts large dsRNAs into siRNAs suitable for gene silencing. Nat Biotechnol 21:324–328.

Penninger JM, Irie-Sasaki J, Sasaki T, Oliveira-dos-Santos AJ. 2001. CD45: new jobs for an old acquaintance. Nat Immunol 2:389–396.

Phillips RL, Ernst RE, Brunk B, Ivanova N, Mahan MA, Deanehan JK, Moore KA, Overton GC, Lemischka IR. 2000. The genetic program of hematopoietic stem cells. Science 288:1635–1640.

Ramalho-Santos M, Yoon S, Matsuzaki Y, Mulligan RC, Melton DA. 2002. "Stemness": transcriptional profiling of embryonic and adult stem cells. Science 298:597–600.

Rubinson DA, Dillon CP, Kwiatkowski AV, Sievers C, Yang L, Kopinja J, Zhang M, McManus MT, Gertler FB, Scott ML, Van Parijs L. 2003. A lentivirus-based system to functionally silence genes in primary mammalian cells, stem cells and transgenic mice by RNA interference. Nat Genet 33:401–406.

Sohail M, Doran G, Riedemann J, Macaulay V, Southern EM. 2003. A

simple and cost-effective method for producing small interfering RNAs with high efficacy. Nucleic Acids Res 31:e38.-

Spangrude GJ, Heimfeld S, Weissman IL. 1988. Purification and characterization of mouse hematopoietic stem cells. Science 241:58-62.

Sui G, Soohoo C, Affar el B, Gay F, Shi Y, Forrester WC. 2002. A DNA vector-based RNAi technology to suppress gene expression in mammalian cells. Proc Natl Acad Sci USA 99:5515-5520.

Terskikh AV, Easterday MC, Li L, Hood L, Kornblum HI, Geschwind DH, Weissman IL. 2001. From hematopoiesis to neuropoiesis: evidence of overlapping genetic programs. Proc Natl Acad Sci USA 98:7934-7939.

Trowbridge IS, Thomas ML. 1994. CD45: an emerging role as a protein tyrosine phosphatase required for lymphocyte activation and development. Annu Rev Immunol 12:85-116.

Zambrowicz BP, Imamoto A, Fiering S, Herzenberg LA, Kerr WG, Soriano P. 1997. Disruption of overlapping transcripts in the ROSA beta geo 26 gene trap strain leads to widespread expression of beta-galactosidase in mouse embryos and hematopoietic cells. Proc Natl Acad Sci USA 94:3789-3794.

Retroviral delivery of small interfering RNA into primary cells

Gregory M. Barton and Ruslan Medzhitov*

Section of Immunobiology and The Howard Hughes Medical Institute, Yale University School of Medicine, 310 Cedar Street, New Haven, CT 06520

Communicated by Peter Cresswell, Yale University School of Medicine, New Haven, CT, October 2, 2002 (received for review August 9, 2002)

RNA interference is an evolutionarily conserved process in which recognition of double-stranded RNA ultimately leads to posttranscriptional suppression of gene expression. This suppression is mediated by short (21- to 22-nt) small interfering RNAs (siRNAs), which induce degradation of mRNA based on complementary base pairing. The silencing of gene expression by siRNAs is emerging rapidly as a powerful method for genetic analysis. Recently, several groups have reported systems designed to express siRNAs in mammalian cells through transfection of either oligonucleotides or plasmids encoding siRNAs. Because these systems rely on transfection for delivery, the cell types available for study are restricted generally to transformed cell lines. Here, we describe a retroviral system for delivery of siRNA into cells. The use of retroviral vectors can greatly expand the types of cells available for RNA interference analysis. Furthermore, we demonstrate that this retroviral system allows for stable inactivation of genes in primary cells.

It has long been appreciated that detection of double-stranded RNA (dsRNA) within mammalian cells leads to an IFN response initiated by the sequence-independent recognition of dsRNA (1). More recently, it was discovered that dsRNA also could induce a sequence-specific degradation of mRNA, effectively silencing expression of a given gene (2). This process of RNA interference (RNAi) initially was discovered in the nematode *Caenorhabditis elegans* (3), but it is now clear that RNAi is an ancient, evolutionarily conserved process. Within invertebrate organisms, which lack the sequence-independent dsRNA response, RNAi has become a powerful method to quickly perform genetic analysis of a given gene.

The complete molecular mechanism responsible for RNAi is not yet known, although it has been shown that silencing does involve cleavage of both the initiating dsRNA and the target mRNA into 21- to 23-nt fragments (4). Furthermore, 21- to 23-nt dsRNAs, or small interfering RNAs (siRNAs), are capable of inducing RNAi in mammalian cells without initiating the sequence-independent dsRNA response (5). Consequently, the challenge to mammalian biologists has been to develop systems that deliver siRNAs efficiently into mammalian cells. Recently, a number of groups reported a solution based on transcription of short hairpin RNAs by RNA polymerase III (pol III) (6–10). The hairpins of these short RNAs are processed to generate siRNAs and induce gene silencing. Transfection of plasmids with pol III promoters driving hairpin RNAs can eliminate expression of a target gene.

The limitation of any plasmid- or oligonucleotide-based system is the dependence on transfection. Only certain cell lines can be transfected, and efficient transfection of primary cells is virtually impossible. In contrast, retroviral gene delivery is effective in most cell lines and many primary cell types. We have developed a retroviral system for delivery of siRNA into mammalian cells. This system can be used to silence gene expression in any cell line or primary cell type that can be infected by a retrovirus.

Materials and Methods

Constructs. The RVH1 and LTRH1 vectors are based on the pQCXIH vector (CLONTECH). The hygromycin resistance gene was replaced with the human CD4 gene, which was cloned from splenic cDNA. To eliminate any potential signaling, a premature stop codon was introduced after amino acid 425, just after the transmembrane domain. The human H1 promoter was cloned from genomic DNA and inserted either upstream of the cytomegalovirus (CMV) promoter (RVH1) by using previously introduced *Xho*I and *Eco*RI sites or within the 3′ LTR by using *Sal*I. The oligonucleotides encoding the human p53 siRNA, described by Brummelkamp *et al.* (6), were 5′-GATCCCCGACTCCAGTGGTAATCTACTTCAAGAGAGTAGATTACCACTGGAGTCTTTTTGGAAC-3′ and 5′-TCGAGTTCCAAAAAGACTCCAGTGGTAATCTACTCTCTTGAAGTAGATTACCACTGGAGTCGGG-3′. These oligonucleotides were annealed and ligated downstream of the H1 promoter. All oligonucleotides were synthesized by the Keck Facility at Yale University.

Generation of Virus. The packaging cell line GP2-293 (CLONTECH) was grown in DMEM with 10% FCS/10 mM Hepes/2 mM L-glutamine/1 mM MEM sodium pyruvate/100 units/ml penicillin/100 μg/ml streptomycin (all from Invitrogen). Cells in 10-cm dishes were transfected by calcium phosphate precipitation with 15 μg pVSV-G (CLONTECH) and 15 μg of RVH1 or LTRH1. Chloroquine (Sigma) was added to a final concentration of 25 μM 5 min before transfection. The medium was replaced 8 h posttransfection. Twenty-four hours posttransfection, cells were placed at 32°C to increase viral titer. Forty-eight hours posttransfection, the supernatant was collected, filtered through a 0.45-μm syringe filter, and spun at 50,000 × *g* for 1.5 h. Pelleted virus was resuspended in 0.1 or 0.05 the original volume of medium at 4°C for several hours.

Infection of Target Cells. HEK293T cells were grown in DMEM with 10% FCS/10 mM Hepes/2 mM L-glutamine/1 mM MEM sodium pyruvate/100 units/ml penicillin/100 μg/ml streptomycin. Primary human fibroblasts (AG01522C cells; Coriell Cell Repositories, Camden, NJ) were grown in MEM α (Invitrogen) with 15% FCS/2 mM L-glutamine/100 units/ml penicillin/100 μg/ml streptomycin. The day before infection, 3×10^5 293T cells or 2×10^5 AG01522 cells were plated per well of six-well plates. The next day, virus supernatant was added with polybrene (5 μg/ml final concentration), and the cells were placed at 32°C overnight. The next day, the medium was replaced and the cells were returned to 37°C until analysis. Etoposide, used to treat AG01522 cells, was purchased from Calbiochem.

Western Blots. Cells were harvested at the indicated times, washed twice with cold PBS, and lysed in TNT lysis buffer (20 mM Tris/200 mM NaCl/1% Triton X-100) plus protease inhibitors. After 20 min on ice, lysates were spun at 15,000 × *g* for 10 min to remove insoluble material. Protein concentrations were de-

Abbreviations: dsRNA, double-stranded RNA; RNAi, RNA interference; siRNA, small interfering RNA; pol III, RNA polymerase III; CMV, cytomegalovirus.

*To whom correspondence should be addressed at: Section of Immunobiology, Yale University School of Medicine, 310 Cedar Street, BML 458, New Haven, CT 06510. E-mail: ruslan.medzhitov@yale.edu.

GENETICS

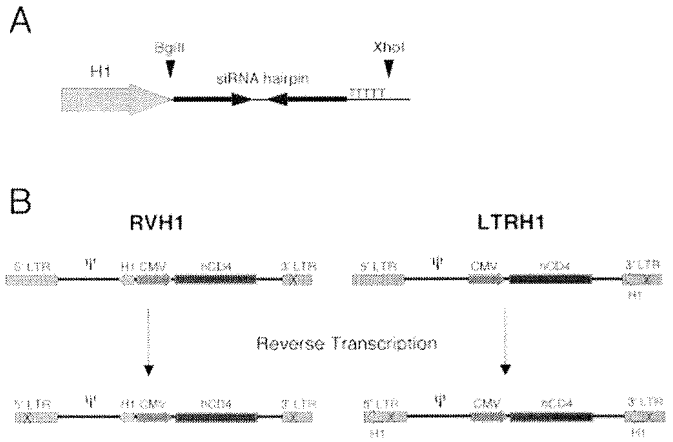

Fig. 1. (*A*) Schematic representation of the H1 promoter cassette. Unique restriction endonuclease sites allow cloning of hairpin-encoding oligonucleotides directly into the retroviral vectors. The five thymidines serve as a termination signal for RNA pol III. (*B*) Schematic representations of RVH1 and LTRH1 retroviral vectors. The vectors are shown above and the integrated proviruses are shown below. During reverse transcription, portions of the 3′ LTR serve as the template for generating the new 5′ LTR. The "X" in the 3′ LTR in the upper schematics represents deletion of the U3 region, which is copied into the 5′ LTR.

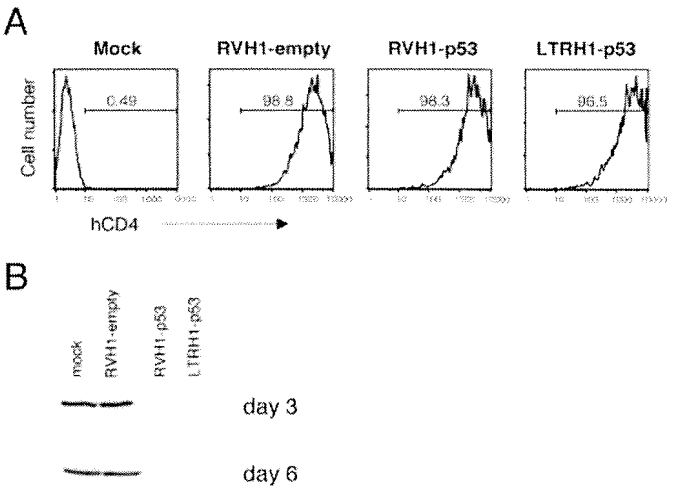

Fig. 2. Infection of 293T cells with RVH1-p53 or LTRH1-p53 eliminates expression of p53. (*A*) CD4 expression on 293T cells infected with RVH1 vector, RVH1-p53, or LTRH1-p53 or mock-infected, as measured by flow cytometry. The percentage of infected cells 3 days postinfection is indicated. (*B*) 293T cells infected as in *A* were analyzed for p53 expression by Western blotting. Western blots are shown 3 and 6 days postinfection.

termined by BCA assay (Pierce). Thirty micrograms of lysate was separated on 10% or 12% SDS/PAGE gels, transferred to Immobilon-P membrane (Millipore), and incubated with anti-p53 or anti-p21 antisera (both from Santa Cruz Biotechnology), followed by incubation with donkey anti-rabbit secondary antibody conjugated to horseradish peroxidase (Amersham Pharmacia). Western blots were developed by using enhanced chemiluminescence (Amersham Pharmacia).

Flow Cytometry. Infected cells were harvested, washed twice with FACS buffer (PBS/3% FCS/0.0025% sodium azide), and incubated for 30 min with anti-hCD4-PE antibody (PharMingen). Cell analysis was performed with a FACScan or FACSCalibur instrument by using CELLQUEST software (PharMingen).

Southern Blots. Genomic DNA (10 μg) was digested with *Eco*RI and *Nhe*I overnight, separated on a 1.2% agarose gel, and transferred to Hybond nylon membrane (Amersham Pharmacia) under alkaline conditions. A DNA probe consisting of an *Eco*RI/*Xba*I fragment from RVH1 (encoding the CMV promoter) was labeled with horseradish peroxidase by using the North2South Direct HRP Labeling and Detection Kit (Pierce). Hybridization and developing of the blot were performed according to the manufacturer's instructions.

Results and Discussion

It has been demonstrated recently that pol III-dependent promoters can be used to drive expression of short hairpin RNAs, which then are processed into siRNAs (6–10). We sought to develop a retroviral vector that would drive expression of siRNAs from the pol III-dependent H1 promoter. Anticipating that expression of a pol III promoter from within a provirus would be hampered by interference from the strong LTR promoter (11), we constructed two viruses to circumvent this problem (Fig. 1). The first, RVH1, lacks the U3 portion of the 3′ LTR. Through the course of reverse transcription, this deletion is copied into the 5′ LTR. Consequently, the 5′ LTR of the integrated provirus is transcriptionally inactive. The second vector, LTRH1, contains the H1 cassette within the 3′ LTR such that the entire cassette is copied into the 5′ LTR, upstream of the promoter elements, during reverse transcription. This design has the added benefit of duplicating the H1 cassette such that the integrated provirus has two copies. Unique restriction endonuclease sites allow the hairpin-encoding oligonucleotides to be cloned directly into both retroviral vectors. In addition, both vectors express a version of human CD4 that lacks the intracellular domain, so infected cells can be identified by cell surface staining with anti-CD4 antibodies.

We initially targeted human p53 gene expression in HEK293T cells, using a 21-nt sequence previously shown to induce RNAi against human p53 (6). 293T cells have high endogenous levels of p53 because of expression of SV40 large T antigen, which stabilizes and inactivates p53. To produce high titer virus, we generated pseudotyped virus by using the vesicular stomatitis virus G protein in place of the normal retroviral envelope. The stability of vesicular stomatitis virus G protein permits concentration of virus by ultracentrifugation (12). Consequently, we were able to infect all cells in a given experiment, eliminating the need to select or sort for infected cells (Fig. 2*A*). Infection of 293T cells with high titer RVH1-p53 or LTRH1-p53 virus eliminated p53 expression completely when compared with mock-infected cells or cells infected with a virus lacking the p53 hairpin, RVH1-empty (Fig. 2*B*). Importantly, because these retroviral vectors integrate into the genomes of the target cells, the elimination of expression was stable over time, effectively creating a mutant cell line.

Through the course of our analysis, we noticed that the reduction in p53 expression in infected cells correlated with expression of CD4 (Fig. 3). The best silencing was achieved in superinfected cells, i.e., cells infected by multiple viruses. As shown in Fig. 3*A*, populations of 293T cells infected with serial dilutions of virus expressed decreasing levels of CD4 even though all of the cells within the population were infected. When we examined p53 expression in these cells, we found that the higher expression of CD4 correlated with more efficient silencing of p53 (Fig. 3*B*). In fact, in cases in which all of the cells expressed CD4, but at relatively low levels, silencing was not always complete. These data indicate that silencing is most efficient when multiple virions infect a given cell, leading to multiple copies of the H1 cassette integrated within the cellular genome. To demonstrate this directly, we performed Southern

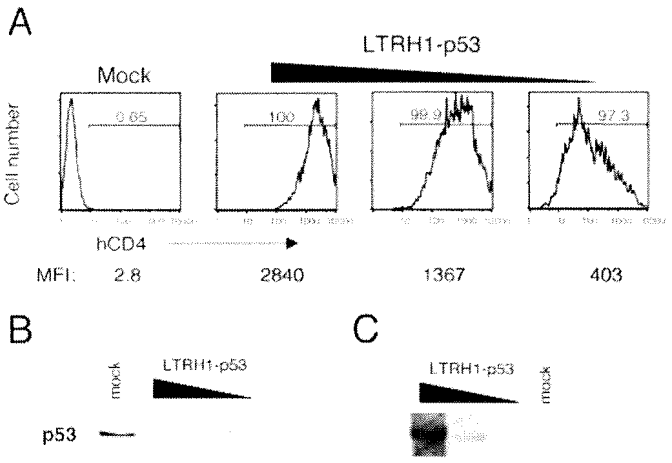

Fig. 3. Multiple copies of the H1 cassette are necessary for complete silencing. (*A*) 293T cells were infected with serial dilutions of LTRH1-p53, and p53 expression was measured 3 days postinfection. The percentage of infected cells was determined by measuring CD4 expression by flow cytometry. The infection percentage and mean fluorescence intensity corresponding to each dilution are indicated. (*B*) 293T cells infected as described in *A* were analyzed for p53 expression by Western blot. (*C*) 293T cells infected as in *A* were analyzed for integration of the retroviral vector by Southern blot. A probe corresponding to the CMV promoter was used to detect the integrated viruses within genomic DNA from infected cells.

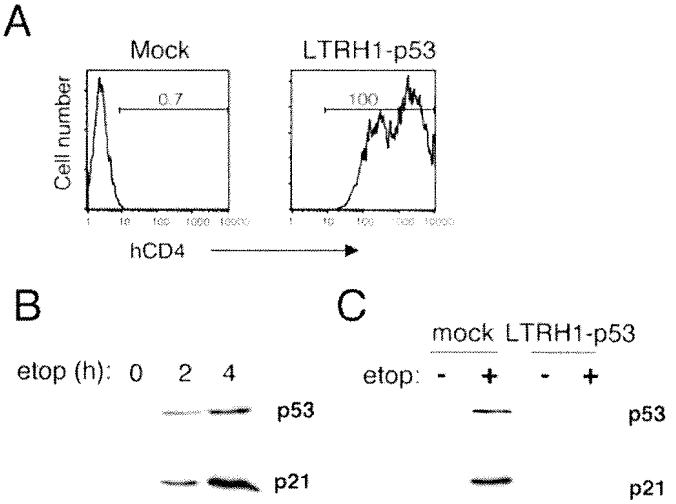

Fig. 4. Retroviral delivery of siRNA into primary fibroblasts eliminates p53 expression. (*A*) FACS analysis of CD4 expression on primary human fibroblasts infected with LTRH1-p53 or mock-infected. (*B*) Primary human fibroblasts (AG01522 cells) were treated with 100 μM etoposide for the indicated times, after which the cells were harvested and p53 and p21 expression levels were determined by Western blot analysis. (*C*) Primary fibroblasts were infected with LTRH1-p53 virus as in *A*. Three days postinfection, cells were treated with 100 μM etoposide (etop). After 4 h of etoposide treatment, cells were harvested and expression levels of p53 and p21 were measured by Western blot analysis.

blot analysis on genomic DNA from infected cells by using a probe for the retroviral vector. As suggested by the analysis of CD4 expression, populations of infected cells with more complete silencing of p53 had more copies of the integrated retroviral vectors within their genomes (Fig. 3*C*). These data agree with the reports of plasmid-based pol III siRNA systems in which silencing was dose-dependent and may suggest that expression from pol III promoters is relatively weak (6), although the need for high expression may vary depending on which gene is targeted. Generation of vectors with multiple copies of the H1 cassette may overcome the need for high copy number or superinfection.

One of the powerful aspects of retroviral gene delivery is the ability to introduce genes into otherwise intractable cell types. In particular, primary cells often can be transduced efficiently by using retroviral vectors. Using high-titer virus, we were able to infect primary human fibroblasts at efficiencies of greater than 99% (Fig. 4*A*). We infected AG01522 cells (primary human fibroblasts) with the LTRH1-p53 vector and analyzed p53 induction after treatment with the topoisomerase inhibitor, etoposide, which induces DNA damage (Fig. 4). Etoposide treatment of AG01522 cells led to up-regulation of p53 after 2 h (Fig. 4*B*), demonstrating that these cells have an intact DNA damage response. DNA damage also led to induction of the p53-dependent gene $p21^{WAF1}$, which inhibits cell cycle progression. Infection of primary fibroblasts with LTRH1-p53 virus before etoposide treatment blocked the up-regulation of p53 and $p21^{WAF1}$, whereas mock-infected cells were still able to mount the appropriate DNA damage response (Fig. 4*B*). These data demonstrate that LTRH1-p53-infected cells are functionally p53-deficient. Not only is p53 expression abrogated, but induction of p53-dependent genes is also prevented.

In conclusion, we have developed a retroviral system capable of initiating RNAi against target genes in infected cells. This system can be used to assess rapidly the effect of specific genetic deficiencies in a wide range of cell lines and primary cell types. Furthermore, the ability to stably inactivate target genes in primary cells, in many cases, will save researchers the considerable expense and time required for generation of knockout mice. The approaches we have taken to increase the efficiency of retroviral-mediated RNAi can be applied easily to other retroviral vectors, most notably lentiviral systems with even broader host ranges. The development of appropriate siRNA delivery vectors eventually may have important clinical applications, especially in combating viruses that prove resistant to treatment, such as HIV (10, 13–15).

We thank A. Unni for thoughtful advice and discussions, C. Pasare for helpful comments on the manuscript, and T. Horng for providing the H1 promoter. This work was supported by the National Institutes of Health and The Howard Hughes Medical Institute.

1. Williams, B. R. (1999) *Oncogene* **18,** 6112–6120.
2. Sharp, P. A. (2001) *Genes Dev.* **15,** 485–490.
3. Fire, A., Xu, S., Montgomery, M. K., Kostas, S. A., Driver, S. E. & Mello, C. C. (1998) *Nature* **391,** 806–811.
4. Elbashir, S. M., Lendeckel, W. & Tuschl, T. (2001) *Genes Dev.* **15,** 188–200.
5. Elbashir, S. M., Harborth, J., Lendeckel, W., Yalcin, A., Weber, K. & Tuschl, T. (2001) *Nature* **411,** 494–498.
6. Brummelkamp, T. R., Bernards, R. & Agami, R. (2002) *Science* **296,** 550–553.
7. Paddison, P. J., Caudy, A. A., Bernstein, E., Hannon, G. J. & Conklin, D. S. (2002) *Genes Dev.* **16,** 948–958.
8. Paul, C. P., Good, P. D., Winer, I. & Engelke, D. R. (2002) *Nat. Biotechnol.* **20,** 505–508.
9. Miyagishi, M. & Taira, K. (2002) *Nat. Biotechnol.* **20,** 497–500.
10. Lee, N. S., Dohjima, T., Bauer, G., Li, H., Li, M. J., Ehsani, A., Salvaterra, P. & Rossi, J. (2002) *Nat. Biotechnol.* **20,** 500–505.
11. Emerman, M. & Temin, H. M. (1984) *Cell* **39,** 449–467.
12. Burns, J. C., Friedmann, T., Driever, W., Burrascano, M. & Yee, J. K. (1993) *Proc. Natl. Acad. Sci. USA* **90,** 8033–8037.
13. Gitlin, L., Karelsky, S. & Andino, R. (2002) *Nature* **418,** 430–434.
14. Jacque, J. M., Triques, K. & Stevenson, M. (2002) *Nature* **418,** 435–438.
15. Novina, C. D., Murray, M. F., Dykxhoorn, D. M., Beresford, P. J., Riess, J., Lee, S. K., Collman, R. G., Lieberman, J., Shankar, P. & Sharp, P. A. (2002) *Nat. Med.* **8,** 681–686.

[CANCER RESEARCH 62, 6400–6404, November 15, 2002]

Advances in Brief

Silencing Expression of the Catalytic Subunit of DNA-dependent Protein Kinase by Small Interfering RNA Sensitizes Human Cells for Radiation-induced Chromosome Damage, Cell Killing, and Mutation

Yuanlin Peng,[1] Qinming Zhang,[2] Hatsumi Nagasawa,[1] Ryuichi Okayasu,[1] Howard L. Liber,[2] and Joel S. Bedford[1,3]

Department of Environmental and Radiological Health Sciences, Colorado State University Fort Collins, Colorado 80523-1681

Abstract

Targeted gene silencing in mammalian cells by RNA interference (RNAi) using small interfering RNAs (siRNAs) was recently described by Elbashir *et al.* (S. M. Elbashir *et al.*, Nature (Lond.), *411:* 494–498, 2001). We have used this methodology in several human cell strains to reduce expression of the *Prkdc* (*DNA-PKcs*) gene coding for the catalytic subunit of the DNA-dependent protein kinase (DNA-PKcs) that is involved in the nonhomologous end joining of DNA double-strand breaks. We have also demonstrated a radiosensitization for several phenotypic endpoints of radiation damage. In low-passage normal human fibroblasts, siRNA knock-down of DNA-PKcs resulted in a reduced capacity for restitution of radiation-induced interphase chromosome breaks as measured by premature chromosome condensation, an increased yield of acentric chromosome fragments at the first postirradiation mitosis, and an increased radiosensitivity for cell killing. For three strains of related human lymphoblasts, DNA-PKcs-targeted siRNA transfection resulted in little or no increase in radiosensitivity with respect to cell killing, a 1.5-fold decrease in induced mutant yield in TK6- and p53-null NH32 cells, but about a 2-fold increase in induced mutant yield in p53-mutant WTK1 cells at both the hypoxanthine quanine phosphoribosyl transferase (hprt) and the thymidine kinase loci.

Introduction

Isolation and characterization of mammalian cell mutants hypersensitive to ionizing radiation has provided key evidence that a principal underlying defect involves faulty processing of DNA double-strand breaks (1–3). Many of the genes involved and their products are now known, including both the main system of NHEJ,[4] and homology directed repair (4). For prokaryotic or lower eukaryotic cells, the ability to obtain and study double or even triple mutants has been very useful, but such mutants are not easily obtained for mammalian cells, and in some cases even single (let alone multiple) mutant phenotypes are lethal. Last year, Elbashir *et al.* (5) reported a highly specific targeted gene silencing in mammalian cells by RNAi using siRNAs. To examine the potential general use of this approach for studying the genetic control of radiosensitivity in human cells and in what situations comparisons could be made easily with cells of identical genetic backgrounds, we targeted the mRNA transcript of the *Prkdc* (*DNA-PKcs*) gene coding for the DNA-PKcs. This protein is central to the NHEJ process as well as being involved in the maintenance of telomere stability (6, 7). The aim for the present experiments was to measure the effectiveness of this siRNA approach for "knocking down" DNA-PKcs levels using Western blot analysis and immunocytochemistry and, also, to measure functional (phenotypic) effects on radiosensitization. The latter included measurements to determine whether the knock-down resulted in (*a*) reduced interphase (G_1) chromosome break restitution as measured by PCC 4 h after irradiation; (*b*) increased frequencies of chromosome aberrations in the first postirradiation mitosis; and (*c*) increased cell killing in low-passage normal human fibroblasts. In addition, experiments were included to detect changes in radiation-induced mutant yields as well as cell killing in three strains of TK6 human lymphoblasts differing in p53 status.

Materials and Methods

Cells

Low-passage normal human fibroblast cultures GM08399 were obtained from the National Institute of General Medical Sciences Coriell Cell Repositories. These cells were routinely grown in αMEM containing 15% fetal bovine serum as described previously (8–10). Three strains of WIL2 lymphoblast-derived cells were used. The TK6, WTK1, and NH32 derivatives are heterozygous for the *thymidine kinase* gene ($TK^{+/-}$). WTK1 cells produce a mutant form of p53, and NH32 cells are p53 null. Growth and use of these cells for mutagenesis assays were identical to the procedures described on previous occasions (11–14).

siRNA Transfections

The siRNA sequence used for targeted silencing of *DNA-PKcs* was chosen as described by Tuschl (http://www.mpibpc.gwdg.de/abteilungen/100/105/sirna_u.html) and recommended by the siRNA supplier (Dharmacon). We used two duplex siRNA sequences separately or together. One was targeted 352 bases downstream from the start codon. This double-stranded siRNA was

GAUCGCACCUUACUCUGUUdTdT
dTdTCUAGCGUGGAAUGAGACAA.

The other siRNA, targeted to the kinase domain, was

CUUUAUGGUGGCCAUGGAGdTdT
dTdTGAAAUACCACCGGUACCUC.

Searches of the human genome database (BLAST) were carried out to ensure the sequences would not target other gene transcripts. The concentration of siRNAs was 0.15 μM during transfections, which were facilitated by Oligofectamine (In Vitrogen), also according to the protocol of Tuschl and the siRNA supplier. For controls, we used Lamin A/C or Ku80-targeted siRNAs, or, in more recent experiments, a *DNA-PKcs*-derived sequence in which 2 or 3 bp were changed. None of these control siRNAs affected DNA-PKcs protein levels or the radiosensitivity phenotypes studied. Because protein turnover rates will determine the optimal transfection and irradiation- or assay-timing protocol, we carried out preliminary experiments to establish that two successive transfections of log phase of cultures (~50% confluent) at 2-day intervals produced marked reductions in DNA-PKcs. Of course, other protocols we have not tried may also produce similar or superior DNA-PKcs knock-downs. In most experiments with the fibroblasts, 2 days after inoculation and 1 day after siRNA transfection, cells were subcultured to one-half of the cell density and transfected again 1 day later. Then, 3 days later, when irradiations were carried out and other assays performed, cells were still

Received 8/20/02; accepted 10/4/02.

The costs of publication of this article were defrayed in part by the payment of page charges. This article must therefore be hereby marked *advertisement* in accordance with 18 U.S.C. Section 1734 solely to indicate this fact.

[1] Y. P., H. N., R. O., and J. S. B. contributed to the studies involving the normal human fibroblasts.

[2] Q. Z. and H. L. L. contributed to the studies involving the lymphoblast-derived cells.

[3] To whom requests for reprints should be addressed, at Department of Environmental and Radiological Health Sciences, Colorado State University, Fort Collins, Colorado 80523-1681. Phone: (970) 491-7492; Fax: (970) 491-0623; E-mail: jbedford@colostate.edu.

[4] The abbreviations used are: NHEJ, nonhomologous end joining; RNAi, RNA interference; siRNA, small interfering RNA; PCC, premature chromosome condensation; DNA-PKcs, catalytic subunit of DNA-dependent protein kinase; DAPI, 4′,6-diamidino-2-phenylindole.

growing and cultures were about 80–90% confluent. In one of the human normal fibroblast experiments, the cells were not subcultured after the first transfection; after the second transfection, cells were allowed to reach confluence, and the following day, the irradiations were carried out. Then, 1 day later, the cells were subcultured, and aberrations were scored after colcemid collection of cells in the first postirradiation mitosis, as reported in Fig. 2*C*.

During the 6-day siRNA transfection protocol for the fibroblasts, in preparation for irradiation or other assays, we estimate that the growth rate (doubling time) of the DNA-PKcs-targeted siRNA-transfected cell populations decreased by ~10% relative to control (altered sequence) siRNA transfection, but the growth was interrupted twice for ~20 h for each transfection in serum-free medium; and in most cases, cells were subcultured to one-half density between transfections. For the lymphoblast-derived cell lines, the siRNA transfections had no effect on the cell population growth.

Western Blot and Immunocytochemistry

For Western blot analysis, cells were prepared as described by Song *et al.* (15). Gels were loaded with 20 μg of protein and, after electrophoresis in 6% Tris-glycine polyacrylamide gels, proteins were transferred to nitrocellulose membranes. After blocking in Tris-buffered saline (TBS) containing 7% nonfat dry milk, membranes were incubated in TBS with 5% nonfat dry milk containing mouse antibodies against DNA-PKcs (AB-4) or Ku 80 (Ab2) obtained from Neomarkers. Goat antimouse secondary antibodies labeled with horseradish peroxidase were then used to bind the primary antibodies, and detection was by chemiluminescence (ECL kit; Amersham Pharmacia). X-ray films to detect the chemiluminescence were then exposed for appropriate times depending on luminescence intensity.

For immunocytochemistry, after the siRNA transfections and at the time selected for optimum knock-down, human fibroblast cultures of attached cells were fixed *in situ* in 4% paraformaldehyde in PBS and were then permeabilized in PBS containing 0.2% Triton X-100. In the case of lymphoblast-derived cells, which grow in suspension culture, cells were prepared for analysis after being centrifuged onto slides (Cytocentrifuge) before fixation in a manner similar to that described above. To detect DNA-PKcs, the same primary antibodies were used, but detection in this case was with rhodamine-labeled goat antimouse IgG and was viewed by fluorescence microscopy.

Chromosome Damage Assays

Interphase PCC. Four h after irradiation of confluent cultures, to allow for completion of much of the postirradiation damage processing, cells were resuspended and fused to mitotic HeLa cells to induce PCC, and the total number of PCCs and fragments was scored as described previously (8–10, 16). The frequency of "excess PCC fragments per cell" was then estimated by subtracting the total number per cell in unirradiated samples from that for irradiated samples. For unirradiated cells, the total number of PCCs per cell was tightly distributed around 45–46.

Mitotic Cells. In the same experiments described for PCC break measurements, other parallel samples were subcultured and allowed to progress to mitosis for scoring aberrations in metaphase cells. Samples were fixed after incubation in the presence of 0.1 μg/ml Colcemid during the intervals 18–22, 22–26, 26–30, and 30–34 h after subculture. We have shown that virtually no second-division cells are present during these fixation intervals after irradiation, incubation, and subculture of these contact-inhibited cells. Aberration scoring was carried out as described previously (10, 17–19).

Cell Survival

Cell survival responses were measured after irradiation of log phase cultures using colony formation as the criterion for cell survival. The siRNA transfection protocol for log phase cultures was similar to that for the treatment of the contact-inhibited plateau-phase cultures except, as mentioned earlier, cells were subcultured after the first siRNA transfection so that they would still be growing and cultures would be ~80% confluent 2 days after the second transfection.

Mutation Assays

Lymphoblast cells were transfected with siRNA as described above. The next day (day 1), they were treated with CHAT medium to eliminate preexisting hprt and tk mutants. A second siRNA treatment was performed on day 3, and cells were used for irradiation on day 5. Cells were untreated or irradiated with 1, 3, 5, or 7 Gy for cytotoxicity experiments, or 1.5 Gy for mutation experiments.

To determine surviving fractions, cells were seeded into 96-well microtiter dishes immediately after treatment, at concentrations ranging from 1 to 10,000 cells per well, depending on the expected surviving fractions.

To determine mutation frequencies, cells were grown in nonselective media for 3 or 6 days to allow phenotypic expression of newly induced mutants at tk or hprt, respectively. At those times, cells were seeded at high density in 96-well microtiter dishes in the presence of trifluorothymidine to measure mutation at tk, or 6-thioguanine to measure mutation at hprt. Cells were also seeded at low density to determine plating efficiency. Plates were scored 12–20 days later, and mutant fractions were calculated as described previously (11).

Results and Discussion

Studies Using Low-Passage Normal Human Fibroblasts. Fig. 1*A* shows a Western blot analysis for one experiment in which two different concentrations were used of the siRNA targeted to DNA-PKcs mRNA, as well as a Ku80-targeted siRNA or a mock transfection without siRNA. The blots were incubated simultaneously with mouse anti-DNA-PKcs and mouse anti-Ku80 antibody followed by detection with horseradish peroxidase-labeled goat antimouse IgG and a chemiluminescence assay. A more severe knock-down of DNA-PKcs was seen for the 0.15 μM concentration of siRNA targeted to DNA-PK_{cs} than for the 5-fold lower (0.03 μM) concentration. In several other experiments, the level of knock-down of DNA-PKcs varied somewhat depending on the protocol. No effect of DNA-PKcs-targeted siRNA transfection on Ku 80 was seen, nor did Ku 80-targeted siRNA affect DNA-PKcs levels. Similar results were obtained in other experiments showing a lack of cross-reactivity with Lamin A/C-targeted siRNAs (data not shown), although, in those cases, the Lamin A/C-targeted siRNA drastically reduced Lamin A/C protein. In the experimental result shown here, Ku80 protein was only partially reduced by Ku80-targeted siRNA. In this case, either the Ku80-targeted siRNA sequence was relatively ineffective or the turnover time of Ku80 was sufficiently different that the timing, or other aspects of the transfection protocol, were suboptimal for that protein.

Fig. 1*B*) shows two fluorescence microscope fields from an experiment in which DNA-PKcs was measured by immunocytochemistry. The siRNA transfection protocol was similar to that used for the result shown in Fig. 1*A* but was from an experiment carried out on another occasion. In Fig. 1*B*, *panels a* and *b* are the same field of cells from a mock-transfected culture showing the cells with a DAPI filter to identify DAPI-stained nuclei (Fig. 1*B*, *a*); and with a rhodamine filter to identify nuclei containing measurable DNA-PKcs (Fig. 1*B*, *b*). Of 156 cells examined, strong DNA-PKcs signals appeared in 85% of the cells, weaker signals in 12%, and no detectable signals in 3%. In cells transfected with DNA-PKcs-targeted siRNA (Fig. 1*B*, *c* and *d*), it appeared that one cell was virtually unaffected, (normal level of DNA-PKcs) another showed reduced DNA-PKcs, but the rest did not have obviously detectable levels. Scoring numerous other microscope fields from this experiment (322 cells total) indicated an average of ~22% unaffected cells (strong signals comparable with controls mentioned above); or with slightly reduced levels of DNA-PKcs, ~13% had appreciably reduced levels, and the remainder had no visibly detectable levels. Similar results were obtained in several replicate experiments, although the proportion unaffected differed. DNA-PKcs is a very abundant protein in human cells and the immunocytochemical detection efficiency range in our experiments from minimum to maximum is not known. For this reason and known nonlinearities in film densitometry (at both low- and high-exposure levels), the Western blot and immunocytochemical analyses in

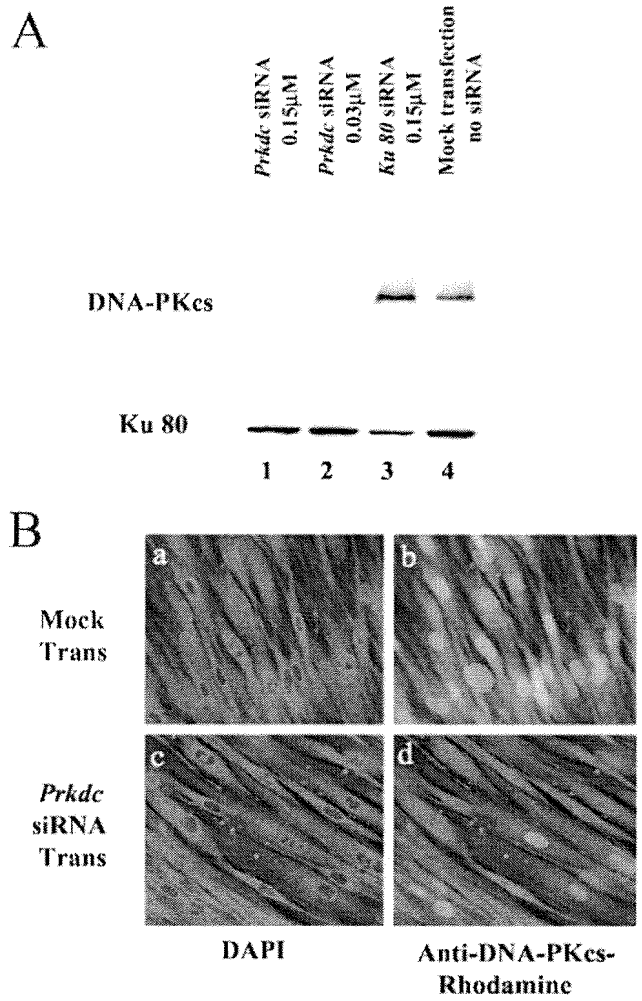

Fig. 1. Expression of DNA-PKcs in low-passage normal human fibroblasts (GM08399) after transfection of siRNA targeted to DNA-PKcs mRNA. *A*, a Western blot from cells after two Oligofectamine-mediated transfections (see "Materials and Methods"); the measurement of both DNA-PKcs and Ku80 protein from cells using siRNA targeted to DNA-PKcs at a concentration of 0.15 μM (*Lane 1*) and at a concentration of 0.03 μM (*Lane 2*). *Lanes 3* and *4*, respectively, cells that were transfected with Ku80-targeted siRNA or mock transfected (two Oligofectamine treatments but without RNA). *B*, fluorescence microscope images of cells either mock transfected (*Mock Trans*, *a* and *b*, same cells) or transfected twice with siRNA targeted to DNA-PKcs (*c* and *d*, same cells). Cells were stained with DAPI (*blue nuclei*) and Vybrant CFDA SE (*green cytoplasm*) and with rhodamine-labeled mouse anti-DNA-PKcs; photographs were taken with DAPI and FITC filters and images merged (*a* and *c*) or with a rhodamine filter and an FITC filter and merged (*b* and *d*).

the present study are not quantitatively comparable. The immunocytochemistry was carried out principally for the purpose of indicating heterogeneity among cells, which was not reflected in Western blots. Another unknown for these studies is the quantitative level of DNA-PKcs reduction necessary for radiosensitization.

Fig. 2, *A* and *B*, shows the result of an experiment to test the effect of DNA-PKcs-targeted knock-down on the rejoining of broken chromosomes during interphase as measured by inducing PCC 4 h after irradiation. Because the immunocytochemical studies showed that the cells in the population irradiated were not likely to be uniformly reduced in DNA-PKcs, we might expect differences among cells in levels below which radiosensitization occurs and, therefore, a nonuniform radiosensitization. Cytogenetic assays such as those carried out to obtain the results shown in Fig. 2, *A* and *B*, are capable of detecting such heterogeneity because damage (excess PCC fragments) is measured in each individual cell. Fig. 2 shows for control (*A*) and siRNA-transfected cells (*B*) the distribution of cells with various numbers of excess fragments 4 h after irradiation with 5 Gy of ^{137}Cs γ rays. Each chromosome break results in an excess fragment. After some time elapses for rejoining, remaining excess fragments can result from either unrejoined breaks or, as is often the case, for longer times in normal human cells, from mis-rejoined breaks that result in acentric or centric rings, *i.e.*, asymmetrical intra-arm intrachanges (8, 10). At the shortest time measurement possible after irradiation with the PCC system (~20 min), a dose of 5 Gy results in an average of ~25–30 excess PCC fragments per cell for several other human fibroblast cell strains, and the excess fragment frequency decreases because of rejoining with a half-time of about 1.5 to 1.7 h (8–10). If these fibroblasts were similar in response, we would expect some five or six excess fragments per cell at the 4-h sample time after a dose of 5 Gy. Fig. 2*A* shows that an average of about eight excess fragments per cell remained, a value not far from the expectation. For cells transfected with DNA-PKcs-targeted siRNA (Fig. 2*B*), the distribution of excess fragments appeared to be bimodal with one peak around 8 and another around 18 excess fragments per cell. These results suggest a sensitization factor of about 2-fold (for the subpopulation sensitized) assuming an approximately linear dose response in the 5-Gy dose range for excess fragments 4 h after irradiation.

The result of an experiment to measure radiosensitivity for induction of chromosomal aberrations measured in the first post-irradiation mitosis, is shown in Fig. 2*C*. We would expect fewer excess acentric fragments than in the interphase PCC experiments because cells were incubated 24 h after irradiation and are required to progress to mitosis for the assay. For nontransfected cells, there were about 0.8 induced dicentrics (a dicentric is scored as one dicentric plus its associated acentric fragment) and 1.0 deletions per cell (acentric fragments not associated with dicentrics or centric rings). For DNA-PKcs-targeted siRNA-transfected cells, we observed about 1.0 induced dicentric and 1.9 deletions per cell. This represents a nearly 2-fold increase in excess fragments or deletions for the DNA-PKcs-targeted siRNA-transfected cells. In this experiment, we did not observe the greatly

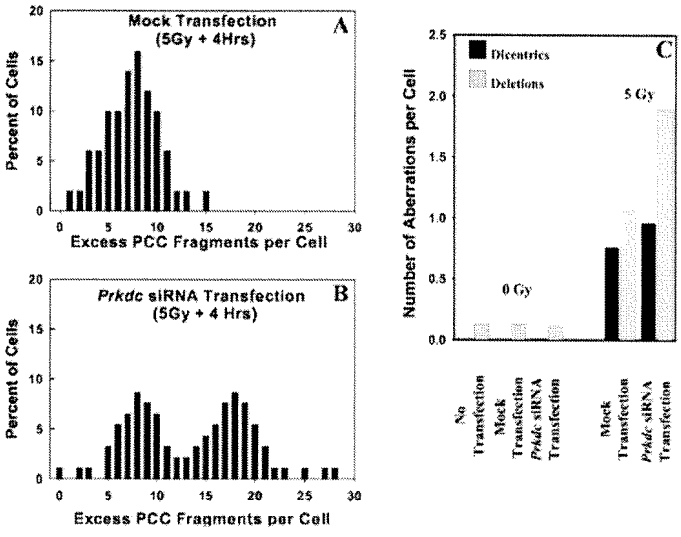

Fig. 2. Changes in chromosomal radiosensitivity of GM08399 human fibroblasts after two transfections with siRNA targeted to DNA-PKcs mRNA. Excess PCC fragments in interphase G_1 cells 4 h after 5-Gy Cs-137 γ rays were measured in mock-transfected cells (*A*) or cells transfected with siRNA targeted to DNA-PKcs mRNA (*B*). Approximately 50–60% of the cells apparently suffered sufficient knock-down of DNA-PKcs to impair their ability to rejoin broken chromosomes or to result in excessive incorrect rejoining to yield other excess fragments. *C*, the result of an experiment in which chromosome-type aberrations were scored after cells entered their first postirradiation mitosis. Dicentrics (*solid bars*) and deletions (*shaded bars*) were not produced by either mock or siRNA transfections alone. Five Gy of γ rays increased the dicentric yield, although not significantly more in the siRNA- than in the mock-transfected cells. In contrast, deletions from either unrejoined chromosome breaks or interstitial deletions (asymmetric intra-arm intrachanges) were increased about 2-fold by transfection with siRNA targeted to DNA-PKcs mRNA.

increased frequency of induced chromatid-type aberrations after irradiation of G_1 or G_0 cells that is usually seen for X-ray-sensitive cells with defects in NHEJ (3, 20–22).

The result of an experiment to examine DNA-PKcs-targeted siRNA radiosensitization with respect to cell killing is shown in Fig. 3. In addition to the heterogeneity in radiosensitivity always present for log phase cultures because of cell cycle-dependent variation in radiosensitivity, and despite some heterogeneity in the proportion of cells with severe or intermediate levels of DNA-PKcs knock-down, there was still a marked radiosensitization of DNA-PKcs-targeted siRNA-transfected cells relative to the two control cell populations. As expected, this was most pronounced in the low-dose region (0–1 Gy), in which survival in mixed heterogeneous cell populations is caused by the killing of the most sensitive subpopulations.

Also shown in Fig. 3 is a curve that passes through the survival estimates for the DNA-PKcs-targeted siRNA-transfected cells that was not fitted to the data but represents a curve for a mixed population of cells consisting of a fraction (20%) of unaffected cells with a radiosensitivity corresponding to curve *R*, and a fraction (80%) of sensitized cells whose response, curve *S*, was derived from the slope of the curve-sensitized cells in the low-dose region between 0 and 0.5 Gy. Thus, despite what appears as a greater knock-down of DNA-PKcs from the immunochemical results illustrated in Fig. 1, we suggest that this result indicates that DNA-PKcs is present in fairly large excess, far above that needed to confer normal radioresistance.

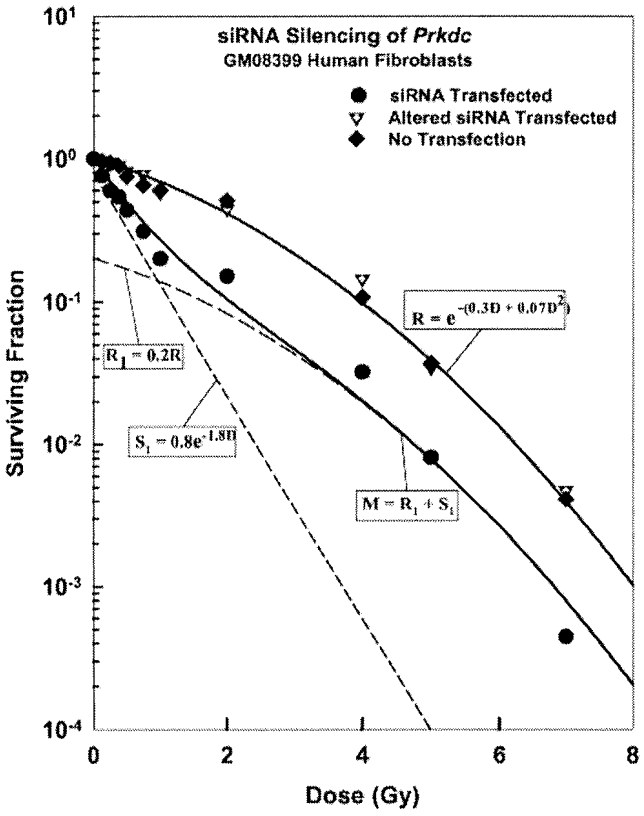

Fig. 3. Sensitization of GM08399 human fibroblasts with respect to cell killing by transfection with siRNA targeted to DNA-PKcs mRNA. Cell survival was measured by colony formation over a range of doses (0–7 Gy) of Cs-137 γ rays after transfection with siRNA targeted to DNA-PKcs mRNA (●, *lower solid curve*), a control siRNA in which the DNA-PKcs siRNA target sequence was altered slightly, as described in the "Results and Discussion" (*inverted triangles, upper solid curve*), or not transfected (◆, *upper solid curve*). The *lower solid curve* (*M*), which reasonably fits the data, is a composite curve that would be expected from a mixed population of cells consisting of 20% with the sensitivity of the cells that did not experience a DNA-PKcs knock-down (*curve labeled* R_1) and 80% with a sensitivity illustrated by *curve* S_1 estimated from the survival estimates for the sensitized cells in the low-dose (0–0.5 Gy) range. R and M represent surviving fraction, and D represents the doses.

It is also worth noting that one of the "control" cell populations in this experiment was not a "mock" transfection but, instead, cells that were transfected with a siRNA control duplex ($siRNA_c$) in which an adenine-uracil bp was substituted for a uracil-adenine bp in position 3 from the 5′ end of the strand of the duplex siRNA equivalent to the mRNA target, and also in which an AC sequence was replaced with a CA sequence in positions 12 and 13 from the 5′ end in the same strand. Transfection with this $siRNA_c$ duplex did not radiosensitize the cells, nor did it knock-down DNA-PKcs as measured in Western blots.

Toxicity and Mutagenesis Studies in Lymphoblast Cells. In our original report of the isolation of NH32 cells, we found that the background MF and the X-ray-induced MF were very similar to TK6, with both lines being much lower than WTK1 (14). However, in this study, we incubated the dishes for longer times (20 instead of 17 days), and observed a substantial increase in the MF for NH32. (The additional incubation time does not affect the MF at TK6 or WTK1.) Therefore, we now conclude that background and induced MF in these cell lines are: WTK1 (ile237 p53) > NH32 (p53 null) > TK6 (p53 wild-type).

As can be seen in Fig. 4*A*, knock-down of DNA-PKcs was achieved in all three of the lymphoblast lines. This result was mirrored in Western blot studies (data not shown). As expected, the two lines with mutant or null p53 were more resistant to radiation-induced cell killing than was the TK6 p53 wild-type. However, in all three lines, there was little or no effect of knocking down DNA-PKcs on cell killing, (data not shown). Surviving fractions were somewhat lower in cells transfected with siRNAs, with values ranging from 49 to 76% of those for the untransfected or mock-transfected cells. However the slopes of the survival curves for each particular cell line were not significantly different, with or without knock-down by siRNA.

Fig. 4*B* shows the results obtained for mutagenesis at the hprt and tk loci. At X-linked hprt, spontaneous mutations consist of one-half large deletions in both TK6 and WTK1 (23). The spectrum for NH32 cells is not known. In the present study, we saw no evidence that DNA-PKcs knock-down affected the quantitative levels of spontaneous mutations at either the hprt or the tk loci. After irradiation, however, there were clear, statistically significant differences for the mutation frequencies observed at the tk locus. The MF after knock-down was decreased in TK6 ($P = 0.002$ for the comparison of mock treated with siRNA), and in NH32 ($P < 0.001$), but, in contrast, the MF increased in WTK1 ($P = 0.004$). Although none of the MFs were significantly different at the hprt locus, nevertheless, there was a similar trend, in that TK6 ($P = 0.10$) and NH32 ($P = 0.10$) were lower and WTK1 ($P = 0.06$) was higher.

It is not straightforward to predict what effect the perturbation of the NHEJ system will have on the mutagenic impact of double-strand breaks. When damage is sustained on the X chromosome, for a cell that has not yet replicated the region (*i.e.,* in G_1 or early S phase), we would imagine that either it will die or it will require some kind of alternative end-joining reaction. In the former case, we would expect the observed MF to be reduced. In the latter case, it could be either increased or decreased, depending on the "error-proneness" of the mechanism, relative to NHEJ. We would have similar expectations for damage on chromosome 17, where tk is located, although it is more complicated because cells in G_1 or early S phase might be able to make use of the homologous chromosome as a template for repair. The fact that mutation was increased in WTK1 is intriguing. It is tempting to speculate that disruption of NHEJ, with the presence of large amounts of mutant p53, led to the operation of a more mutagenic mechanism.

Other approaches, involving stable expression of interfering RNAs for selective knock-down of gene products by introducing vectors that stably integrate and express interfering double-strand RNA hairpins

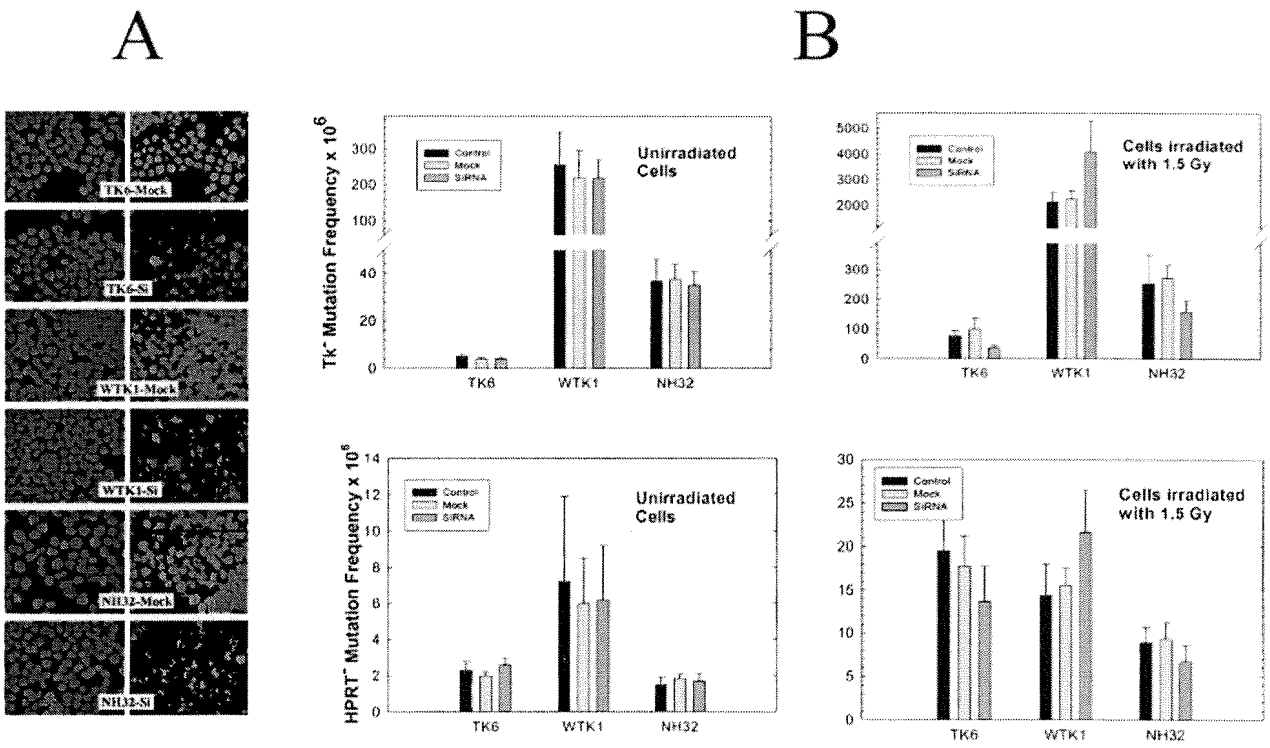

Fig. 4. Mutagenesis studies in human lymphoblast cell lines with altered DNA-PKcs expression. *A*, cells were mock transfected or transfected with siRNA as described in "Materials and Methods." The *left panel* in all cases is a DAPI stain; the *right panel* is immunofluorescence with antibody to DNA-PKcs. Cells were examined 3 days after transfection. *B*, spontaneous and induced mutation frequencies in lymphoblast cells. Experiments were performed 5 days after the initial transfection. Irradiation was with 1.5 Gy γ-irradiation. *Error bars*, SDs.

(24, 25), may offer some advantages over the transient transfection methods used in the present studies, but there may also be some disadvantages. With a stable expression approach, for example, if sufficient expression is achieved to produce a phenotypic change, and the cellular life span is not limiting, it should be possible to obtain clonal populations in which there is much less heterogeneity in levels of knock-down among cells than is possible with the transient expression knock-down. The transient approach, on the other hand may be more appropriate if the long-term knock-down is lethal, or for studies involving multiple gene silencing with little or no restriction on the choice of cells for study; therefore, it should be possible, for example, to study effects on cells with the same or different genetic backgrounds. Clearly the new approaches for RNAi in mammalian cells has many obvious applications as well as its intrinsic interest regarding regulation of gene expression in general.

References

1. Jeggo, P. A. DNA breakage and repair. Adv. Genet., *38:* 185–218, 1998.
2. Thompson, L. H., and Schild, D. Homologous recombinatorial repair of DNA ensures mammalian chromosome stability. Mutat. Res., *477:* 131–153, 2001.
3. Bedford, J. S., and Dewey, W. C. Historical and current highlights in radiation biology: has anything important been learned by irradiating cells? Radiat. Res., *158:* 251–291, 2002.
4. Wood, R. D., Mitchell, M., Sgouros, J., and Lindahl, T. Human DNA repair genes. Science (Wash. DC), *291:* 1284–1289, 2001.
5. Elbashir, S. M., Harborth, J., Lendeckel, W., Yalcin, A., Weber, K., and Tuschl, T. Duplexes of 21-nucleotide RNAs mediate RNA interference in cultured mammalian cells. Nature (Lond.), *411:* 494–498, 2001.
6. Bailey, S. M., Cornforth, M. N., Kurimasa, A., Chen, D. J., and Goodwin, E. H. Strand-specific postreplicative processing of mammalian telomeres. Science (Wash. DC), *293:* 2462–2465, 2001.
7. Bailey, S. M., Meyne, J., Chen, D. J., Kurimasa, A., Li, G. C., Lehnert, B. E., and Goodwin, E. H. DNA double-strand break repair proteins are required to cap the ends of mammalian chromosomes. Proc. Natl. Acad. Sci. USA, *96:* 14899–14904, 1999.
8. Cornforth, M. N., and Bedford, J. S. X-ray induced breakage and rejoining of human interphase chromosomes. Science (Wash. DC), *222:* 1141–1143, 1983.
9. Cornforth, M. N., and Bedford, J. S. On the nature of a defect in cells from individuals with ataxia telangiectasia. Science (Wash. DC), *227:* 1589–1591, 1985.
10. Cornforth, M. N., and Bedford, J. S. A quantitative comparison of potentially lethal damage repair and the rejoining of interphase chromosome breaks in low passage normal human fibroblasts. Radiat. Res., *111:* 385–405, 1987.
11. Furth, E. E., Thilly, W. G., Penman, B. W., Liber, H. L., and Rand, W. M. Quantitative assay for mutation in diploid human lymphoblasts using microtiter plates. Anal. Biochem., *110:* 1–8, 1981.
12. Liber, H. L., and Thilly, W. G. Mutation assay at the thymidine kinase locus in diploid human lymphoblasts. Mutat. Res., *94:* 467–485, 1982.
13. Liber, H. L., LeMotte, P. K., and Little, J. B. Toxicity and mutagenicity of X-rays and (125-I)dUrd or (3-H)TdR incorporated in the DNA of human lymphoblast cells. Mutat. Res., *111:* 387–404, 1983.
14. Chuang, Y. Y., Chen, Q., Brown, J. P., Sedivy, J. M., and Liber, H. L. Radiation-induced mutations at the autosomal thymidine kinase locus are not elevated in p53-null cells. Cancer Res., *59:* 3073–3076, 1999.
15. Song, Q., Lees-Miller, S. P., Kumar, S., Zhang, Z., Chan, D. W., Smith, G. C., Jackson, S. P., Alnemri, E. S., Litwack, G., Khanna, K. K., and Lavin, M. F. DNA-dependent protein kinase catalytic subunit: a target for an ICE-like protease in apoptosis. EMBO J., *15:* 3238–3246, 1996.
16. Cornforth, M. N., and Bedford, J. S. High-resolution measurement of breaks in prematurely condensed chromosomes by differential staining. Chromosoma (Berl.), *88:* 315–318, 1983.
17. Bender, M. A., Bedford, J. S., and Mitchell, J. B. Mechanisms of chromosomal aberration production. II. Aberrations induced by 5 BUdR and visible light. Mutat. Res., *20:* 403–416, 1973.
18. Bender, M. A., Griggs, H. G., and Bedford, J. S. Mechanisms of chromosomal aberration production. III. Chemicals and ionizing radiation. Mutat. Res., *23:* 197–212, 1974.
19. Bedford, J. S., Mitchell, J. B., Griggs, H. G., and Bender, M. A. Radiation-induced cellular reproductive death and chromosome aberrations. Radiat. Res., *76:* 573–586, 1978.
20. Bahari, I. B., and Bedford, J. S. Chromosomal radiosensitivity and its implications to the radiosensitivity of Chinese hamster XR-1 mutant cells. Sains Malaysiana, *18:* 65–80, 1989.
21. Cornforth, M. N., and Bedford, J. S. Ionizing radiation damage and its early development in chromosomes. Adv. Radiat. Biol., *17:* 423–496, 1993.
22. Stackhouse, M. A., and Bedford, J. S. An ionizing radiation-sensitive mutant of CHO cells: irs-20. III. Chromosome aberrations, DNA breaks and mitotic delay. Int. J. Radiat. Biol., *65:* 571–582, 1994.
23. Phillips, E. N., Xia, F., Kelsey, K. T., and Liber, H. L. Spectra of spontaneous and X-ray-induced mutations at the *hprt* locus in related human lymphoblast cell lines that express wild-type or mutant p53. Radiat. Res., *143:* 255–262, 1995.
24. Brummelkamp, T. R., Bernards, R., and Agami, R. A system for stable expression of short interfering RNAs in mammalian cells. Science (Wash. DC), *296:* 550–553, 2002.
25. Paddison, P. J., Caudy, A. A., and Hannon, G. J. Stable suppression of gene expression by RNAi in mammalian cells. Proc. Natl. Acad. Sci. USA, *99:* 1443–1448, 2002.

Small Interfering RNA-Mediated Gene Silencing in T Lymphocytes[1]

Michael T. McManus, Brian B. Haines, Christopher P. Dillon, Charles E. Whitehurst, Luk van Parijs, Jianzhu Chen, and Phillip A. Sharp[2]

Introduction of small interfering RNAs (siRNAs) into a cell can cause a specific interference of gene expression known as RNA interference (RNAi). However, RNAi activity in lymphocytes and in normal primary mammalian cells has not been thoroughly demonstrated. In this report, we show that siRNAs complementary to CD4 and CD8α specifically reduce surface expression of these coreceptors and their respective mRNA in a thymoma cell line model. We show that RNAi activity is only caused by a subset of siRNAs complementary to the mRNA target and that ineffective siRNAs can compete with effective siRNAs. Using primary differentiated T lymphocytes, we provide the first evidence of siRNA-mediated RNAi gene silencing in normal nontransformed somatic mammalian lymphocytes. ***The Journal of Immunology,*** **2002, 169: 5754–5760.**

Introduction of dsRNA into an organism can cause specific interference of gene expression (1). This phenomenon, known as RNA interference (RNAi),[3] results from a specific targeting of mRNA for degradation by an incompletely characterized cellular machinery present in plant, invertebrate, and mammalian cells (2, 3). The proteins mediating RNAi are part of an evolutionarily conserved cellular pathway that processes endogenous cellular RNAs to silence developmentally important genes (4, 5). In RNAi, the protein Dicer, an RNase III enzyme, is probably responsible for the processing of dsRNA into short interfering RNA (siRNA). Functional screens conducted in plants and worms have identified a number of other conserved genes participating in the RNAi pathway. These genes include a number of different helicases, a RNA-dependent RNA polymerase, an exonuclease, dsRNA-binding proteins, and novel genes of unknown function (for recent reviews, Refs. 6, 7, 8, 9, and 10).

Mammalian RNAi was first described in mouse embryos using long dsRNA (11, 12). Then, following the analysis of the structure of the intermediate in this process, small interfering RNAs (siRNAs) were used to silence genes in mammalian tissue culture (13, 14). Most of the RNAi pathway genes discovered in plant and worm screens are also present in mouse and human sequence databases, supporting evidence that a conserved RNAi pathway exists in mammals. One of the more notable exceptions is the RNA-dependent RNA polymerase gene, which has been shown to be involved in the amplification of the dsRNA in *Caenorhabditis elegans* (15, 16). This might imply that perpetuation of the RNAi response in mammals differs from that of lower organisms.

Recent reports have demonstrated gene silencing by siRNA in mammalian cells (17–22). However, despite these initial reports, many uncertainties remain concerning the mechanism, physiologic relevance, and ubiquity of RNAi in mammalian cells. Although studies in tumor cell lines have demonstrated siRNA-mediated RNAi, it remains a major question as to whether primary cells from fresh tissues can undergo the RNAi response. Furthermore, little is known about the efficiency and longevity of siRNA-mediated RNAi gene suppression. In this report, we provide fundamental insight into the siRNA-mediated RNAi mechanism using a thymoma-derived cell line model to demonstrate for the first time the occurrence of RNAi in primary T lymphocytes.

Materials and Methods

Cell culture

E10 is an immature double-positive thymocyte line derived from a TCR-α and p53 double-mutant mouse of a mixed 129/Sv × C57BL/6 background as described (23). These cells, which proliferated vigorously, were maintained at a maximal concentration of 2×10^6 cells/ml and were propagated in complete medium: DMEM supplemented with 10% heat-inactivated FCS, 2 mM L-glutamine, 100 U/ml penicillin, 100 μg/ml streptomycin, and 50 μM 2-ME. Cell culture of primary lymphocytes: cells from the spleen and lymph nodes of DO11.10 TCR-transgenic mice (a generous gift from Dr. C. London, University of California, Davis, CA) were activated for 3 days with 1 μg/ml OVA peptide (residues 323–339) in RPMI medium containing 10% FBS.

Transfection

For electroporations, 2.5 μmol dsRNA and/or 20 μg of pEGFP-N3 plasmid (Clontech Laboratories, Palo Alto, CA) were added to prechilled 0.4-cm electrode gap cuvettes (Bio-Rad, Hercules, CA). E10 cells (1.5×10^7) were resuspended to 3×10^7 cells/ml in cold serum-free RPMI, added to the cuvettes, mixed, and pulsed once at 300 mV, 975 μF with a Gene Pulser electroporator II (Bio-Rad). Cells were plated into 6-well culture plates containing 8 ml of complete medium and were incubated at 37°C in a humidified 5% CO_2 chamber. Cell viability immediately after electroporation was typically around 60%. For cationic lipid transfections, 2 μg of plasmid DNA and 100 nmol siRNAs were used per 10^6 cells, and transfection followed manufacturer's recommended protocol. Transfection of primary lymphocytes: activated DO11.10 T cells were electroporated as above, except that the cells were resuspended to 6×10^7 cells/ml in cold serum-free RPMI and the pulse voltage was 310 mV. After electroporation, the cells were put into four wells of a 24-well plate, each containing 1 ml

Center for Cancer Research, Massachusetts Institute of Technology, Cambridge, MA 02139

Received for publication May 28, 2002. Accepted for publication September 12, 2002.

The costs of publication of this article were defrayed in part by the payment of page charges. This article must therefore be hereby marked *advertisement* in accordance with 18 U.S.C. Section 1734 solely to indicate this fact.

[1] This work was supported by postdoctoral American Cancer Society Fellowship No. PF0122801 (to B.B.H.), a Career Development Award from the Arthritis Foundation (to L.v.P.), and National Institutes of Health Grant Nos. R37–6M34277 and P01-CA42063 (to P.A.S.). C.P.D. is a Howard Hughes Medical Institute Predoctoral Fellow. M.T.M. is a fellow of the Cancer Research Institute.

[2] Address correspondence and reprint requests to Dr. Phillip A. Sharp, Center for Cancer Research, Massachusetts Institute of Technology, 40 Ames Street E17-526, Cambridge, MA 02139. E-mail address: sharppa@mit.edu

[3] Abbreviations used in this paper: RNAi, RNA interference; siRNA, small interfering RNA; PI, propidium iodide; GFP, green fluorescent protein; ORF, open reading frame; UTR, untranslated region; stRNA, small temporal RNA.

0022-1767/02/$02.00

of RPMI supplemented with 1 ng/ml IL-2 (BioSource International, Camarillo, CA). siRNA oligos (Dharmacon, Lafayette, CO) used were as follows (sense strand is given): effective CD4 siRNA, CD4 no. 4, (sense) gagccauaaaucucaucugadgdg, (anti-sense) ucagaugagauuauggcucdtdt; effective CD8 siRNA, CD8 no. 4, (sense) gcuacaacuacuacaugacdtdt, (antisense) gucauguaguaguuguagcdtdt; ineffective siRNAs, CD8 no. 1, (sense) gaaaa uggacgccgaacuudgdg, (anti-sense), aaguucggcguccauuuucdtdt; CD8 no. 2, (sense) cgugggacgagaagcugaadtdt, (antisense) uucagcuucucgucccacgdtdt; CD8 no. 3 (sense) aauuguguaaaaauggcaccgcdcda, (antisense) μggcgguge cauuuuacacaadtdt; CD4 no. 1, (sense) ggagaccaccaugugccgadgdc, (antisense) ucggcacaugguggucucccdtdt; CD4 no. 2, (sense) ggcagagaaggauucu uucdtdt, (anti-sense) gaaagaauccuucucugccdtdt; CD4 no. 3, (sense) ccaccugcgucccugucucadtdc, (antisense) gugguggacgcaggacagadgdt; CD4 no. 5 (sense) ccaccugcgucccugucucadtdc, (antisense) ucagaugagauuauggcucdtdt.

Flow cytometry

E10 cells (~1 × 10^6) were washed once in FACS buffer (PBS supplemented with 2% FCS and 0.01% sodium azide), resuspended to 100 μl, and stained directly with PE-conjugated anti-CD4 (clone RM4-5) or allophycocyanin-conjugated anti-CD8α mAbs, and in some experiments with PE- or allophycocyanin-conjugated anti-mouse Thy-1.2 (clone 53-2.1) mAb. All mAbs were from BD PharMingen (San Diego, CA). The stained cells were washed once, then resuspended in 200 μl FACS buffer containing 200 ng/ml propidium iodide (PI). Unstained and singly stained controls were included in every experiment. 3A9, a T cell hybridoma line that had been infected with a MIGW green fluorescent protein (GFP) retrovirus was included when GFP expression was analyzed. Cell data were collected on a FACSCalibur flow cytometer (BD Biosciences, San Jose, CA) and four-color analyses (GFP, PE, PI, and allophycocyanin) were done with CellQuest software (BD Biosciences). All data were collected by analyses performed on 1 × 10^4 PI-negative events (viable cells). For the primary T cell studies, activated cells were analyzed as above, except that allophycocyanin-conjugated anti-CD4 and PE-conjugated anti-CD8α were used, and 5 × 10^4 PI-negative events were analyzed.

Northern blot analysis of mRNA

Cells were lysed in TRIzol reagent (Life Technologies, Grand Island, NY) and total cellular RNA was purified according to manufacturer's instructions. RNA (10 μg) was fractionated on a denaturing 1% formaldehyde/agarose gel and transferred to a nitrocellulose membrane. Blots were hybridized overnight with ^{32}P-labeled CD4 (818 bp) or CD8α (596 bp) cDNA fragments. After washes, blots were analyzed by a PhosphorImager (Molecular Dynamics).

Results

siRNAs transiently induce silencing in murine thymocyte cell lines

To study RNAi, siRNAs are typically delivered into cells by carrier-mediated transfection reagents. We developed an experimental system using a thymoma-derived cell line, E10 (23), wherein we studied the use of siRNAs to silence either CD4 or CD8α, using the other marker as an internal specificity control. However, typical of lymphocytes, E10 is insensitive to several different cationic and noncationic transfection reagents and thus electroporation was used to introduce siRNAs. Using this method, ~20% of the cell population expressed GFP from a transfected reporter vector. When CD4 or CD8α siRNAs were electroporated into E10, a marked reduction in surface CD4 or CD8α expression, respectively, occurred 36 h later. Flow cytometry analysis showed that most of the cells were transfected and expression levels were reduced >5-fold below wild-type expression levels (Fig. 1*A*). The degree of reduction of CD8α was frequently more pronounced than that of CD4 and, in both cases, a small population of cells appeared to be either untransfected or not responsive to the siRNA treatment. In repeated experiments, typically 70–95% of the cells exhibited a >5-fold reduction in CD8α expression, although sometimes a smaller fraction of cells down-regulated CD8α to a greater degree (Fig. 1*A*).

Elbashir et al. (13) reported that RNAi-induced silencing could be maintained for ~2 wk in HeLa cells, although neither the extent of silencing nor the number of cell divisions was reported. A time course assay was performed in CD8α siRNA-transfected E10 cells. GFP was included in these transfections to investigate the relationship between the uptake and expression of plasmid DNA and siRNAs. Because these experiments were transient transfections, cell doubling results in a decrease in GFP fluorescence intensity and number of GFP-positive cells (Fig. 1*B*, NS RNA). When CD8α siRNAs were cotransfected with the GFP reporter vector, CD8α expression, but not GFP expression, was markedly reduced (see Fig. 1*B*, 24 h). Several cell populations were evident, with the major CD8α silenced population displaying >5-fold reduced CD8α expression. The majority of cells within this population did not express GFP. However, cells that did express GFP also silenced CD8α. This corresponded to ~20% of the total cells, similar to the control GFP alone (Fig. 1*B*, NS siRNA, 24 h). This indicates that all of the cells expressing GFP also received an adequate level of siRNAs to silence CD8α. In addition, a large fraction of cells incorporated biologically active levels of siRNAs and

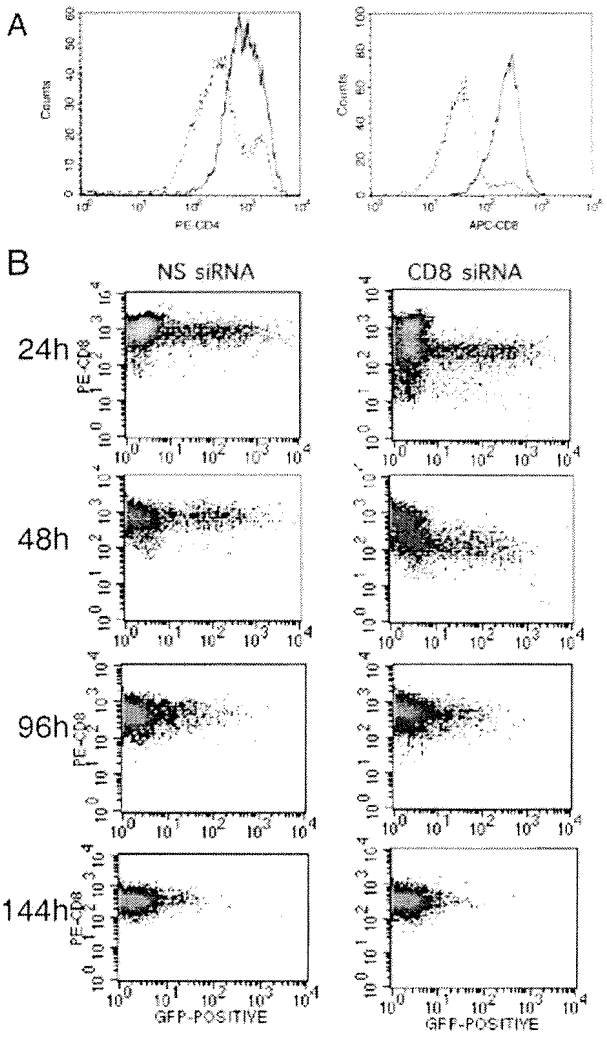

FIGURE 1. CD4 and CD8α siRNAs transiently silence gene expression. *A*, Histogram showing the typical reduction of CD4 and CD8α gene expression seen 36 h post siRNA transfection in E10 T cells. Solid and dashed lines indicate untransfected and siRNA-transfected E10 cells. Approximately 85% of $CD4^+$ cells and 94% of $CD8^+$ cells down-regulated surface expression. *B*, Flow cytometry analysis of transiently transfected GFP and either CD8α or luciferase siRNAs (NS siRNA) in the E10 T cell line. At 24 h, ~60% of the CD8 siRNA-transfected cells down-regulated surface CD8 expression. Gated live cells are shown, and the numbers at the left correspond to the times in hours after electroporation transfection.

yet did not express plasmid DNA. In this experiment, time points were taken over a period of 6 days. At each time point, one-half of the cells were removed from the dish and replaced with fresh medium. The collected cells were stained for CD8α and analyzed by flow cytometry (Fig. 1). A decrease in CD8α surface expression was detectable at 12 h posttransfection, with maximal silencing at 36 h. By 96 h, nearly all of the cells expressed wild-type levels of CD8α. Thus, the RNAi effect in these T cells is a transient phenomena.

In these experiments, there was a dramatic decrease in GFP expression over time, which was likely a result of dilution of the plasmid or potentially due to toxicity of high GFP expression. Because 100% of the GFP-expressing cells exhibited CD8α silencing, it was possible to monitor the "fate" of this subset of silenced cells. The T cells that actively underwent CD8α silencing continued to express GFP over the time course, to the same level as the control population of cells that were not transfected with siRNAs (compare nonspecific RNA to CD8 siRNA). At 96 h, $<5\%$ of the total cells were GFP-positive in cells treated with nonspecific siRNAs and in CD8α siRNA-treated samples. These few remaining GFP-positive cells exhibited normal levels of CD8α expression. This suggests that the cells did not specifically undergo apoptosis as a result of siRNA transfection and subsequent CD8α silencing.

Specificity of siRNA-mediated silencing

Although the GFP transgene expression was not affected during CD8α silencing, the expression of endogenous genes might have been nonspecifically affected. To address this question, the expression levels of CD4 and Thy1.2 T cell markers were examined in cells actively undergoing CD8α silencing. Examination of these markers revealed that there was no reduction of nontargeted gene expression when compared with the control nontransfected cells (Fig. 2*A*), even over extended times (not shown). Although unlikely for this cell line, an additional analysis confirmed that the T cells did not become activated, as they do not up-regulate CD69 (Fig. 2*A*). Together, these experiments confirm the specificity of siRNA-mediated CD8α silencing.

Stability of targeted CD8α mRNA

Short temporal RNAs such as *lin-4* and *let-7* mediate silencing by binding to the 3′-untranslated region (UTR), thus suppressing translation (24–26). This is in marked contrast to the posttranscriptional mRNA degradation effected by siRNAs. To distinguish between these two potential mechanisms for CD8α silencing, a time course Northern blot analysis of CD8α mRNA was performed. The process of silencing did not appreciably affect the growth rate, as compared with control nonspecific siRNA transfections performed in parallel (not shown). Flow cytometry analysis indicated that the RNAi response in these cells lasted 3–4 days (8–10 cell doublings), which corresponds to an ~100-fold increase in cell mass (Fig. 2*B*). Time course analysis was performed in four independent experiments and expression of CD8α was typically suppressed ~5-fold or greater.

At various time points, a fraction of the cells was used to isolate total RNA for Northern blot analysis (Fig. 2*C*). The CD8α mRNA was resolved into two bands, due to alternative splicing (27, 28). Levels of CD8α mRNA decreased during the course of CD8α silencing. Densitometric analysis of the CD8α mRNA bands was performed and normalized to the internal control CD4 band. At the point of maximal silencing, mRNA levels decrease only 2.5-fold. This value is not commensurate with the ~5-fold decrease in protein expression determined by the flow cytometric analysis. However, this RNA was prepared from total cells in which 30% of the

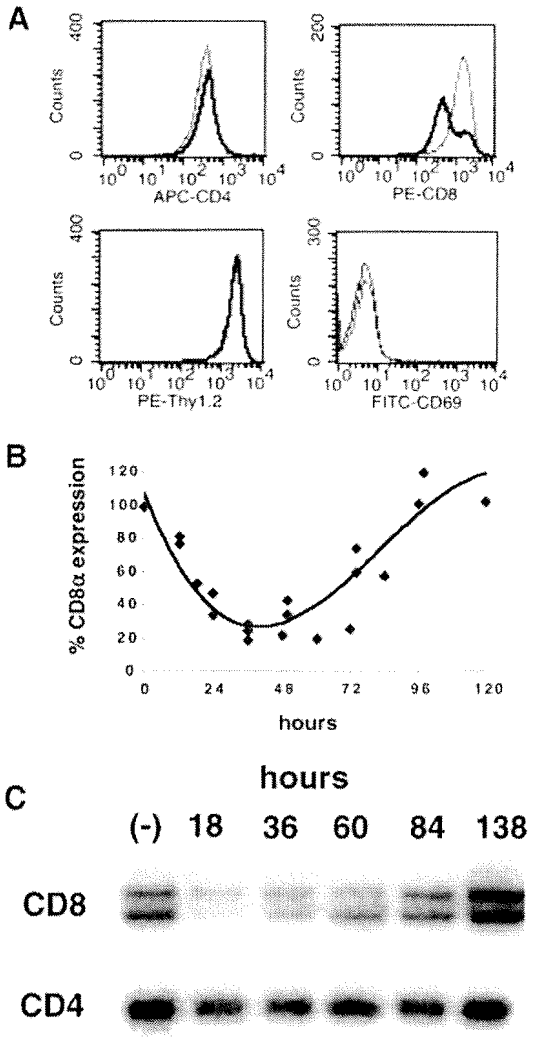

FIGURE 2. Characterization of CD8α siRNA-mediated silencing. *A*, CD8α siRNAs reduce the expression of CD8α, but do not affect the expression of CD4, Thy1.2, or CD69. E10 cells undergoing CD8α silencing at 36 h were immunostained and analyzed via flow cytometry. Histograms plot the number of cells (counts) vs the expression level of each marker (*bottom axis*). Bold line: with siRNA; thin line: without siRNA. *B*, Time course of CD8α silencing. E10 T cells were transfected with siRNAs and cultured over 10 days. During that time, cells were removed from the dish and flow cytometry was performed. Shown are collected data points from three independent experiments. Percent cells expressing normal levels of CD8α are plotted against the time (hours). *C*, Northern blot depicting CD8α mRNA during silencing. At different time points in *A*, RNA was harvested from the cells and probed for CD8α mRNA (the two bands correspond to alternative splicing of CD8). The blot was stripped and reprobed for CD4 mRNA as a loading control.

cells did not exhibit any silencing. When corrected for this reduction, CD8α mRNA was nearly proportionate to levels in reduction of CD8α protein. These Northern blots were performed multiple times with similar results. Thus, although it is clear that CD8α mRNA decreases, we cannot rule out additional silencing phenomena such as cotranslational repression.

Regional sensitivity of an mRNA to silencing by a siRNA

A major outstanding question is whether any region of a mRNA can serve as an effective target for siRNA-directed silencing. Several different siRNAs that targeted different regions of the CD8α

mRNA were tested. Of the first two CD8α siRNAs that were transfected, only one was active. To more quantitatively examine this difference, cells were transfected with varying amounts of siRNAs and CD8α expression was measured by flow cytometry. Cells undergoing silencing were quantified and compared with control nonspecific siRNA treatment (Fig. 3*A*). For the effective CD8α siRNA, picomolar amounts were sufficient to induce some silencing and higher amounts produced a graded response. For the noneffective CD8α siRNA, even at the highest concentration tested, there was no activity.

As these studies progressed, we observed that the majority of the synthetic CD4 and CD8α siRNAs were noneffective at silencing. For CD8α, four different siRNAs were synthesized and tested in the flow cytometry assay: one overlapped the start codon, one which targeted the open reading frame (ORF), one which overlapped the stop codon, and one which targeted the 3′-UTR 15 nt after the stop codon. Only the siRNA which targeted the 3′-UTR ~15 nt after the stop codon effectively silenced CD8α expression. For CD4, five siRNAs were synthesized which targeted corresponding regions to those for the CD8α mRNA (Fig. 3*B*). In this case, only the siRNA that targeted the stop codon was effective at reducing CD4 expression levels. An examination of the nucleotide sequences did not reveal any obvious differences between the effective and ineffective siRNAs.

For each of the above siRNAs, the silencing assay was performed at different siRNA concentrations. None of the inactive siRNAs generated detectable silencing at five times the highest concentration of the active siRNAs (Fig. 3*A* and data not shown). However, these inactive siRNAs were able to compete with the silencing of the active siRNAs. In these competition experiments, inactive CD8α siRNAs were added into the cuvettes containing the active CD8α siRNA, so that both could be electroporated into the cells simultaneously. Varying concentrations were tested, and cells were monitored for CD8α silencing at 36 h (Fig. 4). It was found that when the total siRNA pool contained an inactive CD4 or CD8α siRNA, then silencing mediated by an active siRNA was markedly reduced (Fig. 4, *A* and *B*). These results mirror the ability for active siRNAs to compete for other active siRNAs, a response that we observed for attempting silencing of both CD4 and CD8α simultaneously (Fig. 4, *C* and *D*). The inability to silence both CD4 and CD8α simultaneously in the same cell might suggest that siRNA-mediated RNAi is titratable, as has been described for silencing using long dsRNAs in *C. elegans* (29).

To test whether the above siRNAs were also inactive in other cell types, the CD4 and CD8α genes were expressed from CMV-driven promoters in HeLa cells. The CD8α expression construct contained two regions that corresponded to target sites for effective and ineffective siRNAs in E10. In this assay, cationic lipid cotransfection of the mouse CD4 and CD8α plasmid vectors was performed with either the effective or noneffective CD8α siRNA. When compared with the nonspecific siRNA control, CD8α-specific RNAi silencing was recapitulated in HeLa cells, and the ORF-targeted siRNA was still ineffective at silencing (Fig. 5*A*). These results suggested that the noneffective siRNA phenomenon is not unique to the T cell line, but is likely a feature of either the siRNA sequence, or more likely the mRNA. The concentration dependence of the effective and ineffective siRNA was evaluated in the HeLa cell assay. In this experiment, cationic lipid:siRNA complexes were preformed and added to the cells as previously described (13). The effective siRNA exhibited a concentration dependence; however, the ineffective siRNAs remained inactive even at the highest concentrations (Fig. 5*B*).

siRNA-mediated silencing in primary mouse T cells

To test whether primary cells are sensitive to siRNA-mediated silencing, the CD4/CD8α siRNAs characterized above were used to silence in primary mouse T cells taken from spleen. In these

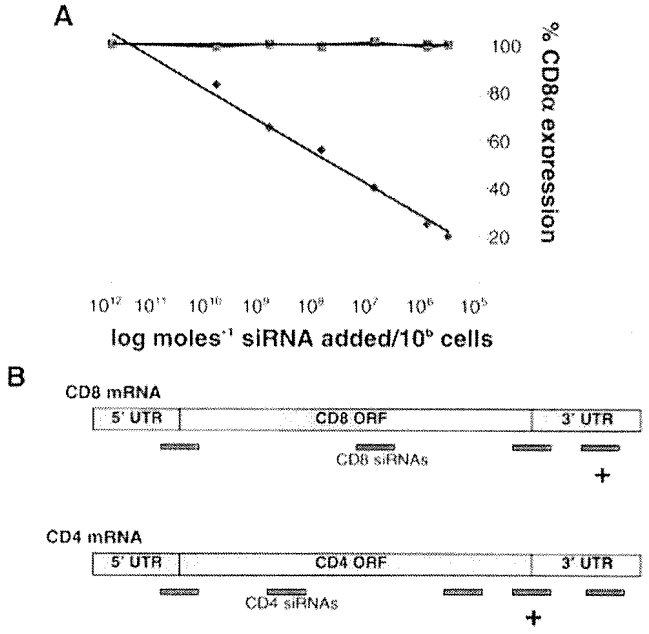

FIGURE 3. A restrictive number of designed siRNA sequences are effective at silencing. *A*, Effect of three different siRNAs targeting CD8α. Effective concentrations of three different CD8α siRNAs were evaluated by titrating increasing amounts of the siRNAs into the cuvettes before electroporation. CD8α expression was evaluated 36 h posttransfection, and is plotted as a percentage of wild-type levels. Effective siRNA (◆); two ineffective siRNAs (▲, ■). *B*, Relative target locations of the siRNAs used in these studies. Schematic of CD4 and CD8α mRNAs (not to scale), showing ORF and 5′- and 3′-UTR. +, Indicates siRNAs that are effective.

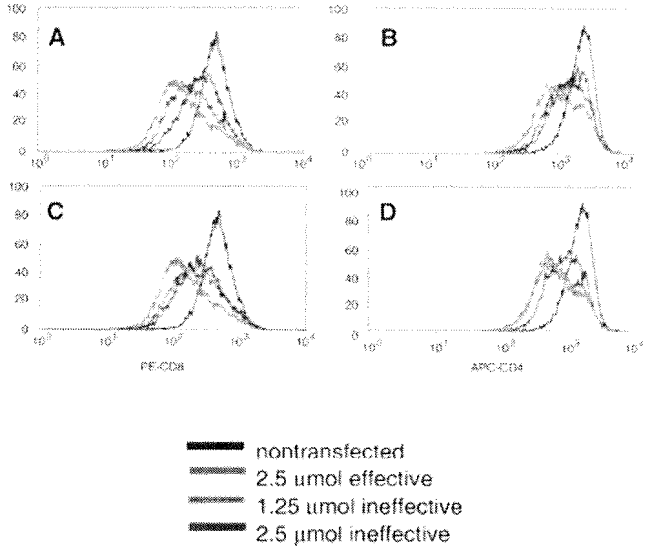

FIGURE 4. Effective and ineffective siRNAs can compete for silencing. Effective CD8α (*A*) and CD4 (*B*) siRNA-mediated silencing is competed by increasing concentration of cotransfected ineffective CD4 and CD8α siRNAs. Effective CD8α (*C*) or CD4 (*D*) siRNA-mediated silencing is competed by increasing concentrations of cotransfected ineffective CD8α or CD4 siRNA. Red indicates E10 cells transfected with 2.5 μmol effective siRNA and black is the nontransfected control. Green and blue indicate the addition of half the amount of an ineffective siRNA.

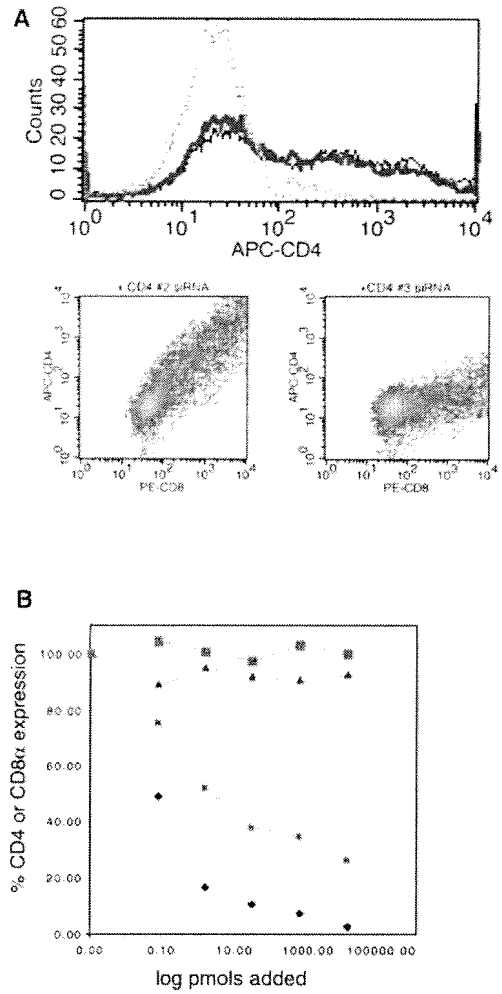

FIGURE 5. Restrictive siRNA usage is not a T cell specific phenomenon. *A*, CD4 silencing in HeLa cells. CD4 and CD8α expression vectors (with or without CD4 siRNAs) were transiently transfected into HeLa cells. The histogram at the top shows the distribution of transfected cells (counts) expressing CD4 (green), and cells that were cotransfected with effective (dotted pink) or ineffective CD4 siRNAs (black). The dotted blue line indicates nontransfected HeLa cells. The bottom two density plots show the specificity of CD4 silencing. CD4-silenced cells were stained for CD4 and CD8α markers. The lower left density plot depicts a typical expression profile of an ineffective siRNA, which is identical to nonspecific siRNA control (not shown). The lower right density plot shows typical results of CD4 silencing using the effective siRNA, which does not affect CD8α expression. *B*, Titration of CD4 or CD8α siRNAs into the HeLa cell system. Effective concentrations of two different CD4 and two different CD8α siRNAs were evaluated by titrating increasing amounts of the siRNAs during cationic lipid cotransfection. CD4 and CD8α expression was evaluated 36 h posttransfection. Effective CD8α siRNAs (green) and CD4 siRNAs (black) reduce CD4 and CD8α expression, while ineffective CD4 (blue) and CD8α (red) maintain high expression levels. Ordinate shows the expression of either CD4 or CD8, which is normalized to 100%. Abscissa depicts the amount of the siRNAs added during transfection.

studies DO11.10 mice, which express a transgenic TCR that recognizes OVA peptide in the context of MHC class II were isolated from these mice are predominantly $CD4^+$; however, a small number (~15%) of $CD8^+$ cells exist in these mice. Efforts to transfect and silence naive T cells were unsuccessful, but if the cells were stimulated to divide by the cognate OVA peptide, CD4 and CD8α silencing could be accomplished similar to the E10 thymoma cell line. Electroporation of CD4 siRNAs into activated primary T cells resulted in an approximate 5-fold decrease in CD4 surface expression compared with an unrelated siRNA control (Fig. 6). Costaining for CD8α on the same cells demonstrated that the down-regulation of CD4 was specific. The maximal degree of silencing was reached at 48 h posttransfection. Later time points could not be collected because of reduced cell viability after 72 h in culture. Similarly, the subset of CD8-positive T cells electroporated with CD8 siRNA exhibited a maximal 3.3-fold decrease in CD8α levels. Furthermore, the degree of silencing in the sample population with the alternate coreceptor (i.e., CD4 in a CD8α siRNA-treated sample) verified that the RNAi response was specific (data not shown). These results demonstrate that primary, mature T cells are able to perform RNAi. The overall degree, kinetics, and specificity of silencing of CD4 or CD8α in primary T cells was comparable to that of the E10 cell line, further supporting the validity of using this line to characterize T cell RNAi.

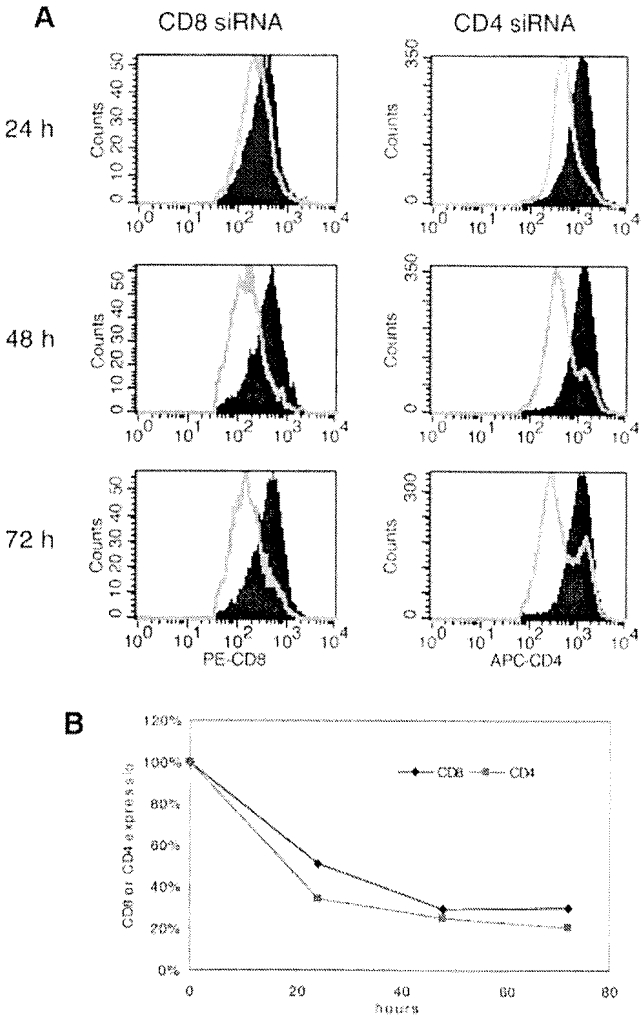

FIGURE 6. Time course of CD4 and CD8α suppression by siRNAs in primary T cells. *A*, Activated DO11 T cells were transfected with siRNAs and cultured for 3 days. Cells at each time point were analyzed by flow cytometry. The histograms are gated on viable cells that express either CD4 or CD8α respectively. The overlays (gray lines) in the histograms represent cells transfected with siRNAs specific for either CD4 or CD8; whereas the underlying histograms (filled) represent controls transfected with a nonspecific siRNA control. *B*, Time course of CD4 and CD8α silencing. The maximal level of suppression was determined by finding the peak fluorescence level of the suppressed curve and expressing it as a percent of the peak fluorescence level of nonspecific siRNA transfection control. Values are expressed as percent silencing and are plotted against time (hours).

Discussion

The CD4 and CD8α T cell surface glycoproteins are of central importance to immune function and disease. We have quantitatively tested the efficacy of a variety of siRNAs to suppress the expression of these glycoproteins. Targeting the CD4 and CD8α markers was attractive since turnover of coreceptor message is fairly rapid (~12 h for CD8α), and changes in surface expression can be rapidly and easily assayed by flow cytometry. In this analysis of two different genes, we observed that T cells and thymocytic cell lines are amenable to siRNA-mediated silencing. These studies revealed that siRNA-mediated RNAi is transient, lasting approximately eight cell doublings. Not every siRNA was able to induce silencing, and the RNAs which targeted the 3′-UTR were effective for both genes. Although small temporal RNAs (stRNAs) mediated translational repression at the mRNA 3′-UTR (for recent reviews, see Refs. 30–34), Northern blot analysis of CD4 and CD8α mRNA indicated posttranscriptional degradation of the mRNA, consistent with a RNAi-type mechanism of silencing. Finally, in primary T cells, the overall penetrance and kinetics of CD4 and CD8α siRNA-mediated RNAi was found to be similar to that observed in the E10 thymoma cell line.

In several experiments, and using electroporation, we found efficient uptake and silencing of >90% of the cells. However, this required the addition of a relatively high amount of siRNA (2.5 μmol/1.5 $\times$ 10^7 cells); Northern blot analysis indicates that only a fraction of the siRNAs (~3 $\times$ 10^4 siRNAs/cell) become associated with the cells (data not shown). Only a fraction of the siRNAs that become associated with cells probably are functional in silencing gene expression. At lower concentrations of siRNAs, a similar fraction (70–95%) of cells exhibit a reduction in CD8 expression, albeit at reduced efficiency. Using either electroporation for T cells or Lipofectamine 2000 for HeLa cells, we found that 100% of the cells that take up and express a cotransfected GFP marker also perform RNAi. Based on this fact, it should be possible to design gene function experiments which enrich the pool of silenced cells by selecting for the activity of a transfected plasmid reporter.

Time course analysis of CD8α silencing in the E10 cell line indicated that the silencing was transient in nature, lasting ~3–4 days. As this cell line doubles rapidly, this value corresponds to approximately eight cell doublings. Northern blots indicated that silencing corresponded to a reduction in mRNA levels, commensurate with the predicted model for RNAi. A translational repression mechanism has been suggested for silencing mediated by stRNAs via the 3′ untranslated region of developmentally important genes. Although the reduction in mRNA level approximated that of CD8α expression, we cannot rule out the possibility of additional translational repression mechanisms.

Only a limited number of the siRNA sequences tested could induce RNAi. For the silencing of most genes, on average one of two candidate siRNAs designed is active in contrast to the one of four and one in five siRNAs tested in targeting CD4 and CD8α (6). It is interesting to note that the siRNAs that were active in silencing targeted the 3′-UTR and stop codon. The restrictive utilization of the 3′-UTR siRNAs did not appear to be cell-type specific, as active and inactive siRNAs gave similar results in HeLa cells. It is unclear why targeting the mouse CD4 and CD8 mRNA 3′-UTRs were effective for performing siRNA-mediated RNAi, while other sites were not. One possibility is that further testing of other mRNA regions would result in productive silencing (35). Alternatively, perhaps the 3′-UTR of these genes is particularly accessible for targeting. Silencing of developmentally timed genes in the endogenous stRNA pathway is specific for the 3′-UTR (25, 36). This could be a common feature of developmentally timed genes, because both CD4 and CD8 are also expressed in a developmentally timed manner.

Attempting to silence both CD4 and CD8α simultaneously resulted in lower levels of silencing of each gene. These results supports a previously recognized observation that the RNAi response is titratable (29). Surprisingly, several of the siRNAs that were inactive competed for silencing when coelectroporated with active siRNAs. While this manuscript was in preparation, another group reported similar findings for the silencing of human coagulation trigger factor (37). However, another group has reported success in dual gene targeting of Lamin A/C and NuMA proteins in HeLa cells (38). The data presented in this study indicate that the inactive siRNAs are recognized by cellular processes but either cannot be converted to an active structure for gene silencing or cannot gain access to their complementary sequences on the target mRNA.

This work presents the first evidence for silencing by siRNA in primary somatic mammalian lymphocytes. In these studies, the degree and kinetics of CD4 and CD8α silencing in the activated primary cells was similar to that of the E10 cell line. In both the primary cells and E10 cells the onset of maximal silencing appeared around three to four cell doublings, which corresponded to 36–48 h posttransfection. In the E10 cells, 100% of the cells had resumed normal CD8α expression by 96 h. Because the viability of the primary cells began to diminish at around 60 h, it was difficult to determine how long the RNAi response would last past 72 h. It is interesting to note that the cells needed to be activated in order for silencing to be accomplished. This could be due to the inability to take up the siRNAs after electroporation, as primary T cells are known to be difficult to transfect with nucleic acids. It is unknown whether mammalian cells must be in a dividing, or "competent", state to perform RNAi. Future studies of siRNA-mediated RNAi in primary cells are required to distinguish between these two possibilities. Nevertheless, these findings provide a precedent upon which future studies of T lymphocyte biology can be designed to validate function by siRNA-mediated silencing.

Acknowledgments

We thank Jane Parnes for the gift of the murine CD4 and CD8 expression constructs. We also acknowledge the Sharp Lab for suggestions and insightful comments.

References

1. Fire, A., S. Xu, M. K. Montgomery, S. A. Kostas, S. E. Driver, and C. C. Mello. 1998. Potent and specific genetic interference by double-stranded RNA in *Caenorhabditis elegans*. *Nature 391:806.*
2. Tuschl, T., P. D. Zamore, R. Lehmann, D. P. Bartel, and P. A. Sharp. 1999. Targeted mRNA degradation by double-stranded RNA in vitro. *Genes Dev. 13: 3191.*
3. Montgomery, M. K., S. Xu, and A. Fire. 1998. RNA as a target of double-stranded RNA-mediated genetic interference in *Caenorhabditis elegans*. *Proc. Natl. Acad. Sci. USA 95:15502.*
4. Grishok, A., A. E. Pasquinelli, D. Conte, N. Li, S. Parrish, I. Ha, D. L. Baillie, A. Fire, G. Ruvkun, and C. C. Mello. 2001. Genes and mechanisms related to RNA interference regulate expression of the small temporal RNAs that control *C. elegans* developmental timing. *Cell 106:23.*
5. Hutvagner, G., J. McLachlan, A. E. Pasquinelli, E. Balint, T. Tuschl, and P. D. Zamore. 2001. A cellular function for the RNA-interference enzyme Dicer in the maturation of the *let*-7 small temporal RNA. *Science 293:834.*
6. McManus, M. T., and P. A. Sharp. 2002. Gene silencing in mammals by siRNAs. *Nat. Genet. Rev. 3:737.*
7. Bernstein, E., A. M. Denli, and G. J. Hannon. 2001. The rest is silence. *RNA 7:1509.*
8. Cullen, B. R. 2002. RNA interference: antiviral defense and genetic tool. *Nat. Immunol. 3:597.*
9. Hannon, G. J. 2002. RNA interference. *Nature 418:244.*
10. Zamore, P. D. 2001. RNA interference: listening to the sound of silence. *Nat. Struct. Biol. 8:746.*
11. Svoboda, P., P. Stein, H. Hayashi, and R. M. Schultz. 2000. Selective reduction of dormant maternal mRNAs in mouse oocytes by RNA interference. *Development 127:4147.*

12. Wianny, F., and M. Zernicka-Goetz. 2000. Specific interference with gene function by double-stranded RNA in early mouse development. *Nat. Cell Biol. 2:70.*
13. Elbashir, S. M., J. Harborth, W. Lendeckel, A. Yalcin, K. Weber, and T. Tuschl. 2001. Duplexes of 21-nucleotide RNAs mediate RNA interference in cultured mammalian cells. *Nature 411:494.*
14. Caplen, N. J., S. Parrish, F. Imani, A. Fire, and R. A. Morgan. 2001. Specific inhibition of gene expression by small double-stranded RNAs in invertebrate and vertebrate systems. *Proc. Natl. Acad. Sci. USA 98:9742.*
15. Sijen, T., J. Fleenor, F. Simmer, K. L. Thijssen, S. Parrish, L. Timmons, R. H. Plasterk, and A. Fire. 2001. On the role of RNA amplification in dsRNA-triggered gene silencing. *Cell 107:465.*
16. Lipardi, C., Q. Wei, and B. M. Paterson. 2001. RNAi as random degradative PCR: siRNA primers convert mRNA into dsRNAs that are degraded to generate new siRNAs. *Cell 107:297.*
17. Cortez, D., S. Guntuku, J. Qin, and S. J. Elledge. 2001. ATR and ATRIP: partners in checkpoint signaling. *Science 294:1713.*
18. Ancellin, N., C. Colmont, J. Su, Q. Li, N. Mittereder, S. S. Chae, S. Stefansson, G. Liau, and T. Hla. 2002. Extracellular export of sphingosine kinase-1 enzyme: sphingosine 1-phosphate generation and the induction of angiogenic vascular maturation. *J. Biol. Chem. 277:6667.*
19. Bai, X., D. Zhou, J. R. Brown, B. E. Crawford, T. Hennet, and J. D. Esko. 2001. Biosynthesis of the linkage region of glycosaminoglycans: cloning and activity of galactosyltransferase II, the sixth member of the β1,3-galactosyltransferase family (β3GalT6). *J. Biol. Chem. 276:48189.*
20. Li, L., J. Mao, L. Sun, W. Liu, and D. Wu. 2001. Second cysteine-rich domain of Dickkopf-2 activates canonical Wnt signaling pathway via LRP-6 independently of dishevelled. *J. Biol. Chem. 12:12.*
21. Koepp, D. M., L. K. Schaefer, X. Ye, K. Keyomarsi, C. Chu, J. W. Harper, and S. J. Elledge. 2001. Phosphorylation-dependent ubiquitination of cyclin E by the SCFFbw7 ubiquitin ligase. *Science 294:173.*
22. Ohta, T., R. Essner, J. Ryu, R. E. Palazzo, Y. Uetake, and R. Kuriyama. 2002. Characterization of CEP135, a novel coiled-coil centrosomal protein involved in microtubule organization in mammalian cells. *J. Cell Biol. 156:87.*
23. Mombaerts, P., C. Terhorst, T. Jacks, S. Tonegawa, and J. Sancho. 1995. Characterization of immature thymocyte lines derived from T cell receptor or recombination activating gene 1 and p53 double mutant mice. *Proc. Natl. Acad. Sci. USA 92:7420.*
24. Reinhart, B. J., F. J. Slack, M. Basson, A. E. Pasquinelli, J. C. Bettinger, A. E. Rougvie, H. R. Horvitz, and G. Ruvkun. 2000. The 21-nucleotide *let-7* RNA regulates developmental timing in *Caenorhabditis elegans. Nature 403:901.*
25. Lee, R. C., R. L. Feinbaum, and V. Ambros. 1993. The *C. elegans* heterochronic gene *lin-4* encodes small RNAs with antisense complementarity to *lin-14. Cell 75:843.*
26. Olsen, P. H., and V. Ambros. 1999. The *lin-4* regulatory RNA controls developmental timing in *Caenorhabditis elegans* by blocking LIN-14 protein synthesis after the initiation of translation. *Dev. Biol. 216:671.*
27. Norment, A. M., N. Lonberg, E. Lacy, and D. R. Littman. 1989. Alternatively spliced mRNA encodes a secreted form of human CD8α: characterization of the human CD8α gene. *J. Immunol. 142:3312.*
28. Giblin, P., J. A. Ledbetter, and P. Kavathas. 1989. A secreted form of the human lymphocyte cell surface molecule CD8 arises from alternative splicing. *Proc. Natl. Acad. Sci. USA 86:998.*
29. Parrish, S., J. Fleenor, S. Xu, C. Mello, and A. Fire. 2000. Functional anatomy of a dsRNA trigger: differential requirement for the two trigger strands in RNA interference. *Mol. Cell 6:1077.*
30. Banerjee, D., and F. Slack. 2002. Control of developmental timing by small temporal RNAs: a paradigm for RNA-mediated regulation of gene expression. *BioEssays 24:119.*
31. Grosshans, H., and F. J. Slack. 2002. Micro-RNAs: small is plentiful. *J. Cell Biol. 156:17.*
32. Pasquinelli, A. E., and G. Ruvkun. 2002. Control and developmental timing by microRNAs and their targets. *Annu. Rev. Cell. Dev. Biol. 28:28.*
33. Moss, E. G. 2002. MicroRNAs: hidden in the genome. *Curr. Biol. 12:R138.*
34. Ambros, V. 2001. microRNAs: tiny regulators with great potential. *Cell 107:823.*
35. Novina, C. D., M. F. Murray, D. M. Dykxhoorn, P. J. Beresford, J. Riess, S. K. Lee, R. G. Collman, J. Lieberman, P. Shankar, and P. A. Sharp. 2002. siRNA-directed inhibition of HIV-1 infection. *Nat. Med. 3:3.*
36. Pasquinelli, A. E., B. J. Reinhart, F. Slack, M. Q. Martindale, M. I. Kuroda, B. Maller, D. C. Hayward, E. E. Ball, B. Degnan, P. Muller, et al. 2000. Conservation of the sequence and temporal expression of *let-7* heterochronic regulatory RNA. *Nature 408:86.*
37. Holen, T., M. Amarzguioui, M. T. Wiiger, E. Babaie, and H. Prydz. 2002. Positional effects of short interfering RNAs targeting the human coagulation trigger tissue factor. *Nucleic Acids Res. 30:1757.*
38. Elbashir, S. M., J. Harborth, K. Weber, and T. Tuschl. 2002. Analysis of gene function in somatic mammalian cells using small interfering RNAs. *Methods 26:199.*

Short RNA duplexes produced by hydrolysis with *Escherichia coli* RNase III mediate effective RNA interference in mammalian cells

Dun Yang*†, Frank Buchholz*‡, Zhongdong Huang*, Andrei Goga§, Chih-Ying Chen*, Frances M. Brodsky*, and J. Michael Bishop*

*G. W. Hooper Foundation and Department of Microbiology and Immunology, and §Division of Hematology/Oncology, Department of Medicine, University of California, San Francisco, CA 94143-0552

Contributed by J. Michael Bishop, May 31, 2002

Small interfering RNA (siRNA) has become a powerful tool for selectively silencing gene expression in cultured mammalian cells. Because different siRNAs of the same gene have variable silencing capacities, RNA interference with synthetic siRNA is inefficient and cost intensive, especially for functional genomic studies. Here we report the use of *Escherichia coli* RNase III to cleave double-stranded RNA (dsRNA) into endoribonuclease-prepared siRNA (esiRNA) that can target multiple sites within an mRNA. esiRNA recapitulates the potent and specific inhibition by long dsRNA in *Drosophila* S2 cells. In contrast to long dsRNA, esiRNA mediates effective RNA interference without apparent nonspecific effect in cultured mammalian cells. We found that sequence-specific interference by esiRNA and the nonspecific IFN response activated by long dsRNA are independent pathways in mammalian cells. esiRNA works by eliciting the destruction of its cognate mRNA. Because of its simplicity and potency, this approach is useful for analysis of mammalian gene functions.

Double-stranded RNA interference (RNAi) has become a powerful genetic tool for selectively silencing gene expression in many eukaryotes (1, 2).

In the RNAi reaction, the cellular RNase III enzyme Dicer cleaves the double-stranded RNA (dsRNA) silencing trigger into 21- to 25-nt RNA called siRNA (small interfering RNA) (3, 4). siRNA pairs with its cognate mRNA, leading to degradation of target mRNA and amplification of gene-specific silencing signals (1–5). Although RNAi has also been observed in mouse oocytes, embryos, embryonic stem cells, and embryonal carcinoma cell lines, dsRNA triggers nonspecific inhibition of gene expression in most mammalian cell lines (6–8). In mammalian cells, dsRNAs longer than 30 bp can activate the dsRNA-dependent kinase PKR and 2′-5′-oligoadenylate synthetase, normally induced by IFN (9). By virtue of its small size, synthetic siRNA avoids activation of the IFN response. The activated PKR inhibits general translation by phosphorylation of the translation factor eukaryotic initiation factor 2α, whereas 2′-5′-oligoadenylate synthetase causes nonspecific mRNA degradation via activation of RNase L (9).

In contrast to the nonspecific effect of long dsRNA, siRNA can mediate selective gene silencing in the mammalian system (10, 11). Hairpin RNA with a short loop and 19–27 bp in the stem also selectively silences expression of genes that are homologous to the sequence in the double-stranded stem (12, 13). Mammalian cells can convert short hairpin RNA into siRNA to mediate selective gene silencing (12, 13). Although many mammalian cells can also convert long dsRNA into siRNA, long dsRNA is incapable of triggering RNAi in these cells (7). The inability of long dsRNA to elicit RNAi in vertebrates has been generally attributed to nonspecific activation of the IFN response (7, 8). However, the relationship between the IFN signaling pathway and RNA interference has not been addressed definitively.

Although siRNA provides a promising tool for assessing the consequences of suppressing gene expression in cultured mammalian cells, RNAi with synthetic siRNA is limited because siRNAs to different sequences within a gene have dramatically varied inhibitory ability (14, 15). Therefore, each mRNA must be screened for an efficient siRNA, a laborious and costly process. However, processing of long dsRNAs should generate a great variety of siRNAs capable of interacting with multiple sites on target mRNAs, increasing the chance that at least one siRNA will pair with its target sequence. Thus, the power of siRNA as a genetic tool in the mammalian system could be greatly enhanced by using siRNA processed from dsRNA.

Although Dicer is involved in the dsRNA cleavage *in vivo*, using Dicer to prepare siRNA *in vitro* may be problematic because dsRNA cleavage by Dicer is very inefficient, particularly for short dsRNAs (3, 16). In contrast, *Escherichia coli* RNase III (EC3.1.24) can digest dsRNA very efficiently into short pieces with the same end structures as siRNA, 5′ phosphate/3′ hydroxyl termini and 2- to 3-nt 3′ overhangs (17). These end structures of siRNA are reported to be important for RNAi activity (18). In addition, large amounts of soluble recombinant *E. coli* RNase III protein can be obtained (17). These attributes make *E. coli* RNase III a promising enzyme for preparing siRNAs *in vitro*.

Exhaustive cleavage of dsRNA by *E. coli* RNase III leads to duplex products averaging 12–15 bp in length (17). These short dsRNA are unable to trigger an RNAi response in mammalian cells (ref. 6 and D.Y., unpublished observation). To obtain siRNA of appropriate length we performed limited RNase III digestion of dsRNA, efficiently generating 20- to 25-bp siRNA. These siRNAs recapitulated the potent and sequence-specific gene silencing by long dsRNA in *Drosphila* S2 cells. More importantly, they also mediated effective RNAi without nonspecific effects in mammalian cells. siRNA produced by the method successfully inhibited various endogenous genes in different mammalian cell lines. Because it is relatively quick and simple, this method may prove to be useful in using siRNA for analysis of gene functions in cultured mammalian cells.

Materials and Methods

Protein Expression and Purification. The *E. coli* RNase III coding sequence was amplified with PCR from the bacterial strain DH5α genomic DNA with the upstream primer cgc gga tcc aac ccc atc gta att aat cgg ctt ca and downstream primer gac gtc cga cga tgg caa t and cloned into *Bam*HI and *Sma*I of pGEX-2T (Amersham Pharmacia). To produce glutathione *S*-transferase (GST)-RNase III protein, the bacterial strain BL21(DE3) carrying the expression vector was grown at 37°C to an OD_{600} of 0.5

Abbreviations: RNAi, RNA interference; dsRNA, double-stranded RNA; siRNA, small interfering RNA; esiRNA, endoribonuclease-prepared siRNA; F-luc, firefly luciferase; R-luc, *Renilla* luciferase; GST, glutathione *S*-transferase; RPE, retinal pigment epithelial; LCa/LCb, clathrin light chain a/b.

†To whom reprint requests should be addressed. E-mail: dyang20@itsa.ucsf.edu.

‡Present address: Max Planck Institute–Molecular Cell Biology and Genetics, Pfotenhauer Strasse 108, 01307 Dresden, Germany.

www.pnas.org/cgi/doi/10.1073/pnas.152327299

and induced with 1 mM isopropyl β-D-thiogalactoside for 2 h. GST-RNase III was purified with glutathione-agarose beads according to the manufacturer's instruction (Amersham Pharmacia), dialyzed against 20 mM Tris·HCl, 0.5 mM EDTA, 5 mM $MgCl_2$, 1 mM DTT, 140 mM NaCl, 2.7 mM KCl, 30% glycerol, pH 7.9 overnight, and kept at −20°C. Approximately 1 mg of RNase III was purified from 1 liter of culture. There was no significant loss of enzyme activity after 6 months of storage.

Single-Strand RNA Synthesis and Preparation of dsRNA. The siRNAs CS1 and CS2 were synthesized chemically (Dharmacon, Lafayette, CO). siRNAs, T1 to T6, and short RNA hairpins, H1 to H6, were synthesized by using the MEGAshortscript kit (Ambion, Austin, TX) from oligo DNA templates carrying a phage T7 promoter at one end. All siRNAs were 21 nt long and had 2-nt 3′ overhangs. All short hairpin RNAs had a 24-bp stem with a UCU loop and an extra GGGA at the 5′ end for efficient transcription *in vitro*. Other RNA strands were individually synthesized by using the MEGAscript kit (Ambion) from PCR-derived linear templates carrying a phage T7 promoter at both ends. dsRNA was formed by annealing as described (16).

The ends of the dsR-457 RNAs corresponded to 1200–1656 in pRL-CMV (Promega). The firefly luciferase (F-*luc*) RNAs corresponded to the following positions in pEGFPLuc (CLONTECH): dsF-592, 1455–2046; CS1, 1520–1538; CS2, 1900–1918; T1, 603–621; T2, 624–642; T3, 2448–2466; T4, 2994–3012; T5, 3013–3031; T6, 3049–3067; H1, 989-1012; H2, 1520–1543; H3, 2529–2552; H4, 2601–2624; H5, 2906–2929; H6, 2947–2970. Templates for *clathrin light chain a* (*LCa*) and *Cdk1* dsRNA represented the full coding sequences of their genes. Templates for the 681-bp c-*myc* dsRNA were amplified with forward primer gactcaacgttagcttcaccaaca and reverse primer ggactccgtcgaggagagcaga. All of these primers had appended 18-base phage promoters.

Production and Purification of Short RNA Duplexes. To prepare endoribonuclease-prepared siRNAs (esiRNAs) for F-luc and *Renilla* luciferase (R-luc), 100 μg of dsRNAs was digested by 1 μg of recombinant RNase III in a 200 μl reaction buffer (same as dialysis buffer except 5% glycerol) for 15 min at 37°C. Reactions were terminated by adding EDTA to 20 mM and the products were separated on 12% polyacrylamide gel, 1 × 89 mM Tris·HCl (pH 8.4)/89 mM boric acid/2 mM EDTA. A 10-bp DNA marker was used to estimate the migration of RNA duplexes. Short RNAs of appropriate sizes were eluted from gel slices by soaking in 1 M $(NH_4)_2AC$ at 37°C overnight and recovered by ethanol precipitation. The precipitate was dissolved in 10 mM Tris·HCl (pH 7.4) and 0.5 mM EDTA at 1.0 μg/μl. For other genes, 100 μg of dsRNAs was digested with 0.2 μg of RNase III for 1 h at 21°C, and reactions were loaded onto QIAquick spin columns after being supplemented with 5 vol of PN buffer (QIAquick nucleotide removal kit, Qiagen, Chatsworth, CA). Flow-through usually contained RNA from 15 to 25 bp, which was precipitated by ethanol and dissolved in TE buffer. The concentration of esiRNA was determined by UV_{260}.

Cell Culture, Nucleic Acid Transfections, and Luciferase Assays. C33A human cervical carcinoma cell line, HeLa human cervical epithelioid carcinoma cell line, and 293 transformed human embryonic kidney cells were obtained from the American Type Culture Collection and grown in DMEM. The hTERT-RPE1 cell line (CLONTECH) is a human retinal pigment epithelial (RPE) cell line that stably expresses the human telomerase reverse transcriptase subunit (hTERT). hTERT-RPE1 cells were permanently transfected with a F-luc expression construct to express F-luc from chromatin templates and grown in DEME/F12 medium. *Drosophila* S2 cells were grown in Schneider medium. All media were from Life Technologies, Grand Island, NY, and supplemented with 10% FBS (vol/vol). Mammalian cells were cultured at 37°C; S2 cells were at room temperature.

To silence luciferase expression from plasmid templates, plasmid DNA and esiRNAs were cotranfected by using Superfect (Qiagen). Cells were transfected at 50–70% confluence in 24-well plates for 2.5 h and then changed to fresh medium. Unless otherwise described, transfections used 1 μg of DNA per well in 0.5 ml transfection medium (0.5 μg pEGFPLuc/0.1 μg pRL-SV40/0.4 μg pUC19/47 nM esiRNA). Data were expressed as mean ratio of relative luciferase activities (F-luc/R-luc or R-luc/F-luc) and normalized to that in cells transfected with DNA only. Error bars equal ± one SD. To silence F-luc expression from chromatin templates in RPE cells, 0.2 μg esiRNA was transfected into each well of a 6-well plate by using Lipofectamine 2000 for 3 h and then changed to the fresh medium. Luciferase activity was measured as described (16). Protein concentrations were measured by Bradford assays (Bio-Rad). To silence endogenous gene expression, cells were co-transfected with 1 μg esiRNA by using Lipofectamine 2000.

***In Vitro* RNAi Assay.** Preparation of cell extracts and *in vitro* RNAi were carried out as described (19). The HeLa cells (2×10^7) were washed in PBS and resuspended in a hypotonic buffer (10 mM Hepes, pH 7.0/2 mM $MgCl_2$/6 mM mercaptoethanol) and lysed. Cell lysates were centrifuged at 20,000 × *g* for 30 min. We stored supernatants at −80°C. As described (16), mRNAs were produced by using a MAXIscript kit (Ambion) and uniformly labeled during the transcription reaction with ^{32}P-labeled UTP. For *in vitro* RNAi, 10 μl of extracts was incubated for indicated times at 37°C with 100 nM esiRNA in a 20 μl of reaction containing 20 mM Hepes (pH 7.0), 1 mM MgOAC, 100 mM K_2(OAC), 5 mM DTT, 500 μM NTP, and 2 units of RNasin (Promega).

Western Blotting. For analysis of clathrin light chain and heavy chain, cells extracts were prepared as described (20, 21). For c-myc, Cdk1, and Cdk2, transfected cells grown in 6-well plates were harvested in PBS buffer containing 1% Nonidet P-40 and mixed with an equal volume of SDS sample buffer. Equal amounts of total protein were separated on 12.5% polyacrylamide gels and transferred to nitrocellulose. Standard immunostaining was carried out by using ECL (Amersham Pharmacia). Signals were quantified by using Molecular Dynamics equipment. Rabbit serum, which recognizes both LCa and clathrin light chain b (LCb), and monoclonal TD.1 against clathrin heavy chain have been described (20, 21). Anti-c-Myc antibody, N262, and antibodies for cyclin A and Cdk2 were from Santa Cruz Biotechnology, and antiactin antibody was from Sigma.

Results and Discussion

Processing Long dsRNAs into Short RNA Duplexes with *E. coli* RNase III. To prepare a heterogeneous siRNA population that could potentially target multiple sites per mRNA molecule for inhibition, we used *E. coli* RNase III to digest long dsRNAs representing the mRNA targets. We overexpressed *E. coli* RNase III as a GST fusion protein in *E. coli* and purified it to homogeneity (Fig. 1*a*). To make a 592-bp dsRNA (dsF-592) corresponding to the F-*luc* and a 457-bp dsRNA (dsR-457) of R-*luc*, we performed *in vitro* transcription from PCR products that had appended phage promoters at each end (Fig. 2*e*). We found that GST-RNase III fusions were highly active in cleaving these dsRNAs at 37°C. Even at low RNase III concentrations, cleavage products were visible within 1 min incubation, and molecules approximately 15–30 bp in length were accumulated during longer incubation and became the main products (Fig. 1*b*). Similar digestion patterns were also observed with dsRNAs representing more than 20 other genes (data not shown). After optimization, we found that limited RNase III digestion of

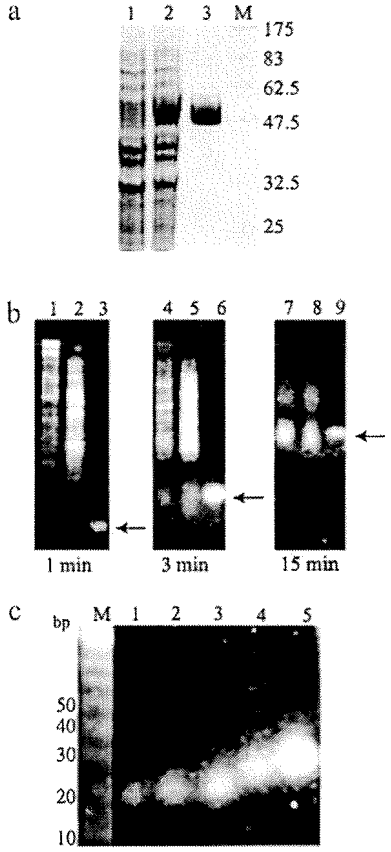

Fig. 1. Preparation of siRNA from dsRNA by hydrolysis with *E. coli* RNase III. (*a*) Overexpression and purification of GST-RNase III fusion. Lanes 1 and 2, *E. coli* extracts before and after isopropyl β-D-thiogalactoside induction; lane 3, purified GST-RNase III fusion; lane M, protein molecular weight marker. (*b*) Time course of RNase III digestion of dsRNA. DsR-457 or dsF-592 RNA was incubated with RNase III for the indicated time, and then separated by electrophoresis in a 4% agarose gel. Lanes 1, 4, and 7 are dsR-457; lanes 2, 5, and 8 are dsF-592; lanes 3, 6, and 9 are 21-bp siRNA marked by an arrow. (*c*) Agarose gel analysis of purified short RNA species processed from dsF-592. Lane M, 10-bp DNA marker; lanes 1 and 2 are chemically synthesized siRNAs; lane 3, 21–23 bp; lane 4, 24–26 bp; lane 5, 27–30 bp.

dsRNA at room temperature for 1 h yielded ample amounts of esiRNA for inhibition of most genes. Efficiently processing dsRNA with high sequence complexity into short species is consistent with the lack of sequence specificity in substrate recognition and cleavage by *E. coli* RNase III (22). We separated RNase III digestion products on polyacrylamid gels and purified the RNAs corresponding to approximately 21–23, 24–26, and 27–30 bp (Fig. 1*c* and data not shown). For simplicity, we named siRNA prepared by RNase III digestion esiRNA.

esiRNA Mediates Effective RNAi Against Reporter Gene Expression in Cultured Insect and Mammalian Cells. To test whether esiRNA has RNAi activity, we cotransfected short RNA duplexes along with expression constructs for F-luc and R-luc into *Drosophila* S2 cells. Inhibition was estimated by measuring the relative F-luc (F-luc/R-luc) or relative R-luc (R-luc/F-luc) activity as described (16). We observed that the 21- to 23-bp esiRNA, processed from dsR-457, caused about 900-fold inhibition of R-luc activity (Fig. 2*a*). The similarly sized esiRNA of F-luc exerted 500-fold of inhibition of F-luc activity (Fig. 2*b*). esiRNAs of 24–26 bp and 27–30 bp showed similarly potent inhibition of their cognate luciferase activity (Fig. 2 *a* and *b*). The unprocessed dsRNAs, dsR-457 and dsF-592, were 2- to 10-fold less potent

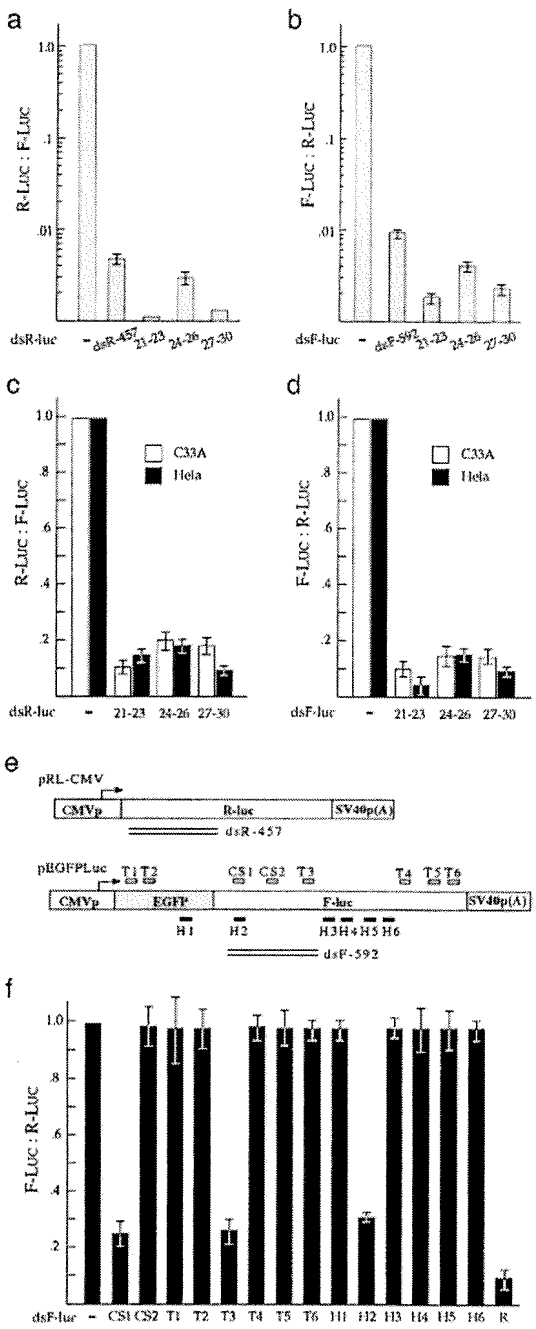

Fig. 2. siRNA-mediated gene silencing in insect and mammalian cells. The effect of esiRNA on R-luc (*a* and *c*) or F-luc (*b* and *d*) expression was determined in *Drosophila* S2 cells (*a* and *b*) and mammalian cell lines, HeLa and C33A (*c* and *d*). Plasmid DNAs with or without various sized dsRNAs were cotransfected into cells. (*e*) Reporter plasmids, siRNAs, dsRNAs, and short hairpin RNAs. The diagram illustrates DNA constructs used to produce *in vivo* mRNA and *in vitro* dsRNA for F-luc and R-luc genes. The positions of dsRNAs, chemically synthesized siRNAs (CS1 and CS2), *in vitro*-transcribed siRNAs (T1 to T6), and short hairpin RNAs (H1 to H6) are indicated. (*f*) The variable effect of synthetic siRNAs or short hairpin RNAs on different sequences within a gene. Plasmid DNAs with or without the various indicated short RNA species were cotransfected into HeLa cells. R is the F-luc esiRNA shorter than 30 bp.

than esiRNA (Fig. 2 *a* and *b*). Recapitulation of RNAi activity of long dsRNA with its esiRNA is consistent with the presumption that siRNA is the bona fide mediator of the RNAi reaction.

We further tested whether esiRNA is a specific gene silencer

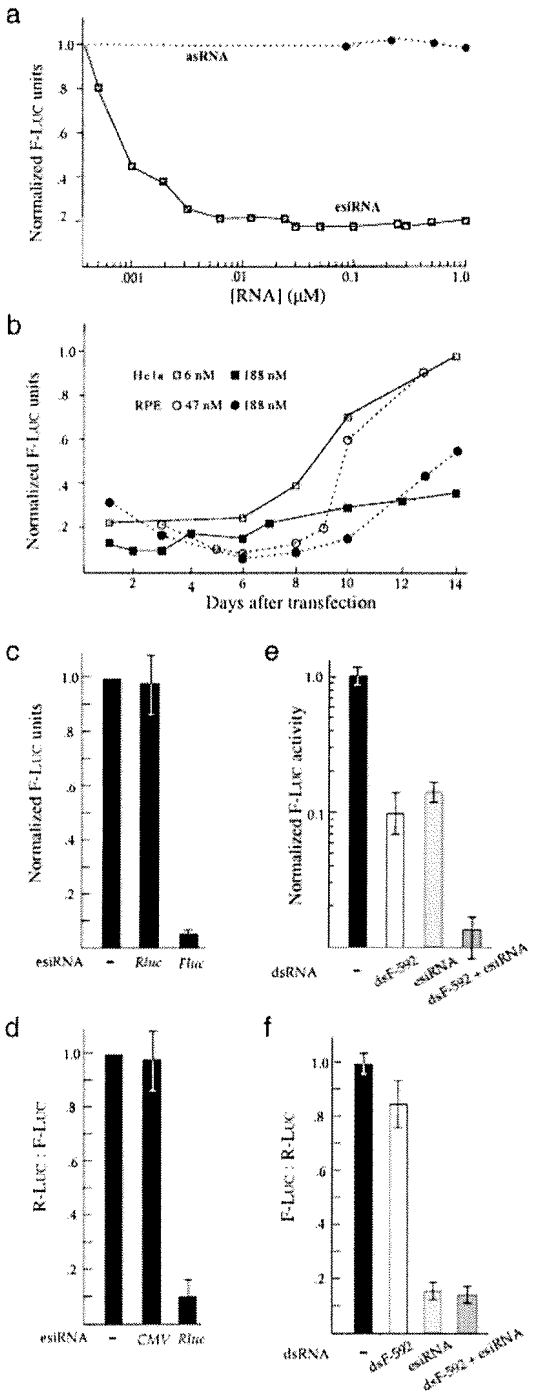

Fig. 3. Characteristics of RNAi. (*a*) Dose–response for antisense RNA (asRNA) and esiRNA against F-luc. Indicated amounts of F-luc esiRNA (21–23 bp) or antisense strand of CS1 were transfected into RPE cells to target F-luc expression from chromatin templates, and luciferase activities were measured at 24 h after transfection. Data represent the average of 3–6 experiments and are expressed as relative luciferase activity after normalization to the luciferase units/μg of protein observed in control cells transfected with R-luc esiRNA. (*b*) Duration of esiRNA-mediated inhibition. F-luc esiRNA (21–23 bp) was transfected into RPE cells, and luciferase activities were measured at the indicated time period. When HeLa cells were used, F-luc target was expressed from cotransfected plasmid DNA. (*c*) esiRNA silences gene expression from mRNA templates. HeLa cells were transfected with 0.5 μg F-luc mRNA with or without 0.1 μg of esiRNA (21–23 bp) for either F-luc or R-luc for 3 h and then collected for luciferase assays. Data are expressed as arbitrary luciferase units and normalized to that produced in cells transfected with mRNA only. (*d*) esiRNA corresponding to the promoter region has no RNAi activity. HeLa cells were transfected with pGL-3-control (Promega) and pRL-CMV with or without 21- to 23-bp esiRNA corresponding to either the cytomegalovirus (CMV) promoter or R-luc. Luciferase activity was measured 24–96 h after cotransfection. (*e* and *f*) Relationship between RNAi and the IFN signaling pathway. DsF-592 and F-luc esiRNA (21–23 bp) were transfected individually or together into HeLa cells to silence F-luc expression from plasmid templates. Luciferase activity was measured 24–48 h after cotransfection. Data are expressed as either F-luc units (*e*) or relative F-luc activity (*f*), normalized to that of DNA-only transfections.

in mammalian cells. We observed that 21- to 23-bp esiRNA of R-luc caused 85–90% inhibition of relative R-luc expression in both HeLa and C33A cells (Fig. 2*c*). Similarly sized esiRNAs of F-luc inhibited 90–95% of relative F-luc expression (Fig. 2*d*). This reciprocal effect indicates that the short RNA duplexes acted in a sequence-specific manner without affecting expression from the noncomplementary templates. Similarly, 24- to 26-bp and 27- to 30-bp esiRNAs exerted sequence-specific inhibition, consistent with a published report that the synthetic enhanced green fluorescent protein siRNAs ranging from 21 to 27 nt all have RNAi activity (Fig. 2 *c* and *d* and ref. 11). Similar results were obtained with column-purified esiRNAs (Fig. 2*f*). We compared inhibitory ability of siRNA and esiRNA. We found that different siRNAs of F-*luc* made by either chemical synthesis or *in vitro* transcription had dramatically varied silencing ability and were less potent inhibitors than esiRNA (Fig. 2 *d* and *f*). This was also true for short RNA hairpins. Of the 14 siRNAs and short hairpin RNAs for F-*luc*, only three showed reasonable RNAi activity (Fig. 2*f*). The synthetic siRNAs or hairpin RNAs recognized only one sequence element, whereas esiRNAs covered comprehensive sequence elements of the target mRNA. Thus, esiRNA likely increases the chance that at least one siRNA can pair with and lead to destruction of its target.

Similar strong and specific inhibition by esiRNA was observed in IMR-90, CHO, hTERT-RPE1, MEF, and 293 cells, suggesting the approach is generally applicable for mammalian cell lines (data not shown). As expected, long dsRNA, either dsF-592 or dsR-457, caused sequence-independent inhibition of both F-luc and R-luc expression, suggesting activation of the IFN signaling pathway (Fig. 3 *e* and *f* and data not shown). In contrast, esiRNA did not cause significant nonspecific inhibition of control luciferase expression in these mammalian cell lines.

Dose Dependence of RNAi Mediated by esiRNA in Mammalian Cells. Cotransfection assays do not allow accurate calculation of the minimal effective esiRNA concentration. To study dose dependence of esiRNA-induced inhibition, we used F-luc esiRNA to inhibit gene expression in the hTERT-RPE1 cells that were stably transfected with an F-luc expression construct. We observed a saturated inhibition when the transfection buffer contained at least 3 nM of esiRNA (Fig. 3*a*). Inhibition decreased at subsaturating esiRNA doses and was undetectable when the esiRNA dose was below 0.5 nM (Fig. 3*a*). The antisense strand of the chemically synthesized siRNA CS1 was incapable of inhibiting F-luc activity even at 10- to 20-fold higher concentrations than the effective concentration used for its double-stranded form, suggesting siRNAs are more potent inhibitors than antisense RNAs (Figs. 2*f* and 3*a*).

Rapid Onset and Prolonged Duration of Inhibition. To further characterize the RNAi reaction, we determined the duration of F-luc esiRNA-mediated inhibition of chromatin templates in the above hTERT-RPE1 cells. We observed 50–65% inhibition of F-luc activity at 8 h after transfection (data not shown), suggesting that silencing was established rapidly. Silencing reached the maximum 5–6 days after transfection and then declined (Fig. 3*b*). When plasmid DNA was used to express targets for inhi-

GENETICS

bition in HeLa cells, we observed that the inhibition could last 2 weeks if high esiRNA doses were used. Low doses of esiRNA caused less potent inhibition that was sustained for several days (Fig. 3*b*). Thus, the longevity of esiRNA-mediated inhibition at least partially depended on esiRNA dose with either episomal or chromatin templates. The rapidity and longevity of esiRNA-mediated inhibition suggest that esiRNAs could be used to inactivate genes whose protein products are relatively stable.

esiRNA Elicits mRNA Decay. A key feature of RNAi in *Caenorhabditis elegans* and *Drosophila* is that it exerts its effect by eliciting the destruction of targeted mRNA (1). To test whether siRNAs also act posttranscriptionally in the mammalian system, we asked whether esiRNA could directly inhibit expression from its cognate mRNA. We cotransfected esiRNA and F-luc mRNA into HeLa cells. Three hours after transfection, control cells that had received F-*luc* mRNA produced 20,000–50,000 units of luciferase activity. However, cotransfected esiRNAs for F-luc but not R-luc caused 15-fold inhibition of F-luc activity, suggesting that siRNA-mediated gene silencing is directed at mRNA in mammalian cells (Fig. 3*c*). Consistent with this result, we found that the esiRNA corresponding to a promoter region had no RNAi activity (Fig. 3*d*). To test whether esiRNA elicits destruction of the target mRNA, we used an extract of HeLa cells to perform an *in vitro* RNAi assay identical to that used to characterize RNAi responses in *Drosophila* embryo extracts (19). We found that esiRNAs for either F-*luc* or R-*luc* accelerated the degradation of their cognate mRNA 4- to 8-fold (Fig. 4). This finding is consistent with previous reports on the effect of siRNA (10, 14).

Nonspecific Gene Silencing by Long dsRNA and Sequence-Specific Interference by siRNA Are Independent Pathways. To test the effect of the IFN signaling pathway on RNAi, we first asked whether we could detect RNAi activity of siRNA in the presence of a nonspecific IFN response activated by long dsRNA in HeLa cells. We found that dsF-592 caused 10- to 20-fold inhibition of both F-luc and R-luc expression, suggesting activation of the nonspecific IFN response (Fig. 3 *e* and *f*). F-luc esiRNA selectively inhibited F-luc expression as observed before. When esiRNA and dsF-592 were cotransfected, we observed additive inhibition of F-luc expression (Fig. 3*e*). However, esiRNA inhibited relative F-luc activity equally with or without cotransfected dsF-592, suggesting that activation of nonspecific IFN response has no effect on the potency of specific RNAi inhibition (Fig. 3*f*).

We then tested whether inactivation of the IFN response suffices to activate specific gene silencing of long dsRNA. We found that mouse embryonic fibroblast cells lacking either PKR or both PKR and RNase L were defective in both nonspecific and specific gene silencing triggered by dsF-592, although siRNA-mediated RNAi could be detected (data not shown). We concluded that sequence-specific RNAi mediated by siRNA is independent of dsRNA-triggered nonspecific gene silencing.

esiRNA Selectively Silences the Expression of Endogenous Genes. To test whether the expression of endogenous genes could be silenced we targeted a wide variety of genes, including those with either abundant long-lived or rare short-lived transcripts/proteins. We first attempted to silence the expression of the LCa in HeLa cells. We examined the level of LCa protein 5 days after esiRNA transfection to allow turnover of the protein, whose half-life is 24 h (20). Western blot analysis revealed that the LCa chain was reduced up to 90% (Fig. 5*a*). LCb was unaffected although it has 66% homology in DNA sequence with LCa and was recognized by the same antibody. A cross-silencing between *LCa* and *LCb* was not expected because these two genes do not share any uninterrupted DNA sequence longer than 21 nt in length (data not shown). LCa turns over independently of the other subunits of clathrin. Accordingly, inhibition of LCa expression did not affect the expression of clathrin heavy chain (Fig. 5*a*). We found that esiRNA-treated cells grew normally despite dramatically reduced LCa protein. This finding is presumably caused by functional redundancy between LCa and LCb. For example, complete loss of LCa in PC12 cells has been reported to have little effect on clathrin-mediated endocytosis and secretion (20).

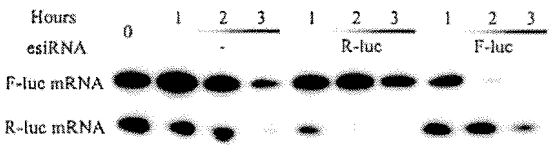

Fig. 4. esiRNA induces degradation of its cognate mRNA. ^{32}P-labeled F-luc or R-luc mRNA was incubated in extracts of HeLa cells with or without the cognate esiRNAs for the indicated time periods and then analyzed in a 4% sequence gel.

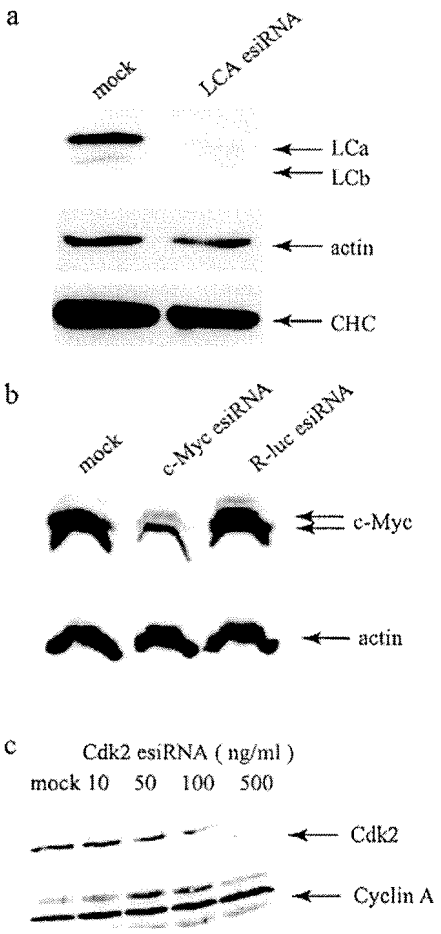

Fig. 5. Silencing of endogenous mammalian genes with esiRNA. (*a*) Specific inhibition of expression of LCa. Western blotting was used to analyze HeLa cells that had been mock-transfected or transfected with LCa esiRNA. Three antibodies were used: rabbit serum that recognizes both LCa and LCb, mAb against actin, and monoclonal TD.1 against the clathrin heavy chain (CHC). (*b*) Selective reduction of c-Myc expression; 293 cells were transfected with buffer, c-*myc* esiRNA, or R-luc esiRNA. Western blotting was performed with antibodies against c-myc and actin 72 h after transfection. (*c*) Dose-dependent inhibition of Cdk2 expression by esiRNA; 293 cells were transfected with indicated doses of Cdk2 esiRNA. Western blotting was performed with antibodies against Cdk2 and cyclin A 5 days after transfection.

We next asked whether esiRNA could be used to inhibit genes whose mRNA and protein products are low in abundance and relatively unstable. As an example, we transfected c-*myc* esiRNA into 293 cells. We observed that the level of c-myc protein was reduced by about 70% (Fig. 5*b*). Inhibition was sequence-specific because actin expression was not affected and unrelated R-luc esiRNA failed to reduce c-myc expression. In addition, we observed specific reduction of cyclin-dependent kinases, Cdk1 and Cdk2, in response to treatment with their corresponding esiRNA (Fig. 5*c* and data not shown). The RNase III/esiRNA protocol was also used to specifically reduce expression of chaperon p23 (K. Yamamoto, personal communication). To date, we have successfully used esiRNA to inhibit the expression of seven diverse genes in cell culture. These examples established esiRNA as a valuable tool for selective depletion of gene products in mammalian cells.

Our results demonstrate that the short RNAs produced by hydrolysis with *E. coli* RNase III can specifically silence gene expression in cultured mammalian cells, in a manner similar to that observed with synthetic siRNA. There are several advantages to the esiRNA protocol presented here. Because esiRNA can potentially target multiple sites within an mRNA, the requirement of screening efficient siRNA for individual genes is eliminated. Targeting of multiple sites would also be important in efforts to reduce viral replication because it can restrict the emergence of siRNA-resistant strains produced by base pair mismatches. The protocol is technically simple and quick, and it is effective on a wide range of proteins in different mammalian cell lines. Large-scale functional genomic studies with dsRNA have already been successful in *C. elegans*, but comparable analysis is still lacking in vertebrates (23, 24). Because of its attributes, RNAi with esiRNA could be easily adapted for analysis of gene functions at the genome scale in cultured mammalian cells. A reverse genetics approach with esiRNA could be particularly useful for identifying genes essential for viability because it is difficult to make stable mutants for those genes. The technique should also be useful in the study of cancer. Cancer cells are genetically different from their normal cell counterparts, often having undergone at least a half-dozen mutations (25). esiRNA could be used to search for genes whose down-regulation specifically kills tumor cells, an approach that would simultaneously identify and validate appropriate new drug targets.

We thank Larry Chasin and James W. Erickson for reviewing the manuscript, John Bell and Raul Andino for PKR−/− and RNase L−/− mouse embryonic fibroblasts, Tim Tian for helpful discussion, and Sue Kim and Kevin Hill for critical reading of the manuscript. This work was supported by National Institutes of Health Grant CA44338 (to J.M.B.), National Institutes of Health Grant GM38093 (to F.M.B.), and the G. W. Hooper Research Foundation. D.Y. is supported by a Postdoctoral Fellowship from the Susan G. Komen Breast Cancer Fund. F.B. was a Fellow of the Leukemia and Lymphoma Society. A.G. is supported by a Postdoctoral Research Fellowship for Physicians from the Howard Hughes Medical Institute. C.-Y.C. is supported by a Postdoctoral Fellowship from the Arthritis Foundation.

1. Sharp, P. A. (2001) *Genes Dev.* **15,** 485–490.
2. Bosher, J. M. & Labouesse, M. (2000) *Nat. Cell Biol.* **2,** E31–E36.
3. Bernstein, E., Caudy, A. A., Hammond, S. M. & Hannon, G. J. (2001) *Nature (London)* **409,** 363–366.
4. Elbashir, S. M., Lendeckel, W. & Tuschl, T. (2001) *Genes Dev.* **15,** 188–200.
5. Nishikura, K. (2001) *Cell* **16,** 415–418.
6. Paddison, P. J., Caudy, A. A. & Hannon, G. J. (2002) *Proc. Natl. Acad. Sci. USA* **99,** 1443–1448.
7. Yang, S., Tutton, S., Pierce, E. & Yoon, K. (2001) *Mol. Cell. Biol.* **21,** 7807–7816.
8. Wianny, F. & Zernicka-Goetz, M. (2000) *Nat. Cell Biol.* **2,** 70–75.
9. Stark, G. R., Kerr, I. M., Williams, B. R., Silverman, R. H. & Schreiber, R. D. (1998) *Annu. Rev. Biochem.* **67,** 227–264.
10. Elbashir, S. M., Harborth, J., Lendeckel, W., Yalcin, A., Weber, K. & Tuschl, T. (2001) *Nature (London)* **411,** 494–498.
11. Caplen, N. J., Parrish, S., Imani, F., Fire, A. & Morgan, R. A. (2001) *Proc. Natl. Acad. Sci. USA* **98,** 9742–9747.
12. Paddison, P. J., Caudy, A. A., Bernstein, E., Hannon, G. J. & Conklin, D. S. (2002) *Genes Dev.* **16,** 948–958.
13. Brummelkamp, T. R., Bernards, R. & Agami, R. (2002) *Science* **296,** 550–553.
14. Holen, T., Amarzguioui, M., Wiiger, M. T., Babaie, E. & Prydz, H. (2002) *Nucleic Acids Res.* **30,** 1757–1766.
15. Harborth, J., Elbashir, S. M., Bechert, K., Tuschl, T. & Weber, K. (2001) *J. Cell Sci.* **114,** 4557–4565.
16. Yang, D., Lu, H. & Erickson, J. W. (2000) *Curr. Biol.* **10,** 1191–1200.
17. Amarasinghe, A. K., Calin-Jageman, I., Harmouch, A., Sun, W. & Nicholson, A. W. (2001) *Methods Enzymol.* **342,** 143–158.
18. Elbashir, S. M., Martinez, J., Patkaniowska, A., Lendeckel, W. & Tuschl, T. (2001) *EMBO J.* **20,** 6877–6888.
19. Zamore, P. D., Tuschl, T., Sharp, P. A. & Bartel, D. P. (2000) *Cell* **101,** 25–33.
20. Action, S. L., Wong, D. H., Parham, P., Brodsky, F. M. & Jackson, A. P. (1993) *Mol. Biol. Cell* **4,** 647–660.
21. Nathke, I. S., Heuser, J., Lupas, A., Stock, J., Turck, C. W. & Brodsky, F. M. (1992) *Cell* **68,** 899–910.
22. Zhang, K. & Nicholson, A. W. (1997) *Proc. Natl. Acad. Sci. USA* **94,** 13437–13441.
23. Gonczy, P., Echeverri, G., Oegema, K., Coulson, A., Jones, S. J., Copley, R. R., Duperon, J., Oegema, J., Brehm, M., Cassin, E., *et al.* (2000) *Nature (London)* **408,** 331–336.
24. Fraser, A. G., Kamath, R. S., Zipperlen, P., Martinez-Campos, M., Sohrmann, M. & Ahringer, J. (2000) *Nature (London)* **408,** 325–330.
25. Hanahan, D. & Weinberg, R. A. (2000) *Cell* **100,** 57–70.

RNA interference in mammalian cells using siRNAs synthesized with T7 RNA polymerase

Olivier Donzé and Didier Picard*

Département de Biologie Cellulaire, Université de Genève, Sciences III, 30 quai Ernest-Ansermet, CH-1211 Genève 4, Switzerland

Received February 28, 2002; Revised and Accepted March 25, 2002

ABSTRACT

Methods that allow the specific silencing of a desired gene are invaluable tools for research. One of these is based on RNA interference (RNAi), a process by which double-stranded RNA (dsRNA) specifically suppresses the expression of a target mRNA. Recently, it has been reported that RNAi also works in mammalian cells if small interfering RNAs (siRNAs) are used to avoid activation of the interferon system by long dsRNA. Thus, RNAi could become a major tool for reverse genetics in mammalian systems. However, the high cost and the limited availability of the short synthetic RNAs and the lack of certainty that a designed siRNA will work present major drawbacks of the siRNA technology. Here we present an alternative method to obtain cheap and large amounts of siRNAs using T7 RNA polymerase. With multiple transfection procedures, including calcium phosphate co-precipitation, we demonstrate silencing of both exogenous and endogenous genes.

INTRODUCTION

Over the last few years, RNA interference (RNAi) has been recognized as a major mechanism of post-transcriptional gene silencing in the nematode *Caenorhabditis elegans* and the fruitfly *Drosophila*, as well as in plants (1). This phenomenon is based on double-stranded RNA (dsRNA) that triggers the silencing of gene expression in a sequence-specific manner. According to the prevailing model, the injected or transfected dsRNA is processed into small RNAs (guide RNAs or small interfering RNAs, siRNAs) of 21–25 nt, depending on the species (2,3). The siRNAs probably associate with a multicomponent nuclease, identified in *Drosophila* and called RISC (RNA-induced silencing complex), and guide this enzyme for sequence-specific degradation of the mRNA (4). In mammalian cells, the interferon-mediated antiviral response to long dsRNA that leads to the shutdown of protein synthesis precludes the use of RNAi (5). To bypass this non-specific effect, short interfering dsRNAs of 21 nt (which do not activate the antiviral response) have been used instead (6). The function of several endogenous genes has recently been investigated with this technique in mammalian cells (7,8). This new approach requires the chemical synthesis of short RNAs involving high cost without a guarantee that the purchased siRNA will be effective in silencing (6). To alleviate these problems, we present a simple alternative to obtain large amounts of short interfering RNAs with T7 RNA polymerase-directed *in vitro* transcription. The obtained siRNAs promote silencing in different mammalian cells of both exogenous and endogenous genes.

MATERIALS AND METHODS

T7 siRNA synthesis

Desalted DNA oligonucleotides were ordered from Microsynth (Switzerland). (i) T7, 5′-TAATACGACTCACTA-TAG-3′. (ii) GFP as in Caplen *et al.* (9): sense, 5′-ATGAACTTCAGGGTCAGCTTGCTATAGTGAGTCGTAT-TA-3′; antisense, 5′-CGGCAAGCTGACCCTGAAGTTCTA-TAGTGAGTCGTATTA-3′. (iii) PKR nucleotides 931–949 relative to the start codon: sense, 5′-AAGATCAAGTTTT-GCCAATGCTATAGTGAGTCGTATTA-3′; antisense, 5′-AAGCATTGGCAAAACTTGATCTATAGTGAGTCGTAT-TA-3′. The oligonucleotide-directed production of small RNA transcripts with T7 RNA polymerase has been described (10). For each transcription reaction, 1 nmol of each oligonucleotide was annealed in 50 µl of TE buffer (10 mM Tris–HCl pH 8.0, and 1 mM EDTA) by heating at 95°C; after 2 min, the heating block was switched off and allowed to cool down slowly to obtain dsDNA. Transcription was performed in 50 µl of transcription mix: 1× T7 transcription buffer (40 mM Tris–HCl pH 7.9, 6 mM $MgCl_2$, 10 mM DTT, 10 mM NaCl and 2 mM spermidine) 1 mM rNTPs, 0.1 U yeast pyrophosphatase (Sigma), 40 U RnaseOUT (Life Technologies) and 100 U T7 RNA polymerase (Fermentas) containing 200 pmol of the dsDNA as template. After incubation at 37°C for 2 h, 1 U RNase free-DNase (Promega) was added at 37°C for 15 min. Sense and antisense 21-nt RNAs generated in separate reactions were annealed by mixing both crude transcription reactions, heating at 95°C for 5 min followed by 1 h at 37°C to obtain 'T7 RNA polymerase synthesized small interfering double-stranded RNA' (T7 siRNA). The mixture (100 µl) was then adjusted to 0.2 M sodium acetate pH 5.2, and precipitated with 2.5 vol ethanol. After centrifugation, the pellet was washed once with 70% ethanol, dried, and resuspended in 50 µl of water.

*To whom correspondence should be addressed. Tel: +41 22 702 6813; Fax: +41 22 702 6928; Email: picard@cellbio.unige.ch

Cell culture

Human HeLa and HEK293T cells were grown at 37°C in Dulbecco's modified Eagle's medium (DMEM) (Life Technologies) supplemented with 5% fetal calf serum, glutamine, penicillin and streptomycin. Cells were seeded into 6-well plates in 2.5 ml of medium 2–3 h prior to transfection by the calcium phosphate co-precipitation technique. Unless noted, 2 µl of T7 siRNA plus 1 µg/well of plasmids pEGFP-C1 (Clontech) and pcDNA3-Luc (11) in 90 µl of water were prepared in a tube to which 30 µl of 1 M $CaCl_2$ was added. The calcium/DNA/siRNA solution was mixed quickly with 120 µl of 2× phosphate solution (140 mM NaCl, 1.5 mM Na_2HPO_4, 50 mM HEPES, pH 7.02) and the precipitate was immediately added to the wells. For silencing of an endogenous gene, 2 µl of T7 siRNA plus 2 µg of vector pcDNA3 were transfected by the calcium phosphate co-precipitation technique. For liposome-mediated transfection, cells were seeded into 6-well plates 4–5 h prior to treatment. Co-transfection of plasmids and T7 siRNAs was carried out with Lipofectamine (Life Technologies) as directed by the manufacturer for adherent cell lines. Unless noted otherwise, 2 µl of T7 siRNA and 0.5 µg of pEGFP-C1 formulated into liposomes were applied per well. The final volume was 1 ml/well. Cells were harvested and lysed 24 and 40 h later for GFP and PKR analysis, respectively.

Western blotting

Cells were lysed in 10 mM Tris–HCl pH 7.5, 150 mM NaCl, 0.1% SDS, 1% Triton X-100, 0.5% deoxycholate, 5% glycerol, protease inhibitors and 1 mM DTT. Equal amounts of total proteins were separated on a 10% polyacrylamide gel and transferred to nitrocellulose. The proteins were revealed either with anti-GFP (Clontech), anti-PKR (Santa-Cruz), anti-luciferase (12) or anti-Hsp90 (a kind gift from Dr David Toft, Mayo Clinic) antibodies.

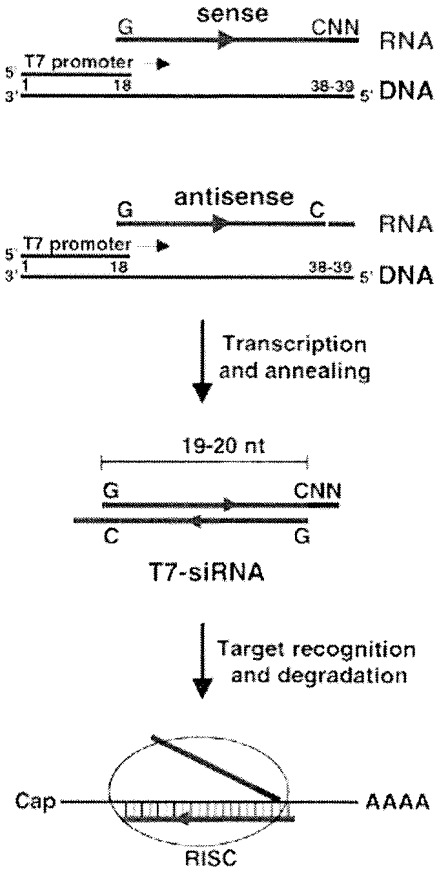

Figure 1. Strategy to generate T7 siRNAs (see Results and Discussion for details). The sequence of the gene of interest is shown in red (sense) or blue (antisense), while the two unrelated nucleotides are in black. RISC stands for the RNA-induced silencing complex that targets the mRNA for cleavage.

RESULTS AND DISCUSSION

To generate siRNAs *in vitro*, we designed the strategy presented in Figure 1. An 18mer oligonucleotide encompassing the T7 promoter is annealed to a 38mer (39mer) oligonucleotide with the complementary sequence of the T7 promoter downstream of the target sequence preceded by two additional nucleotides (reading the sequence 5′→3′). The transcribed sequence is 19 nt (20 nt) plus 2 nt, which can be any nucleotides in the case of the sense RNA but must be complementary nucleotides in the antisense RNA, since it has been shown that the antisense RNA of the siRNA guides target recognition (13). It is noteworthy that T7 RNA polymerase can transcribe a template where only the promoter is double stranded (10). The last guanosine of the T7 promoter is the first ribonucleotide that is incorporated into the RNA by the T7 RNA polymerase during transcription and, therefore, all siRNAs designed by this method will start with a G. Thus, the design of T7 siRNA requires that the sequence starts with a G and has a C at position 19 (position 20) to allow annealing with the complementary RNA, which also starts with a G (see Fig. 1). This G-N17 (N18)-C rule does not restrict the T7 siRNA design since this sequence is frequently found in any gene (on average about five times in a random sequence of 100 bp). To obtain dsRNA for RNAi, only two DNA oligonucleotides corresponding to the sense and antisense sequences of the target gene have to be ordered. The T7 promoter oligonucleotide is invariant and common to any target gene. Following transcription reactions, sense and antisense transcripts are annealed and ethanol precipitated, yielding what we refer to as T7 siRNAs. The integrity of the transcripts was checked on a Nusieve agarose gel (data not shown).

Since our goal was to perform siRNA-mediated silencing with T7 siRNAs, we first selected as a target GFP, which has already been used to study RNAi. The plasmid pEGFP-C1 was transfected together with a 22 nt T7 siRNA into HeLa cells with lipofectamine. Cells were harvested 24 h later and the levels of the exogenously expressed protein were monitored by immunoblot analysis. As shown in Figure 2A, GFP protein levels dropped in the presence of T7 siRNAi targeted to GFP. An unrelated T7 siRNA targeted against the kinase PKR (see below) did not affect GFP levels. Numerous different approaches have been developed to facilitate the transfer of foreign genes into cells, among them the calcium phosphate co-precipitation technique. We thus decided to compare lipofectamine with calcium phosphate. As shown in Figure 2B, GFP expression was also reduced following transfection of T7 siRNAs by the calcium phosphate co-precipitation technique. In the same experiment, the expression of firefly luciferase was not affected by any of the T7 siRNAs, indicating that silencing

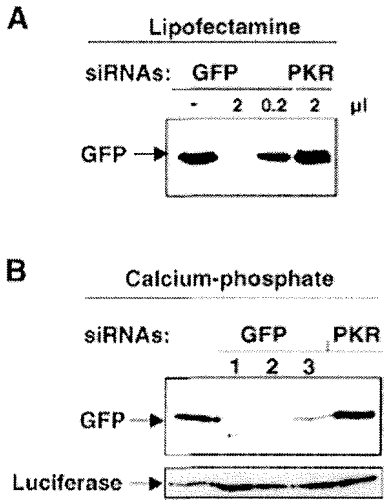

Figure 2. T7 siRNAs silence transfected genes in mammalian cells. (**A**) Plasmid pEGFP-C1 and decreasing amounts of siRNAs were co-transfected using a lipofectamine-based protocol. GFP was revealed with an anti-GFP antibody. T7 siRNA against PKR was transfected as a specificity control. (**B**) T7 siRNAs directed against GFP (1–3 represent siRNAs from three independent transcription reactions) or PKR were transfected using the calcium phosphate co-precipitation technique into HeLa cells with the plasmids pEGFP-C1 and pcDNA3-Luc. GFP and luciferase were detected with anti-GFP and anti-luciferase polyclonal antibodies, respectively.

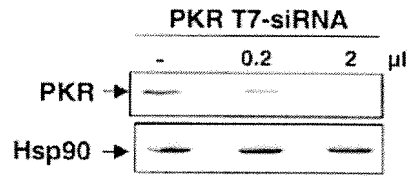

Figure 3. T7 siRNA silences an endogenous gene in mammalian cells. Aliquots of 0.2 or 2 µl of T7 siRNA directed against PKR were transfected using the calcium phosphate co-precipitation technique into 293T cells. Forty hours after transfection, cells were harvested and equal amounts of proteins were loaded on a 10% polyacrylamide gel. PKR was detected using a polyclonal antibody against PKR. Hsp90 was revealed as a specificity and loading control.

triggered by T7 siRNAs in mammalian cells is specific, as reported previously for chemically synthesized siRNAs (6,9). Caplen and colleagues used siRNAs of different lengths and showed that both 21- and 22-nt siRNAs work well to silence GFP (9). We have noticed that 22-nt-long T7 siRNAs may be more efficient for silencing transfected genes than 21 nt T7 siRNAs (data not shown). We conclude that T7 siRNAs can be introduced into cells and mediate their silencing effects with the non-liposome based calcium phosphate co-precipitation method.

To complete our study, we tested T7 siRNA on an endogenous gene, the gene for the interferon-induced protein kinase PKR (14). For this target, the T7 siRNA was 21 nt long, as described recently for other endogenous targets (6,7). In this case, the main challenge for a successful RNAi experiment is to achieve a high transfection efficiency. Using either lipofectamine or calcium phosphate co-precipitation, the transfection efficiency reached almost 80% for HeLa and 293T cells (as judged by transfection of GFP; data not shown). As presented in Figure 3, T7 siRNA targeted against human PKR, transfected into 293T by the calcium phosphate co-precipitation technique, was able to down-regulate endogenous PKR 48 h after the beginning of transfection. The silencing was almost completely effective with 2 µl of T7 siRNA. The residual PKR protein observed by immunoblot may reflect the 10–20% untransfected cells. The T7 siRNA was specific since no effect was observed on the unrelated protein Hsp90 (Fig. 3).

In conclusion, we report here a new protocol for the synthesis of siRNAs by T7 RNA polymerase and their transfer into cells. The main advantage of this technique is its simplicity and its extremely low cost compared with the current prices for synthetic RNA oligonucleotides. The amount of T7 siRNA required for each sample is small and represents ~1–5% of the synthesized short RNA. We estimate that the average yield of T7 siRNA per transcription reaction is 1–5 µg (per 200 pmol template) and that silencing experiments can be carried out with 40–200 ng of T7 siRNA (in 2 µl; see Figs 2 and 3). But even 10 times less was sufficient for a noticeable decrease in GFP expression (Fig. 2A, lane 0.2). The demonstration that RNAi also works with the calcium phosphate technique further contributes to making this powerful technology widely available and applicable. With our approach, RNA interference in mammalian cells may become as easy as in *C.elegans* or *Drosophila*, where long dsRNAs synthesized by T7 RNA polymerase can be used.

ACKNOWLEDGEMENTS

We thank David Toft for the Hsp90 antibody. We are grateful to Katharina Strub and Laurent Huck for experimental advice. This work was supported by the Swiss National Science Foundation, Krebs Forschung Schweiz and the Canton de Genève.

REFERENCES

1. Carthew,R.W. (2001) Gene silencing by double-stranded RNA. *Curr. Opin. Cell Biol.*, **13**, 244–248.
2. Hammond,S.M., Bernstein,E., Beach,D. and Hannon,G.J. (2000) An RNA-directed nuclease mediates post-transcriptional gene silencing in *Drosophila* cells. *Nature*, **404**, 293–296.
3. Zamore,P.D., Tuschl,T., Sharp,P.A. and Bartel,D.P. (2000) RNAi: double-stranded RNA directs the ATP-dependent cleavage of mRNA at 21 to 23 nucleotide intervals. *Cell*, **101**, 25–33.
4. Bernstein,E., Caudy,A.A., Hammond,S.M. and Hannon,G.J. (2001) Role for a bidentate ribonuclease in the initiation step of RNA interference. *Nature*, **409**, 363–366.
5. Williams,B.R. (1999) PKR; a sentinel kinase for cellular stress. *Oncogene*, **18**, 6112–6120.
6. Elbashir,S.M., Harborth,J., Lendeckel,W., Yalcin,A., Weber,K. and Tuschl,T. (2001) Duplexes of 21-nucleotide RNAs mediate RNA interference in cultured mammalian cells. *Nature*, **411**, 494–498.
7. Harborth,J., Elbashir,S.M., Bechert,K., Tuschl,T. and Weber,K. (2001) Identification of essential genes in cultured mammalian cells using small interfering RNAs. *J. Cell Sci.*, **114**, 4557–4565.
8. Garrus,J.E., von Schwedler,U.K., Pornillos,O.W., Morham,S.G., Zavitz,K.H., Wang,H.E., Wettstein,D.A., Stray,K.M., Cote,M., Rich,R.L., Myszka,D.G. and Sundquist,W.I. (2001) Tsg101 and the vacuolar protein sorting pathway are essential for HIV-1 budding. *Cell*, **107**, 55–65.
9. Caplen,N.J., Parrish,S., Imani,F., Fire,A. and Morgan,R.A. (2001) Specific inhibition of gene expression by small double-stranded RNAs in invertebrate and vertebrate systems. *Proc. Natl Acad. Sci. USA*, **98**, 9742–9747.
10. Milligan,J.F. and Uhlenbeck,O.C. (1989) Synthesis of small RNAs using T7 RNA polymerase. *Methods Enzymol.*, **180**, 51–62.

11. Donzé,O., Jagus,R., Koromilas,A.E., Hershey,J.W. and Sonenberg,N. (1995) Abrogation of translation initiation factor eIF-2 phosphorylation causes malignant transformation of NIH 3T3 cells. *EMBO J.*, **14**, 3828–3834.
12. Donzé,O. and Picard,D. (1999) Hsp90 binds and regulates Gcn2, the ligand-inducible kinase of the alpha subunit of eukaryotic translation initiation factor 2. *Mol. Cell. Biol.*, **19**, 8422–8432.
13. Lipardi,C., Wei,Q. and Paterson,B.M. (2001) RNAi as random degradative PCR: siRNA primers convert mRNA into dsRNAs that are degraded to generate new siRNAs. *Cell*, **107**, 297–307.
14. Donzé,O., Abbas-Terki,T. and Picard,D. (2001) The Hsp90 chaperone complex is both a facilitator and a repressor of the dsRNA-dependent kinase PKR. *EMBO J.*, **20**, 3771–3780.

RNAi functions in cultured mammalian neurons

Anna M. Krichevsky* and Kenneth S. Kosik

Center for Neurologic Diseases, Brigham and Women's Hospital, Harvard Medical School, Boston, MA 02115

Edited by Solomon H. Snyder, Johns Hopkins University School of Medicine, Baltimore, MD, and approved July 8, 2002 (received for review May 7, 2002)

In a wide range of organisms, double-stranded RNA triggers posttranscriptional gene silencing or RNA interference (RNAi). Small interfering RNAs, the 21-nt double-stranded RNA intermediates of this natural pathway, have became a powerful tool to knock down specific gene expression in mammalian cell lines and potentially will be useful for the analysis of loss-of-function phenotypes. In mammalian primary neuronal cultures, where genetic manipulations are especially difficult, RNAi might be developed into a highly efficacious tool to study the roles of specific genes in neuron development and functioning. Neurons, however, have been considered the most resistant to RNAi. We report here an application of RNAi to postmitotic primary neuronal cultures. Synthetic siRNA can be readily introduced into neurons and effectively inhibit the expression of endogenous and transfected genes.

Double-stranded RNAs (dsRNAs) are remarkably effective at suppressing specific gene expression in *Caenorhabditis elegans, Drosophila melanogaster, Trypanosoma brucei*, and plants by a pathway involving RNA interference (RNAi) or sequence-specific posttranscriptional gene silencing (1–3). dsRNAs are cleaved by ribonuclease III into 21–22 nucleotide RNA duplexes or small interfering RNAs (siRNAs). These molecules trigger the degradation of the cognate mRNA (4, 5). Although dsRNA induces the global shut-down of protein synthesis in mammalian cells, directly introducing siRNAs of less then 30 nt can suppress expression of specific endogenous and heterologous genes in mammalian cell lines (6, 7). From these studies, the investigators concluded that RNA interference could occur in mammalian cells. The mechanism of the siRNA-triggered RNAi in those cells remains to be elucidated. Until recently, existing approaches to suppress specific gene expression in mammalian cells, mainly antisense and dominant–negative, have proven inefficient and inconsistent. Therefore, RNAi, with its characteristic efficacy at very low concentrations of siRNA, in the low nanomolar range, holds great promise for exploring gene function in mammalian cell cultures. A number of genes were successfully knocked-down in mammalian somatic and embryonic cell lines, including HeLa, HEK293, and P19 (8, 9). However, for reasons that are unclear, neurons seemed more resistant to RNAi than other cell types, perhaps because of differences related to the RNA transport across the cell membrane or the RNAi pathway in these cells. Although RNAi is systemic in *C. elegans* when fed or injected to whole animals, and even silences genes into the next generation, worm neurons seemed resistant to RNAi (10). However, high concentrations of dsRNA (15 μg/ml) can induce a knockdown of targeted gene expression in proliferating and differentiating nematode neuronal culture (11). In *D. melanogaster*, genomic cDNA hybrids predicted to produce dsRNA are able to target genes expressed in neurons (12). Here, we demonstrate that the introduction of very low concentrations of siRNAs into dissociated postmitotic cultures prepared from the rat hippocampus and forebrain can be effective in suppressing endogenous and heterologous genes.

Materials and Methods

Cortical and Hippocampal Cell Culture. Pregnant embryonic day 18 (E18) Sprague–Dawley rats were killed by inhalation of CO_2, and the embryos were removed immediately by Cesarean section. Cerebral cortices and hippocampi were removed and digested in 0.25% trypsin in Hepes-buffered Hanks' balanced salt solution (HBSS) without calcium or magnesium at 37°C for 15 min. The tissue was washed 3× with HBSS and manually dissociated with a fire-bored Pasteur pipette. Cells were plated at a concentration 12,000–20,000/cm^2 on polyL-lysine-coated coverslips in a plating medium containing DMEM and 5% (vol/vol) FBS. After 3 h of incubation, the medium was changed to Neurobasal, containing B27 supplement and 0.5 mM glutamine. All experiments were initiated 5–8 days after plating. Very few glial cells were observed in these cultures.

siRNA Preparation and Transfections. siRNAs corresponding to pEGFP or dsRed2 reporter genes and to MAP2 or YB-1 mRNAs were designed as recommended (13), with 5′ phosphate, 3′ hydroxyl, and two base overhangs on each strand; they were chemically synthesized by Xeragon. The following gene-specific sequences were used successfully: Si-GFP sense 5′-CAAGCUGACCCUGAAGUUCUU-3′ and antisense 5′-GAACUUCAGGGUCAGCUUGUG-3′; Si-DsRed sense 5′-AGUUCCAGUACGGCUCCAAUU-3′ and antisense 5′-UUGGAGCCGUACUGGAACUUG-3′, cognate for MAP2, siRNA1 sense 5′-CGAGAGGAAAGACGAAGGAUU-3′ and antisense 5′-UCCUUCGUCUUUCCUCUCGUG-3′; siRNA2 sense 5′-CAGGGCACCUAUUCAGAUAUU-3′ and antisense 5′-UAUCUGAAUAGGUGCCCUGUG-3′. Annealing for duplex siRNA formation was performed as described (6).

Cotransfections of reporter plasmids and siRNA were performed with Lipofectamine 2000 (Life Technologies) in 6-well plates. Briefly, Lipofectamine diluted in Opti-MEM was applied to the plasmids/dsRNA mixture, and the formulation was continued for 25 min. Per well, 1 μg of pEGFP-C2, 1 μg of pDsRed2, and 0.01–0.2 μg of 21-bp dsRNA (siRNA) formulated with 2 μl of Lipofectamine were applied in the final volume of 1.7 ml. The medium was changed to Neurobasal 2 h after transfection, and cells were incubated for 24–48 h after fixation and analysis. Transfection efficiencies as determined by 4′,6-diamidino-2-phenylindole staining were from 1% to 8%.

Transfections of siRNA for endogenous gene targeting were carried out with TransMessenger transfection reagent (Qiagen, Chatsworth, CA). siRNA (1 μg per well) was condensed with Enhanser R and formulated with 4 μl of TransMessenger reagent, according to the manufacturer's instructions. The transfection complex was diluted in 900 μl of Neurobasal and was added directly to the cells; it was replaced with Neurobasal after 2 h. Cells were stained and analyzed 48–68 h after transfections. The results were confirmed in three independent experiments.

Immunocytochemistry. Double immunofluorescence labeling of MAP2 and several proteins was performed. Neurons grown on glass coverslips were washed with PBS, fixed in 4% (wt/vol) paraformaldehyde, permeabilized with 0.25% Triton X-100, washed two more times with PBS, and blocked for 30 min with

This paper was submitted directly (Track II) to the PNAS office.

Abbreviations: dsRNA, double-stranded RNA; RNAi, RNA interference; siRNA, small interfering RNA; E*n*, embryonic day *n*; siGFP, siRNA cognate to green fluorescent protein; MAP2, microtubule-associated protein 2.

*To whom reprint requests should be addressed. E-mail: krichevsky@cnd.bwh.harvard.edu.

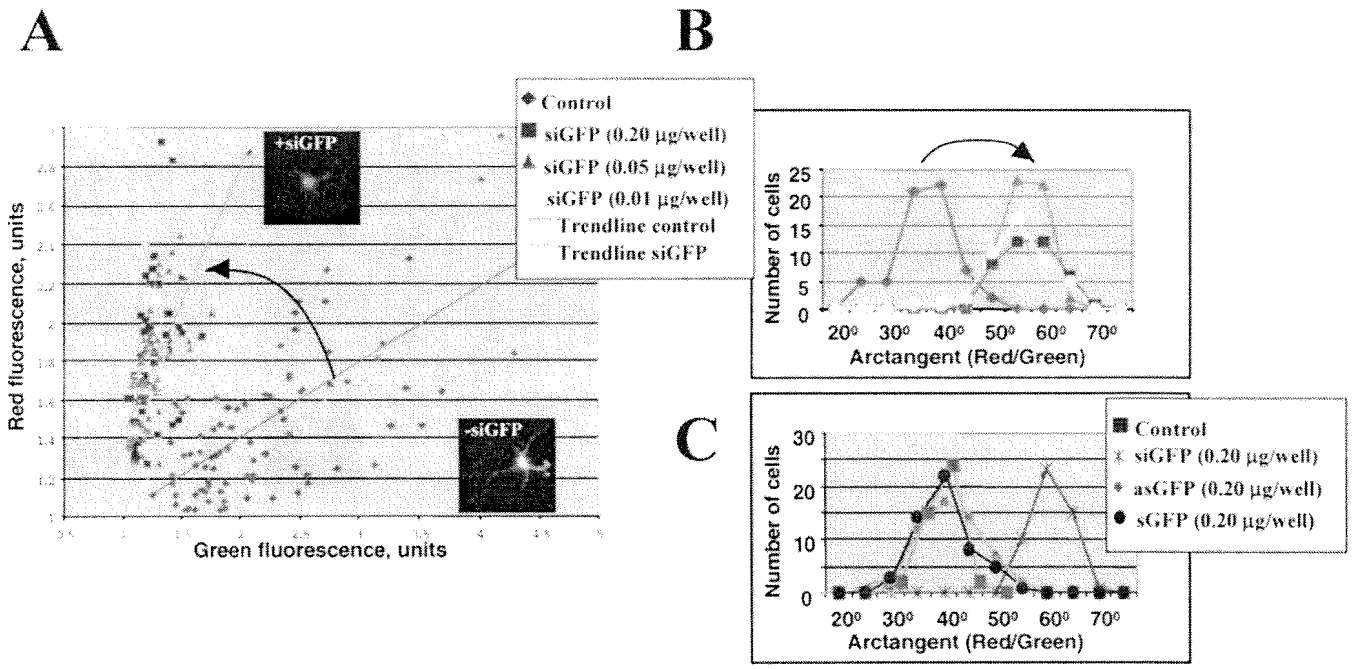

Fig. 1. Effect of 21nt-siRNA targeting GFP expression (siGFP) in primary cortical neurons. (*A*) Primary neurons were cotransfected with pEGFP and DsRed2 plasmids and with siRNA cognate to EGFP (siGFP). For each transfected cell, green and red fluorescence were normalized to a background and plotted. In each experiment, at least 50 randomly chosen transfected control (−siGFP) and targeted (+siGFP) neurons were analyzed. Typical control and targeted cells are shown in *Insets*. (*B*) For each cell in *A*, an arctangent function (that represents the ratio between red and green fluorescence) was calculated, and the results are presented as a distribution function. The shift in this distribution represents specific suppression of GFP expression by siGFP. Similar effects were observed with siGFP concentrations from 0.006–0.12 μg/ml. (*C*) Single strands of siGFP (sense-sGFP and antisense-asGFP 21nt-RNAs) do not suppress GFP expression.

10% (vol/vol) neural goat serum. Cells were incubated with primary antibodies [1:200 in 1% (vol/vol) neural goat serum in PBS] overnight at 4°C and washed three times with PBS. Mouse monoclonal anti-MAP2 antibody was produced in our laboratory (14). Rabbit polyclonal anti-YB1 antibody was generously provided by V. Evdokimova (McGill Univ., Montreal, QC, Canada); rabbit polyclonal anti-cortactin was purchased from Santa Cruz Biotechnology. MAP2 was visualized with Alexa 488- or Alexa 594-conjugated goat anti-mouse secondary antibody [1:500 in 1% (vol/vol) goat serum in PBS; Molecular Probes]. Other antibodies were detected with Alexa 488- or Alexa 594-conjugated goat anti-rabbit secondary antibody. Actin was detected with Alexa Fluor 594 phalloidin (1:100; Molecular Probes). Finally, cells were washed in PBS and mounted on the microscope with Antifade mounting medium.

Microscopy and Image Analysis. Fluorescent microscopy was performed with a confocal laser scanning unit coupled to a Zeiss Axiovert S100. Images were recorded with equal exposure times for specific reporter plasmids or for specific antibodies (in nonsaturating conditions). In each cotransfection experiment, at least 50 randomly chosen transfected neurons were analyzed. In each MAP2-targeting experiment, at least 70 random neurons per experimental condition were analyzed, and gene expression was quantified in both control and targeted cells. Quantification of pixel intensity was performed with Adobe PHOTOSHOP software and normalized to a background.

Results

First, to assess the effectiveness of RNAi on cultured neurons, the 21-nt sense and antisense ssRNAs targeted against EGFP-C2 and DsRed2 reporter vectors were selected from the coding regions and designed as described in *Materials and Methods*. Each strand was synthesized separately, and pairs were annealed to create the duplex dsRNAs with the characteristics of siRNAs (13). Primary neurons were transfected with these two plasmids and one cognate dsRNA 5–8 days after plating. Two hours after transfection, the medium was changed to Neurobasal; cells were fixed, and EGFP and DsRed2 expressions were monitored 24–48 h later. Fluorescent microscopy showed that EGFP or DsRed2 expressions were significantly and specifically inhibited by their corresponding dsRNAs, but not by unrelated dsRNAs in nearly all transfected neurons (Fig. 1 *A* and *B* show the data for GFP targeting). At 24 h after cotransfection with two plasmids, most transfected neurons (1–8% efficiency) expressed a high level of GFP and a lower level of DsRed and, therefore, appeared yellow-green when merged (the typical cell is shown in *Inset* in Fig. 1*A*). siRNA cognate to green fluorescent protein (siGFP) significantly reduced enhanced green fluorescent protein (EGFP) expression without affecting dsRed expression and, therefore, the cells appeared red. To quantify the effect of siRNA on a GFP expression, images were recorded with equal exposure times for specific reporter plasmids under nonsaturating conditions, with further monitoring of green and red fluorescence for randomly chosen transfected cells. For each cell, green and red fluorescence were normalized to a background and plotted (Fig. 1*A*). In each experiment, at least 50 randomly chosen transfected control and targeted neurons were compared. This analysis demonstrated that GFP expression was specifically inhibited by the cognate dsRNA duplex as detected by a 42% reduction in the green fluorescence intensity, whereas the red fluorescence remained unchanged. For each analyzed cell, the ratio between red and green fluorescence was calculated as an arctangent function; the results are presented as a distribution function in Fig. 1*B*. The shift in this distribution represents specific suppression of GFP expression by siGFP. Moreover, almost nonoverlapping distribution functions of control vs. targeted cells clearly indicate that nearly all transfected neurons

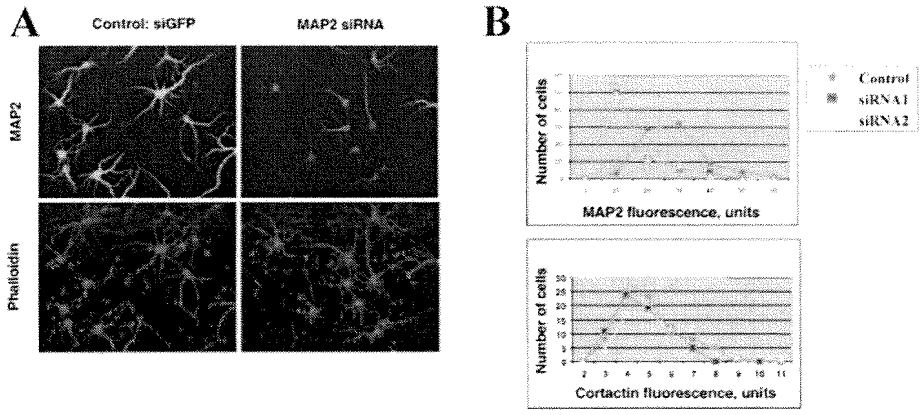

Fig. 2. MAP2 suppression by cognate 21nt-siRNAs. (*A*) Double fluorescence staining of neurons transfected with nonspecific siRNA or with MAP2-siRNA. (*Upper*) Staining with MAP2 monoclonal antibody (green). (*Lower*) Staining with actin-bound toxin phalloidin (red). In each experiment, at least 70 random neurons per experimental condition were analyzed, and gene expression was quantified in both control and targeted cells. (*B*) Distribution of MAP2 and cortactin expression levels in control and targeted cells, two different siRNA (siRNA1 and siRNA2) show a very similar effect.

were affected by siGFP even in its lowest concentration (6 ng/ml). The suppression was specific for dsRNA duplex: both sense and antisense ssRNAs did not inhibit expression of the reporter gene (Fig. 1*C*).

Similar analysis of DsRed2 targeting by its cognate dsRNA demonstrated some overlap between control and targeted cells when plotted as above, with DsRed2 expression inhibited specifically at ≈30% (data not shown). This was due to the later onset of DsRed2 expression and the high variability of its expression level between different control cells.

Next, we tested the effect of siRNAs on microtubule-associated protein 2 (MAP2) and RNA-binding protein YB-1 (also called p50) endogenous mRNAs. In the course of these experiments, we noticed that siRNA could be readily introduced into neurons when compared with plasmid DNA. Therefore, there was no need to introduce the reporter vector as a marker of cells transfected with siRNA. The endogenous mRNA for MAP2 was targeted by transfections of cognate 21-nucleotide dsRNAs with TransMessenger transfection reagent. Double immunofluorescence labeling of MAP2 and three unrelated proteins (cortactin, actin, YB-1) was performed 48–68 h after transfections. The expression of MAP2 was specifically reduced by the cognate dsRNA duplex in 70–80% of cells, whereas expression of unrelated proteins was unaffected (Fig. 2*A*). Among these cells, the decrease in MAP2 fluorescent intensity was ≈4-fold. The fluorescent intensity over the total cell population varied greatly because of variation in transfection efficiency and possibly differential sensitivity of the neurons to siRNA. Nevertheless, even when the fluorescent intensity was measured over the total population of cells, a decrease in MAP2 fluorescence was readily detectable (Fig. 2*B*). Remarkably, this statistical analysis revealed that two different siRNA cognate to MAP2 (siRNA1 and siRNA2) demonstrated the identical inhibitory effect on MAP2 expression.

Phenotypic effects of MAP2 suppression on cultured neurons can be observed early on after plating as neurons consolidate their lamellae and elaborate filopodia. It has been shown (15, 16) that MAP2 is required to overcome early transitions of neuritic development and to begin processes elongation. We targeted primary cultures with the cognate siRNAs 3 h after plating and analyzed the effect over 28–40 h. Within this shorter time-frame, fewer neurons suppressed MAP2 expression. However, the degree of MAP2 suppression correlated with the recognized defect in filopodial elaboration (Fig. 3).

Transfection with two different dsRNAs cognate to YB-1 RNA-binding protein did not suppress the target protein even with a 68-h exposure. The reasons for the ineffectiveness of RNAi in this case may arise from the high stability of the extremely abundant YB-1 protein or from intrinsic features of YB-1 mRNA.

Discussion

The use of small interfering RNAs has become a powerful tool to knock down specific gene expression in a wide range of cells. In *Drosophila* lysate, dsRNA triggers the recognition and targeted cleavage of homologous cellular mRNA (4). In mammalian cells, the mechanism underlying siRNA-mediated gene targeting is unknown; it might interfere with RNA stability and/or translation or, alternatively, transcription.

In cultured mammalian cell lines, chemically synthesized siRNAs can by introduced into cells when formulated with lipophilic reagents (Lipofectamine 2000 or Oligofectamine; refs. 7 and 8). Very recently, several groups developed an alternative approach to suppress genes by intracellular expression of siRNAs from transfected plasmide DNA (17–20). Notably, transfections of postmitotic primary neurons are very inefficient, often toxic, and, therefore, none of the techniques mentioned above would be useful for siRNA-mediated gene targeting in neurons. In principle, RNA can be introduced into a single neuron with cationic lipids (21). We have demonstrated that synthetic 21-nt dsRNA (siRNAs) is readily delivered into primary cortical and hippocampal neurons by

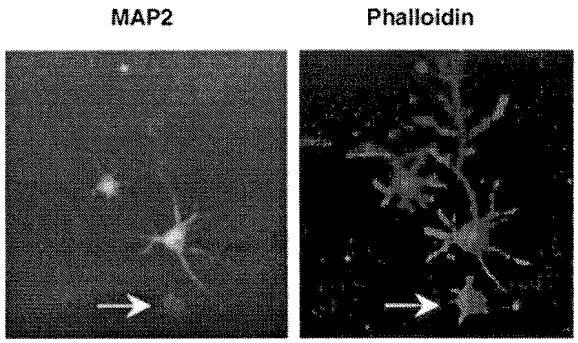

Fig. 3. MAP2 suppression correlates with the defect in early staged neuronal development. Double fluorescence staining of young neurons transfected with MAP2-siRNA. (*Left*) Staining with MAP2 monoclonal antibody (green). (*Right*) Staining with actin-bound toxin phalloidin (red). The cell with silenced MAP2 expression (labeled by arrow) exhibits severe defect in filopodia elaboration.

cationic TransMessenger transfection reagent and can be used to suppress gene expression. Therefore, the RNAi pathway seems operative in primary mammalian neurons. Even a brief (2-h) exposure to a low concentration of siRNAs (0.006–0.6 μg/ml) caused suppression of endogenous and heterologous gene expression. Antisense ssRNAs in that concentration range did not inhibit gene expression. Higher concentrations of siRNA/transfection reagents seemed to be toxic for neuronal cultures. The effect of siRNA on MAP2 expression was slow and usually became visible 2 days after transfections. We also assume that longer incubation of cells is required for better suppression of transfected GFP and DsRed genes; however, we failed to keep neurons transfected with Lipofectamine 2000 healthy more than 48 h. In nematode, the only other neuronal culture system in which RNAi was shown to be effective, the RNAi effect was also quite slow (visible after 3–4 days with dsRNA) and required much higher amounts of dsRNA (15 μg/ml instead of 0.006–0.6 μg/ml). Currently, we do not know what factors are responsible for the rate and the strength of RNAi-induced posttranscriptional gene suppression. Clearly, particular characteristics of a targeted mRNA ("defensive" secondary structures and bound transfactors, causing ineffectiveness of some siRNA) and protein (different life times) affect RNAi efficacy. In addition, cell-specific factors might be involved in differential siRNA delivery and regulation of RNA interference in various cell types. The recent discovery of predominantly brain-specific microRNAs, a previously uncharacterized class of noncoding RNAs sharing processing pathways with siRNAs (22), together with our data, suggest a role of RNAi-related mechanisms of gene regulation in neuronal development and functioning. The ability to knock down expression of a specific gene is likely to have broad application in neurons, a setting where genetic manipulations have proven difficult.

1. Hutvagner, G. & Zamore, P. D. (2002) *Curr. Opin. Genet. Dev.* **12,** 225–232.
2. Sharp, P. A. (2001) *Genes Dev.* **15,** 485–490.
3. Hammond, S. M., Caudy, A. A. & Hannon, G. J. (2001) *Nat. Rev. Genet.* **2,** 110–119.
4. Zamore, P. D., Tuschl, T., Sharp, P. A. & Bartel, D. P. (2000) *Cell* **101,** 25–33.
5. Bernstein, E., Caudy, A. A., Hammond, S. M. & Hannon, G. J. (2001) *Nature (London)* **409,** 363–366.
6. Elbashir, S. M., Harborth, J., Lendeckel, W., Yalcin, A., Weber, K. & Tuschl, T. (2001) *Nature (London)* **411,** 494–498.
7. Caplen, N. J., Parrish, S., Imani, F., Fire, A. & Morgan, R. A. (2001) *Proc. Natl. Acad. Sci. USA* **98,** 9742–9747.
8. Harborth, J., Elbashir, S. M., Bechert, K., Tuschl, T. & Weber, K. (2001) *J. Cell Sci.* **114,** 4557–4565.
9. Paddison, P. J., Caudy, A. A. & Hannon, G. J. (2002) *Proc. Natl. Acad. Sci. USA* **99,** 1443–1448.
10. Timmons, L., Court, D. L. & Fire, A. (2001) *Gene* **263,** 103–112.
11. Christensen, M., Estevez, A., Yin, X., Fox, R., Morrison, R., McDonnell, M., Gleason, C., Miller, D. M., III, & Strange, K. (2002) *Neuron* **33,** 503–514.
12. Kalidas, S. & Smith, D. P. (2002) *Neuron* **33,** 177–184.
13. Elbashir, S. M., Martinez, J., Patkaniowska, A., Lendeckel, W. & Tuschl, T. (2001) *EMBO J.* **20,** 6877–6888.
14. Escobar, M. I., Pimienta, H., Caviness, V. S., Jacobson, M., Crandall, J. E. & Kosik, K. S. (1986) *Neuroscience* **17,** 975–989.
15. Gonzalez-Billault, C., Engelke, M., Jimenez-Mateos, E. M., Wandosell, F., Caceres, A. & Avila, J. (2002) *J. Neurosci. Res.* **67,** 713–719.
16. Caceres, A., Mautino, J. & Kosik, K. S. (1992) *Neuron* **9,** 607–618.
17. Paul, C. P., Good, P. D., Winer, I. & Engelke, D. R. (2002) *Nat. Biotechnol.* **20,** 505–508.
18. Lee, N. S., Dohjima, T., Bauer, G., Li, H., Li, M. J., Ehsani, A., Salvaterra, P. & Rossi, J. (2002) *Nat. Biotechnol.* **20,** 500–505.
19. Miyagishi, M. & Taira, K. (2002) *Nat. Biotechnol.* **20,** 497–500.
20. Yu, J. Y., DeRuiter, S. L. & Turner, D. L. (2002) *Proc. Natl. Acad. Sci. USA* **99,** 6047–6052.
21. Crino, P. B. & Eberwine, J. (1996) *Neuron* **17,** 1173–1186.
22. Lagos-Quintana, M. R. R., Yalcin, A., Meyer, J., Lendeckel, W. & Tuschl, T. (2002) *Curr. Biol.* **12,** 735–739.